METABOLISM OF THE COVALENT PHOSPHATE IN GLYCOGEN

Vincent S. Tagliabracci

Submitted to the faculty of the University Graduate School
in partial fulfillment of the requirements
for the degree
Doctor of Philosophy
in the Department of Biochemistry & Molecular Biology
Indiana University

July 2010

Accepted by the Faculty of Indiana University, in partial fulfillment of the requirements for the degree of Doctor of Philosophy.

Peter J. Roach, Ph.D. -Chair

Doctoral Committee

Anna A. DePaoli-Roach, Ph.D.

June 25, 2010

Thomas D. Hurley, Ph.D.

Nuria Morral, Ph.D.

DEDICATION

This work is dedicated to my parents, Susan and Vince Tagliabracci, whose love and support have made this all possible. You guys have dedicated your lives to me, so I am honored to dedicate this work to you.

I would also like to dedicate this work to my grandmother, Elaine Stillert, who has been the best grandmother any grandson could ever have.

Last but not least, I would also like to dedicate this work to my wife, Jenna L. Jewell, who for the past five years has kept me in check and taught me to strive for perfection

I love you guys!

.

ACKNOWLEDGEMENTS

I would first like to thank my mentor, Dr. Peter Roach. Peter has not only been a great teacher but also a great friend, advising me in the laboratory and in life. He has made me appreciate the difficulty and the diligence needed to apply the scientific method and perhaps most importantly, has taught me how to be my own most severe critic. Because of him, I no longer look at a failed experiment as a failure, but rather an opportunity to thrive by learning from my mistakes.

I would next like to thank Dr. Anna DePaoli-Roach. Anna has made me realize that I am capable of doing things that I never before thought possible. She has made me appreciate and embrace the hard work and dedication that comes with scientific exploration.

I would like to thank everyone in the Roach and DePaoli-Roach labs. Dyann Segvich, Cathy Meyer, Jose Irimia, Sasha Skurat, Sixin Jiang, Chandra Karthik, Punitee Garyali , Chris Contreras, Chiharu Nakai and Katrina Hughes. I think the most imperative attribute of our lab is that we are all close friends as well as colleagues. It was a pleasure coming to work everyday and interacting with you guys.

I would like to thank my committee members, Dr. Tom Hurley and Dr. Nuria Morral. They have given me invaluable advice on my project that helped it move forward.

I would like to thank our collaborators that contributed to this work. Parastoo Azadi, Christian Heiss, Mayumi Ishihara, Vincent Gattone, Caroline Miller, Berge Minassian, Jean-Marie Girard and Julie Turnbull.

I would like to thank everyone in the Department of Biochemistry and Molecular Biology. In particular, Dr. Zhong-Yin Zhang, Jack Arthur, Sandy McClain, Melissa Pearcy, Sheila Reynolds, and Jamie Mayfield.

Last but not least, my family. Without them none of this would be possible. My parents and idols, Susan and Vince, my wife and best friend, Jenna, my grandma Elaine, my mother-in-law Sherry and of course, the dogs- Libby and Chanel.

ABSTRACT

Vincent S. Tagliabracci

METABOLISM OF THE COVALENT PHOSPHATE IN GLYCOGEN

Glycogen is a highly branched polymer of glucose that functions to store glucose residues for future metabolic use. Skeletal muscle and liver comprise the largest glycogen reserves and play critical roles in maintaining whole body glucose homeostasis. In addition to glucose, glycogen contains small amounts of covalent phosphate of unknown function, origin and structure. Evidence to support the involvement of glycogen associated phosphate in glycogen metabolism comes from patients with Lafora Disease. Lafora disease is an autosomal recessive, fatal form of progressive myoclonus epilepsy. Approximately 90% of cases of Lafora disease are caused by mutations in either the *EPM2A* or *EPM2B* genes that encode, respectively, a dual specificity phosphatase called laforin and an E3 ubiquitin ligase called malin. Lafora patients accumulate intracellular inclusion bodies, known as Lafora bodies that are primarily composed of poorly branched, insoluble glycogen-like polymers. We have shown that laforin is a glycogen phosphatase capable of releasing phosphate from glycogen *in vitro* and that this activity is dependent on a functional carbohydrate binding domain. In studies of laforin knockout mice, we observed a progressive change in the properties and structure of glycogen that paralleled the formation of Lafora bodies. Glycogen isolated from these mice showed increased glycogen phosphate, up to 6-fold ($p < 0.001$) compared to WT, providing strong evidence that laforin acts as a glycogen phosphatase *in vivo.* Furthermore we have demonstrated that glycogen synthase introduces phosphate into glycogen during synthesis by transferring the β-phosphate of UDP-glucose into the polymer and that laforin is capable of releasing the phosphate incorporated by glycogen synthase. Analysis of mammalian glycogen revealed the presence of covalently linked phosphate at the 2 hydroxyl and the 3 hydroxyl of glucose residues in the polysaccharide, providing the first direct evidence of the chemical nature of the phosphate linkage. We envision a

glycogen damage/repair process, analogous to errors during DNA synthesis that are subsequently repaired. We propose that laforin action parallels that of DNA repair enzymes and Lafora disease results from the inability of the phosphatase to repair damaged glycogen, adding another biological polymer to the list of those prone to errors by their respective polymerizing enzymes.

Peter J. Roach, Ph.D. -Chair

TABLE OF CONTENTS

LIST OF TABLES

LIST OF FIGURES

LIST OF ABBREVIATIONS

ADP	Adenosine diphosphate
AGL	Amylo-1,6-glucosidase, 4-α-glucanotransferase
AMP	Adenosine monophosphate
AMPK	AMP activated protein kinase
AT	acquisition time
ATP	Adenosine triphosphate
$Ba(OH)_2$	Barium hydroxide
BE	Branching enzyme
$CaCl_2$	Calcium chloride
cAMP	3'-5'-cyclic adenosine monophosphate
cAZY	Carbohydrate active-enzymes
CBM20	Carbohydrate binding domain subtype 20
Ci	Curries
CK-1	Casein kinase-1
CK-2	Casein kinase-2
cpm	Counts per minute
Cys/C	Cysteine
Da	Dalton
DBE	Glycogen debranching enzyme
DCC	Dicyclohexylcarbodiimide
DEAE	Diethylaminoethyl
DFRQ	Decoupler frequency for heteronucleus (^{13}C or ^{31}P)
DHBA	α-Dihydroxybenzoic acid
DNA	Deoxyribonucleic acid
DSP	Dual specificity phosphatase
DTT	Dithiothreitol
DYRK1A	Dual specificity tyrosine-phosphorylation-regulated kinase 1A
EDTA	Ethylenediaminetetraacetic acid

EGTA	Ethyleneglycol-O, O'-bis(2-aminoethyl)-N, N, N', N'-tetraacetic acid
eIF2α	Eukaryotic initiation factor-2α
EM	Electron microscopy
Epm2a	Epilepsy progressive myoclonus type 2a
Epm2aIP	Epm2a interacting protein
Epm2b	Epilepsy progressive myoclonus type 2b
ER	Endoplasmic reticulum
ETC	Electron transport chain
F6P	Fructose-6-phosphate
F-1,6-BP	Fructose-1,6-bisphosphate
G1	Glucose
G2	Maltose
G3	Maltotriose
G4	Maltotetraose
G5	Maltopentaose
G6	Maltohexaose
G7	Maltoheptaose
G8	Maltooctaose
GAA	Lysosomal acid-α-glucosidase
GAPDH	Glyceraldehyde-3-phosphate dehydrogenase
gHMQC	Gradient heteronuclear multiple quantum coherence
Glc	Glucose
G6P	Glucose-6-phosphate
GLUT	Sodium independent glucose transporter
Gly/G	Glycine
GN	Glycogenin
GP	Glycogen phosphorylase
G6PT	Glucose-6-phosphate translocase
G6Pase	Glucose-6-phosphatase
GS	Glycogen synthase

GSK3	Glycogen synthase kinase-3
GSD	Glycogen storage disorder
HBR	Hydrobromic acid
HCl	Hydrochloric acid
$HClO_4$	Perchloric acid
HK	Hexokinase
HMQC	Heteronuclear multiple quantum coherence
HPAEC	High performance anion exchange chromatography
HPTLC	High performance thin layer chromatography
H_2SO_4	Sulfuric acid
Hz	Hertz
I_2	Iodide
IR	Insulin receptor
IRS	Insulin receptor substrate
kDa	Kilodalton
KH_2PO_4	Potassium dihydrogen phosphate
KI	Potassium iodine
KOH	Potassium hydroxide
KOMP	Knockout mouse project repository
LDH	Lactate dehydrogenase
LB	Lafora body
LD	Lafora disease
LiCl	Lithium chloride
LSS	Low speed supernatant
LSP	Low speed pellet
MALDI	Matrix assisted laser desorption/ionization
MCT-1	Monocarboxylate transporter-1
MCT-2	Monocarboxylate transporter-2
$MgCl_2$	Magnesium chloride
$MnCl_2$	Manganese chloride
MGSKO	Muscle glycogen synthase knockout

MIX	Mixing (spinlock) time
MS	Mass spectrometry
NaCl	Sodium chloride
NaCl	Sodium chloride
NaOH	Sodium hydroxide
$NADP^+$	Nicotinamide adenine dinucleotide phosphate
NaOAc	Sodium acetate
ND	Not detectable
NH_4HCO_3	Ammonium bicarbonate
NHL	NCL-1, HT2A and LIN-41
NHLRC1	NHL repeat-containing protein 1
NH_4OH	Ammonium hydroxide
NI	Number of increments
NMR	Nuclear magnetic resonance
NP:	Number of points in the directly detected dimension
NT	Number of transients
OH	Hydroxyl
PAS	Periodic acid/Shiff
PASD	Periodic acid/Shiff α-amylase resistant
PCR	Polymerase chain reaction
PDK-1	Phosphoinositide-dependent kinase-1
PFK	Phosphofructokinase
PGI	Phosphoglucose isomerase
PGM	Phosphoglucomutase
Ph	Phosphorylase
PIP2	Phosphatidylinositol (4,5) bisphosphate
PIP3	Phosphatidylinositol (3,4,5) triphosphate
PKA	cAMP dependent protein kinase / protein kinase A
PI3K	Phosphatidylinositol-3-kinase
PKB/Akt	Protein kinase B
PM	Plasma membrane

PMSF	Phenylmethylsulfonylfluoride
*p*NPP	*para*-Nitrophenylphosphate
PP1c	Protein phosphatase-1, catalytic subunit
PP1G	Glycogen associated phosphatase
PTG	Protein targeted to glycogen
RING	Really interesting new gene
RNA	Ribonucleic acid
RT	Room temperature
RTPCR	Real time polymerase chain reaction
SDS	Sodium dodecyl sulfate
SDS-PAGE	Sodium dodecyl sulfate polyacrylamide gel electrophresis
Ser/S	Serine
SEX4	Starch excess-4
SFRQ	Spectrometer frequency for proton nucleus
SM	Skeletal muscle
SW	Spectral width in the directly detected dimension (^{1}H)
SW1	Spectral width in the indirectly detected dimension (^{13}C or ^{31}P)
TBS	Tris-buffered saline
TBST	Tris-buffered salin containing tween-20
TCA	Trichloroacetic acid
TCA cycle	Tricarboxylic acid cycle
TFA	Trifluoroacetic acid
Thr	Threonine
Tris	Tris(hydroxymethyl)aminomethane
TLC	Thin layer chromatography
Trp/W	Tryptophan
Tyr	Tyrosine
THAP	2',4',6'-Trihydroxyacetophenone monohydrate
Thr/T	Threonine
TOCSY	Total correlation spectroscopy

TOF	Time of flight
Tyr/Y	Tyrosine
Ub	Ubiquitin
UDP	Uridine diphosphate
UDP-glucose	Uridine diphosphate glucose
UGP	UDP-glucose pyrophosphorylase
UGPPase	UDP-glucose pyrophosphatase
UMP	Uridine monophosphate
UTP	Uridine triphosphate
WT	Wild type

INTRODUCTION

1. Glycogen Structure

Glycogen is a highly branched polymer of glucose that functions to store glucose residues for future metabolic use. The large majority of glycogen in animals is found in the liver and skeletal muscle, but heart, brain, adipose, as well as many other tissues are capable of synthesizing the polymer (1). The mobilization of glucose from glycogen deposits in the liver provides a constant supply of glucose for tissues, such as the brain, which depends on this sugar for an energy source. Skeletal muscle, on the other hand, lacks the enzymatic machinery for mobilization of glucose to the blood stream and glucose released from glycogen is catabolized locally. Polymerization of glycogen occurs by the formation of α-1,4-glycosidic linkages between glucose residues, forming an elongated polymer. Branch points are introduced at the C6 hydroxyl of a glucose residue in the chain forming an α-1,6-glycosidic linkage (Figure 1). The frequency of α-1,6-glycosidic linkages (about 1 every 8-12 glucose residues), determines the topology, structure and solubility of glycogen and distinguishes it from the carbohydrate moiety of plant starch. A unique three dimensional structure of glycogen cannot be determined experimentally due to the fact that glycogen is polydisperse. However much is known about the branching structure of glycogen and a widely accepted model has been proposed (2) (Figure 2). In this model the average chain consists of 13 glucose residues where the inner B chains contain two branch points and the outer A chains are unbranched. A full size glycogen molecule would consist of 12 tiers, have Mr ~10^7, a diameter of ~40 nm and contain about 55,000 glucose residues (2). Based on this model there is an equal number of A chains and B chains with a uniform distribution of chain lengths. Furthermore, each B chain has two chains attached to it, and all the A chains are on the outermost tier. The branching frequency of 1 branch point every 8-12 glucose residues is somewhat misleading, as it is the average over the entire glycogen molecule. Given that the A chains are unbranched, the

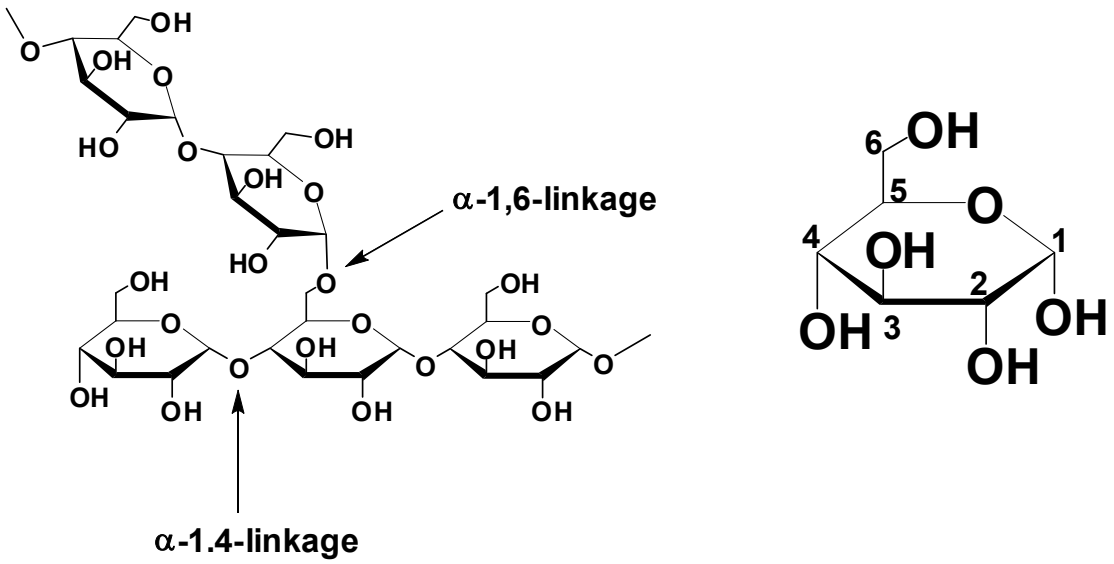

Figure 1. Glycosidic linkages in glycogen. The traditional α-1,4- and α-1,6-glycosidic linkages account for the bulk of the polymerization of glycogen (left). The structure of glucose, indicating the numerical nomenclature of the carbons (right).

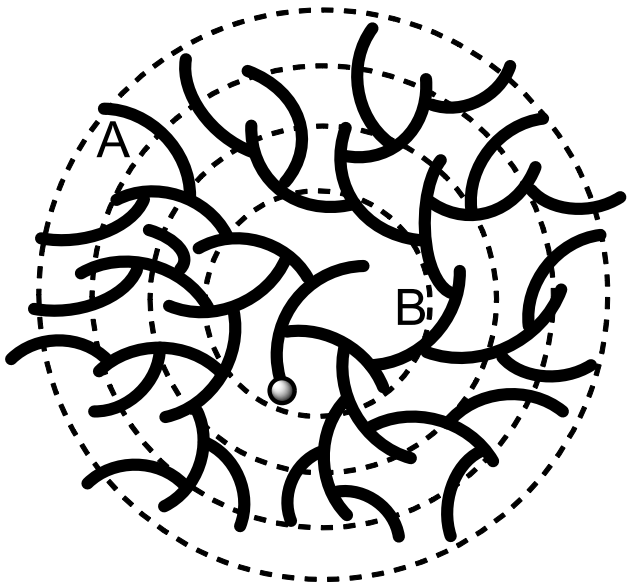

Figure 2. Glycogen structure. A portion of a molecule is shown, indicating the branching pattern, the tiered structure and the A and B chains. The unbranched A chains account for about 50% of the total number of glucoses in the glycogen molecule.

average distance between branches would only apply to the B chains. However, the A chains account for about 50% of the entire glycogen molecule, assuming they are of full length, so the distance between branch points on the B chains would be about 4 glucoses.

In addition to glucose, glycogen also contains small amounts of covalently linked phosphate whose function and origin, until recently, was not well understood (3-7). Rabbit skeletal muscle glycogen for example contains 0.064% by weight of phosphate or 0.12% mol phosphate/mol glucose. This value corresponds to about 1 phosphate molecule for approximately every 650 glucose residues. Covalently bound phosphate has been proposed to exist as a phosphomonoester at the C6-OH and a phosphodiester, linking C1 of one glucose residue to C6 of another residue forming an alternative branch point (4). Lomako et al. (4) proposed that a specific enzyme, termed UDP-glucose: glycogen glucose-1-phosphotransferase introduces this diester linkage, with the source of the phosphate from UDP-glucose. The enzyme was not, however, fully characterized at the molecular level. Covalently bound phosphate in plant amylopectin, a complex carbohydrate similar in structure to mammalian glycogen, is well accepted and alterations in starch phosphate levels have profound impact on starch metabolism (8). Specific protein dikinases, unique to plants, are known to catalyze this phosphorylation (9). Glucan water dikinase and phosphoglucan water dikinase transfer the β phosphate of ATP to C6 and C3 hydroxyl residues in amylopectin respectively. Phosphorylation at C6 is thought to prime the polysaccharide for phosphorylation at the C3 hydroxyl (9). Extensive analysis of mammalian genomes reveals no mammalian homologues of the dikinases identifiable by sequence comparison. Furthermore, the starch phosphatase, starch excess 4 (SEX4), hydrolyzes both C6 and C3 phosphate from amylopectin. Genetic depletion of SEX4 in Arabidopsis leads to the accumulation of starch (10), presumably by preventing the degradation of the starch granule due to excessive phosphate (11).

Besides phosphate, trace amounts of glucosamine have also been detected in rabbit liver glycogen, but not in skeletal muscle and heart glycogen

(12). The glucosamine in liver glycogen has not been studied thoroughly and its importance in glycogen structure and metabolism, if any, is not understood. Glucosamine is thought to be incorporated into glycogen by glycogen synthase using UDP-glucosamine as the glucosyl donor (12). Glucosamine is present as an α-1,4-linkage and liver glycogen purified from rats injected with galactosamine contained as much as 10% glucosamine in the polysaccharide (12).

The physiological relevance of these atypical, covalent structural components of glycogen is unknown. Nevertheless emerging evidence points to a particularly important role for covalent phosphate in maintaining glycogen structure and solubility.

2. Glycogen Metabolism

2.1 Preamble

Glycogen metabolism is regulated largely by the coordinated action of glycogen synthase and glycogen phosphorylase, the rate limiting enzymes in glycogenesis and glycogenolysis, respectively. The synthesis of glycogen can be initiated once sufficient uridine diphosphate glucose (UDP-glucose) is formed from the combined actions of a series of enzymes that convert glucose to UDP-glucose. This conversion is highly dependent on the nutritional status of the organism. For example, when nutrients are limiting, the majority of ingested glucose will be oxidized through glycolysis and oxidative phosphorylation. In times of nutritional abundance glucose can be converted to UDP-glucose and stored as glycogen. In muscle, glucose is taken from the bloodstream by facilitated diffusion mediated by the GLUT4 transporter, whose translocation to the plasma membrane is dependent on the hormone insulin. In liver, the constitutively active GLUT2 transporter facilitates glucose entry into hepatocytes, a process that is not dependent on insulin. The intracellular glucose is rapidly converted to glucose-6-phosphate (glucose-6P) by glucokinase in the liver and hexokinase in muscle, at which time the cell's nutritional status decides the fate of glucose-6P. In times of low nutrient availability, glucose is oxidized whereas in

times of nutritional abundance, the glucose-6P is converted to glucose-1-phosphate (glucose-1P) by phosphoglucomutase (PGM). Glucose-1P is a substrate for UDP-glucose pyrophosphorylase (UGP), a uridylyltransferase that catalyzes the formation of UDP-glucose from UTP and glucose-1P. Glycogen synthase then initiates bulk glycogen biosynthesis from a short oligosaccharide primer covalently linked to and synthesized by glycogenin.

2.2 Glycogenin

The necessity for a 'primer' in polysaccharide synthesis was suggested by the Cori's in the early 1930's (13), with the observation that glycogen synthesis by phosphorylase and glucose-1P proceeded only in the presence of a trace of glycogen. Work by Whelan and Krisman (14, 15) led to the discovery of a specialized self glycosylating protein, glycogenin, that was found to be necessary for the initiation of glycogen biosynthesis. Primates have two glycogenin genes, glycogenin-1, corresponding to the originally described enzyme, and glycogenin-2. In humans, glycogenin-1, encoded by the *GYG1* gene, is widely expressed and predominates in muscle. Glycogenin-2 is restricted to liver, heart, and to a lesser degree, pancreas. (16). A patient has been described with a mutation in the *GYG1* gene, resulting in the depletion of glycogen in skeletal muscle, and cardiac arrhythmia, associated with the accumulation of abnormal storage material in the heart (17). Glycogenin is a member of the family 8 retaining glycosyltransferases (GT8) and initiates the synthesis of glycogen through repeated self glycosylation reactions using UDP-glucose as a substrate to form a short glucose polymer approximately ten residues long (18, 19). Two chemically distinct reactions are catalyzed by glycogenin, the first involving glucosylation of Tyr194 through the formation of a C1-O-tyrosyl linkage and the second involving the subsequent formation of the α-1,4-glycosidic linkages. The resulting α-1,4-linked oligosaccharide acts as a primer for bulk glycogen synthesis (20, 21). Glycogenin is an unusual enzyme, since it is the catalyst, a substrate and a product of the reaction. The crystal structure of rabbit muscle glycogenin has been solved revealing the basic functional unit as a dimer (22).

2.3 Glycogen synthase

The rate limiting intracellular enzyme in glycogen biosynthesis is glycogen synthase. Glycogen synthase catalyzes the formation of the α-1,4-glycosidic linkages in glycogen by transferring a glucosyl moiety from UDP-glucose to the non-reducing end (C4-OH) of a glycogen molecule with the release of UDP (Figure 3). Although the mechanism of this reaction is not completely understood, it has been proposed that an unstable oxonium ion intermediate is formed, giving the anomeric carbon on the glucosyl moiety positive character, allowing for attack of the C4-OH at the non-reducing end of the glycogen particle (23). Glycogen synthase belongs to the family 3 retaining glycosyltransferases (GT3) and mammals express two isoforms, one of which is liver specific and the other expressed in muscle and other tissues (1). The regulation of glycogen synthase is complex, as both phosphorylation and allosteric regulation play major roles in controlling enzyme activity. In fact, glycogen synthase was the third enzyme shown to be controlled by reversible phosphorylation (24). Normally, phosphorylation by protein kinases inactivates the enzyme but this inactivation can be overcome by the potent allosteric activator glucose-6P (25). In the laboratory, glycogen synthase activity is measured in the absence and presence of glucose-6P. The ratio of the two activities, (minus glucose-6P divided by plus glucose-6P), generates an activity ratio which is used as a kinetic index of the state of activation of the enzyme due to its covalent phosphorylation status (25). For example, a low activity ratio would be indicative of a highly phosphorylated and inactivated enzyme, whereas a high activity ratio is indicative of an active, dephosphorylated enzyme. Rabbit muscle glycogen synthase contains at least 9 different serine residues located at the N and C termini that can be phosphorylated *in vivo* (1). *In vitro*, a number of protein kinases phosphorylate glycogen synthase, including glycogen synthase kinase-3 (GSK3) (26, 27), phosphorylase kinase (PhK) (28), cAMP dependent protein kinase (PKA) (29), casein kinase 1 (CK1) (30, 31), casein kinase 2 (CK2) (32), AMP activated protein kinase (AMPK) (33), PAS kinase (34), DYRK1A (35) and p38 MAPK (36). The phosphorylation sites of glycogen synthase were named before the

sequence of the protein was determined. Sites 1a, 1b, 2, 2a, 3a, 3b, 3c, 4 and 5 correspond, respectively to residues 697, 710, 7, 10, 640, 644, 648, 652, and 656 in rabbit muscle glycogen synthase (Figure 4). The mammalian N terminus contains two sites that are phosphorylated *in vivo*, sites 2 and 2a (Figure 4). *In vitro*, site 2 is phosphorylated by cyclic AMP-dependent protein kinase (29) and phosphorylase kinase (28). Site 2a is phosphorylated by casein kinase 1 *in vitro*, but only when site 2 has been phosphorylated (30). Consistent with this idea, mutation of site 2 eliminates phosphorylation of site 2a in COS cells (37). These phosphorylation events inactivate the enzyme and exemplify a phenomenon termed hierarchal phosphorylation, a mechanism in which a phosphorylation event at one residue is a prerequisite for phosphorylation of another residue (38). The C terminus of glycogen synthase contains 7 phosphorylation sites in the muscle isoform and 5 in the liver isoform, as sites 1a and 1b are absent in the liver enzyme. Phosphorylation of sites 3a and 3b in the C termini have the most influence on enzyme activity (1). GSK-3 phosphorylates these regulatory sites and, *in vitro*, catalyzes sequential phosphorylation of sites 4, 3c, 3b, and 3a (26, 32). These sites are phosphorylated in a hierarchal manner involving GSK3 and casein kinase II. Casein kinase II phosphorylates site 5, creating a recognition motif –S-X-X-X-S(P), (where X is any amino acid) for GSK3. This primes glycogen synthase for sequential phosphorylation at sites 4, 3c, 3b, and 3a by GSK3 (26, 32, 39). GSK-3, however, is not the only kinase that phosphorylates the C terminal regulatory sites 3a and 3b. This is based on the observations that glycogen synthase expressed in COS cells or Rat1 fibroblasts can still be phosphorylated and inactivated when site 2 and site 2a are mutated to alanine, and the GSK-3 recognition motif is disrupted by serine-to-alanine substitutions at sites 3c, 4, and/or 5 (40). The mutant enzyme could still be phosphorylated at site 3a and/or 3b suggesting the presence of another site 3a and/or 3b kinase. A site 3a kinase was originally purified from rabbit skeletal muscle and identified as DYRK1A, a member of the dual-specificity tyrosine phosphorylated and regulated protein kinase family (35). Another site 3a kinase was identified as PAS kinase, (34), after the identification of orthologues in *S. cerevisiae* that were genetically

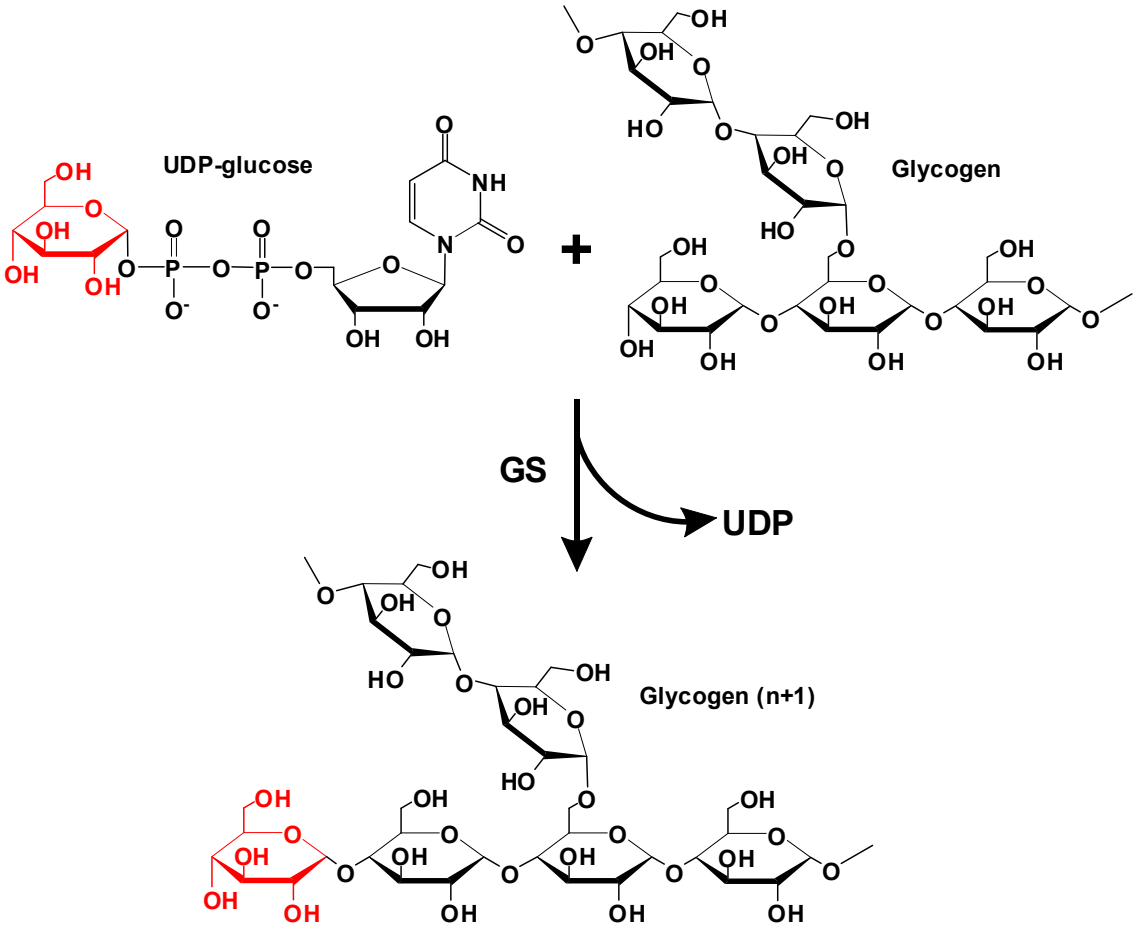

Figure 3. The glycogen synthase reaction. Glycogen synthase transfers a glucosyl moiety (red) from UDP-glucose to the non-reducing end (C4-OH) of a glycogen particle.

required for the maintenance of normal glycogen stores (41). *In vitro*, site 3b and 4 can be phosphorylated by the stress activated protein kinase p38 MAPK (36)

Activity can be restored to glycogen synthase by the action of the glycogen associated phosphatases (PP1G) that remove the inhibitory phosphates (see Introduction Section 2.8). In muscle, PP1G is composed of the type 1 protein phosphatase catalytic subunit (PP1c) and the regulatory subunits PTG, R6, and R_{GL}. The regulatory subunits have carbohydrate binding domains that localize the phosphatase to glycogen to dephosphorylate enzymes involved in glycogen metabolism (42).

Activation of glycogen synthase leads to the formation of an elongated polymer of glucose that would eventually become insoluble and perhaps toxic to the cell. Keeping the polymer soluble by the formation of branch points necessitates the action of another glycogen metabolic enzyme, the branching enzyme.

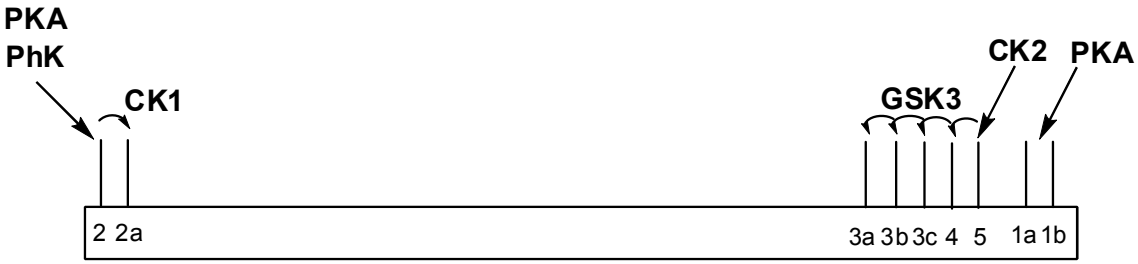

Figure 4. Schematic of glycogen synthase. Vertical lines indicate the phosphorylation sites associated with different protein kinases. PKA; protein kinase A (cAMP dependent protein kinase); PhK, phosphorylase kinase; CK1, casein kinase-1; CK2, casein kinase-2; GSK3, glycogen synthase kinase-3. Modified from Roach. 2, 101-120. (2002) Curr Mol Med.

2.4 The branching enzyme

The branching enzyme adds branch points to a growing glycogen particle in the form of α-1,6-glycosidic linkages, thereby influencing the structure and solubility of the polysaccharide. These branch points are introduced by cleavage of an α-1,4-glycosidic linkage, excising a segment of existing oligosaccharide, and reforming an α-1,6-linkage (43) (Figure 5). The mammalian enzyme is a monomer with M_r of 77 kDa (44) and shares sequence similarity with α-amylase and other polysaccharide modifying enzymes that act on branched structures. The degree of branching of polysaccharides determines the solubility of the polymer. For example, a polysaccharide with frequent branches, like glycogen, is soluble in aqueous solution. A polysaccharide with less frequent branch points, like the amylopectin found in starch, is far less soluble in aqueous solution. Glycogen branching is therefore a central feature in the maintenance of a functional, non toxic polymer; indeed, defects in the human branching enzyme are found in type IV glycogen storage disease (see Introduction Section 4.6). Common to all patients is the formation of poorly branched insoluble glycogen particles or polyglucosans that can have devastating effects due to their lack of solubility. Unlike glycogen synthase, not much is known about the regulation of the branching enzyme.

The synthesis of glycogen thus requires the combined action of three enzymes, glycogenin, glycogen synthase and the branching enzyme. In times of metabolic demand, such as fasting or exercise, glycogen is broken down and the stored glucose can be oxidized and used as fuel. The degradation of glycogen is mediated by the combined actions of glycogen phosphorylase and the debranching enzyme.

2.5 Glycogen phosphorylase

A key enzyme in glycogenolysis is glycogen phosphorylase. Glycogen phosphorylase catalyzes the phosphorolysis of the α-1,4-glycosidic linkages of glycogen producing glucose-1-phosphate and $glycogen_{(n-1)}$ (Figure 6). Phosphorylase uses pyridoxal phosphate as a necessary cofactor and three

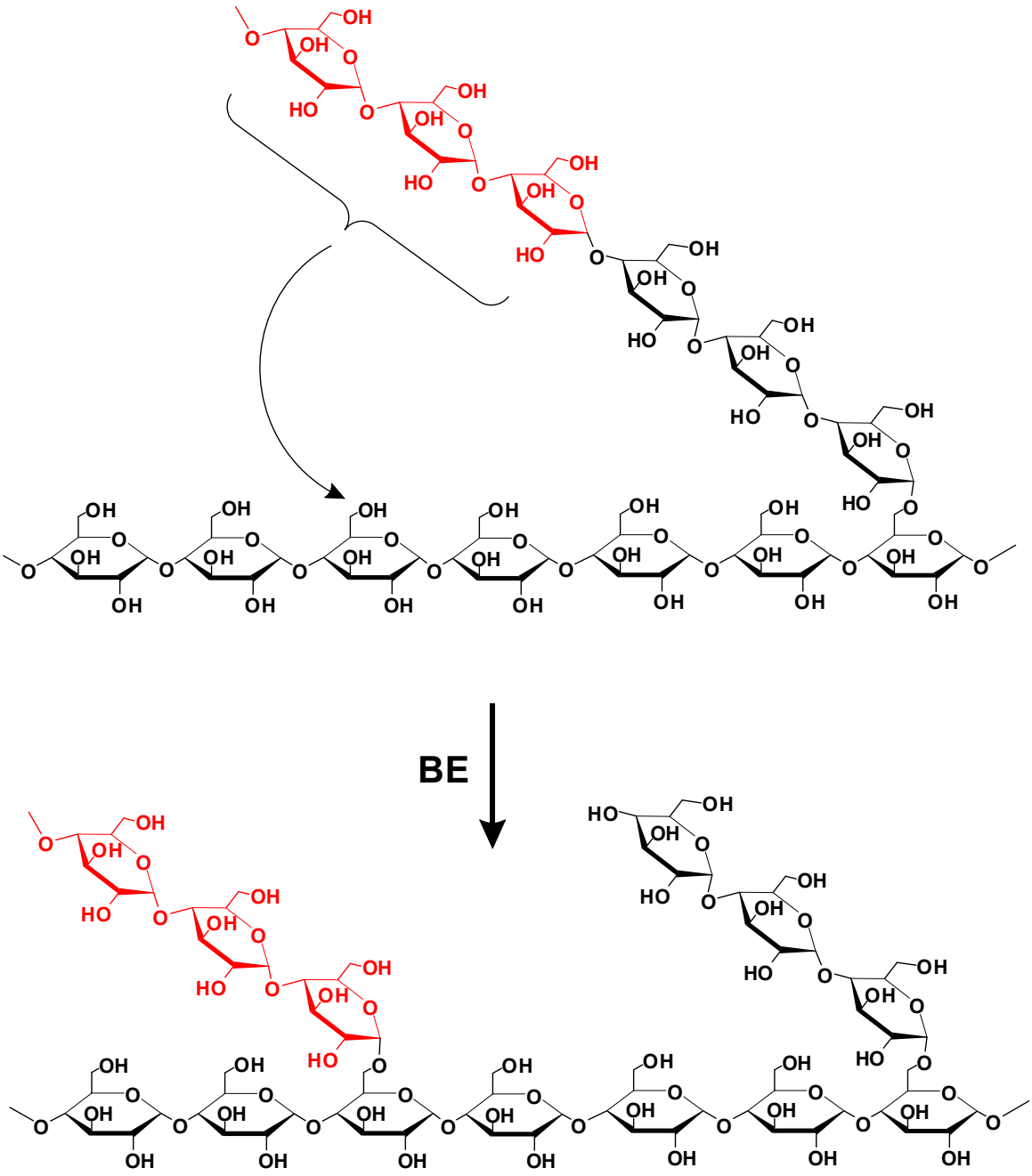

Figure 5. The branching enzyme reaction. The reaction catalyzed by the branching enzyme (BE) involves excising a segment of existing oligosaccharide by cleavage of an existing α-1,4-glycosidic linkage followed by the formation of an α-1,6-linkage.

isoforms of the enzyme, expressed in skeletal muscle, liver and brain are present in mammals. The most active form of the enzyme is thought to be a homodimer with a subunit of 97,000 Da (45) which undergoes transitions between an active R state and a less active T state. The transition between these 2 states is dependent on the phosphorylation state of the enzyme and its interaction with allosteric ligands. The phosphorylated form of the enzyme, phosphorylase a, has a single phosphorylated serine, Ser^{14}. Phosphorylation by phosphorylase kinase activates the enzyme by promoting a large conformational change and shifting the enzyme's equilibrium from the less active T state to the more active R state. The allosteric activator AMP also shifts the equilibrium in favor of the R state and can restore activity to the dephosphorylated form of the enzyme, phosphorylase b. As for glycogen synthase, phosphorylase activity is measured in the absence and presence of its allosteric regulator AMP. The resulting activity ratio is used as a kinetic index on the state of activation of the enzyme due to its covalent phosphorylation status (46). The protein phosphatase that dephosphorylates phosphorylase is PP1G, containing the R_{GL}, PTG/R5 or R6 regulatory subunits in skeletal muscle and PTG/R5, R6 or G_L in liver (47).

2.6 The debranching enzyme

Mechanistically, phosphorylase stalls four glucose residues from an α-1,6-glycosidic linkage necessitating the action of another enzyme, the glycogen debranching enzyme. The glycogen debranching enzyme or amylo-1,6-glucosidase, 4-α-glucanotransferase, (AGL), is a relatively large protein with Mr of 165 kDa. The substrate for AGL is a branch with 4 glucose residues formed by phosphorylase. AGL has two separate catalytic activities and two different active sites. The N terminal domain catalyzes the hydrolysis of an α-1,4-linkage to leave a single branched residue in an α-1,6-linkage, and reforms an α-1,4-linkage between the detached glucose residues and the main chain (Figure 7). The C terminus of AGL contains a domain with amylo-1,6-glucosidase activity that removes the remaining branched glucose residue. Mutations in AGL lead to

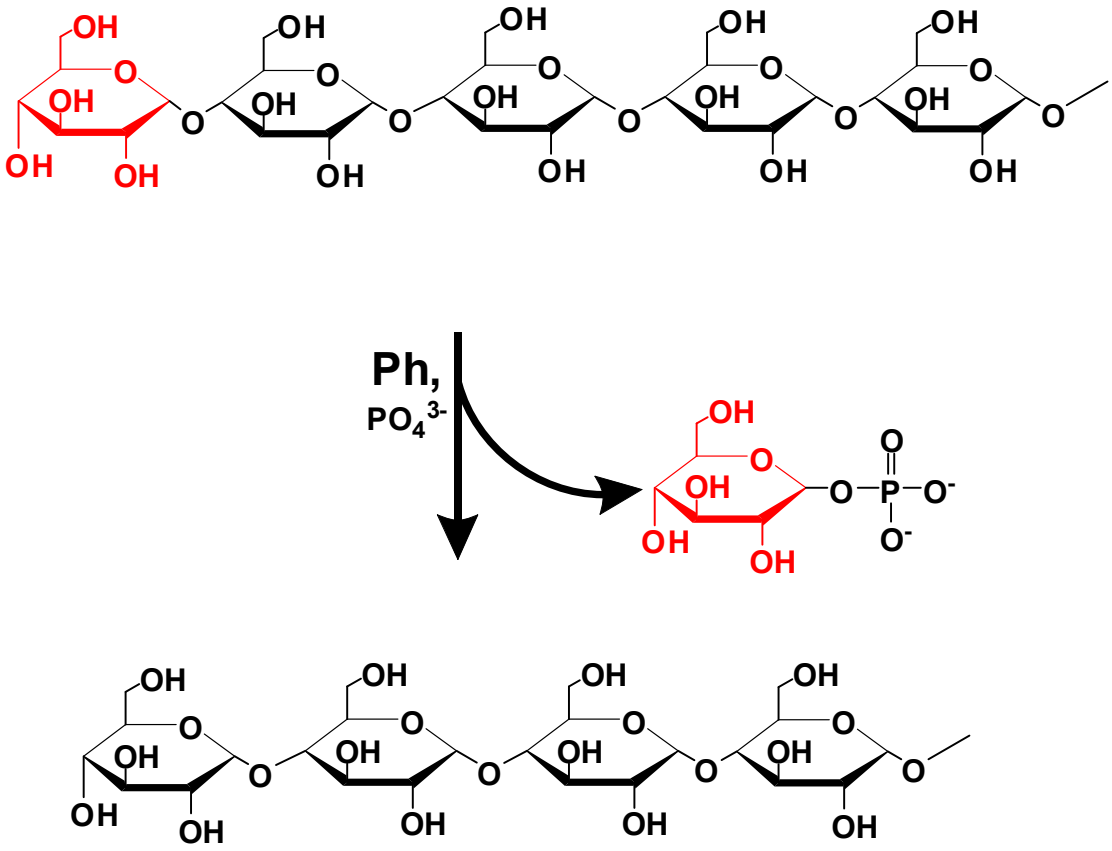

Figure 6. The glycogen phosphorylase reaction. Glycogen phosphorylase transfers a molecule of inorganic phosphate to the terminal glucose residue in a glycogen chain and subsequent cleavage of the α-1-4 glycosidic linkage.

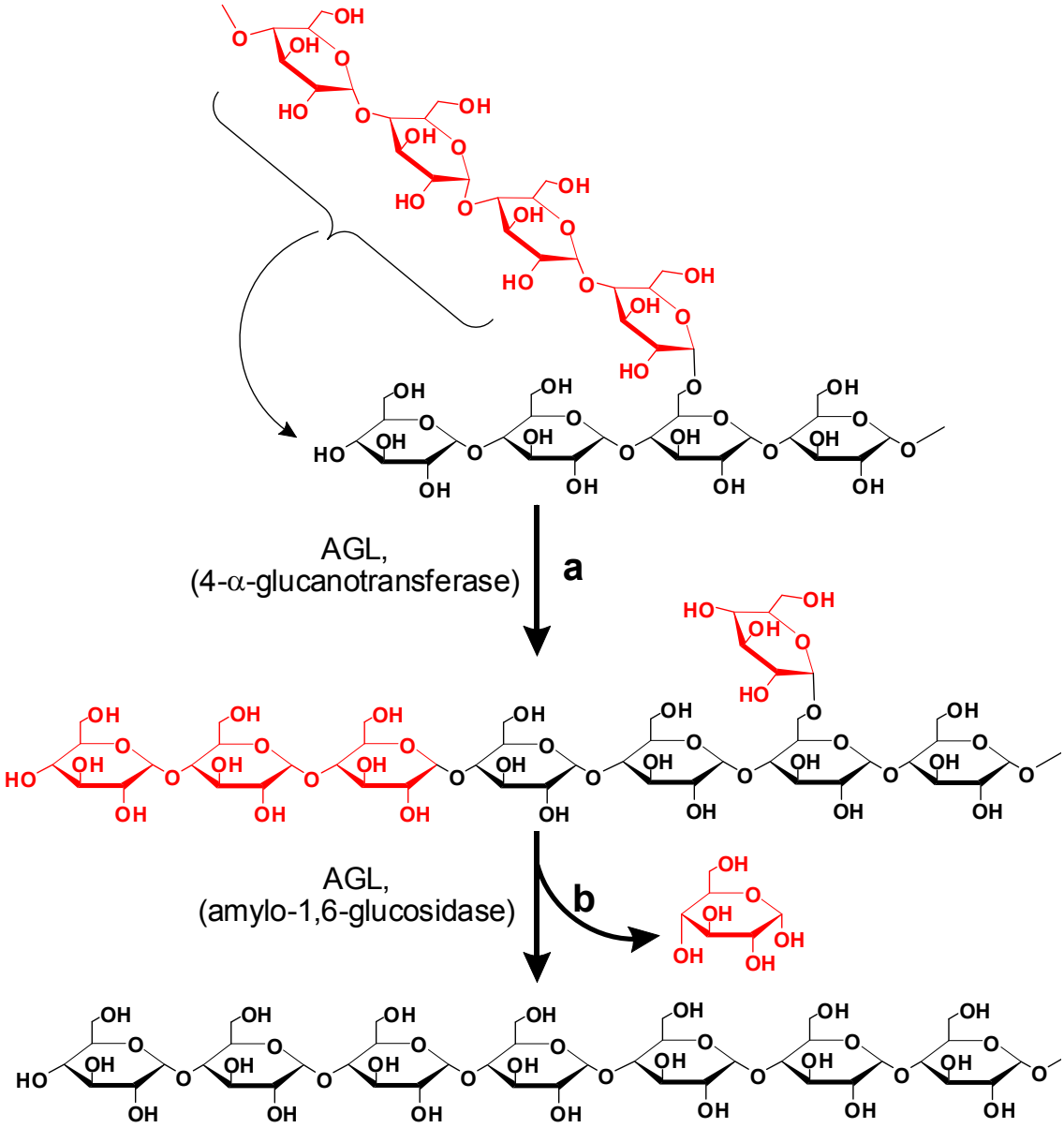

Figure 7. The glycogen debranching enzyme (AGL) reaction. AGL has 2 separate catalytic activities that work sequentially to debranch a glycogen molecule. After phosphorylase stalls 4 glucoses from a branch point, AGL excises three glucoses of existing oligosaccharide by cleavage of an α-1,4-glycosidic linkage followed by the formation of a new α-1,4-linkage at the non-reducing end of the main chain (a). The second reaction involves hydrolysis of the α-1,6-linkage with the release of glucose (b).

a type III glycogen storage disease or Cori's disease, characterized by abnormal glycogen structure with very short outer chains.

2.7 Acid-α-glucosidase

Glycogen resides and is metabolized by the above enzymes in the cytosol. However, a small fraction of glycogen makes its way to the lysosomes where it is degraded by another glycogen metabolizing enzyme, acid-α-glucosidase. Acid-α-glucosidase is the enzyme responsible for the breakdown of lysosomal glycogen by catalyzing the hydrolysis of both the α-1,4- and α-1,6-linkages to produce glucose. Although the mechanism of glycogen transfer to the lysosomes for degradation is still not well understood, the importance of lysosomal glycogen degradation is highlighted in patients with Pompe's disease. Pompe's patients have defects in acid-α-glucosidase and hyperaccumulate lysosmal glycogen resulting in a severe phenotype in heart and muscle that usually results in death within the first year of life. There is evidence for the transcriptional regulation of the human acid α-glucosidase gene (48) but regulation of acid-α-glucosidase activity for the most part seems to be strictly dependent on pH.

2.8 Glycogen associated phosphatases

The glycogen associated phosphatases (PP1G) consist of the catalytic subunit of protein phosphatase 1 (PP1c) and a regulatory or targeting subunit that binds glycogen with high affinity. These targeting subunits localize PP1c to glycogen in the vicinity of glycogen metabolizing enzymes. The result is dephosphorylation of target substrates leading to a net accumulation of glycogen, mainly through activation of glycogen synthase and inactivation of phosphorylase. Common to all glycogen targeting subunits is a PP1 binding motif (RVXF) and a glycogen binding domain (49). Mammalian genomes contain no fewer than seven glycogen targeting subunits but only four have been extensively characterized, PTG/R5, R_{GL} R6 and G_L (49). Ceulemans et al. (50) undertook a bioinformatic approach to trace the evolution of regulatory subunits of PP1. By

searching completed genome sequences, they identified three novel regulatory subunits of PP1 that were named PPP1R3E, PPP1R3F and PPP1R3G. These putative proteins all contained the canonical RVXF motif that mediates interaction with PP1, as well as putative glycogen binding domains. R_{GL}/ G_M, (PPP1R3A) was the first glycogen-binding subunit of PP1 identified (51). The R_{GL}/G_m subunit is expressed only in striated muscle and is necessary for the activation of glycogen synthase in response to exercise (52). Furthermore, R_{GL} knockout mice have decreased glycogen levels as well as a decrease in the activity ratio of glycogen synthase (53). G_L, (PPP1R3B), a 33 kDa protein, is expressed predominantly in liver and skeletal muscle in humans but only in liver of rodents (54). PP1G/G_L is controlled allosterically by glucose and phosphorylase (55, 56). R5/PTG (PPP1R3C) interacts with glycogen metabolizing enzymes and has been suggested to control glycogen synthase activity in response to insulin stimulation (57, 58). Crosson et al. (58) reported that genetic depletion of PTG in mice is embryonically lethal. Heterozygous deletion of the PTG gene resulted in mice with reduced glycogen stores in adipose tissue, liver, heart, and skeletal muscle, correlating with decreased glycogen synthase activity and glycogen synthesis. Furthermore, these mice were glucose intolerant, hyperinsulinemic, and insulin resistant, conditions that worsened as the mice aged (58). Distruption of the PTG gene, in the laboratory of Dr. Anna DePaoli-Roach, leads to viable mice that have a decrease in the glycogen synthase -/+ glucose-6P activity ratio and a corresponding 30% decrease in skeletal muscle glycogen. Fold activation of glycogen synthase activity in response to insulin is unchanged in these mice suggesting that PTG is not required for the activation of glycogen synthase in response to insulin. Most importantly, and contrary to the report by Crosson et al. (58), the homozygous null mice are viable and more insulin sensitive as judged by insulin tolerance tests and by hyperinsulinemic-euglycemic clamp studies (DePaoli-Roach, unpublished data). There is a clear increase in PTG protein levels in response to exercise, suggesting that PTG, like R_{GL}, may be essential for the activation of glycogen synthase in response to exercise (see Results). Recently, PTG has been implicated in a fatal form of

progressive myoclonus epilepsy known as Lafora Disease (see Introduction Section 5). R6 is a 33kDa protein that is ubiquitously expressed, with highest levels in heart and skeletal muscle and much lower levels in the liver (59). PP1/PPP1R3E activity has been proposed to be under long-term control by insulin in rodent liver yet absent from skeletal muscle. However, PPP1R3E mRNA is found at appreciable levels in human skeletal muscle (60).

There is strong evidence to support critical roles for these targeting subunits in controlling glycogen accumulation also in humans, as a prevalent variant in *PPP1R3A,* the gene encoding human R_{GL}, impairs glycogen synthesis and decreases glycogen levels in human, as well as mouse, skeletal muscle (61).

3. Hormonal Regulation of Glycogen Metabolism

3.1 Insulin regulation of glycogen metabolism

Skeletal muscle and liver comprise the largest glycogen reserves and play critical roles in whole body glucose homeostasis. The mobilization of glucose from glycogen deposits in the liver provides a constant supply of glucose for tissues, such as the brain, which depend primarily on this sugar as an energy source. In the fasted state, the enzyme-catalyzed isomerization of glucose-1P released by phosphorolysis of glycogen, results in the production of glucose-6P. The liver expresses glucose-6-phosphatase, which converts glucose-6P to glucose that can enter the blood stream and supply other organs with a source of energy. Skeletal muscle lacks glucose-6-phosphatase and glucose released from glycogen is catabolized locally. The metabolism of glycogen in these tissues is linked hormonally to nutritional status by regulation of the enzymes that participate in both the synthesis and degradation of the polymer.

Insulin is the primary hormone responsible for promoting the conversion of glucose into glycogen in the muscle. In the diabetic state, impairment of insulin action is associated with defective muscle glycogen metabolism (1). Insulin stimulates glucose uptake in the muscle, leading to an increase in glucose-6P levels, which drives glycogen synthesis by allosterically activating glycogen

synthase. Insulin also triggers a signaling cascade in both muscle and liver involving phosphatidylinositol-3-kinase (PI3K). Binding of insulin to the extracellular α-subunit of the insulin receptor tyrosine kinase results in activation of tyrosine kinase activity. Autophosphorylation of a series of tyrosine residues in the intracellular β-subunit activates the kinase towards intracellular substrates, including the insulin receptor substrate-1 (IRS-1). Phosphorylation of IRS-1 by the insulin receptor signals to PI3K, which in turn phosphorylates the 3' position of phosphatidylinositol-4,5-bisphosphate producing phosphatidylinositol-3,4,5-bisphosphate. Recruitment of 3'-phosphatidylinositol dependent kinase 1 (PDK1) activates protein kinase B (PKB/AKT) which phosphorylates an N terminal serine of GSK3, inhibiting the enzyme. The phospho-serine occupies the region of the active site of GSK3 that would interact with the 'primed' phosphate groups in a target substrate (62). The inactivation of GSK3 prevents phosphorylation of sites 3a, 3b, 3c and 4 in glycogen synthase and activates the enzyme. Not all of the insulin control of glycogen synthase can be explained by the regulation of GSK-3, because insulin stimulation causes dephosphorylation of both the N and C terminal phosphorylation sites; GSK3 phosphorylates 3a, 3b, 3c and 4 all in the C terminus. The glycogen-associated phosphatases have been implicated in hormonal control of glycogen synthase activity. An obvious mechanism to explain the dephosphorylation of glycogen synthase in response to insulin stimulation would be activation of an insulin-stimulated glycogen synthase phosphatase. In muscle, it has been proposed that stimulation with insulin activates a PP1G containing the striated muscle specific glycogen targeting subunit R_{GL} (63) or PTG (57, 64). However, mice lacking the R_{GL} subunit are still capable of activating glycogen synthase in response to insulin (53), suggesting that another targeting subunit of PP1 may be involved in insulin stimulated dephosphorylation of glycogen synthase in muscle. An alternate proposal is the inactivation of cAMP dependent protein kinase, (PKA) by insulin-stimulated activation of cAMP phosphodiesterases which has been observed in adipocytes (65). In liver, a rise in blood glucose and the subsequent increase in plasma insulin levels promotes glycogenesis by allosteric mechanisms mediated by

glucose and phosphorylase *a*. Binding of glucose to an allosteric site on the phosphorylated form of glycogen phosphorylase causes a conformational change that makes phosphorylase a better substrate for PP1G/G_L and provides a mechanism for negative feedback control by glucose upon its own production by glycogen degradation (66). Furthermore, the glucose induced conversion of phosphorylase into its *b* form indirectly promotes dephosphorylation and activation of glycogen synthase. Phosphorylase *a* is an allosteric inhibitor of PP1G/G_L, and the transition of phosphorylase *a* to phosphorylase *b* relieves the inhibition on PP1G/G_L resulting in dephosphorylation and activation of glycogen synthase (66).

3.2 Epinephrine and glucagon regulation of glycogen metabolism

In contrast to insulin, epinephrine promotes glycogenolysis in muscle, and glucagon is the main hormone inducing glycogen degradation in the liver. Acting through β-adrenergic receptors, epinephrine initiates a signaling cascade that activates adenyl cyclase catalyzing the conversion of ATP to cAMP. cAMP activates PKA by binding the regulatory subunit and releasing the active catalytic subunit to phosphorylate target substrates. Phosphorylation of the α and β subunits of phosphorylase kinase by PKA in response to epinephrine relieves the inhibitory effects of these subunits on the catalytic subunit. Active phosphorylase kinase phosphorylates glycogen phosphorylase at Ser^{14} shifting the equilibrium from the less active T state to the more active R state, thus promoting glycogenolysis. Inhibition of glycogen synthesis is mediated by PKA dependent phosphorylation of glycogen synthase at sites 2, 1a and 1b (1), as well as phosphorylase kinase dependent phosphorylation of site 2. It has been proposed that epinephrine signalling through PKA decreases the activity of PP1G by PKA dependent phosphorylation of R_{GL}, leading to dissociation of the catalytic subunit PP1c (67). PKA also phosphorylates the PP1 inhibitory protein, inhibitor-1 in response to epinephrine stimulation (68). In the liver, glucagon activates liver adenyl cyclase, which increases cAMP levels and stimulates PKA dependent phosphorylation and inactivation of glycogen synthase.

Phosphorylation of phosphorylase kinase by PKA results in phosphorylation and activation of phosphorylase. In addition to degrading glycogen, activated phosphorylase (phosphorylase *a*) prevents glycogen synthesis by binding G_L and altering its glycogen synthase phosphatase activity, thereby inhibiting glycogen synthase activity (56, 69).

4. Glycogen Storage Diseases

4.1 Preamble

The overall importance of glycogen is illustrated by the physiological effects of deficiencies in the enzymes involved in its metabolism (Figure 8). Glycogen storage diseases are inherited metabolic disorders of glycogen metabolism affecting either the synthesis or degradation of the polysaccharide. These disorders result in a polysaccharide that is altered either in quantity and/or quality.

4.2 Glycogen storage disease type 0

Glycogen storage disease type 0 (GSD0) is a rare autosomal recessive form of fasting hypoglycemia that presents in infancy. GSD0 is caused by mutations in the *GYS2* gene, which encodes the liver isoform of glycogen synthase and results in an almost complete loss of liver glycogen. Patients have high blood ketones, low alanine and lactate concentrations and postprandial hyperglycemia, hyperlactatemia and hyperlipidemia (70). Mice lacking the *Gys2* gene have a 95% reduction in liver glycogen content, develop mild hypoglycemia, with an elevated rate of basal gluconeogenesis and an impairment in insulin suppression of endogenous glucose production (71). Recently, a mutation in the *GYS1* gene was described that resulted in sudden cardiac death of an 8 year old patient after collapsing during a bout of exercise (72). Similarly, approximately 90% of *Gys1* null mice died soon after birth due to impaired cardiac function (73).

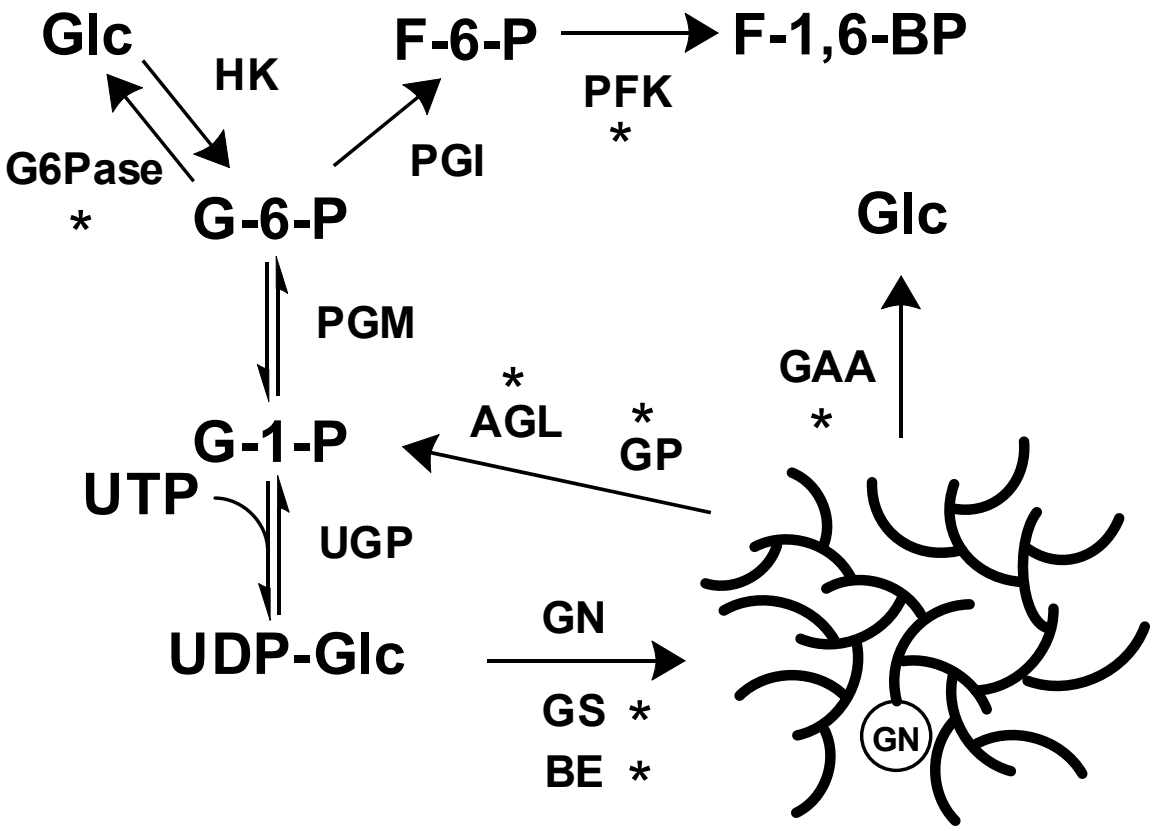

Figure 8. Glycogen metabolism. The asterisks indicate enzymes implicated in glycogen storage disorders. HK, hexokinase/glucokinase; PGM, phosphoglucomutase; UGP, UDP-glucose pyrophosphorylase; GN, glycogenin; GS, glycogen synthase; BE, branching enzyme; GP, glycogen phosphorylase; AGL, debranching enzyme; GAA, lysosomal acid α-glucosidase; G6Pase, glucose-6-phosphatase; PGI, phosphoglucose isomerase; PFK, phosphofructokinase.

4.3 Glycogen storage disease type I: von Gierke's disease

Glycogen storage disease type I (GSDI) or von Gierke's disease is characterized by the accumulation of glycogen and fat in the liver and kidneys, resulting in hypoglycemic seizures, hepatomegaly, growth retardation and life-threatening lactic acidosis (74). GSD1 is caused by mutations in the *G6PC* and *G6PT* genes and is the most common type of glycogenosis. *G6PC* and *G6PT* encode glucose-6-phosphatase and glucose-6P translocase (G6PT) respectively. Glucose-6-phosphatase hydrolyzes phosphate from glucose-6-P, a product of glycogenolysis or gluconeogenesis, to allow mobilization of glucose from the liver to the blood stream in the fasting state. Similarly, loss of the G6PT results in the same phenotype (75). In the terminal steps of gluconeogenesis and glycogenolysis, cytoplasmic glucose-6P is translocated into the lumen of the endoplasmic reticulum by G6PT, where glucose-6-phosphatase resides (75). The inability to dephosphorylate glucose-6P results in severe hypoglycemia with a concomitant increase in the intracellular glucose-6P concentrations driving excessive glycogen accumulation (76).

4.4 Glycogen storage disease type II: Pompe's disease

Glycogen storage disease type II or Pompe's disease is an autosomal recessive disorder caused by a deficiency in the lysosomal acid-α-glucosidase. Pompe's patients have mutations in the *GAA* gene, resulting in the most devastating form of the glycogen storage disorders (77). Pompe's patients overeraccumulate glycogen in the lysosomes of the heart and skeletal muscle leading to death usually within a year after birth (78). Acid-α-glucosidase is restricted to glycogen catabolism in the lysosomes and does not appear to play a role in the cytosolic degradation of the polysaccharide. The phenotype of the *gaa-/-* mice resembles the human disease closely, with the exception that pathological symptoms develop late relative to the onset of the human disease (79). Crossing *Gaa-/-* mice with a transgenic mouse overexpressing a hyperactivated form of glycogen synthase accelerated the course of the disease and resulted in the formation of abnormally structured polyglucosan, reminiscent

of that observed in patients with Lafora disease, glycogenosis type IV, and glycogenosis type VII (80). Douillard-Guilloux et al. (81) generated a *Gaa/Gys1* double knockout mouse model that exhibited a profound reduction in the amount of heart and skeletal muscle glycogen, a significant decrease in lysosomal swelling and autophagic build-up as well as a complete correction of cardiomegaly. These data suggest that long-term elimination of muscle glycogen synthesis may lead to a significant improvement of the structural, metabolic and functional defects in patients with Pompe's disease.

4.5 Glycogen storage disease type III: Cori's disease

Glycogen storage disease type III or Cori's disease is an autosomal recessive disorder caused by mutations in the *AGL/DBE* gene leading to defects in the glycogen debranching enzyme, AGL (82). Symptoms usually present during infancy with hypoglycemia and failure to thrive (82). Since the removal of branch points is required for complete phosphorolysis by phosphorylase, patients accumulate glycogen with very short outer chains.

4.6 Glycogen storage disease type IV: Andersen's disease

Glycogen storage disease type IV or Andersen's disease is one of the most severe of the glycogen storage disorders. It is caused by mutations in the *GBE1 gene,* whose protein product is the branching enzyme (83). Patients present with hepatosplenomegaly, failure to thrive, and progressive liver cirrhosis, and the severity of the disease is related to the degree of accumulation of polyglucosan (84). The polyglucosan in Andersen's patients has long stretches of unbranched chains resulting in a loss of solubility of the polysasccharide, eventually leading to cellular dysfunction and degeneration.

4.7 Glycogen storage disease type V: McArdle's disease

Glycogen storage disease type V or McArdle's disease is caused by mutations in the *PYGM* gene encoding the muscle form of glycogen phosphorylase. Symptoms are surprisingly mild and begin in young adulthood

with exercise intolerance and muscle cramps due to the inability to breakdown glycogen and use the released glucose as fuel (85).

4.8 Glycogen storage disease type VI: Hers' disease

Glycogen storage disease type VI or Hers' disease is caused by mutations in the *PYGL* gene which encodes the liver isoform of glycogen phosphorylase. Patients experience mild hypoglycemia, hepatomegaly and growth retardation (86).

4.9 Glycogen storage disease type VII: Tarui's disease

Glycogen storage disease type VII or Tarui's disease is caused by mutations in the *PFKM* gene, encoding the muscle form of phosphofructokinase. Phosphofructokinase catalyzes a rate limiting step in glycolysis by phosphorylating fructose-6P to fructose-1,6-bisphosphate. Loss of function mutations in *PFKM* causes a a build up of glycolytic intermediates which are thought to drive excessive glycogen synthesis through elevation of the allosteric activator of glycogen synthase, glucose-6-P (87).

5. Lafora Disease

5.1 Etiology

Lafora Disease (LD) is an autosomal recessive neurodegenerative disorder that falls into the category of progressive myoclonus epilepsies with onset typically in the teenage years followed by death within ten years (88, 89). Although not thought of as a classical example of a glycogen storage disorder, characteristic to all Lafora patients is the presence of periodic acid-Schiff (PAS) positive staining intracellular inclusion bodies that are composed of poorly branched, insoluble glycogen-like polymers known as Lafora bodies (Figure 9). The detection of Lafora bodies in biopsies from the sweat glands in the arm pit is used diagnostically. Lafora bodies are most commonly found in organs with the highest rate of glucose metabolism, including the brain, skeletal muscle, heart

and liver. Lafora patients experience symptoms starting in early adolescence as stimulus sensitive grand mal tonic-clonic, absence, visual and myoclonic seizures. Rapid progressive dementia ensues with psychosis, cerebellar ataxia, dysarthria, amaurosis, mutism, muscle wasting and respiratory failure leading to death within ten years of first symptom (90). Lafora disease is relatively rare in the outbred populations of the United States, Canada, China and Japan, and it most commonly found in parts of the world where a high rate of consanguinity is practiced. This would include ethnic isolates in the United States, Canada, Spain, France and Italy, and in isolated regions of Asia, India, Pakistan, Africa, and in the Middle East (91). To date no preventative or curative treatment is available. Mutations in two genes, Epilepsy progressive myoclonus type 2A (*EPM2A*) and Epilepsy progressive myoclonus type 2B (*EPM2B*), account for approximately 90% of Lafora cases (89, 91). The remaining cases could result from mutations in a third, yet to be identified gene, or could be mutations in promoter or enhancer regions of the two known genes (92). The *EPM2A* gene is composed of 4 exons encoding, by sequence similarity, a dual specificity protein phosphatase termed laforin (Figure 10A). Laforin also contains an N terminal carbohydrate binding domain that binds tightly to glycogen. The second gene, *EPM2B* (*NHLRC1*), encodes malin, an E3 ubiquitin ligase, containing an N terminal RING finger domain, common to all E3 ubiquitin ligases, followed by 6 NHL domains thought to be involved in protein-protein interactions (93) (Figure 10B). Most recent Lafora research has focused on understanding the functions of laforin and malin, and their relationship to the development of the disease.

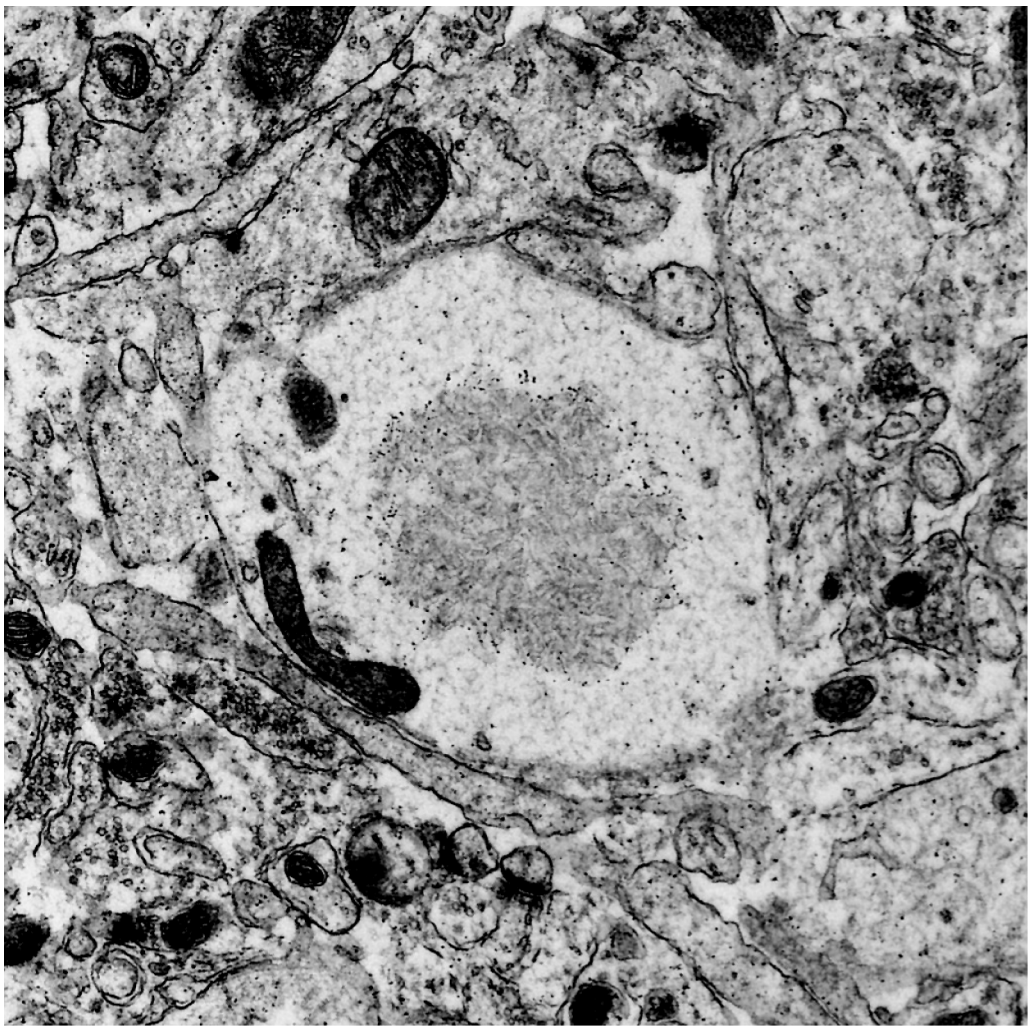

Figure 9. Lafora bodies. An electron micrograph depicting a Lafora body in a neuropil of an *Epm2a-/-* mouse. Courtesy of Cameron Ackerley, The Hospital for Sick Children, University of Toronto.

5.2 Mouse models of Lafora disease

Three mouse models of Lafora disease have been developed (94-96). Disruption of the mouse *Epm2a* gene resulted in viable homozygous null mice that had many, but not all, the features of the human disease (94). Neuronal degeneration was observed at two months, when relatively few Lafora bodies were present, followed by a much more robust accumulation of the polyglucosan after 4 months. The second mouse model utilized transgenic over-expression of a dominant negative form of laforin generated by mutating the catalytic Cys266 to Ser inactivating the phosphatase activity of the enzyme and driving expression under the control of the chicken β-actin promoter (95). The mutant human laforin was overexpressed in skeletal muscle to a level of 150 times that of the endogenous protein (97). The mice developed Lafora bodies in muscle, liver and neurons and, by immunogold electron microscopy, laforin was shown to be in proximity of the polyglucosan deposits. Our laboratory has recently generated and initially characterized the malin knockout mouse. Disruption of the *Epm2b* gene resulted in viable animals with homozygotes produced at the expected frequency for Mendelian inheritance. The animals developed Lafora bodies at 3 months of age in brain, and to a lesser degree in skeletal muscle and heart (96) (see Results).

5.3 Laforin

Laforin was first identified by Minassian and colleagues using a positional cloning approach. They identified *EPM2A* on chromosome 6q24 that encodes laforin (98) (Figure 10A). Laforin is a ubiquitously expressed protein with highest expression level in skeletal muscle, liver, kidney, heart, and brain (99). Laforin contains the signature dual specificity phosphatase (DSP) motif HCXXGXXRS/T and can dephosphorylate phospho-serine/threonine and phospho-tyrosine as well as the generic phosphatase substrate *p*-nitrophenyl phosphate (*p*NPP) *in vitro* (100). Additionally, laforin contains a highly conserved carbohydrate binding domain (CBM20) that can bind complex carbohydrates including glycogen, amylopectin and polyglucosan (95, 101). Laforin is conserved in all vertebrates

and in a small, defined group of protists including *Toxoplasma gondii* (102) (Figure 11). Niittyla et al. (10) described a gene in plants called starch excess 4 (SEX4) whose protein product contains an N terminal DSP and a C terminal CBM, the same domains as laforin but in the opposite orientation. SEX4 has a well established role as a starch phosphatase that hydrolyzes C3 and C6 phosphate from amylopectin (11) and genetic depletion of SEX4 in *Arabidopsis* results in the accumulation of insoluble polysaccharide (10). Furthermore, laforin complements the SEX4 phenotype in *Arabidopsis* providing evidence that laforin and SEX4 are functional equivalents (102). In mammals, laforin has been proposed to bind many proteins involved in glycogen metabolism including glycogen synthase, GSK3, PTG and malin (90, 103-105). Two other proteins HIRIP5, a cytosolic protein involved in iron metabolism and *Epm2a* interacting protein 1 (106), a protein with unknown function, have also been reported to interact with laforin. Fifty six mutations in the *EPM2A* gene have been found and the large majority of these mutations affect either the polysaccharide binding and/or the dual specificity phosphatase activities of laforin (The Lafora

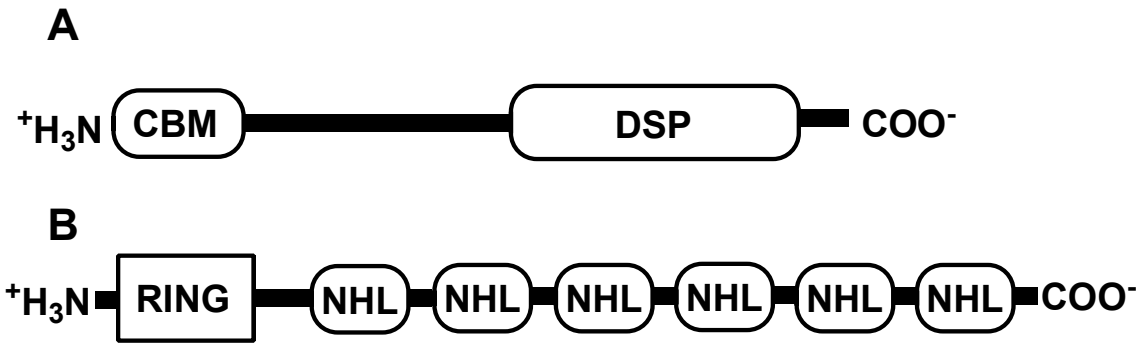

Figure 10. Lafora disease proteins, laforin and malin. A. Schematic of laforin depicting its N terminal carbohydrate binding module (CBM) and its C terminal dual specificity phosphatase domain (DSP). **B.** Schematic of malin depicting its N terminal RING finger domain followed by 6 NHL domains.

Progressive Myoclonus Epilepsy Mutation and Polymorphism Database, http://projects.tcag.ca/lafora/). One mutation was also described that had no effect on phosphatase and polysaccharide binding activity but did affect interaction with PTG (103). Laforin is very sensitive to inhibition by polysaccharides, when assayed using the generic phosphatase substrate *p*-nitrophenyl phosphate (*p*NPP) (107). One disease mutation, W32G (91), is located in the conserved carbohydrate binding domain and, when transferred to recombinant laforin, eliminates glycogen binding by laforin without completely abolishing *p*NPPase activity (101, 107). Thus impaired glycogen binding by laforin may be sufficient to cause disease. Another link between laforin and glycogen comes from the observation that the laforin protein levels correlate with the amount of glycogen in a series of mouse models in which the muscle glycogen content was genetically manipulated (108).

A prominent hypothesis in Lafora research has been that the polyglucosan might result from an imbalance between the activities of glycogen synthase and branching enzyme. There is precedent for this proposal. Andersen's disease, caused by mutations in the branching enzyme gene, leads to the accumulation of polyglucosan (109). A somewhat similar situation exists in glycogen storage disorder type VII, Tarui's disease, in which mutation of the phosphofructokinase gene causes a build up of glycolytic intermediates which are thought to drive excessive glycogen synthesis through elevation of the allosteric activator of glycogen synthase, glucose-6-P (87). In addition, our laboratory previously observed that a mouse in which hyperactive glycogen synthase is overexpressed in muscle overaccumulated glycogen and developed structures reminiscent of Lafora bodies (80, 110). Therefore, several groups have looked for ways by which laforin could affect glycogen synthesizing enzymes. Glycogen synthase is inactivated through phosphorylation by the protein kinase GSK-3 which itself contains an inhibitory phosphorylation site (111). Two groups have proposed that the inhibitory phosphate of GSK-3 can be removed by laforin (104, 112), thus potentially leading to activation of glycogen synthase to cause the biosynthetic imbalance. Lohi et al. (104) suggested that laforin's role is to detect

polyglucosan appearance during glycogen synthesis and to initiate mechanisms to down-regulate glycogen synthase. They reported that laforin is capable of dephosphorylating glycogen synthase kinase 3β (GSK3β), thereby activating it to phosphorylate and inhibit glycogen synthase. Loss of function of laforin should result in a hyperphosphorylated GSK3β and a hyperactivated glycogen synthase. This would lead to an imbalance between glycogen synthase and the branching enzyme resulting in insufficient branching and the formation of polyglucosan. More recently, these same groups have reported that laforin is a regulator of the cellular response to energy deprivation and that it confers cancer resistance to 2-deoxyglucose induced apoptosis via dephosphorylation of GSK3β. However, several studies argue against GSK-3 being a laforin substrate (3, 7, 97, 113). Perhaps most important is the observation that the GSK3 phosphorylation state is unchanged in two different genetic mouse models of Lafora disease in which the *Epm2a* gene is either disrupted (3) or the dominant-negative laforin is over-expressed (97). Measurements of glycogen synthase and branching enzyme activities in these mice also argued against the "branching imbalance" hypothesis.

An emerging hypothesis in Lafora research was first introduced by Worby et al. (113), who showed that laforin was capable of dephosphorylating amylopectin, the major component of plant starch with similar chemistry to glycogen (α-1,4-glycosidic linkages with less frequent α-1,6-branch points). This hypothesis was further supported by Gentry et al. (102) who demonstrated that laforin was a functional equivalent to SEX4, the phosphatase responsible for removing phosphate from plant starch. Further insight was provided by our laboratory, demonstrating that laforin was able to dephosphorylate mammalian glycogen and more notably, *Epm2a*-/- mice contained elevated levels of glycogen phosphate, supporting the hypothesis that laforin is a physiological glycogen phosphatase (3) (see Results). It should also be noted that laforin activity to dephosphorylate glycogen was dependent not only on a functional dual specificity phosphatase domain but also a functional carbohydrate binding domain (3).

Figure 11. Sequence alignment of Laforin. Laforin is found in all vertebrates and a small subset of protists including *T. gondii*. The red, blue and green amino acids demonstrate 100%, 75% and 50% conservation across the shown species respectively. The CBM is highlighted in yellow and the DSP in grey. The catalytic HCXXGXXRS/T motif is in bold.

5.4 Malin

The *EPM2B* gene (also called *NHLRC1*) encodes malin, a 395 residue protein that contains an NH_2-terminal RING finger domain followed by six NHL domains (114). Fifty eight disease causing mutations in the *EPM2B* gene have been identified (The Lafora Progressive Myoclonus Epilepsy Mutation and Polymorphism Database, http://projects.tcag.ca/lafora/). The RING finger domain is characteristic of E3 ubiquitin ligases (115) and Gentry et al. (105) reported that malin interacts with laforin and catalyzes its polyubiquitination *in vitro* and in cultured cells. In cells, the result is proteosome-dependent degradation of laforin. Furthermore, Chan et al. (95) were unable to detect endogenous laforin in tissue from non-Lafora disease patients by using multiple polyclonal antibodies to laforin. However, they were able to detect endogenous laforin surrounding Lafora bodies in tissue from Lafora patients with malin mutations. Nevertheless, laforin protein levels correlate with glycogen in a series of mouse models in which the muscle glycogen content was genetically manipulated (108). Disruption of the *Gys1* gene in mice, which encodes the muscle isoform of glycogen synthase, and whose skeletal muscle is completely devoid of glycogen, have a 60% reduction in laforin protein levels. Overexpression of a hyperactive form of glycogen synthase results in a massive overaccumulation of glycogen and a subsequent 7-fold elevation in laforin protein levels (108). So it is unclear whether the increase in laforin protein levels in patients with malin mutations is a cause of over accumulation of glycogen, lack of laforin degradation due to malin mutations or a combination of both. Nonetheless, if the physiological function of malin is to mediate the destruction of laforin, then it is hard to reconcile with the fact that Lafora disease is caused by recessive mutations in either *EPM2A* or *EPM2B*. Based on the model of Gentry et al. (105), defective malin should up-regulate laforin.

Recent studies using cell culture overexpression systems have reported that several proteins involved in glycogen metabolism are substrates for malin, including glycogen synthase, PTG and AGL (116-118). Two independent laboratories have reported that co-expression of malin and laforin resulted in the

ubiquitination and proteosome-dependent degradation of the regulatory subunit of protein phosphatase 1, PTG (117, 118). They proposed that laforin, via its glycogen binding domain, could recruit malin to the glycogen particle to promote the degradation of PTG and glycogen synthase thereby inhibiting glycogen synthesis. They also suggest that neurons contain the enzymatic machinery capable of synthesizing glycogen, yet do not do so because glycogen synthase is in an inactivated, hyperphosphorylated form (117). Loss of laforin or malin would inhibit malin-mediated degradation of PTG and glycogen synthase, driving excessive glycogen accumulation by dephosphorylation of glycogen synthase. Interestingly, co-expression of the catalytically inactive form of laforin had the same effect on the degradation of PTG. It is hard to envision control of PTG as a key event in the formation of Lafora bodies since patients with mutations in laforin that abolish phosphatase activity still develop Lafora bodies and the neurological sequalae, unless the phosphatase domain is required for an independent but interrelated function. Another proposal for the formation of Lafora bodies comes from work in cell culture overexpression systems with the identification of the glycogen debranching enzyme (AGL) as a substrate for malin-mediated ubiquitination and proteosome-dependent degradation (119). This ubiquitination event, unlike the ones discussed above, was independent of laforin. The authors proposed that mutations in malin would prevent the ubiquitination and proteosome-dependent degradation of AGL resulting in increased AGL protein promoting the removal of α-1,6-glycosidic linkages and resulting in polyglucosan formation. However, based on the two stage degradation of glycogen by phosphorylase and debranching enzyme, excessive AGL activity should only reduce branching frequency if phosphorylase, normally an abundant enzyme, becomes limiting. Solaz-Fuster et al. (116) have proposed that AMPK phosphorylates laforin, controls its association with malin and thereby regulates laforin and malin targets. AMPK was also reported to phosphorylate the PTG protein phosphatase subunit and target it for degradation by the malin-laforin complex (120). Other studies have suggested that laforin and malin are recruited to aggresomes upon proteosomal inhibition (121). The authors

proposed that the centrosomal accumulation of malin and laforin enhances the ubiquitination of malin substrates, facilitating their efficient degradation by the proteosome. (121). Furthermore, laforin and malin were shown to form a functional complex with HSP70 to suppress the cellular toxicity of misfolded proteins by promoting their degradation through the unfolded protein response (122).

Our laboratory has recently generated the malin knockout mouse (*Epm2b-/-*) and analyses of these mice have refuted many of the proposed mechanisms of action of malin (96) (see Results).

6. Glycogen in the Brain

6.1 Location

Although Lafora bodies are present in many tissues, their formation in neurons likely contributes to the neurological deterioration and subsequent death in patients with Lafora disease (123, 124). The brain contains low levels of glycogen relative to muscle and liver. In mice for example, brain glycogen concentrations are about 5-10 times lower than muscle and ~100 times lower than liver. It is thought that brain glycogen is almost exclusively produced in astrocytes in the adult animal, whereas in the embryo, glycogen is produced in both neurons and glial cells, but as animals age neuronal glycogen disappears and polysaccharide synthesis is predominantly restricted to astrocytes, a subtype of glial cells (125, 126). Electron microscopy studies of glycogen granules suggests that the polysaccharide is not uniformly distributed throughout the brain but concentrated in areas with the greatest synaptic density (127), suggesting a role for glycogen in the energy-dependent process of synaptic transmission. However, white matter, which is devoid of synapses has also been reported to contain significant amounts of glycogen (128).

Since Lafora bodies are primarily composed of glycogen, how is it that Lafora patients accumulate the polymer in neurons if these cells do not synthesize glycogen? Most studies on the location of brain glycogen have been

performed with cultured tissue cells, conditions not always conducive for glycogen accumulation. Neurons in culture may not produce detectable levels of glycogen, but may still produce the polysaccharide *in vivo*. Furthermore, brain glycogen is rapidly depleted after the death of an animal (129), much more so than that of muscle and liver glycogen. Perhaps neurons do accumulate glycogen *in vivo*, but detection goes unnoticed due to the rapid degradation of the polymer post mortem. Neurons do express the muscle isoform of glycogen synthase which based on cell culture studies, has been proposed to be hyperphosphorylated and thus inactive (117). However, considering that glycogen synthase is activated allosterically by glucose-6P, which overcomes the inactivation by phosphorylation, it is not unreasonable to assume that neuronal glycogen synthase *in vivo* would have the capacity to synthesize glycogen.

6.2 Brain glycogen metabolism

Glycogen in astrocytes is thought to serve as an energy reserve for neighboring neurons. The degradation of glycogen by the brain isoform of glycogen phosphorylase produces glucose-1P which is isomerized to glucose-6P by PGM. The resulting glucose-6P is oxidized through glycolysis forming pyruvate, which is subsequently converted to lactate by lactate dehydrogenase (Figure 12). Several lines of evidence suggest that lactate exits the astrocytes and is then taken up by neurons to be used as a fuel. For example, neurons operate normally if lactate is substituted for glucose (130, 131) and during hypoglycemia, glycogen is rapidly degraded and appears mainly as extracellular lactate (132). Furthermore, astrocytes do not express glucose-6-phosphatase and therefore cannot make free glucose from glycogen phosphorolysis to be transported to neurons. Astrocytes do however, express lactate dehydrogenase and readily oxidize glucose-6P to lactate via glycolysis. Lactate is exported from astrocytes by the monocarboxylate transporter-1 (MCT1) (133, 134) and enters neurons via MCT2 where it is aerobically metabolized by oxidative phosphorylation (Figure 12).

The concentration of brain glycogen seems to be sensitive to brain glucose levels. In rats, an episode of hypoglycemia resulted in glycogenolysis but only after glucose levels in the brain had fallen to zero (135). These data imply that glycogen is rapidly metabolized in the brain when glucose transport becomes rate limiting and provides a significant source of energy during hypoglycemia. Moreover, re-establishment of euglycemia resulted in an increase in glycogen well above basal levels. This super-compensation phenomenon has been implicated as a possible mechanism for hypoglycemia unawareness (136). Further insight into the metabolic importance of brain glycogen was demonstrated by Suh et al. (137). Manipulation of brain glycogen levels by the glycogen phosphorylase inhibitor CP316819 resulted in an increase in brain glycogen levels that prevented the pathological effects of insulin-induced systemic hypoglycemia by delaying the onset of isoelectric encephalogram, a recognizable sign of transmembrane ion gradient failure. The glycogen stores preserved brain function for up to 90 minutes during an episode of severe hypoglycemia.

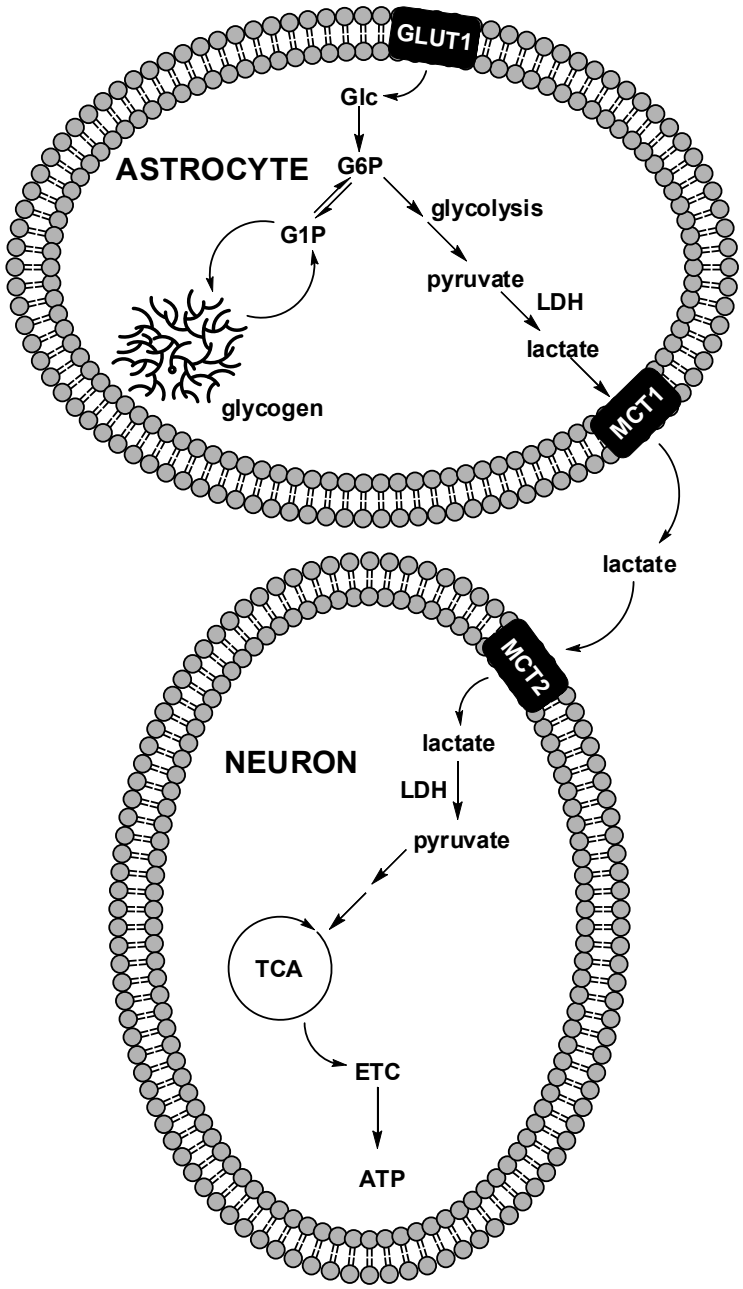

Figure 12. Brain glycogen metabolism. Glycogen is synthesized and stored in astrocytes. The degradation of glycogen by phosphorylase produces glucose-1P which is isomerized to glucose-6P by PGM. The resulting glucose-6P is oxidized through glycolysis forming pyruvate, which is subsequently converted to lactate by lactate dehydrogenase (LDH). The lactate is exported from the astrocytes by the monocarboxylate transporter-1 (MCT1) and taken up by the neuron via monocarboxylate transporter-2 (MCT2). The neuronal lactate is further oxidized by the tricarboxylic acid cycle (TCA) and the electron transport chain (ETC) producing ATP to fuel the neuron.

RESEARCH OBJECTIVE

Since the discovery that mutations in the *EPM2A* and *EPM2B* genes caused Lafora disease, most Lafora research has focused on understanding the functions of these two proteins, and their relationship to the development of Lafora bodies. When I started my studies, the majority of work had focused on ways in which laforin and malin might down-regulate glycogen synthesis, with the hypothesis that a biosynthetic imbalance between glycogen synthase and the branching enzyme leads to the formation of Lafora bodies. The search for protein substrates of laforin led to a proposal that it dephosphorylated the inhibitory N terminal phosphorylation site of GSK3 (104), a negative regulator of glycogen synthase. If laforin was a GSK3 phosphatase it would act as a negative regulator of glycogen synthesis, dephosphorylating GSK3, which in turn would phosphorylate and inhibit glycogen synthase. So in patients with *EPM2A* mutations, GSK3 would remain phosphorylated and inactivated, resulting in activation of glycogen synthase. Work from a previous graduate student in our laboratory found no changes in the phosphorylation status of GSK3 in two mouse models of Lafora disease (138) and furthermore found no differences in the activity of glycogen synthase and the branching enzyme in these mice, providing strong evidence that laforin was not a GSK3 phosphatase. These negative results prompted us to begin looking for other laforin substrates when a report from the Dixon laboratory (113) demonstrated that laforin was capable of dephosphorylating amylopectin. This group was unable to detect activity towards rabbit liver glycogen however (113). Earlier reports from the 1990's by Whelan and colleagues had demonstrated that rabbit liver glycogen contains significantly less phosphate than muscle glycogen (5). My original goal was to determine if laforin was a physiological glycogen phosphatase and what role covalent phosphate plays in glycogen structure and metabolism. More specifically, how is phosphate incorporated into glycogen? Which hydroxyl in glucose is it attached to? Can excessive glycogen phosphate cause Lafora disease? Therefore, my

research objective was to understand how phosphate in glycogen is metabolized and the possible role it plays in the etiology of Lafora disease.

EXPERIMENTAL PROCEDURES

1. Purification of rabbit skeletal muscle glycogen

Two male rabbits were sacrificed by injection with pentobarbital and decapitation. The back and hind limb muscles were immediately removed and placed on ice. The muscle was cut up into small pieces and homogenized in a Waring blender with 3 volumes of 4 mM EDTA pH 7.8. The homogenate was centrifuged at 9,000 x g for 45 minutes. The supernatant was passed through Miracloth to remove the floating fat and 100% trichloracetic acid (TCA) added to a final concentration of 10%. The solution was cleared by centrifugation at 9,000 x g and 1 volume of -80^{o}C 100% ethanol was added to the supernatant to precipitate the glycogen. The glycogen was collected by centrifugation at 8,000 x g for 45 minutes and resuspended in ~80mL of water purified by reverse osmosis (H_2O). Nonpolar contaminants were extracted twice with an equal volume of chloroform:octanol (3:1). To the aqueous phase was added 1 volume of ethanol and the glycogen was allowed to precipitate overnight at -20^{o}C. The glycogen was again collected by centrifugation at 12,000 x g for 30 minutes and resuspended in 45 mL of 1% sodium dodecyl sulfate (SDS). After high speed centrifugation at 196,000 x g for 2 hours, the glycogen pellet was resuspended in H_2O and placed in an ice bath for 1 hour to precipitate the SDS that had come out of solution and pelleted during the high speed centrifugation. After centrifugation to remove SDS, the glycogen was precipitated with 2 volumes of 100% ethanol, collected by centrifugation at 12,000 x g and again resuspended in H_2O at which time it was dialyzed against 2 changes of 3 L H_2O. The glycogen was precipitated with 1 volume of 100% ethanol, collected by centrifugation and washed with 100% ethanol. After evaporation of residual ethanol at room temperature for several days, the glycogen, (yield ~3.5 g) was stored at -20^{o}C until use.

2. Preparation of the Malachite green reagent

The Malachite green reagent was prepared essentially as described in (139). All solutions were made in polypropylene conical screw cap tubes as used glassware had contaminating phosphate. Briefly, 13.5 mg of Malachite green oxalate was dissolved in 30 mL of H_2O. Ten mL of a 4.2% (w/v) ammonium molybdate in 4 M HCl was added and the solution incubated at 4^oC on a nutator for a minimum of 45 minutes. Immediately before use, the solution was filtered through a 22 μm filter and Tween 20 added to a final concentration of 0.01%.

3. Laforin phosphatase activity assays

Recombinant His-tagged laforin was expressed in *Escherichia Coli* and purified by affinity chromatography using Ni-NTA agarose as described previously (107). To measure laforin phosphatase activity with amylopectin and/or rabbit skeletal muscle glycogen as substrate, a 100 μL reaction mix consisting of phosphatase buffer (100 mM sodium acetate, 50 mM bis-Tris, 50 mM Tris HCl, 2 mM DTT, pH 6.5), 25 μg/mL laforin and varying concentrations of polysaccharide substrate were incubated at 37^oC for the indicated time points. The reaction was terminated by the addition of 100 μL N-ethyl maleimide at which time 400 μL of Malachite green reagent was added. The samples were mixed and the OD at 620 nm recorded to assess inorganic phosphate levels by comparison to a standard curve generated using KH_2PO_4. The Malachite green reagent prepared under these conditions had a linear range from 0.5-7 nmoles KH_2PO_4.

Hydrolysis of *p*-nitrophenyl phosphate (*p*NPP) was performed in a 100 μL reaction volume containing 1X phosphatase buffer with 25 μg/mL recombinant laforin and varying amounts of *p*NPP. The reaction was terminated by the addition of 400 μL of 0.25 M NaOH and the absorbance was read at 410 nm. Activity was measured taking the extinction coefficient of *p*-nitrophenolate to be 18.3 $mM^{-1}cm^{-1}$.

4. Purification of mouse skeletal muscle and liver glycogen for covalent phosphate determination

Frozen mouse muscle (minimum 500-600 mg) or liver (minimum 150 mg, for fed animals) was pulverized under liquid nitrogen and hydrolyzed in 10 volumes (w/v) of 30% KOH at 100°C for 1 hour in a sterile 15 mL polypropylene conical screw cap tube. The solution was cooled, centrifuged at 10,000 x g for 10 minutes, the supernatant passed through Miracloth to remove the floating fat and collected in a 15 mL polypropylene conical tube. The filtrate was precipitated with 2 volumes of -20°C 100% ethanol with addition of approximately 25 μL of 1 M LiCl and allowed to stand at -20°C overnight. The glycogen was recovered by centrifugation at 10,000 x g for 30 minutes, redissolved in 500 μL of H_2O (occasionally with heat), transferred to an Eppendorf tube and centrifuged at 17,500 x g at 4°C on a table top centrifuge to remove insoluble material. The supernatant was transferred to a clean Eppendorf tube, precipitated with 2 volumes of -20°C 100% ethanol and LiCl added after the ethanol to a final concentration of 6.7 mM (10 μL of 1M LiCl). The glycogen was allowed to precipitate at -20°C for a minimum of 1 hour, recovered by centrifugation at 17,500 x g for 20 minutes and resuspended in 100 μL of H_2O (occasionally with heat). Ten volumes of a 4:1 methanol:chloroform solution were added and the solution heated at 80°C for 5 minutes. The methanol:chloroform solution was prepared in an extensively water-washed glass beaker using clean glass pipettes. After cooling, the precipitated glycogen was recovered by centrifugation at 17,500 x g for 20 minutes. For liver glycogen, the pellet was resuspended in 100 μL of H_2O and the methanol:chloroform extraction repeated. The glycogen pellet was dried in a Speed Vac and resuspended in 500 μL of H_2O and precipitated again with 2 volumes -20°C 100% ethanol and 6.7 mM LiCl, and allowed to precipitate at -20°C for a minimum of 1 hour. The glycogen was again collected by centrifugation at 17,500 x g for 20 minutes and redissolved in 400 μL of H_2O. To ensure that all the glycogen was resuspended, the sample was placed in a boiling water bath for 5 minutes, cooled and 100 μL of 50% TCA was added (final concentration of 10%). The solution was centrifuged at 17,500 x g for 20 minutes,

the supernatant transferred to a new clean Eppendorf tube and precipitated with 2 volumes of -20°C 100% ethanol. The glycogen was allowed to precipitate for a minimum of 1 hour at -20°C and collected again by centrifugation at 17,500 x g for 20 min at 4°C. The glycogen pellet was dried in a speed vac and resuspended in 500 μL of H_2O and dialyzed using Spectra/Por®Dialysis Membrane (MWCO: 12-14,000Da, Vol/length: 0.32 mL/cm) overnight against 4 L of H_2O with constant stirring. The glycogen was transferred from the dialysis tubing to a clean Eppendorf tube, precipitated with 2 volumes of -20°C 100% ethanol and allowed to stand at -20°C for a minimum of 1 hour. Occasionally LiCl was omitted from this step in order to assess glycogen solubility in the absence of chaotropic salts. However, after some time 10 μL of 1 M LiCl was added and the glycogen was allowed to stand at -20°C for an additional 1 hour. After collection by centrifugation at 17,500 x g for 20 minutes, the glycogen was dried in a Speed Vac until the pellet became dislodged from the side of the Eppendorf tube. The pellet was transferred into a tared, clean Eppendorf tube and the mass recorded. The glycogen was redissolved to 5 mg/mL for skeletal muscle and 10 mg/mL for liver with H_2O. An aliquot was used to measure glucose equivalents after digestion with α-amylase and amyloglucosidase (see below). Glycogen phosphate was measured according to the protocol of Hess and Derr (140). For skeletal muscle glycogen, 250-400 μg and for liver glycogen, 750-1,000 μg was dried in a speed vac and hydrolyzed with 10 μL of 10N HCl and 30 μL of 60% perchloric acid at 190°C for 2 hours in clean borosilicate glass tubes (VWR). After hydrolysis, 100 μL of H_2O was added followed by 400 μL of the Malachite green reagent. The solution was transferred with a clean Pasteur pipette into a 1 mL disposable cuvette and the OD 620 nm recorded and compared to a standard curves using glucose-6P subjected to the same hydrolysis conditions and KH_2PO_4. Under these conditions the standard curve was linear in the range of 0.5-7 nmoles KH_2PO_4 or glucose-6P. By this procedure, lipids were removed by the methanol:chloroform extraction. Proteins and nucleic acids were absent as determined by the Bradford protein determination assay (141) and by A260 absorbance, respectively. The recovery

of glycogen was ~75-80% of that obtained by the KOH protocol (see Experimental Procedures Section 9) used for the isolation and determination of glycogen from mouse skeletal muscle (53).

5. Preparation of mouse tissue samples for Western blot analysis

Animals were sacrificed by cervical dislocation and the heads immediately decapitated into liquid nitrogen. The hind limb skeletal muscle and liver was immediately excised and frozen in liquid nitrogen. The frozen tissues were stored at -80^{o}C for later use. Tissues were pulverized under liquid nitrogen and stored at -80^{o}C until use. Brains were dissected from the frozen heads under liquid nitrogen, powdered as above and stored at -80^{o}C until use. Frozen tissue samples (30-100 mg) were homogenized in 10 volumes (w/v) of a buffer containing 50 mM Tris HCl, pH 7.8, 10 mM EDTA, 2 mM EGTA, 100 mM NaF, 2 mM benzamidine, 0.1 mM N$^{\alpha}$-p-tosyl-L-lysine chloromethyl ketone, 50 mM β-mercaptoethanol, 0.5 mM PMSF, 10 μg/ml leupeptin and 1 mM sodium orthovanadate) (0.1-0.2% Triton X-100 was included for brain samples) with a tissue Tearer at maximal speed for 20-30 sec. Muscle homogenates were centrifuged at 6,500-8,000 x g and brain homogenates at 8,000-10,000 x g for 10 minutes. The supernatant, denoted LSS (low speed supernatant), was used for Western blot analysis, measurement of enzyme activities and quantitation of glycogen (see below). The pellet denoted LSP (low speed pellet) was resuspended in the same or two thirds to half the original homogenization volume for skeletal muscle and brain, respectively. The resuspended LSP was used for Western analyses, measurement of enzyme activities, and quantitation of glycogen in parallel with the LSS. In some cases, the LSS was subjected to high speed centrifugation (100,000 x g for 90 minutes) to generate a glycogen pellet. The glycogen pellet was enriched, usually 5 fold compared to the high speed supernatant, and used for Western analyses.

6. Glycogen synthase and glycogen phosphorylase activity assays

Tissues were homogenized as above and the LSS and the LSP were used to measure glycogen synthase and glycogen phosphorylase activity. Glycogen synthase activity was measured by the incorporation of [U-^{14}C]-glucose into glycogen using UDP-[U-^{14}C]glucose as the glucosyl donor in the presence or absence of 7.2 mM glucose-6-P (142). A reaction mixture (60 μL) consisting of 50 mM Tris-HCl pH 7.8, 20 mM EDTA, 25 mM KF, 6.67 mM UDP-glucose, 10 mg/mL treated rabbit liver glycogen (Type III) (see Experimental Procedures Section 7), -/+ 10.9 mM glucose-6P pH 7.6-7.8 and UDP-[U-^{14}C]glucose for a specific activity of ~1100 cpm/nmol (usually ~15 μCi in 12 mL) was preheated for 5 minutes at 30^{o}C. Thirty μL of either the LSS or the LSP appropriately diluted (see below) was added and the reaction mix incubated at 30^{o}C for various times depending on tissue and fraction. Typically for muscle, the LSS was diluted 1:4 in homogenization buffer and the LSP, which was resuspended in the original volume, was diluted 1:2. The reaction time was 15 minutes. For brain, the LSS was used undiluted and the LSP, resuspended in ½ the original volume, was also undiluted. The reaction time was 45 minutes. All reactions were stopped by spotting 75 μL onto 2 cm x 2 cm square 31ET filter paper and immediately immersed in -20^{o}C 66% ethanol under stirring. The filter papers were allowed to wash for ~10-15 minutes with stirring, at which time the ethanol was discarded and fresh RT, 66% ethanol added with stirring for an additional 1 hour. A third wash was performed for 15 minutes with fresh 66% ethanol and after removing the ethanol, the filter papers were washed with acetone for 5 minutes with stirring. The filter papers were dried under a heat lamp and placed in scintillation vials with 5 mL of Bio-Safe II scintillation cocktail and the radioactivity detected by scintillation counting.

Glycogen phosphorylase was measured by the incorporation of [U-^{14}C]-glucose into glycogen using [U-^{14}C]-glucose-1-phosphate as the glucosyl donor in the presence or absence of 2 mM AMP (46). A reaction mixture (60 μL) consisting of 200 mM KF, 100 mM glucose-1P, 10 mg/mL treated rabbit liver glycogen (Type III) , -/+ 3 mM AMP pH 6 and [U-^{14}C]-glucose-1-phosphate for a

specific activity of ~23 cpm/nmol (usually ~10 μCi in 12 ml) was preheated for 5 minutes at 30°C. The reaction mixture without AMP contained 0.15 mg/mL caffeine. Thirty μL of either the LSS or the LSP appropriately diluted (see below) was added and the reaction mixture incubated at 30°C for various times depending on tissue and fraction. Typically for muscle, the LSS was diluted 1:4 in homogenization and the LSP, which was resuspended in the original volume, was diluted 1:2. The reaction time was 6.5 minutes. For brain, the LSS was used undiluted and the LSP, resuspended in ½ the original volume, was also undiluted. The reaction time was 15 minutes. All reactions were stopped by spotting 75 μL onto 2 cm X 2 cm square 31ET filter paper and immediately immersed in -20°C 66% ethanol. Filters were washed as described for the glycogen synthase assay. Radioactivity incorporated into glycogen was quantified as for glycogen synthase activity using scintillation counting.

7. Preparation of treated glycogen

Rabbit liver glycogen, Type III (Sigma) was passed over a mixed bed ion exchange resin to remove contaminating ions. Ten grams of glycogen was dissolved in 100 mL of H_2O in a glass beaker with stirring. Aldrich mixed bed TMD-8 ion exchange resin (~200 mL bed volume) was washed with 500 mL of H_2O in a beaker three times with stirring for approximately 10 minutes each. The resin was packed into a column (4.3 cm X 50 cm), and washed with an additional 1 L of H_2O at a free flow rate. Immediately before applying the glycogen, the flow rate was adjusted to ~50 mL/hr., and the glycogen was collected in a beaker. The glycogen was precipitated by slowly adding 100% ethanol at -80°C to a final concentration of 66% with stirring. To facilitate the precipitation, 2 drops of 1M NaCl were added (~50 μL). The suspension was kept stirring in an ice bath for 15 minutes and then transferred to Beckmann centrifuge tubes pre-cooled to 4°C. The glycogen was centrifuged at 8,000 rpm for 20 minutes at 4°C using a JA.10 rotor. The pellet was washed twice with 100% ethanol, collected by centrifugation and allowed to dry in a mortar covered with parafilm with holes.

The dried glycogen was ground with a pestle, transferred to a 50 mL conical tube and stored at 4°C until use.

8. Western blot analysis

Samples prepared as above were diluted with 5X loading buffer to 1X and boiled for 5 minutes (5X loading buffer: 62.5 mM Tris-PO_4 pH 6.8, 50% (w/v) glycerol, 6.25% (w/v) SDS, 0.1% (w/v) bromphenol blue and 5% β-mercaptoethanol) and subjected to SDS polyacrylamide gel electrophoresis (SDS PAGE) using a 10% polyacrylamide gel. The gel was run at 200 V until the bromphenol blue reached the bottom of the gel. The proteins were transferred to nitrocellulose membranes overnight at 15 volts and stained with Ponceau S to assess loading. The membranes were blocked for 1 hour with 5% non-fat milk dissolved in filtered Tris-buffered saline containing Tween 20 (TBST, 10 mM Tris-HCl, 150 mM NaCl, 0.1% Tween 20 pH 8) and filtered through Miracloth immediately before use. The TBST was filtered through a bottle top, 0.22 μm, Stericup sterile filter (Millipore). The membranes were probed for a minimum of 1 hour at room temperature or a maximum of overnight at 4°C with various antibodies diluted appropriately in 2% milk dissolved in TBST and washed 3 X 5-10 minutes each with TBST before incubation with the secondary antibody. The secondary antibody was incubated with the membranes for 1 hour at room temperature followed by washing with TBST 3 times for 5-10 minutes each. Detection was by enhanced chemiluminescence and autoradiography. The levels of protein expression were quantitated by densitometric scanning of the autoradiogram using Quantity One software (BioRad). Anti-glycogen synthase, anti-glycogen synthase phospho-site 3a, anti phospho-GSK-3, anti-phospho- and nonphospho-AMPK, and anti-phospho-eIF2α were from Cell Signaling Technology, anti-laforin and anti-branching enzyme antibodies were from Abnova, anti-GSK-3 from Invitrogen Corporation, anti-GAPDH antibody was from Biodesign, anti-AGL antibody was from Abgent, anti-ubiquitin antibody was from Santa Cruz Biotechnology. Anti-glycogenin-1 (143) and anti R_{GL} (61) are as

previously described. Anti-PTG antibodies were a generous gift from Dr. Alan Saltiel (University of Michigan, Ann Arbor, MI).

9. Determination of glycogen concentration

Total glycogen in skeletal muscle, liver and brain was assayed by slight modifications of Suzuki et al. (53). For skeletal muscle and liver, approximately 30 mg of frozen powdered tissue was weighed in a 1.5 mL screw cap tube and hydrolyzed in 200 μL of 30% KOH for 1 hour, cooled on ice and precipitated with 2 volumes of 100% ethanol at -20°C. To aid the precipitation of glycogen, 67 μL of 2% Na_2SO_4 was added prior to the addition of the ethanol. After precipitating for 1 hour at -20°C, the glycogen was collected by centrifugation at 17500 x g, resuspended in 100 μL (200 μL for liver) of H_2O and precipitated again with 2 volumes of -20°C, 100% ethanol for a minimum of 1 hour at -20°C. This procedure was repeated once more (total of 3 ethanol precipitations) and the glycogen pellet dried in a Speed Vac and digested overnight in 100 μL of 0.2 mM sodium acetate pH 4.8 and 0.3 mg/mL amyloglucosidase. Glucose equivalents were determined by a coupled reaction involving the conversion of glucose to glucose-6P by hexokinase followed by the reduction of nicotinamide adenine dinucleotide phosphate ($NADP^+$), by glucose-6P dehydrogenase and recording the OD at 340 nm. Typically for muscle, the glycogen digest was diluted 1:2 and 10μL added to a 300 μL reaction mix consisting of 300 mM triethanolamine pH 7.6, 4 mM $MgCl_2$, 0.9 mM $NADP^+$, 2 mM ATP and 2 μg/mL glucose-6P dehydrogenase (Roche). The OD 340nm of an aliquot (100μL) was recorded and to the remaining reaction mix was added 1μL hexokinase (diluted with an equal volume of $(NH_4)_2SO_4$ to 750 units/mL) (Roche). The reaction was allowed to proceed for 25-30 minutes at room temperature and the OD 340nm recorded. For brain glycogen determination, 40-50 mg of frozen powdered tissue was weighed in 1.5 mL screw cap tubes and hydrolyzed in 300 μL of 30% KOH for 1 hour, cooled on ice and precipitated with 2 volumes of -20°C, 100% ethanol. To aid the precipitation of the glycogen, 100 μL of 2% Na_2SO_4 was added prior to

the addition of the ethanol. After precipitating for 1 hour at -20°C, the glycogen was collected by centrifugation and resuspended in 100 μL of H_2O. Ten volumes of a 4:1 methanol:chloroform solution was added and the lipids extracted by heating the resulting solution at 80°C for 5 minutes. After recovery of the precipitated glycogen by centrifugation at 17,500 x g for 20 minutes, the lipid extraction was repeated and the glycogen again recovered by centrifugation. The glycogen pellet was resuspended in 100 μL of H_2O and precipitated with 2 volumes -20°C 100% ethanol. After standing at -20°C for 1 hour, the glycogen was collected by centrifugation, dried in a speed vac, digested with amyloglucosidase and glucose equivalents quantitated as described above.

For glycogen determination of the LSS and the LSP, typically, for skeletal muscle ~200 μL of the LSS and 300 μL of the LSP (resuspended in the same volume as the original homogenization) was brought to 30% KOH and hydrolyzed for 1 hour at 100°C. Glycogen levels were determined as above with the exception that the final digestion volume with amyloglucosidase was 50 μL. Ten μL and 20 μL of the LSS and LSP respectively, were used to measure glucose equivalents. For brain homogenates, 200-300 μL of the LSS and no less than 400 μL of the LSP (resuspended in 2/3 the original homogenization volume) were used. Again, the glycogen was purified and quantitated as described above for total brain glycogen with the exception that the final amyloglucosidase digestion volume was 50 μL. Twenty μL of both the LSS and LSP was used to determine glucose equivalents.

10. Glycogen branching determination

The degree of branching of polysaccharides was analyzed by the protocol of Krisman (30) using mouse skeletal muscle glycogen purified for covalent phosphate determination (see Experimental Procedures Section 4). Briefly, 125 μL of an iodine-iodide solution containing 1.5 M KI and 100 mM I_2 was added to 32.5 mL of a saturated solution of $CaCl_2$ and mixed. Glycogen, 100 μL of ~0.5 mg/mL was added to 600 μL of the $CaCl_2$ solution containing the iodine-iodide

reagent and incubated for 7 minutes at room temperature, at which point the spectrum of the sample was recorded from 400-750 nm in a disposable plastic cuvette.

11. Electron microscopy

Purified glycogen (15-25 μg), whether from whole tissue or from the LSS and LSP was spotted on a Formvar coated grid and allowed to settle for 30-60 s, at which time a drop of NanoVan (Nanoprobes) was added and wicked off 30 seconds later. The glycogen was viewed with a Technia G12 Biotwin transmission electron microscope (FEI, Hillsboro, OR) equipped with an AMT CCD camera (Advanced Microscopy Techniques, Danvers, MA) at 80 kEV and 150,000 X magnification at the Indiana University Electron Microscopy Center. Particle diameters were measured, and a histogram was constructed depicting the size distribution of the particles for different age groups and genotypes.

12. Ethanol solubility assay

Purified skeletal muscle glycogen from 9 month old *Epm2a-/-* mice was subjected to treatment with wild type laforin or catalytically inactive C266S laforin (see Experimental Procedures Section 3). The reaction was terminated by boiling for 10 minutes in a H_2O bath, cooled, and the denatured protein removed by centrifugation. The supernatant was dialyzed overnight against H_2O, and the glycogen recovered by ethanol precipitation. This glycogen was also used for electron microscopy studies as described above.

13. Synthesis and purification of [β^{32}P]UDP-glucose, [β^{32}P]UDP-[2-deoxy]-glucose and [β^{32}P]UDP-[3-deoxy]-glucose

[β^{32}P]UDP-glucose, [β^{32}P]UDP-[2-deoxy]-glucose and [β^{32}P]UDP-[3-deoxy]-glucose were synthesized enzymatically and purified essentially as in (144, 145) (Figure 13). Briefly, 1-5 mCi of [γ-^{32}P]-ATP (3000 Ci/mmol) was dried under N_2 gas and resuspended in a reaction mixture containing 45 mM Tris-HCl, pH 7.5, 6 mM $MgCl_2$, 0.8 mM UTP, 0.9 mM DTT, 3 units of UDP-glucose

pyrophosphorylase (Sigma), 3 units of inorganic pyrophosphatase (Roche) and 6 units of phosphoglucomutase (Roche). The reaction was initiated by the addition of 5.6 units of hexokinase (Roche) and incubated at 30°C for 3-18 hours and then terminated by boiling in a H_2O bath for 10 minutes. For [β^{32}P]UDP-glucose synthesis, the reaction mixture contained 9 mM glucose and was terminated after 3-4 hours. For [β^{32}P]UDP-[2-deoxy]-glucose and [β^{32}P]UDP-[3-deoxy]-glucose synthesis, the reaction mixtures contained 20 mM 2-deoxy- glucose and 20mM 3-deoxy-glucose, respectively and were terminated after ~18 hours. The denatured protein was removed by centrifugation at 17,500 x g and the supernatant was added to 5 mg activated charcoal and vortexed vigorously for 2-3 minutes. After centrifugation 5000 x g for 1 minute, the pellet was washed 3 times with 1 mL ice cold H_2O, with vigorous vortexing for 30 sec and the [β^{32}P]UDP-glucose was eluted with 200 μL of a 50% (v/v) ethanol solution containing 0.16 M ammonium hydroxide by vigorously vortexing for 2-3 minutes and centrifugation at 5,000 x g for 1 minute. The eluent was dried in a Speed Vac and the [β^{32}P]UDP-glucose and derivatives were resuspended in 100-200 μL of H_2O, aliquoted and stored at -80°C until use.

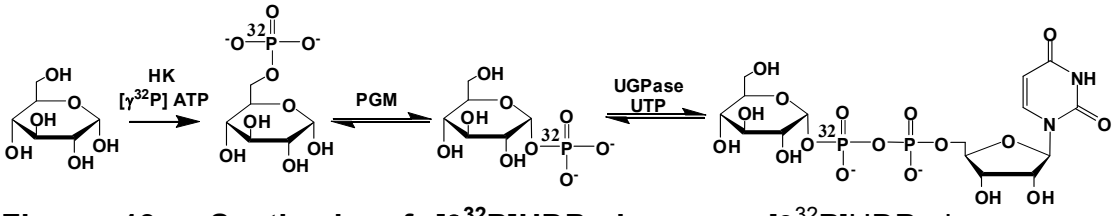

Figure 13. Synthesis of [β^{32}P]UDP-glucose. [β^{32}P]UDP-glucose was synthesized enzymatically starting with [γ-^{32}P]ATP. HK, hexokinase; ATP, adenosine triphosphate; PGM, phosphoglucomutase; UGP, UDP-glucose pyrophosphorylase; UTP, uridine triphosphate.

14. Thin layer chromatography

To asses purity of the radio isotopes, ascending thin layer chromatography was performed in a solvent consisting of n-propanol:ethyl acetate:H_2O (7:1:4) using high performance thin layer chromatography (HPTLC) silica gel plates (Alltech). The plates were allowed to dry at room temperature and radioactivity visualized by autoradiography.

15. Phosphorylation of glycogen by glycogen synthase

A reaction mixture consisting of 62.5 mM Tris-HCl pH 7.6, 8.3 mg/mL deionized rabbit liver glycogen, 9 mM glucose-6P, 6.25 mM EDTA and 1.25 μM [β^{32}P]UDP-glucose (50,000-100,000 cpm/pmol) or 1.25 μM UDP-[U-^{14}C]glucose, (500-2000 cpm/pmol) was preheated to 30^{o}C at which time partially purified D-form glycogen synthase from rabbit skeletal muscle or recombinant His-tagged yeast glycogen synthase was added to a final concentration of 1.0-1.2 μg/mL. The final concentration of the reaction components were 50 mM Tris-HCl pH 7.6, 6.7 mg/mL deionized rabbit liver glycogen, 7.2 mM glucose-6P, 5 mM EDTA and 1 μM [β^{32}P]UDP-glucose or 1 μM UDP-[U-^{14}C]glucose. The reaction mixture was incubated for the indicated time or, if not stated, 30 minutes, and terminated either by boiling in a 100^{o}C H_2O bath or by the addition of 2 volumes of 100% ethanol at -20^{o}C. Immediately before termination of the reaction, KH_2PO_4 was added to both the ^{14}C and ^{32}P reactions to a final concentration of 50 mM to reduce background ^{32}P. All reactions, whether stopped by boiling or ethanol precipitation, were placed at -20^{o}C for a minimum of 1 hr in 66% ethanol containing 5-15 mM LiCl to precipitate the radiolabeled glycogen. After boiling in a H_2O bath for 2 minutes, the glycogen was recovered by centrifugation at 17,500 x g for 20 minutes at 4^{o}C and dried in a Speed Vac. The glycogen pellet was redissolved in H_2O to a final concentration of 6.67 mg/mL and SDS loading buffer added to 1X. In most cases, the glycogen pellet was redissolved in H_2O to a final concentration of ~8.3 mg/ml, aliquoted and brought to 6.7 mg/mL by the addition of α-amylase and amyloglucosidase (final concentration of 300 μg/mL for each glucosidase and 20 mM NaOAc pH 4.8) or laforin (see Experimental

Procedures Section 17). The reaction was for a minimum of 1 hour at 37-40^{o}C, and was terminated by the addition of SDS loading buffer. After boiling, the glycogen (~200-250 μg) was subjected to SDS PAGE using 10 % gels (1.5 mm plate separation), the gels stained with Commassie blue, destained with 25% methanol containing 7% glacial acetic acid, dried with a gel dryer and the radioactivity detected using a phosphorimager.

16. Phosphorylation of glycogen using skeletal muscle extracts

Rabbit liver glycogen was phosphorylated using skeletal muscle extracts from WT and *Gys1-/-* mice (MGSKO) mice similarly to above with the exception that the source of the enzyme was muscle extract. Approximately 30 mg of mouse skeletal muscle was homogenized as above, and 20 μL of the LSS (~5 mg/mL) added to 80 μL of a reaction mixture containing 62.5 mM Tris-HCl pH 7.6, 8.3mg/mL deionized rabbit liver glycogen, 9 mM glucose-6P, 6.25 mM EDTA and 1.25 μM [β^{32}P]UDP-glucose (50,000-100,000cpm/pmol) or 1.25 μM UDP-[U-^{14}C]glucose (500-2000 cpm/pmol). The reaction was incubated at 30^{o}C for 30 minutes and the glycogen was purified, treated with or without glucosidases and visualized as above.

17. Dephosphorylation of ^{32}P-labeled glycogen with laforin

Phosphorylated glycogen (40 μL of an ~8.3 mg/mL solution) whether prepared with rabbit skeletal muscle glycogen synthase or recombinant yeast glycogen synthase was incubated with 50 μg/mL active WT laforin or catalytically inactive C266S laforin in phosphatase buffer in a final reaction volume of 50 μL for a minimum of 1.5 hrs at 37^{o}C. The reaction was terminated by the addition of SDS loading buffer and subjected to SDS PAGE and subsequent phosphorimaging to visualize the radiolabeled glycogen.

18. Purification of phosphorylated oligosaccharides from rabbit skeletal muscle glycogen

Approximately 240-250 mg (80-85 mg/mL) of rabbit skeletal muscle was digested overnight at 37-40^{o}C with 0.3 mg/mL amyloglucosidase and 0.3 mg/mL α-amylase containing 1 mM $CaCl_2$, and 10 mM sodium acetate pH 4.8 in a 3 mL reaction volume. After digestion, a precipitate formed which was inferred to be glycogenin, as it is a hydrophobic protein (146). Glycogenin was removed by centrifugation at 10,000 x g for 5 minutes at 4^{o}C and the digest was transferred to clean Eppendorf tubes and placed in a boiling H_2O bath for 10 minutes to denature the α-amylase and amyloglucosidase. After cooling, the protein was removed by centrifugation at 17,500 x g for 10 minutes at 4^{o}C and the cleared supernatant was added to 2 mL (bed volume) of DEAE sepharose resin and incubated overnight on a Nutator at 4^{o}C. Prior to addition of the supernatant, the DEAE sepharose resin was washed three times with 10 mL of 10 mM NaOAc pH=4.8 for 10 minutes on a Nutator at 4^{o}C. The resin was poured into a column and washed with 20 column volumes of H_2O. The anionic species were eluted stepwise (flow rate of ~0.5 mL/min) with 10 mM, 50 mM, 100 mM, 500 mM, and 1 M ammonium bicarbonate (NH_4HCO_3). Four mL of each concentration was used and 1 mL fractions were collected. An aliquot (40-60 μL) of each fraction was used to measure covalent phosphate (see Experimental Procedures Section 4). The remainder was dried in a Speed Vac and redissolved in ~500 μL H_2O, and dried further until there was no visible NH_4HCO_3. Typically this procedure was repeated 2-3 times to remove all the NH_4HCO_3. The fractions containing phosphate were dissolved in H_2O to a final concentration of 1 mM phosphate and stored at -20^{o}C until use.

19. Dephosphorylation of phosphorylated oligosaccharides purified from rabbit skeletal muscle glycogen

Phosphorylated oligosaccharides (10 μL of 1 mM phosphate) were treated with either WT laforin (25 μg/mL) or C266S laforin (25 μg/mL) in 25 mM sodium acetate pH 5.5 in a final reaction volume of 20 μL overnight at 37^{o}C to ensure

completion. A different buffer was chosen because the components in the phosphatase buffer described in Experimental Procedures Section 3 gave a strong signal on the HPAEC that eluted from the column around the same retention time as glucose. The reactions were terminated by boiling in a 100^{o}C H_2O bath for 10 minutes and the precipitated protein removed by centrifugation at 17,500 x g for 10 minutes at 4^{o}C, filtered using spin filters and the products analyzed as described below.

20. Analysis of purified phosphorylated oligosaccharides by high performance thin layer chromatography (HPTLC)

Phosphorylated and dephosphorylated oligosaccharides purified from glycogen were analyzed by HPTLC on silica gel plates in a solvent system consisting of n-propanol:ethyl acetate:H_2O (7:1:4). Approximately 3 nmoles (based on phosphate) of phosphorylated oligosaccharides were developed using ascending thin layer chromatography in the above solvent and stained for sugars by dipping the plates in a 95% methanolic solution containing 0.3% N-(1-Naphthyl)ethylene-diamine dihydrochloride and 5% H_2SO_4 (for 100 mL: dissolve 300 mg of N-(1-Naphthyl)ethylene-diamine dihydrochloride in 95 mL methanol and 5 mL of concentrated H_2SO_4). The plates were allowed to dry at room temperature and were placed in an oven at 110^{o}C for 10 minutes. Approximately 10 nmoles of sugar and sugar phosphate standards were developed in parallel.

21. Analysis of purified phosphorylated oligosaccharides by high performance anion exchange chromatography (HPAEC)

Phosphorylated oligosaccharides purified from glycogen were analyzed by HPAEC on an ICS3000 from Dionex using a PA1 column and detected by pulsed amperometric detection. All samples were filtered using a spin column before injection into a 25 μL injection loop. Eluent A consisted of 100 mM NaOH and Eluent B 100 mM NaOH containing 1 M sodium acetate. The fractions were eluted with a continuous gradient from 0-75% Eluent B over 60 minutes with a flow rate of 0.25 mL/min. Five to 10 nmoles of phosphorylated oligosaccharides

were analyzed (based on phosphate concentration). Carbohydrate standards, maltose, maltotriose, maltotetraose, maltopentaose, maltohexaose, maltoheptaose, maltooctaose, glucose-1P, glucose-6P, and glucose-2P were analyzed at a concentration of 10-100 μM (250 pmoles-2.5 nmoles).

22. Synthesis of glucose-1,2-cyclic phosphate

Glucose-1,2-cyclic phosphate was synthesized essentially as described by Zmudzka and Shugar (147). One gram of the disodium salt of glucose-1P was dissolved in 5 mL of H_2O and converted to the free acid by cation exchange chromatography using Dowex (H+) 50W-X8 resin. The resin was washed with H_2O and the free acid of glucose-1P was neutralized with pyridine and concentrated in a Speed Vac to approximately 10 mL using clean borosilicate glass tubes. Pyridine (30 mL) and 3 g of dicyclohexylcarbodiimide (DCC) were added and the solution incubated at 0^oC for 48 hours in a round bottom flask at which time 10 mL of H_2O was added to the reaction and the precipitated cyclohexylurea filtered away by vacuum filtration. The filtrate was extracted 3 times with an equal volume of diethyl ether and the aqueous phase concentrated under vacuum in a Speed Vac to about 5 mL using clean borosilicate glass tubes. The insoluble material was removed by vacuum filtration and the filtrate was passed through a Dowex (H+) cation exchange resin and rapidly neutralized with a saturated solution of barium hydroxide ($Ba(OH)_2$) to pH 8. The resulting solution was concentrated under reduced pressure in a Speed Vac to about 1 mL in borosilicate glass tubes, freed from cloudiness by centrifugation at 5,000 x g for 5 minutes and 3 mL of acetone added to the supernatant to precipitate a white powder. The solution was centrifuged 5,000 x g for 5 minutes and the barium salt of glucose-1,2-cyclic phosphate washed 3 times with 10 mL of 100% ethanol at -20^oC by mixing well and centrifugation at 5,000 x g for 5 minutes followed by 3 washes with an equal volume of acetone. The barium salt of glucose-1,2-cyclic phosphate was dried under reduced pressure in a Speed Vac and stored at -20^oC until use.

23. Synthesis of glucose-2-phosphate

Glucose-2-phosphate (glucose-2P) was synthesized by acid hydrolysis of glucose-1,2-cyclic phosphate and purified as the barium salt (148, 149) (Figure 14). The conditions for acid hydrolysis are chosen to be sufficient to open the ring and hydrolyze the very labile glucose-1P without hydrolyzing the glucose-2P (149). Therefore 100 μmols of glucose-1,2-cyclic phosphate was dissolved in 9 mL of H_2O and preheated to 100°C at which time 1 mL of 1 M hydrobromic acid was added and the solution incubated for 5 minutes at 100°C in a 15 mL polypropylene conical screw cap tube. The solution was cooled and a saturated solution of $Ba(OH)_2$ was added until the pH was between 9-10. The solution was kept on ice until the barium phosphate formed began to settle at which time the precipitate was collected by centrifugation at 10,000 x g for 10 minutes and the supernatant saved on ice. The precipitate was redissolved in 100 mM HBr, the pH adjusted to 9 and the solution kept on ice until once again the barium phosphate began to settle. This procedure was repeated for a third time and to the combined supernatants was added 3 volumes of cold 100% ethanol. After cooling overnight on ice, the precipitated barium salt of glucose-2P was collected by centrifugation at 10,000 x g for 10 minutes, washed with 100% ethanol, dried under reduced pressure in a Speed Vac and stored at -20°C until use.

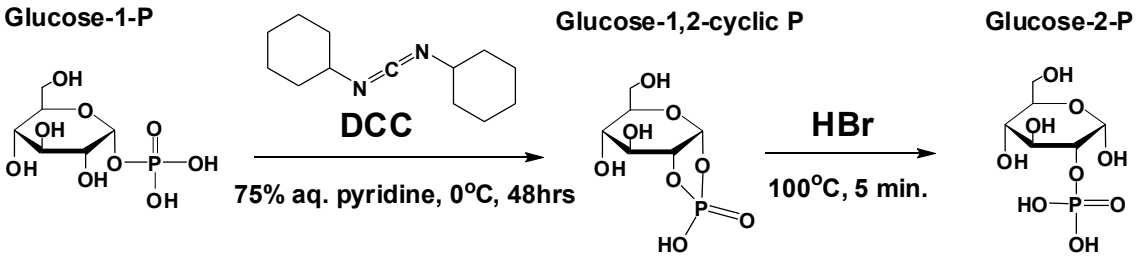

Figure 14. Synthesis of glucose-2-phosphate. Glucose-2P was synthesized by cyclization of glucose-1P with dicyclohexylcarbodiimide (DCC) in aqueous pyridine at °C for 48 hours, followed by mild acid hydrolysis of the labile cyclic phosphate. HBr, hydrobromic acid.

24. Matrix assisted laser desorption ionization time of flight mass spectrometry (MALDI-TOF-MS) analysis of phosphorylated oligosaccharides

MALDI-TOF-MS analysis was performed by the Complex Carbohydrate Research Center, The University of Georgia. Briefly, an aliquot (2 μL, 1 mM phosphate) of purified phosphorylated oligosaccharides were analyzed by MALDI/TOF-MS. The matrix was 2',4',6'-trihydroxyacetophenone monohydrate (THAP, 0.5 M 2,4,6 THAP in ethanol:0.1 M diammonium hydrogen citrate in H_2O : 2:1 (v/v)). The matrix solution (1 μL) was deposited first on the target and then an equal volume of the sample was deposited. All spectra were obtained using a Microflex LRF (Bruker). MALDI-TOF-MS analysis was performed in the reflector negative ion mode. Positive ion mode, using α-dihydroxybenzoic acid (DHBA, 20 mg/mL solution in 50% methanol:H_2O was tried also but the sample produced stronger signals in negative ion mode with THAP matrix.

25. Nuclear magnetic resonance (NMR) spectroscopy

The phosphorylated oligosaccharides were deuterium-exchanged by lyophilization from D_2O, dissolved in D_2O, and transferred to an NMR tube with magnetic susceptibility plugs matched to D_2O (Shigemi). The pD of the sample was 5.9. Proton-proton and proton-carbon correlated spectra were acquired on a Varian Inova 600 MHz spectrometer equipped with a 3-mm cryoprobe or a Varian Inova-800 MHz spectrometer, equipped with a 5-mm cryoprobe. Proton-phosphorous correlated spectra were acquired on a Varian Inova 500 MHz spectrometer, equipped with an 8-mm XH room temperature probe. All spectra were taken at 25°C. Chemical shifts were referenced to internal acetone [$\delta(^1H)$ = 2.218 ppm, $\delta(^{13}C)$ = 33.0 ppm] (150). All experiments except the ^1H-^{31}P correlated spectra were acquired with standard Varian pulse sequences. For ^1H-^{31}P correlated experiments, the regular gHMQC and HMQC-TOCSY experiments were modified for ^{31}P in the X channel, using a π pulse of 13 ms at a level of 60 dB, and a $^3J_{H-P}$ coupling constant of 7 Hz. Chemical shifts were referenced to

external 85% phosphoric acid [δ(31P) = 0.00 ppm]. Additional acquisition parameters are listed in Table 1.

experiment	SFRQ	DFRQ	SW	SW1	NT	NI	AT	MIX	NP
proton	600		5040		32		1998		10070
^{1}H-^{1}H gCOSY	600		5040	5040	8	512	203		1024
^{1}H-^{1}H TOCSY	800		3721	3721	32	128	138	100	512
^{1}H-^{1}H ROESY	800		3721	3721	32	128	138	300	512
^{1}H-^{13}C gHSQC	600	150	5040	10555	256	100	150		756
^{1}H-^{31}P gHMQC	500	200	3470	8000	360	32	400		1388
^{1}H-^{31}P HMQC-TOCSY	500	200	3470	3000	400	24	300	40	1041

Table 1. NMR acquisition parameters. Abbreviations used: SFRQ, spectrometer frequency for proton nucleus in Hz, DFRQ, decoupler frequency for heteronucleus (^{13}C or ^{31}P) in Hz, SW, spectral width in the directly detected dimension (^{1}H) in Hz, SW1, spectral width in the indirectly detected dimension (^{13}C or ^{31}P) in Hz, NT number of transients, nNI, number of increments, AT, acquisition time in ms,MIX, Mixing (spinlock) time in ms, np: number of points in the directly detected dimension.

RESULTS

1. Laforin is a Glycogen Phosphatase

1.1 Laforin dephosphorylates glycogen and amylopectin *in vitro*

Our initial attempts to identify a substrate for laforin were primarily focused on sugar phosphate metabolites such as glucose-6P and glucose-1P, with no success (data not shown). During the course of these studies a report by Worby et al. (113) demonstrated that laforin was capable of dephosphorylating amylopectin (113). In addition to glucose, α-1,4-linked polysaccharides like amylopectin and mammalian glycogen contain small amounts of covalent phosphate. In amylopectin ~0.25% by weight of the molecule contains phosphate, corresponding to about 1 phosphate every 150 glucose residues. The values for mammalian glycogen vary depending on tissue and species, but are nonetheless relatively small compared to the amount of glucose. In our hands, rabbit muscle glycogen contains 4-5 times more phosphate than rabbit liver glycogen. In muscle, a molecule of phosphate is present approximately every 650 glucoses, which corresponds to about 0.07% of the polysaccharide weight. In liver this value is about 1 phosphate every 3,000 glucose residues. Worby et al. (113) attempted to measure dephosphorylation of commercially available rabbit liver glycogen by laforin but were unsuccessful, possibly because of the lack of assay sensitivity and/or the low phosphate content of liver glycogen. We initially confirmed the observation that amylopectin is a substrate for recombinant laforin (Figure 15A & B). Some 80-90% of the phosphate was released in a time dependent manner. Varying the amylopectin concentration indicated a saturable process that followed a hyperbolic curve. We then analyzed rabbit skeletal muscle glycogen purified by relatively mild conditions (see Experimental Procedures Section 1). This glycogen contained 0.38% by weight of protein as judged by the Bradford protein determination assay. SDS PAGE and Coomassie staining revealed the presence of a 38 kDa protein that was only apparent after the glycogen had been hydrolyzed with α-amylase (data

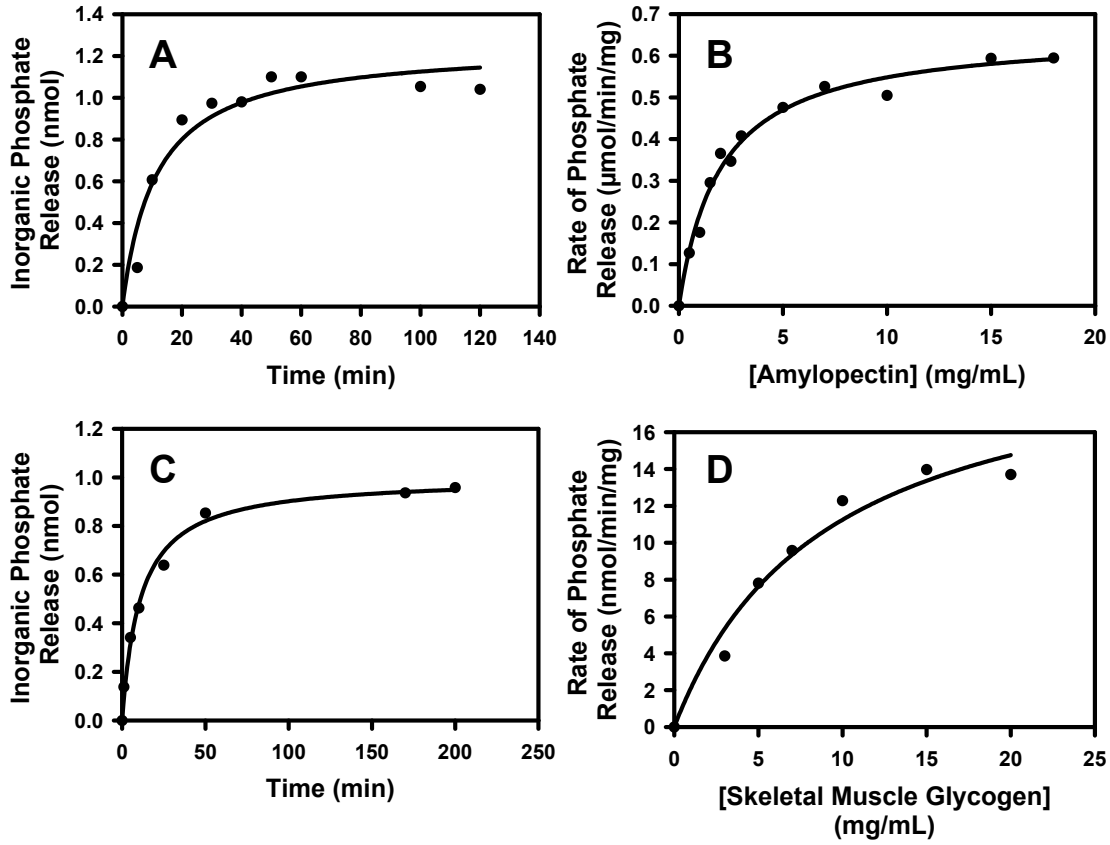

Figure 15. Laforin dephosphorylates amylopectin and rabbit skeletal muscle glycogen *in vitro*. A. Time dependent release of phosphate from potato amylopectin (0.5 mg/ml) by purified, recombinant laforin (2.5 μg/ml). **B.** Concentration dependence of the rate of dephosphorylation of amylopectin by laforin. The reaction was for 15 minutes in the presence of 2.5 μg/ml laforin. **C.** Time dependent release of phosphate from rabbit skeletal muscle glycogen (5 mg/ml) by purified, recombinant laforin (25 μg/ml). **D.** Concentration dependence of the rate of dephosphorylation of rabbit skeletal muscle glycogen by laforin. The reaction was for 40 min in the presence of 25 μg/ml laforin.

not shown). Western analysis using anti glycogenin antibody demonstrated that the protein was glycogenin (data not shown). Analysis of total phosphate content by acid hydrolysis and detection of inorganic phosphate indicated that the glycogen contained 0.07% covalent phosphate by weight. Laforin released 20–25% of the total phosphate present, and the glycogen concentration dependence of the reaction was close to hyperbolic (Figure 15C & D). Unlike amylopectin, glycogen is believed to exist as a series of concentric shells of glucose residues (Figure 16B) and phosphate in the interior layers may not be accessible to laforin in the intact glycogen molecule. Therefore, after phosphate release had reached a maximum, we added the glycogen-degrading enzymes, α-amylase and amyloglucosidase, to disrupt the glycogen structure. Most of the remaining phosphate was now released and was by inference present in the inner tiers of the molecule (Figure 16A). Exposure of glycogen to the glucosidases in the absence of laforin did not release inorganic phosphate, and likewise treatment of laforin with the glucosidases led to no phosphate release (data not shown).

1.2 Glycogen dephosphorylation requires the carbohydrate binding domain of laforin

The laforin mutant C266S, in which a critical active site residue is mutated (Figure 11), did not hydrolyze phosphate from glycogen confirming that phosphate release was not an artifact and was an enzyme-catalyzed reaction (Figure 17B). Some Lafora disease mutations are located in the glycogen binding domain and, with one of these, W32G, previous work has demonstrated that the enzyme does not bind glycogen yet retains significant activity towards the artificial phosphatase substrate *p*-nitrophenyl phosphate (*p*NPP) (101, 107). Recombinant W32G laforin was partially active towards *p*NPP but was unable to dephosphorylate glycogen (Figure 17A & B) demonstrating that laforin action requires binding to glycogen by this non-catalytic domain. This finding is consistent with the idea that laforin is associated with glycogen during its metabolism, monitoring and opposing the excessive introduction of phosphate.

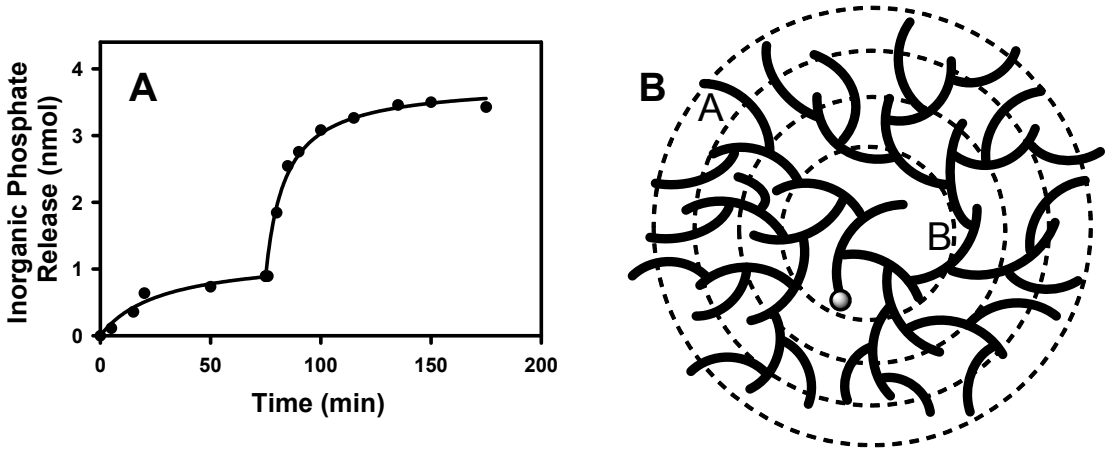

Figure 16. Dephosphorylation of glycogen in the presence of glycogen hydrolyzing enzymes. A. Dephosphorylation of rabbit skeletal muscle glycogen in the presence of α-amylase and amyloglucosidase. Glycogen (5 mg/ml) dephosphorylation by laforin (25 μg/ml) was allowed to proceed until the reaction was essentially complete, at which time α-amylase (0.3 mg/ml) and amyloglucosidase (0.3 mg/ml) were added. Subsequent phosphate release was monitored. **B.** Model for glycogen structure. Glycogen is believed to exist as a series of concentric shells of glucose residues, so that inner tiers would not be on the surface of the molecule. A full size molecule would consist of twelve tiers.

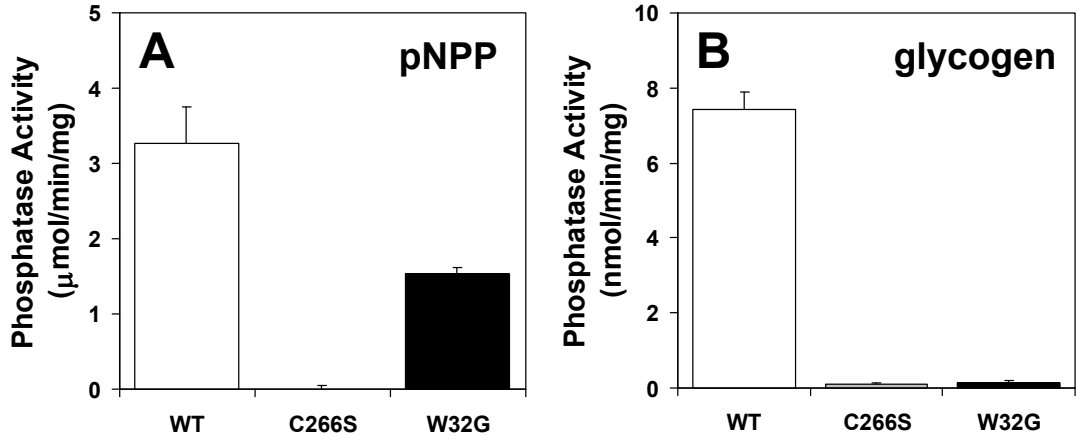

Figure 17. Glycogen dephosphorylation requires the carbohydrate binding domain of laforin. A. WT laforin and W32G laforin are active towards *p*NPP. Mutation at the active site (C266S) eliminated activity. **B.** WT laforin releases phosphate from rabbit skeletal muscle glycogen. Mutation at the active site (C266S) essentially eliminated activity. Mutation in the carbohydrate binding domain (W32G), which is known to eliminate binding to polysaccharides, also abolished laforin's ability to dephosphorylate glycogen.

2. Analysis of *Epm2a-/-* Mice

2.1 Glycogen and glycogen phosphate levels increase with age in the absence of laforin

Mice with the *Epm2a* gene disrupted develop many of the characteristics of Lafora disease (151). The animals had Lafora bodies in muscle and brain, impaired behavioral responses, and ataxia, and they ultimately underwent myoclonic seizures. Lafora disease is a progressive disorder and in the *Epm2a*-/- mice neurological symptoms are only apparent in older, 9 month old, animals; however Lafora bodies begin to develop around 3 months of age. We therefore compared young animals, 3 months of age, with mice 9-12 months old, beginning with the measurement of glycogen and glycogen phosphate content. Analysis of muscle glycogen isolated from the 3 month animals showed no difference in total glycogen levels between wild type and *Epm2a*-/- mice (Figure 19A open bars) and an approximately four-fold increase in the phosphate content (Figure 18A, open bars). In the older animals, there was a three-fold elevation in total glycogen content (Figure 19A, filled bars) and a further increase in phosphate to around six times that present in wild type animals (Figure 18A, filled bars). Phosphate content of wild type glycogen was unchanged as animals aged from 3 to 9-12 months. A similar trend was observed in liver glycogen phosphate levels. At 3 months of age, there was an approximately 30% increase in liver glycogen phosphate (Figure 18B, open bars). As the animals aged to 9-12 months, glycogen phosphate levels increased to 4 times that of age-matched wild type controls (Figure 18B, filled bars). Glycogen phosphate levels were significantly lower as the WT mice aged from 3 to 9-12 months of age, possibly due to the high turnover of the glycogen in the liver as compared to muscle (see Discussion). Brain glycogen levels were already increased at 3 months and progressed to a five-fold elevation in the old animals (Figure 19B). Because of the much lower amounts of glycogen recoverable from brain, it was not feasible to measure phosphate content. The greater sensitivity of brain glycogen

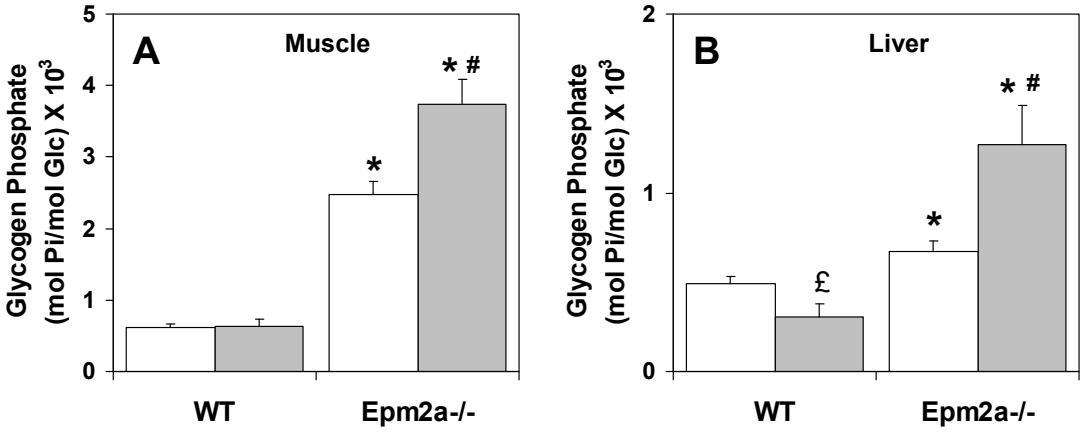

Figure 18. Skeletal muscle and liver glycogen phosphate levels are increased in *Epm2a-/-* mice. Glycogen was purified from muscle and liver for analysis of covalent phosphate**. A.** Skeletal muscle glycogen phosphate levels in 3 month (open bars) and 9-12 month (filled bars) WT and *Epm2a-/-* mice. *p< 0.001 vs WT, $^{\#}$p< 0.01 vs 3 month *Epm2a-/-*, (n=7-8). **B.** Liver glycogen phosphate levels in 3 month (open bars) and 9-12 month (filled bars) WT and *Epm2a-/-* mice. $^{£}$p< 0.05 vs 3 month WT, *p< 0.05 vs WT, $^{\#}$p< 0.05 vs 3 month *Epm2a-/-*, (n=6-8).

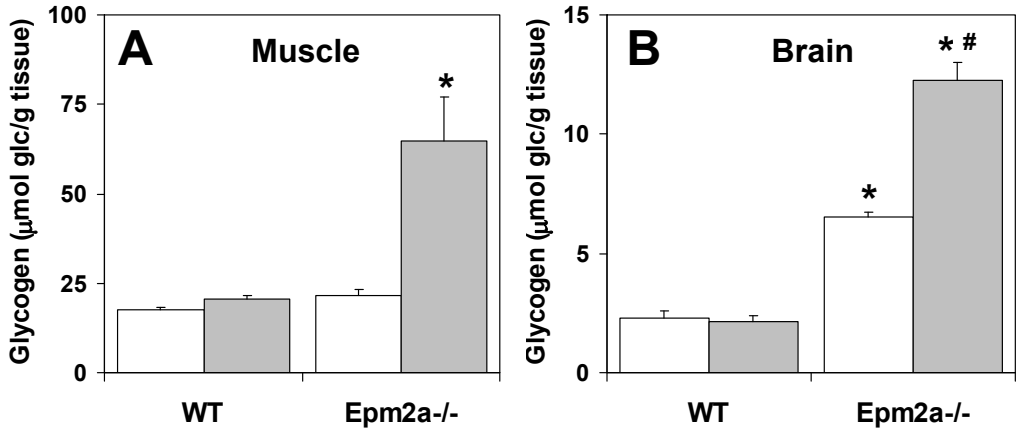

Figure 19. Skeletal muscle and brain glycogen levels increase with age in *Epm2a-/-* mice. Total glycogen content was analyzed from 3 month and 9-12 month old animals. **A.** Skeletal muscle glycogen levels in 3 month (open bars) and 9-12 month (filled bars) WT and *Epm2a-/-* mice. *p< 0.001 vs WT and 3 month *Epm2a-/-*, (n=11-15). **B.** Brain glycogen content in 3 month (open bars) and 9-12 month (filled bars) WT and *Epm2a-/-* mice. *p= 0.0001 vs WT, $^{\#}$p< 0.002 vs 3 month *Epm2a-/-*, (n=3-4).

accumulation in the absence of laforin could reflect differences in brain glycogen metabolism and explain the potentially more serious consequences in this tissue.

2.2 Age-dependent changes in chemical and physical properties of glycogen in *Epm2a-/-* mice

Lafora disease is characterized by poorly branched glycogen-like polymers in the Lafora bodies (89-91). We therefore monitored the degree of branching of glycogen purified from laforin deficient mice by recording the visible absorption spectrum in the presence of iodine. Iodine intercalates into polysaccharide helices to give a characteristic spectrum whose absorption maximum is influenced by the degree of branching and hence the length of uninterrupted helical segments (152). This technique readily distinguishes wild type mouse glycogen from amylopectin which has one α-1,6-linkage on average every ~30 glucoses and whose absorption spectrum maximum is at a much higher wavelength (Figure 20A, red). Mammalian glycogen typically has branches every ~12 glucose residues. The iodine spectra of muscle glycogen from 3 month or 9-12 month old wild type mice are super-imposable, with absorption maximum around 470 nm, indicating no change in branching with age in WT animals (Figure 20A & B). Muscle glycogen from 3 month old *Epm2a*-/- mice had an iodine spectrum slightly, but significantly, shifted to longer wavelength (Figure 20A, green, & B). However, the spectrum for 9-12 month old knockout animals was dramatically altered, such that it was approaching that of amylopectin and indicative of a substantial reduction in the number of branches (Figure 20A, blue & B). Removal of the phosphate by laforin treatment did not alter the iodine spectrum (data not shown). In liver there were no significant alterations in the iodine spectrum of glycogen purified from young or old *Epm2a*-/- mice (data not shown).

Poorly branched glucose polymers, like amylopectin, are less soluble in water than highly branched polysaccharides. Indeed, during isolation (see Experimental Procedures Section 4), it was more difficult to dissolve precipitated glycogen from the 9-12 month *Epm2a*-/- mice than glycogen from any of the

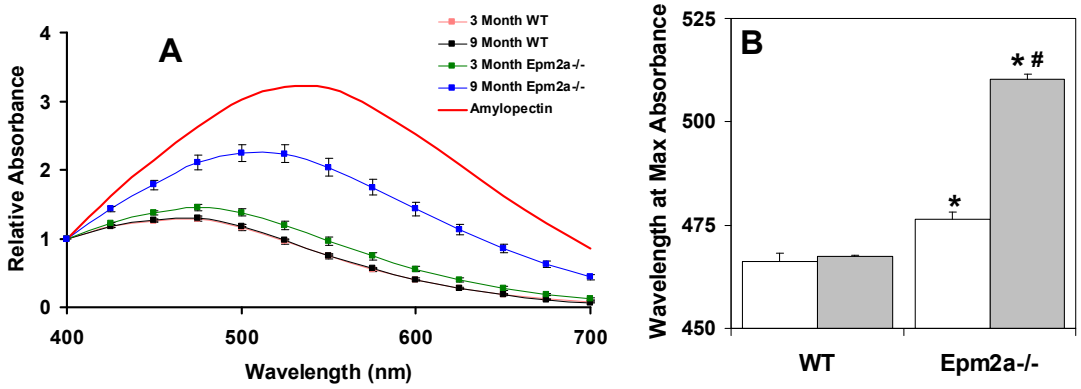

Figure 20. Glycogen becomes poorly branched with age in *Epm2a-/-* mice. A. Iodine spectra of skeletal muscle glycogen (50-75 μg/mL) purified from WT and *Epm2a-/-* mice. Amylopectin is shown for reference. **B.** Quantitation of A. 3 month old animals are depicted with open bars and 9-12 month old animals with filled bars. The wavelength at maximum absorbance indicates the degree of branching of polysaccharides. *p< 0.002 vs WT, #p< 0.0001 vs 3 month *Epm2a-/-*, (n=3-8).

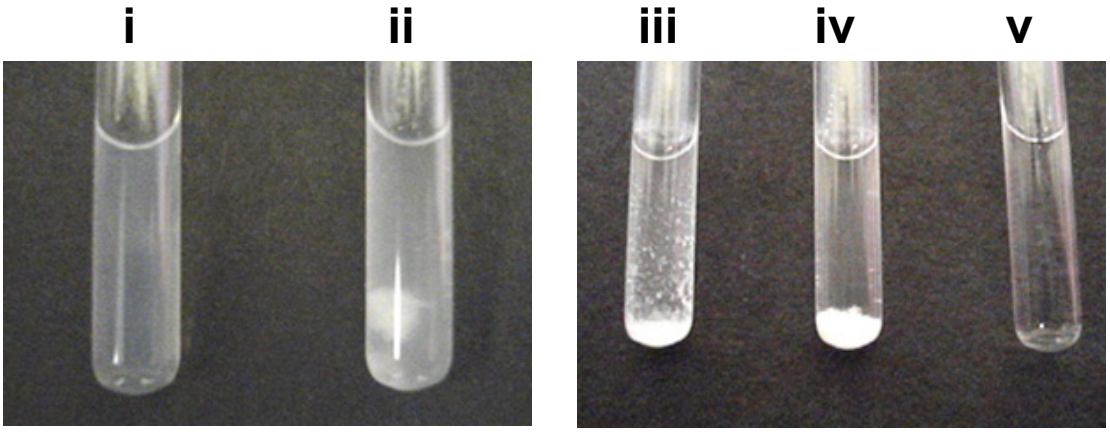

Figure 21. Glycogen phosphate contributes to glycogen solubility in ethanol. Skeletal muscle glycogen (5 mg/mL) purified from a 9 month old *Epm2a-/-* mice that was treated with catalytically inactive laforin (C266S) (i) or active laforin (ii), and brought to 66% (v/v) ethanol. (iii) Addition of LiCl to (i). (iv) Addition of LiCl to (ii). (v) Addition of LiCl to a 66% ethanol solution without glycogen (v).

other mouse groups analyzed. Likewise, after storage at -20^{o}C, thawing of 9-12 month mouse glycogen solution resulted in a precipitate that required heating to re-dissolve. Similar treatment of glycogen from wild type or 3 month old *Epm2a-/-* mice did not result in precipitated material.

Polysaccharides like glycogen are insoluble in ethanol, a property that is useful for their separation from ethanol soluble constituents. Thus, as part of our normal isolation protocol of glycogen from tissues (see Experimental Procedures Section 4), we utilize precipitation in 66% (v/v) ethanol. In the course of this work, we observed that muscle glycogen from *Epm2a*-/- mice, regardless of age, was much more soluble in 66% ethanol than wild type glycogen and did not come readily out of solution (data not shown). Addition of trace amounts of a chaotropic salt, like LiCl, used to ensure complete precipitation of polysaccharides from ethanol, was effective in precipitating glycogen from both the 3 month and the 9-12 month *Epm2a-/-* mice. Glycogen from 9-12 month *Epm2a*-/- mice was exposed under aqueous conditions to either the catalytically inactive C266S mutant laforin or wild type laforin followed by addition of ethanol to 66% (v/v). Treatment with inactive laforin recapitulated the results described for glycogen from tissue extracts, with the glycogen remaining in solution (Figure 21C, i). Treatment with active laforin, conditions which remove most of the phosphate, resulted in a polysaccharide that precipitated normally (Figure 21C, ii). Addition of LiCl to both samples hastened precipitation, although the phosphorylated glycogen formed more flocculent material that, under gravity, pelleted at a slower rate (Figure 21C, iii & iv). The visible material was not salt since it was absent in the control sample lacking any glycogen (Figure 21C, v).

2.3 Age dependent changes in glycogen structure in *Epm2a-/-* mice

The high molecular weight of glycogen makes it large enough to be analyzed by electron microscopy and the literature contains numerous examples. Analysis of the glycogen purified from the muscle of wild type mice by transmission electron microscopy indicated particles reminiscent of these structures, whether from old or young animals (Figure 22A & B). Glycogen from

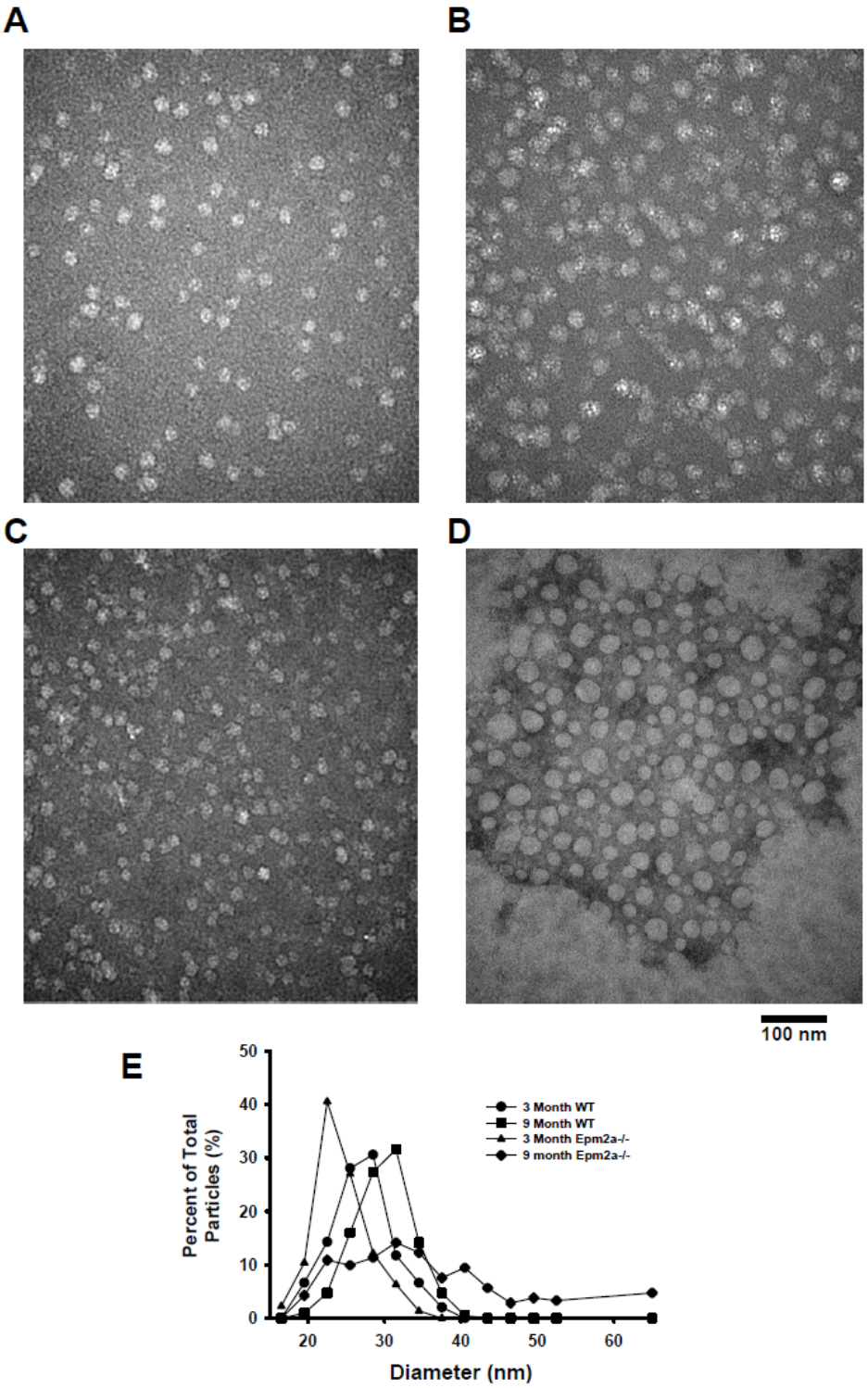

Figure 22. Age-dependent changes in glycogen structure in *Epm2a-/-* mice. Electron micrographs of skeletal muscle glycogen purified from: **A.** 3 month old WT; **B.** 9-12 month old WT; **C.** 3 month old *Epm2a-/-,* **D.** 9-12 month old *Epm2a-/-;* **E.** Size distribution of skeletal muscle glycogen particles purified from WT and *Epm2a-/-* mice.

3 month old *Epm2a*-/- mice had generally a similar appearance, although perhaps with a tendency to slightly smaller particles (Figure 22C). In contrast, glycogen from the 9-12 month old mice had a strikingly distinct appearance, with a more defined boundary, less granularity and a more even density (Figure 22D). Furthermore, many fields had large regions where particles appear to have coalesced or aggregated, either before or during preparation of the grids. The size distribution of the particles was estimated by measuring apparent particle diameter. Glycogen particles from 3 month old wild type mice had an average diameter of 27.1 nm, which is in the range reported for native muscle glycogen particles (153). Interestingly, with age, there appeared to be a shift in the population to a slightly larger size (average 35.1 nm) but retaining the approximately Gaussian distribution seen in the younger animals. Glycogen particles from the 3 month old knockout animals, as noted, were smaller, with average diameter 24.2 nm, but still normally distributed. The comparable analysis of the particles from old *Epm2a*-/- mice was hampered by the presence of the large conglomerates. Although individual particles were visible, their dimensions could not be estimated. From counting particles in regions outside of the conglomerates, it was apparent that there was much greater variability in size, with many particles of diameter well beyond that anticipated for a normal glycogen particle (Figure 22D). This could be due to a different density of the polysaccharide or more likely an aggregation of individual molecules that cannot be resolved by this analysis.

Compared with the other samples analyzed, the glycogen from the old knockout mice was characterized by having the highest phosphate content and much reduced branching. Thus, purified muscle glycogen from the 9-12 month old *Epm2a*-/- animals was subjected to treatment with laforin to remove phosphate and, in a parallel control, treatment with the catalytically inactive laforin mutant C266S. After removing protein and buffer, the glycogen was visualized by electron microscopy. Glycogen from the control sample had an appearance comparable to that shown in Figure 22D (Figure 23A). Treatment of 9-12 month old glycogen with active laforin caused a significant change in

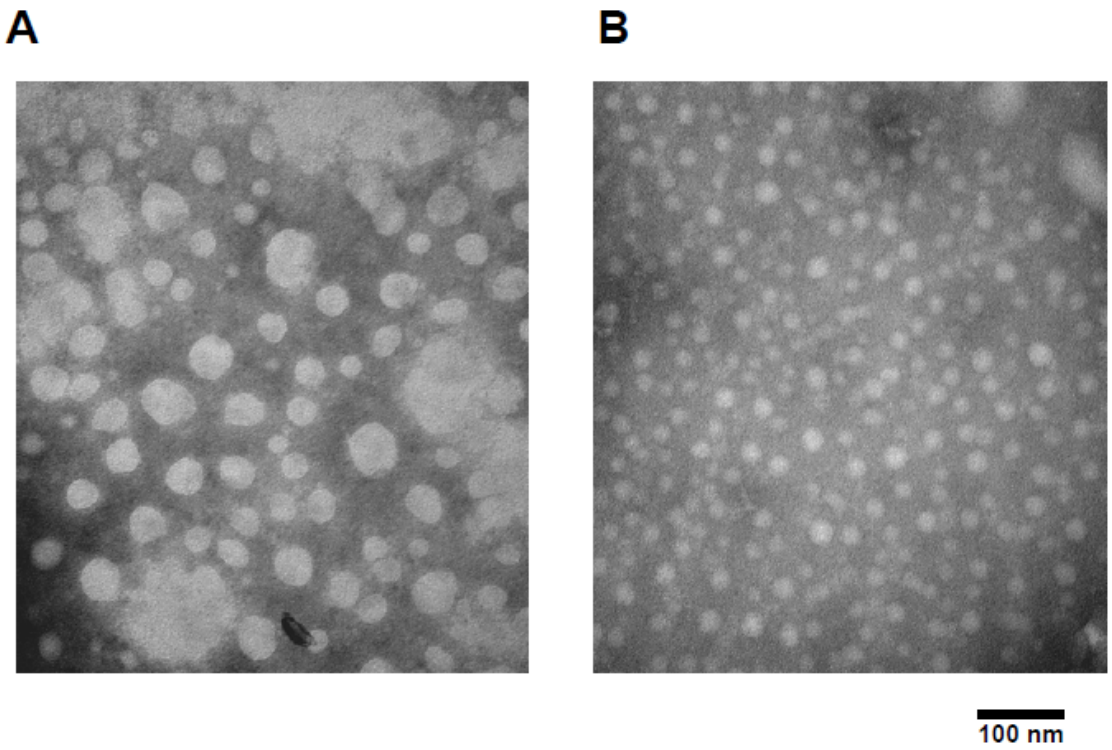

Figure 23. Effect of phosphate removal on skeletal muscle glycogen from 9-12 month old *Epm2a-/-* mice. Electron micrographs of glycogen treated with **A.** the catalytically inactive laforin (C266S) or **B.** active WT laforin.

individual appearance tending more to that of wild type (Figure 23B). However, the granularity of the normal particles was not completely restored. Since the removal of phosphate by laforin did not affect branching (previous section), we conclude that the phosphate is primarily responsible for the abnormal morphology of the glycogen from the 9-12 month old animals, in particular the presence of larger particles and aggregates.

With the possibility that abnormal glycogen phosphorylation might affect the aggregation of glycogen, at least in the samples from older *Epm2a*-/- mice, we wondered whether our standard sample preparation for enzyme analysis, in which a low speed centrifugation is included to remove gross cellular debris from tissue extracts, may have actually removed some of the glycogen. This separation is not an issue for samples directly processed for measurement of glycogen. We found that in extracts from the muscle of 9-12 month old *Epm2a*-/- mice, about 60% of the glycogen was recovered in the low speed pellet (LSP), compared with ~25% for wild type muscle (Figure 24A). In brain extracts, over 75% of the glycogen was in the pellet from knockout mouse extracts (Figure 24B). The increased glycogen in the old knockout mice was associated with the LSP as the glycogen level in the low speed supernatant (LSS) was the same as wild type. Glycogen was purified from the LSS and LSP fractions of muscle extracts of the 9-12 month old *Epm2a*-/- animals for analysis by electron microscopy (Figure 24C & D). During this procedure, it was noted that the LSP glycogen was significantly harder to dissolve in water than the LSS fraction. The pellet fraction was highly enriched for the morphologically abnormal structures described in Figure 22, whereas in the supernatant the particles were predominantly of more wild type appearance. The glycogen in the pellet also had significantly higher glycogen phosphate content (Figure 24E). The phosphorylation of the LSS glycogen was, in absolute terms, comparable to that of the whole glycogen fraction of 3 month old *Epm2a*-/- mice (see Figure 18A, open bars). Analysis of glycogen branching by iodine spectra indicated that the pellet was enriched for poorly branched glycogen, with an absorption maximum close to that of amylopectin (Figure 24F). In these old knockout mice, it appears that low speed

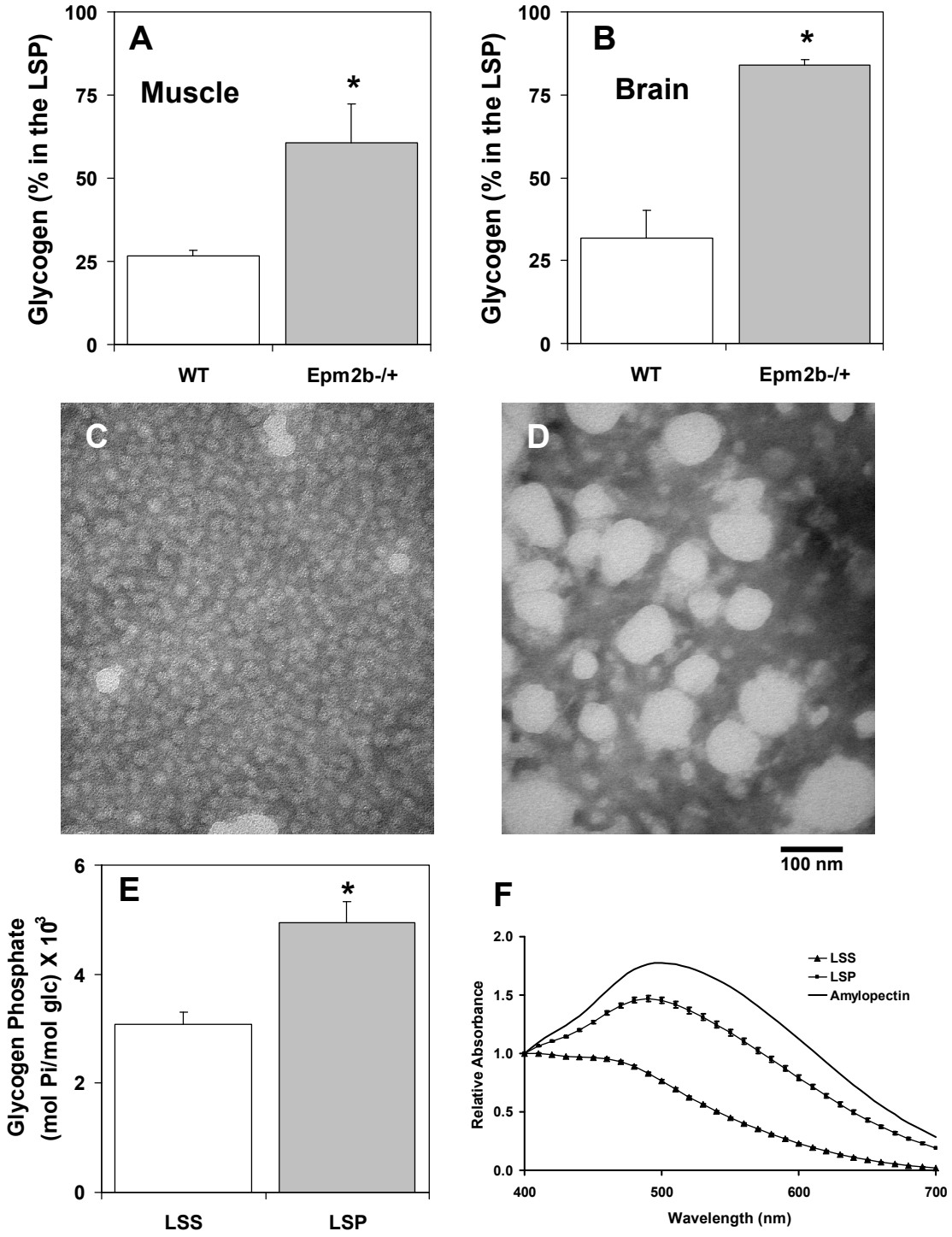

Figure 24. Fractionation of glycogen from 9-12 month old *Epm2a-/-* mice. Total skeletal muscle or brain extracts from 9-12 month old WT and *Epm2a*-/- mice were subjected to low speed centrifugation to generate supernatant (LSS) and pellet (LSP). **A.** Percentage of total muscle glycogen, in the LSP. *p< 0.05, (n=6). **B.** Percentage of total brain glycogen in the LSP. *p< 0.005, (n=3). **C.**

centrifugation can effectively separate a polyglucosan fraction from normal glycogen that remains in the supernatant.

2.4 Analysis of glycogen metabolizing enzymes and related proteins in 9-12 month old *Epm2a-/-* mice

We extended our analysis of glycogen metabolism in the old *Epm2a-/-* mice, quantitating some potentially relevant proteins and also taking into account the partitioning of the glycogen between the LSS and LSP. In wild type mice, most laforin is present in the LSS in muscle and brain (Figure 25A & 26A). As judged by Western analysis, total glycogen synthase protein level (LSS plus LSP) was increased by ~50% in the muscle (Figure 25A) and ~2.5-fold in brain (Figure 26A) of knockout animals and this elevation could be attributed to an increase in the protein associated with the LSP. There was in fact a slight decrease in the soluble glycogen synthase protein. Glycogen synthase activity measured in the presence of glucose-6P, usually taken as a measure of total glycogen synthase (25), however, was statistically unchanged between genotypes in either the LSS or LSP fractions (Figure 27B,D & 28B,D). In *Epm2a*-/- muscle extracts (Figure 27B & D) or brain extracts (Figure 28B & D), the activity in the LSP fractions was lower than in the LSS, despite the presence of as much or more glycogen synthase protein in the LSP (Figure 25A & 26A). In other words, the measured glycogen synthase specific activity was reduced in the LSP. In contrast, the activity associated with the LSP fraction of wild type mice was commensurate with the relatively small amount of glycogen synthase protein present. The reason for the unexpectedly low specific activity in the LSP fractions, muscle or brain, of the glycogen synthase of the knockout mice is not immediately obvious. One possibility would be the occurrence of some stable and novel modification of the protein. Alternatively, the activity assay in this fraction may somehow be inaccurate. This result is also consistent with the *in vitro* observation that purified rabbit muscle glycogen synthase binds more effectively to the abnormal glycogen isolated from old *Epm2a*-/- muscle (Figure 29). The -/+ glucose-6P activity ratio has been used as a kinetic index of

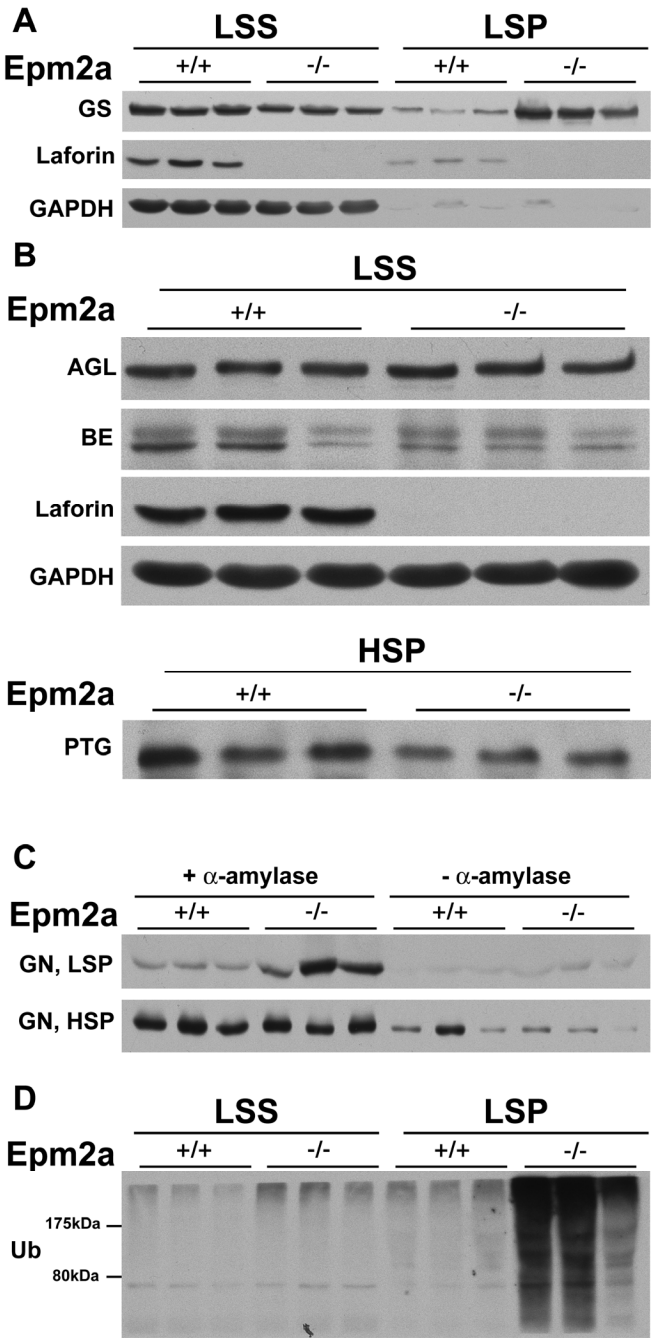

Figure 25. Analysis of glycogen metabolizing enzymes and related proteins in skeletal muscle of 9-12 month old *Epm2a-/-* mice. Muscle extracts WT and *Epm2a*-/- mice were analyzed. **A.** Glycogen synthase (GS) protein levels in the LSS and the LSP of muscle extracts. **B.** Glycogen debranching enzyme (AGL) and branching enzyme (BE) protein levels in muscle extracts. Muscle PTG protein levels in the high speed centrifugation glycogen pellet. **C.** Glycogenin (GN) protein levels in the LSP and the HSP of muscle treated or not with α-amylase. **D.** Ubiquitinated proteins in the LSS and LSP.

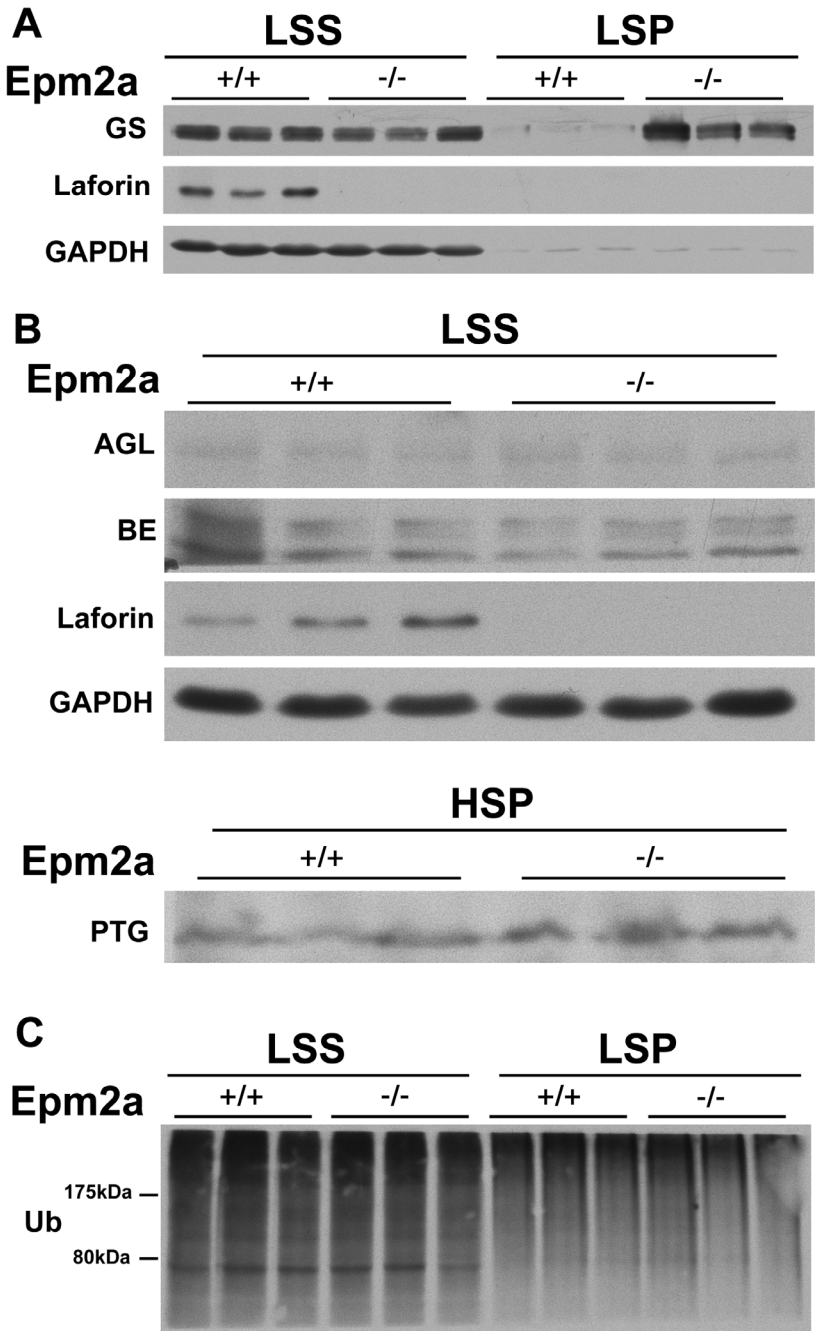

Figure 26. Analysis of glycogen metabolizing enzymes and related proteins in brain of 9-12 month old *Epm2a-/-* mice. Brain extracts from WT and *Epm2a-/-* mice were analyzed. **A.** Glycogen synthase protein levels in the LSS and the LSP. **B.** Glycogen debranching enzyme (AGL) and branching enzyme (BE) protein levels in the LSS. PTG protein levels in the high speed centrifugation glycogen pellet of brain extracts. **C.** Ubiquitinated proteins in the LSS and LSP.

glycogen synthase inactivation by reversible phosphorylation. In muscle, but not brain, there was a significant reduction in the activity ratio in the *Epm2a*-/- samples in both fractions (Figure 27A,C & 28A,C).

Based on Western blotting, the levels of branching enzyme (BE) and debranching enzyme (AGL) were not greatly changed in extracts of muscle (Figure 25B) or brain (Figure 26B) from *Epm2a*-/- mice. Small levels of both proteins were detectable in the LSP with a small increase in the knockout animals tracking with the elevated levels of glycogen in this fraction. However quantitation of total protein (LSS+LSP) showed no differences between WT and knockout mice (data not shown). PTG is a type 1 protein phosphatase regulatory subunit (64) that has been implicated in laforin action, first as a protein capable of interacting with laforin (103) and secondly as a potential target for a malin-laforin ubiquitylating complex, leading to its proteosomal degradation (117, 118). PTG associates with glycogen and, with the available antibodies, we can only detect PTG when enriched in high speed glycogen pellets. Analysis of PTG protein levels revealed, if anything, a decrease in PTG protein in the muscle of *Epm2a*-/- mice (Figure 25B) and no change in the brain (Figure 26B).

Glycogenin is the self-glucosylating initiator protein of glycogen synthesis (154-156) which is thought to remain covalently attached to glycogen. As such, its level will index the number of glycogen molecules present. Glycogenin can only be detected by Western blotting once glycogen has been degraded by treatment with α-amylase (Figure 25C). Consistent with this idea, the large majority of the glycogenin is only detected after α-amylase digestion. In these experiments, the glycogenin level essentially correlates with the amount of glycogen present, as analyzed in the LSP of the knockout mice where there is more glycogen (Figure 25C). The high speed pellet concentrates the glycogen present in the LSS. Analysis of glycogenin protein levels in this fraction revealed no changes between the WT and *Epm2a-/-* mice. If the measured glycogen level in the different fractions is normalized to the amount of glycogenin, there is no great variation. This ratio is increased in the LSP fraction from the *Epm2a*-/- mice, but only by ~60%. The main conclusion from this analysis is that the

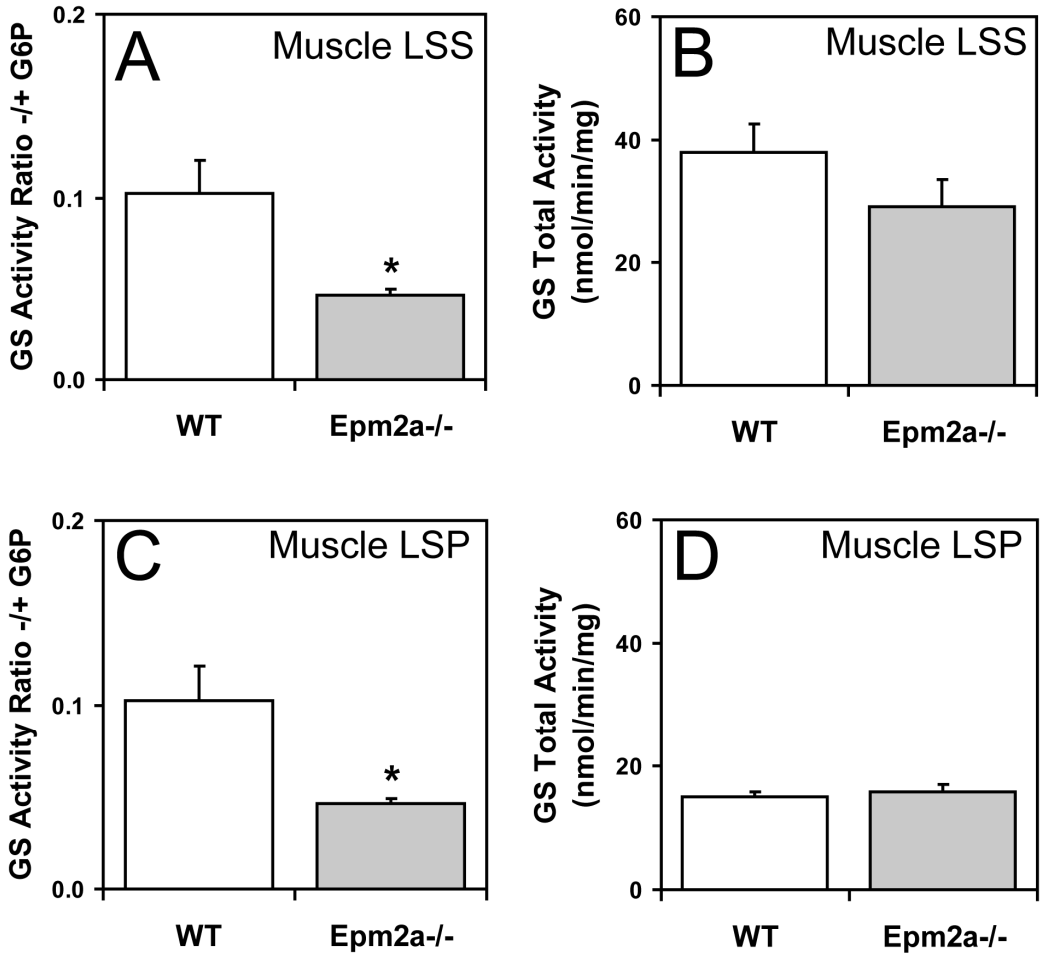

Figure 27. Skeletal muscle glycogen synthase activity in the LSS and LSP of 9-12 month old *Epm2a-/-* mice. Skeletal muscle extracts WT and *Epm2a-/-* mice were analyzed. **A.** Glycogen synthase activity ratio in the LSS of WT (open bars) and *Epm2a-/-* (filled bars) mice. *p< 0.05, (n=3). **B.** Total glycogen synthase activity measured in the presence of glucose-6P in the LSS of WT (open bars) and *Epm2a-/-* (filled bars) mice. **C.** Glycogen synthase activity ratio in the LSP of WT (open bars) and *Epm2a-/-* (filled bars) mice. **D.** Total glycogen synthase activity measured in the presence of glucose-6P in the LSP of WT (open bars) and *Epm2a-/-* (filled bars) mice. *p< 0.05, (n=3).

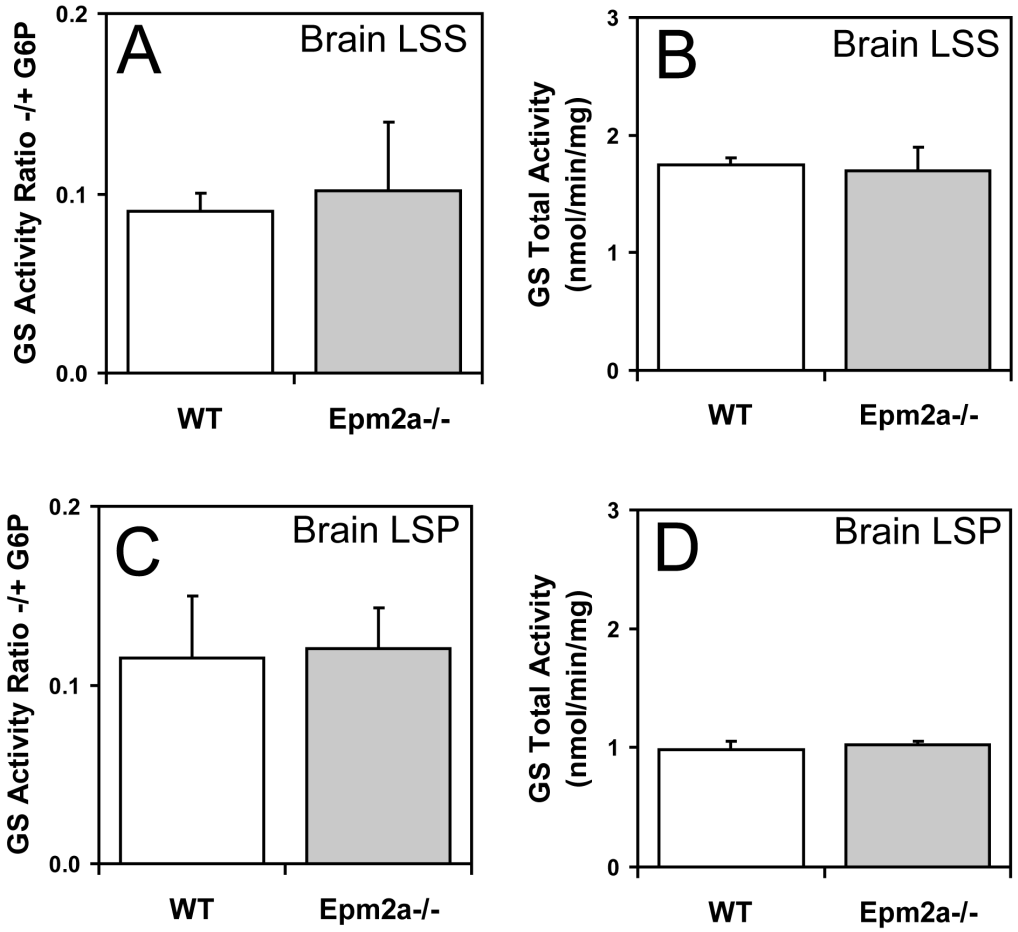

Figure 28. Brain glycogen synthase activity in the LSS and LSP of 9-12 month old *Epm2a-/-* mice. Brain extracts from WT and *Epm2a-/-* mice were analyzed. **A.** Glycogen synthase activity ratio in the LSS of WT (open bars) and *Epm2a-/-* (filled bars) mice. **B.** Total glycogen synthase activity measured in the presence of glucose-6P in the LSS of WT (open bars) and *Epm2a-/-* (filled bars) mice. **C.** Glycogen synthase activity ratio in the LSP of WT (open bars) and *Epm2a-/-* (filled bars) mice. **D.** Total glycogen synthase activity measured in the presence of glucose-6P in the LSP of WT (open bars) and *Epm2a-/-* (filled bars) mice.

morphologically abnormal glycogen in the old knockout mice consists of glycogen molecules whose molecular mass is not greatly different from wild type.

A pathological hallmark of many neurodegenerative disorders, including Lafora disease, is the presence of ubiquitin-positive, intracellular inclusion bodies in regions of the brain (157). Western analysis of skeletal muscle revealed a remarkable increase in ubiquitin positive proteins in the LSP of the old *Epm2a-/-* mice (Figure 25D). The signal was comparable between genotypes in the LSS and analysis of ubiquitin positive proteins in brain, failed to reveal any noticeable changes between the WT and *Epm2a-/-* animals (Figure 26D).

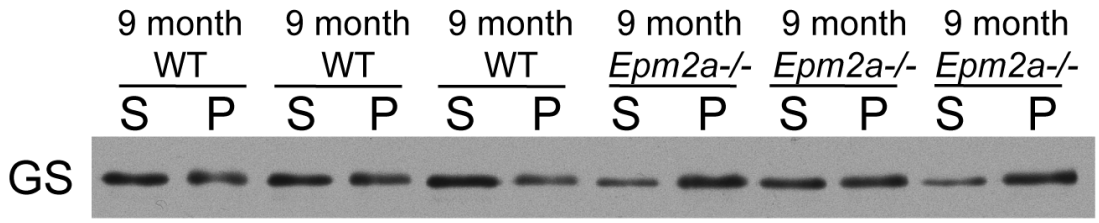

Figure 29. Glycogen synthase binds more effectively to the abnormal glycogen isolated from 9-12 month old *Epm2a-/-* muscle. Purified rabbit muscle glycogen synthase (GS, I-form) was incubated with purified muscle glycogen from 9 month old WT and *Epm2a-/-* mice and subjected to high speed centrifugation to pellet glycogen. S, supernatant after centrifugation at 100,000 x g; P, pellet after centrifugation at 100,000 x g.

2.5 Analysis of glycogen metabolism in 3 month old *Epm2a-/-* mice

Our characterization of the 3 month old *Epm2a-/-* is not as thorough as in the older animals. In brain, glycogen levels are elevated in the knockout animals as early as 3 months of age (Figure 19B, open bars). Total skeletal muscle glycogen levels in the 3 month old *Epm2a-/-* mice are relatively normal compared to WT, although there is a trend for an increase in the knockout animals that didn't quite reach statistical significance ($p=0.06$, Figure 19A, open bars). The major biochemical change observed at this age was a 4 fold increase in the covalent phosphate content of skeletal muscle glycogen in the *Epm2a-/-* animals (Figure 18A, open bars), with a corresponding increase in ethanol solubility (data not shown). Morphologically, the muscle glycogen granules in the 3 month old *Epm2a-/-* mice are relatively normal when viewed under the electron microscope (Figure 22C). Although this glycogen is somewhat poorly branched as judged by the iodine spectra (Figure 20A & B), the physico-chemical properties of the polysaccharide are for the most part, comparable to those of WT glycogen. Distribution of muscle glycogen between the LSS and the LSP displayed a similar trend to the older *Epm2a-/-* animals. Approximately 60-65% of the glycogen was recovered in the LSP after centrifugation of muscle extracts of the *Epm2a-/-* mice (Figure 30A & B). The glycogen synthase activity ratio (-/+ glucose-6P), as well as total glycogen synthase activity measured in the presence glucose-6P was unchanged in the knockout mice in both the LSS and the LSP (Figure 30C-F). Based on Western analysis, the level of AGL was unchanged in the *Epm2a-/-* in the LSS with no detectable protein in the LSP (Figure 31). As early as 3 months of age, the *Epm2a-/-* mice exhibit a redistribution of glycogen synthase protein from a soluble LSS to an insoluble LSP fraction (Figure 31).

During the preparation of this thesis, Moreno et al. (158) reported that a functional laforin-malin complex promotes the ubiquitination of AMP-activated protein kinase (AMPK), a heterotrimeric serine/threonine protein kinase that acts as an energy sensor. This ubiquitination occurred through the formation of lysine -63 linked ubiquitin chains which did not target AMPK for proteosomal

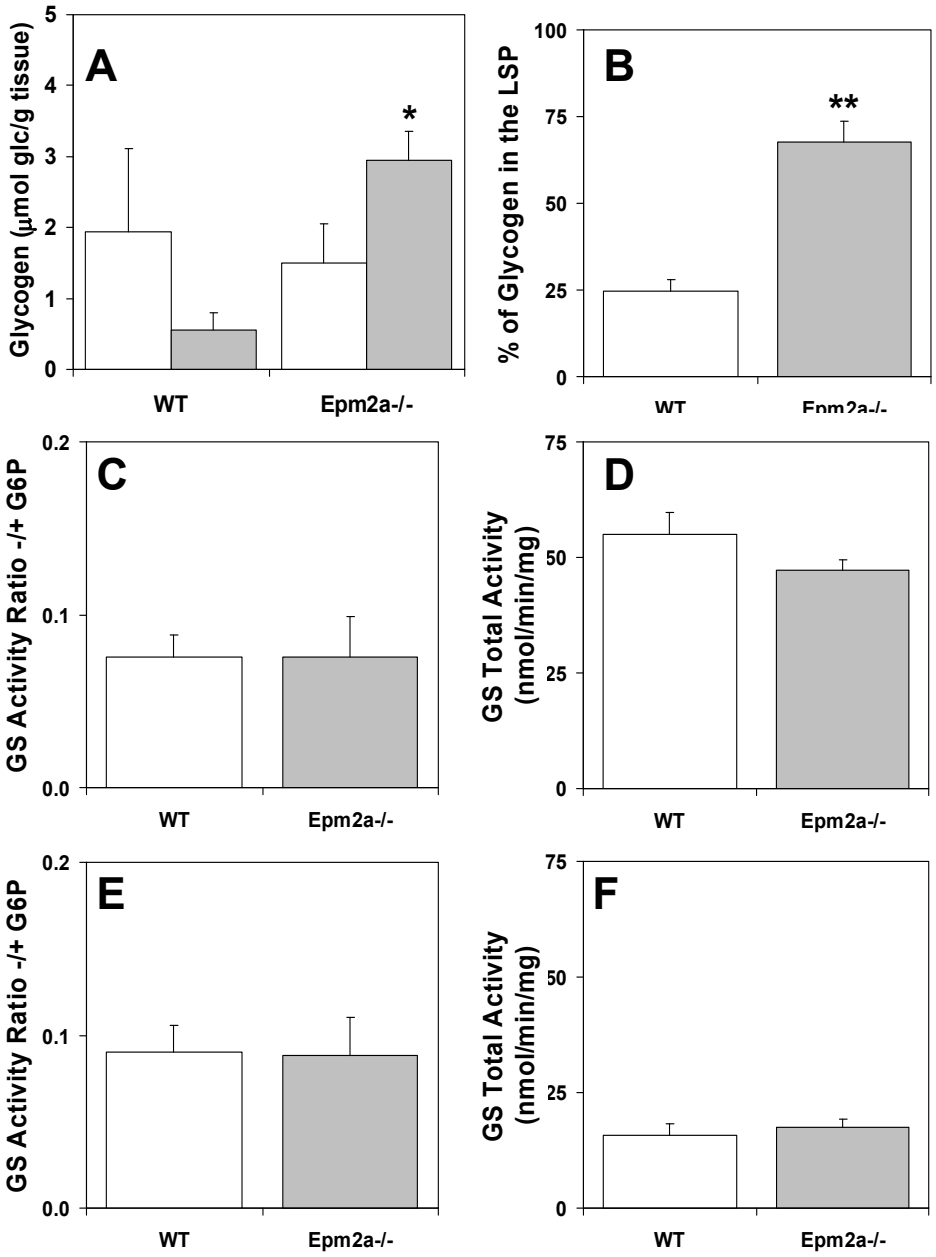

Figure 30. Skeletal muscle glycogen and glycogen synthase activity in 3 month old *Epm2a-/-* mice. Skeletal muscle extracts of WT and *Epm2a-/-* mice were analyzed. **A.** Glycogen levels in the LSS (open bars) and LSP (filled bars) of WT and *Epm2a-/-* mice. *p= 0.0078 vs WT LSP, (n=3). **B.** Percentage of glycogen in the LSP. **p= 0.004, (n=3). **C.** Glycogen synthase activity ratio in the LSS, (n=3). **D.** Total glycogen synthase activity in the LSS measured in the presence of glucose-6P, (n=3). **E.** Glycogen synthase activity ratio in the LSP, (n=3). **F.** Total glycogen synthase activity in the LSS measured in the presence of glucose-6P, (n=3).

degradation. However, the authors suggested that this modification increases the steady-state levels of at least the β-subunit of AMPK, possibly because it alters the subcellular distribution of the protein. AMPK is a trimer of three different subunits, α, β and γ. AMPKα is the catalytic subunit and contains a highly conserved kinase domain located at the N terminus of the protein (159). AMPKγ and AMPKβ are regulatory subunits and the latter contains a carbohydrate binding domain that associate with glycogen and has been proposed to be a sensor of glycogen levels (160). AMPK is regulated by allosteric activation by AMP and by the phosphorylation of Thr172 within the catalytic domain of the α-subunit by upstream kinases (161). Western analysis of the α-subunit of AMPK in the 3 month old *Epm2a-/-* mice revealed no changes between genotypes in the LSS. The level of AMPKα in the LSP was also unchanged in the knockout animals. These results are inconsistent with the model of Moreno et al. (158), as loss of laforin would disrupt the laforin-malin complex and lysine ubiquitination of AMPK resulting in lower levels of AMPK, or possibly an alteration in the distribution between the LSS and the LSP. Furthermore, phosphorylation of AMPK at Thr172 in the α-subunit, taken as a measure of protein kinase activity, was unaffected by disruption of the *Epm2a* gene (Figure 31).

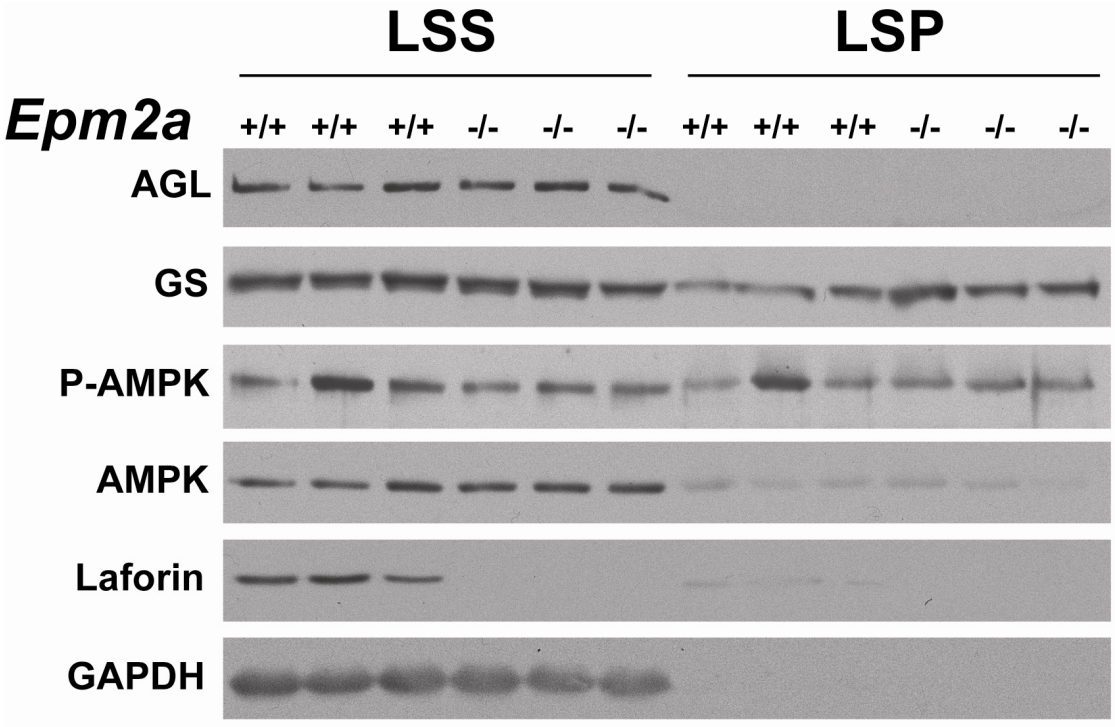

Figure 31. Analysis of glycogen metabolizing enzymes and related proteins in 3 month old *Epm2a-/-* mice. Skeletal muscle extracts from WT and *Epm2a*-/- mice were analyzed. AGL, glycogen synthase (GS), P-AMPK, AMPK and laforin protein levels in the LSS and LSP of WT and *Epm2a-/-* mice. GAPDH is shown as a loading control.

3. Generation and Analysis of *Epm2b-/-* Mice

3.1 Preamble

Dr. DePaoli-Roach's laboratory and our laboratory have recently developed and initially characterized mice in which the second gene involved in Lafora disease, *Epm2b* has been deleted**.** The data presented below were generated by a number of individuals in both laboratories. My contributions included: glycogen synthase and phosphorylase activity measurements, glycogen determinations, glycogen phosphate determinations, data collection and participation in the preparation of the manuscript that was recently published (96). The mice were generated and characterized under the leadership of Dr. Anna DePaoli-Roach. Processing of tissue was done by Anna DePaoli-Roach, Dyann M. Segvich, and Catalina Meyer. RTPCR and exercising of mice were performed by Jose M. Irimia who also helped with the histology. Western blot analysis and genotyping were performed by Anna DePaoli-Roach and Dyann M. Segvich. The manuscript was written by Peter Roach and Anna DePaoli-Roach.

3.2 Generation of *Epm2b-/-* mice

Disrupted ES C57BL/6N (10571D-E2) cells were purchased from the Knockout Mouse Project Repository (KOMP), University of California, Davis. The strategy for the disruption was to replace the complete *Epm2b* coding region plus 391 nucleotides of 3' UTR with a cassette containing the LacZ and the neo genes. The LacZ gene was fused in frame at the *Epm2b* ATG (Figure 32A). After expansion and confirmation of targeting by PCR analyses (Figure 32B), the cells were injected into C57Bl/6J blastocysts and the injected blastocysts were implanted in the uterus of pseudo-pregnant C57Bl/6J females for generation of chimeric mice. PCR genotyping of the chimeric mice showed that one male was positive for the disruption and was mated with C57Bl/6J females to test for germline transmission. Germline transmission of the disrupted allele gave heterozygous *Epm2b-/+* mice in a C57/Bl6 background. Progeny from crosses of heterozygous mice generated animals for characterization. Since we have been

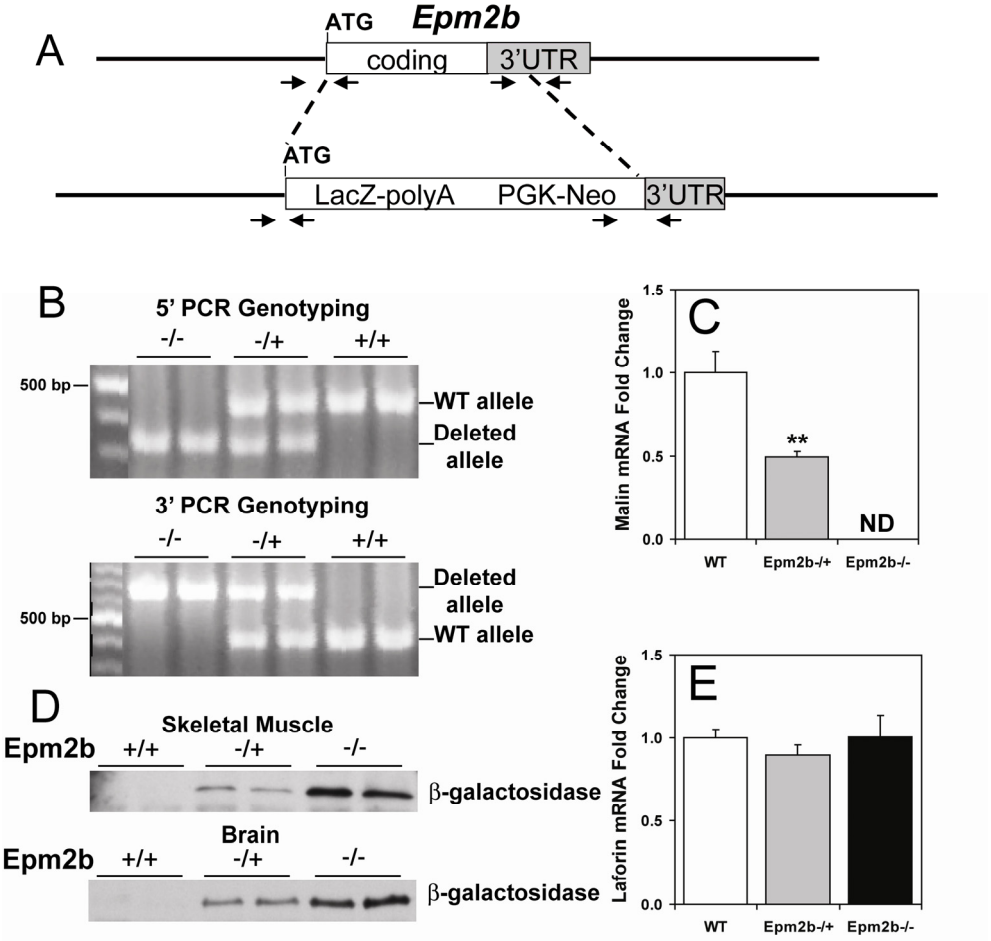

Figure 32. Targeted disruption of *Epm2b*. A. Strategy for the distruption of the *Epm2b* gene. Diagram of the *Epm2b* locus and targeted disruption of the coding region. Arrowheads indicate the position of the oligonucleode primers used for PCR genotyping. **B.** 5' and 3' PCR genotyping. The wild type and the disrupted alleles are indicated. **C, E.** Malin and laforin transcript levels. Malin and laforin mRNA levels were determined in skeletal muscle of 3 month old mice. **p< 0.01 vs WT, (n=4). ND indicates not detectable. **D.** β-galactosidase expression. Shown is a representative Western blot of β-galactosidase expression in skeletal muscle and brain of WT, heterozygous and homozygous null *Epm2b* mice, (n=8).

unable to obtain usable antibodies against mouse malin, we adopted several independent approaches to assure deletion. Standard PCR directed at both the 5'- and 3'-ends of the insertion clearly distinguished the wild type and mutant alleles (Figure 32B). Quantitative PCR was applied to determine message levels and did not detect malin message in *Epm2b-/- mice* (Figure 32C). Finally, the gene disruption strategy places β-galactosidase under the control of the malin promoter. Therefore, the presence of β-galactosidase marks the targeted deletion of *Epm2b* in tissues that express malin. Samples from brain and muscle of *Epm2b*-/+ and *Epm2b-/-* mice were positive for β-galactosidase by Western blotting whereas no signal was detected in the wild type mice (Figure 32D). From all of these criteria, we conclude that the *Epm2b-/-* mice indeed carry a disruption in both alleles of the gene. We also used quantitative PCR to analyze the laforin mRNA level and found no change in the *Epm2b-/-* mice (Figure 32E).

3.3 *Epm2b-/-* mice develop Lafora bodies by 3 months of age

A characteristic feature of Lafora disease is the presence of Lafora bodies in tissues. Therefore we analyzed various tissues for their presence. Sections from brain, skeletal muscle, heart and liver of 3 month old wild type and knockout mice were treated with diastase and then stained with periodic acid/Schiff (PASD) to visualize α-amylase resistant polysaccharide. PASD positive structures, indicative of Lafora bodies, were visible in most areas of the brain. They were most abundant in the cerebellum (Figure 33A) and were also plentiful in the hippocampus (Figure 33C) and cortex (data not shown) of *Epm2b-/-* animals. Comparable structures were absent in corresponding sections from wild type littermates (Figure 33B & D). Though less abundant than in brain, Lafora bodies were also readily detectable in heart muscle from knockout mice (Figure 33E) but not wild type littermates (Figure 33F). We have yet to complete a systematic survey of skeletal muscle but it is apparent that Lafora bodies are much more scarce in muscle than in brains or even hearts from *Epm2b-/-* mice at this age. We found some Lafora bodies in soleus muscle (Figure 33G) but not in wild type controls (Figure 33H). The lower incidence of Lafora bodies in skeletal

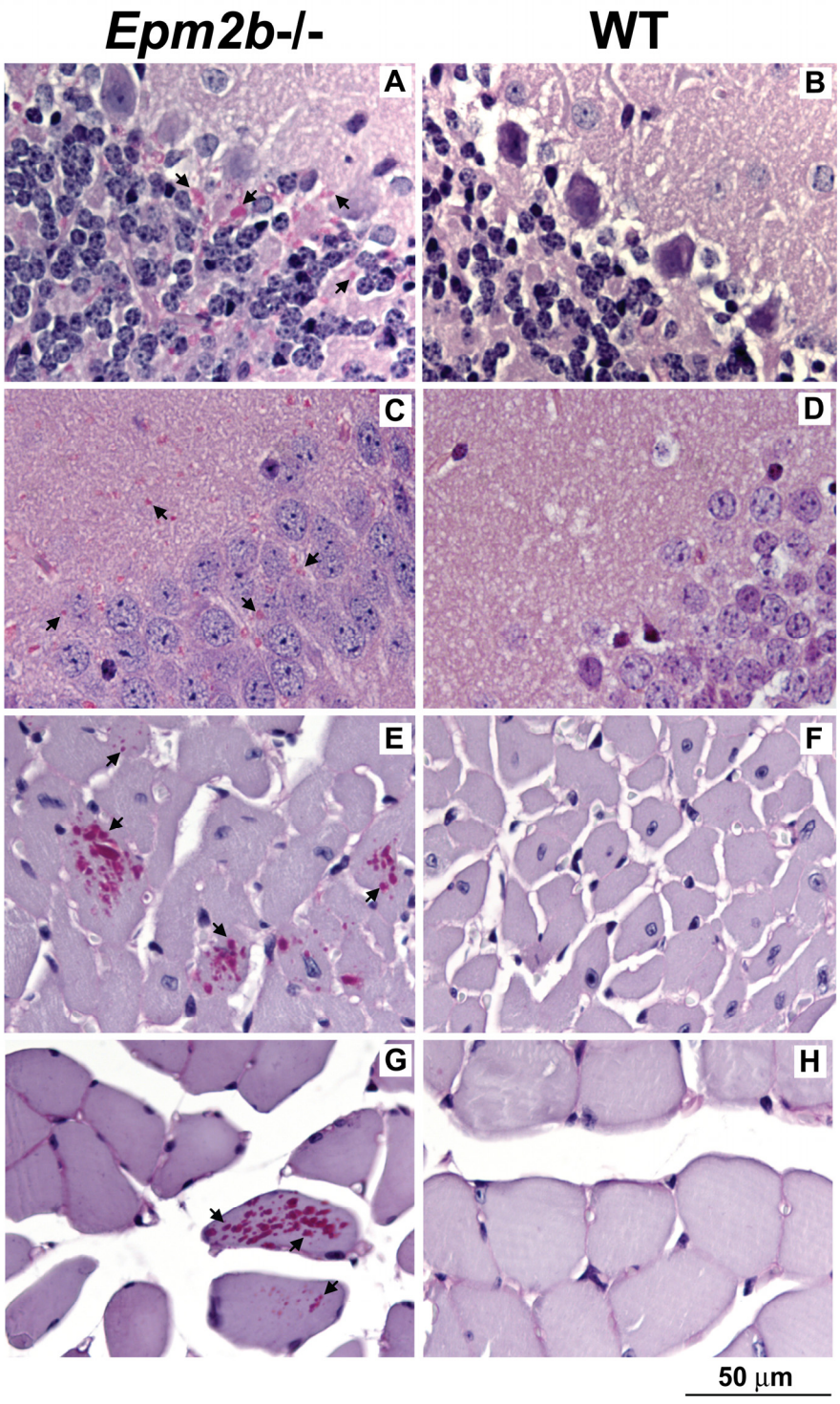

Figure 33. Lafora bodies in tissues of *Epm2b-/-* mice. Sections of brain, heart and skeletal muscle from 3 month old mice were stained with periodic acid/Schiff/diastase (PASD) to visualize α-amylase resistant polysaccharide, indicated by arrows. **A.** Cerebellum, *Epm2b-/-*; **B.** Cerebellum, wild type; **C.** Hippocampus, *Epm2b-/-*; **D.** Hippocampus, wild type; **E.** Heart, *Epm2b-/-*; **F.** Heart, wild type; G, soleus muscle, *Epm2b-/-*; **H.** soleus muscle, wild type.

muscle as compared with brain is consistent with the lesser degree of glycogen synthase and laforin redistribution to the insoluble LSP in these tissues (see Results Section 3.4). No Lafora bodies were detected in the livers of *Epm2b-/-* mice (data not shown).

3.4 Glycogen, glycogen metabolizing enzymes and related proteins in 3 month old *Epm2b-/-* mice.

Our systematic analysis of the *Epm2a-/-* mice found no evidence to support the imbalance hypothesis for the formation of Lafora bodies. Perhaps more important was the fact that glycogen synthase activity was unchanged and there were no significant alterations in any of the potential laforin-malin targets. Therefore, we extended our analyses of glycogen metabolism to the *Epm2b-/-* mice with emphasis on the levels of proteins proposed to be targets of malin, as *in vivo* substrates of the E3 ubiquitin ligase should be elevated in its absence. A small, but significant, increase in total glycogen was observed in muscle and brain from *Epm2b-/-* mice (Figure 34A & 35A). Low speed centrifugation of tissue extracts separates glycogen into the soluble supernatant (LSS) and the insoluble pellet (LSP). In muscle, the distribution of glycogen was unchanged (Figure 34B & C) but in brain there was a significant increase in the proportion of insoluble glycogen in tissue from *Epm2b-/-* mice (Figure 35B & C). Glycogen synthase total activity and -/+ glucose-6P activity ratios were unchanged in the knockout animals (Figure 36A-D & 37A-D), although in brain there was a trend to increased total activity in the LSP (Figure 37D). These results were confirmed by Western blotting with anti-glycogen synthase antibodies (Figure 40A & 41A), and in the case of brain the increased proportion of glycogen synthase in the LSP was statistically significant. Glycogen phosphorylase total activity, activation state (-/+ AMP activity ratio) and distribution between soluble and insoluble fractions in muscle and brain were unaffected by loss of the *Epm2b* gene (Figure 38A-D & 39A-D). The knockout animals did however display a significant increase in total phosphorylase activity in the LSP (Figure 39D). The level of the other metabolic enzyme analyzed debranching enzyme, was also unaltered in

,

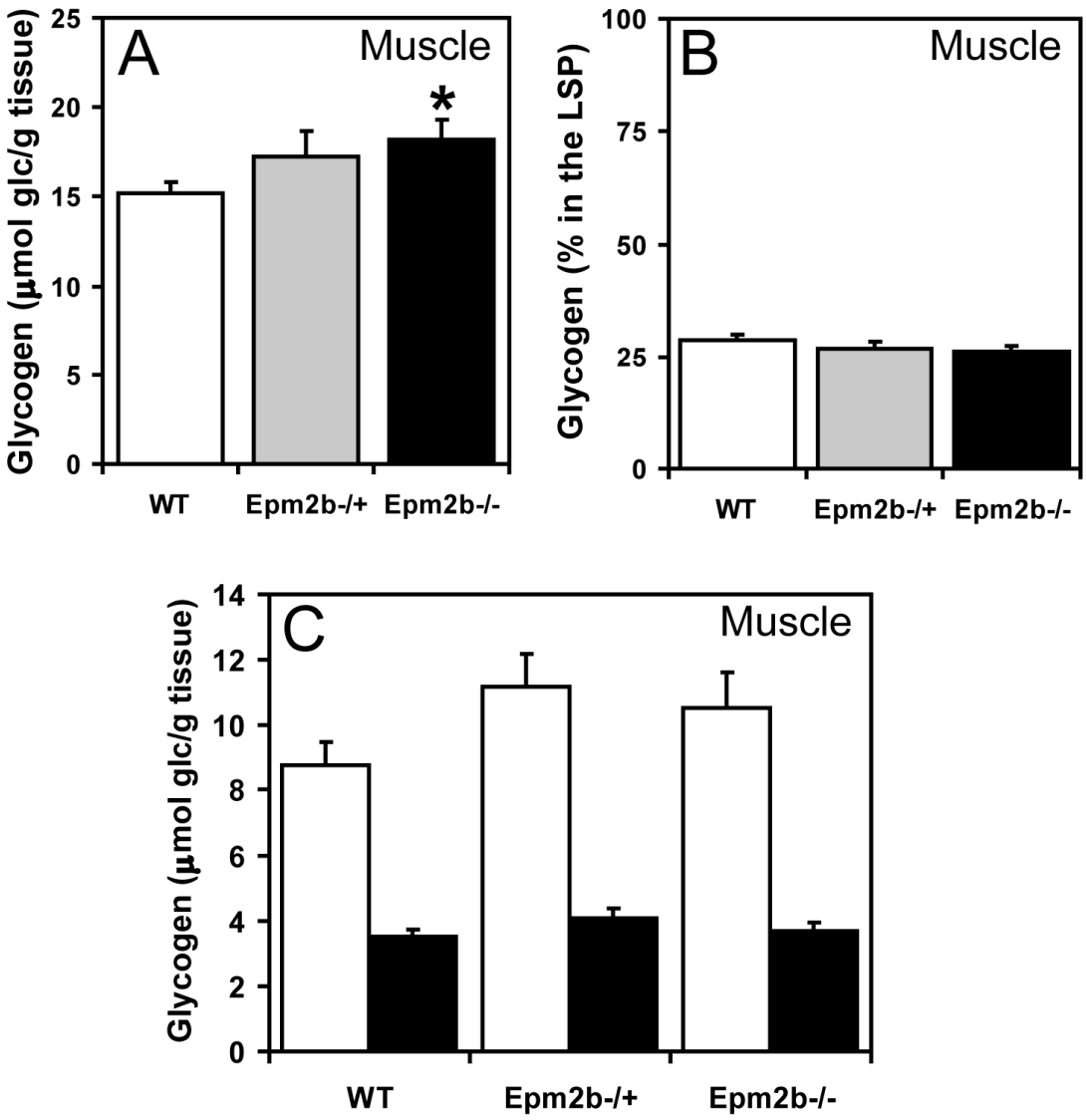

Figure 34. Glycogen levels in skeletal muscle of *Epm2b-/-* mice. Total glycogen levels and distribution of glycogen between the LSS and the LSP from 3 month old male WT, *Epm2b-/+* and *Epm2b-/-* mice was analyzed. **A.** Total skeletal muscle glycogen levels. *p< 0.05 vs WT, (n=8). **B.** Percentage of skeletal muscle glycogen in the LSP, (n=4). **C.** Skeletal muscle glycogen levels in the LSS (open bars) and LSP (filled bars), (n=4).

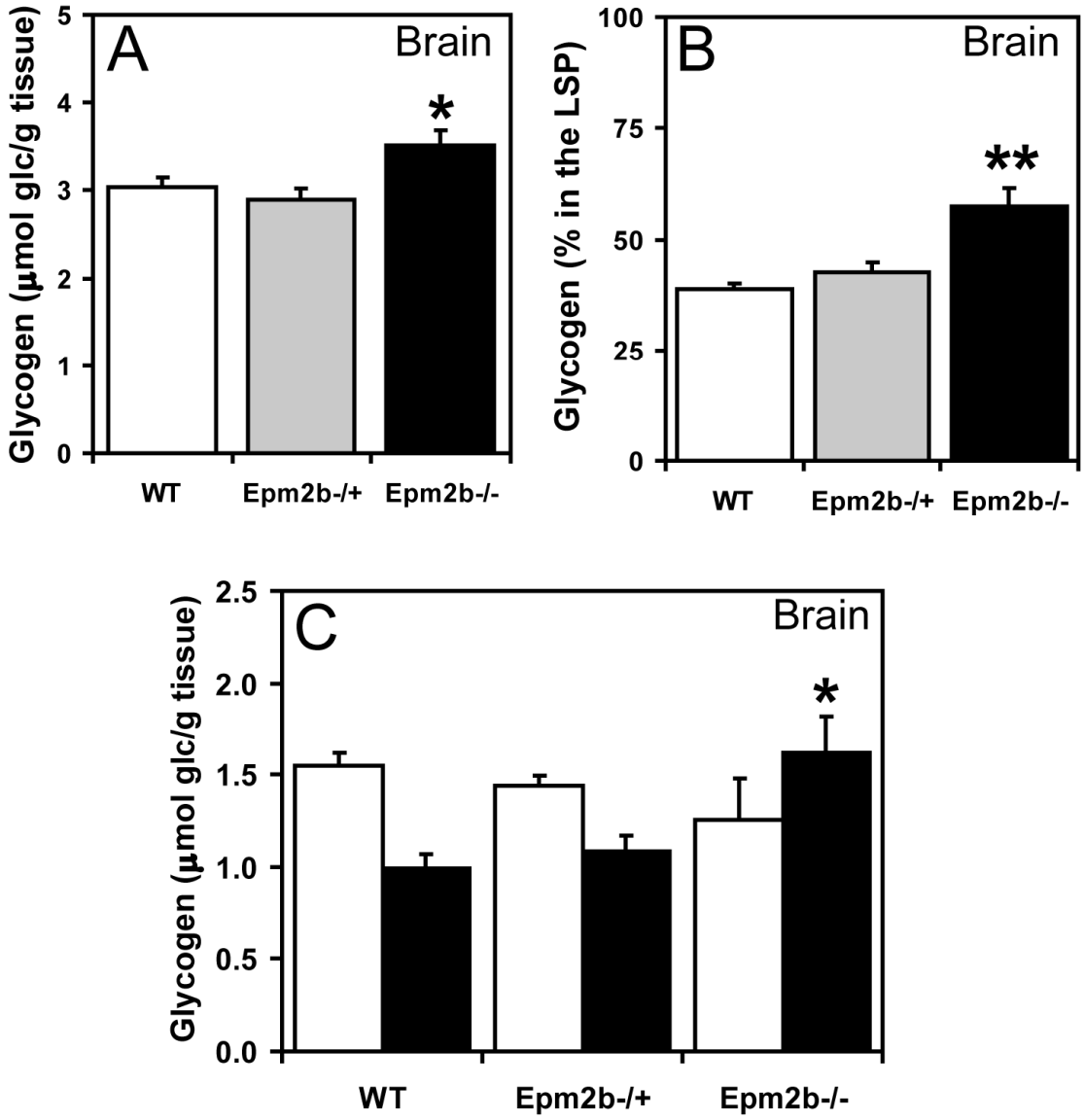

Figure 35. Glycogen levels in brain of *Epm2b-/-* mice. Total glycogen levels and distribution of glycogen between the LSS and the LSP from 3 month old male WT, *Epm2b-/+* and *Epm2b-/-* mice was analyzed. **A.** Total brain glycogen levels. *p< 0.05 vs WT, (n=8). **B.** Percentage of brain glycogen in the LSP. **p< 0.01 vs WT and *Epm2b-/+*, (n=6). **C.** Brain glycogen levels in the LSS (open bars) and LSP (filled bars). *p< 0.05 vs WT LSP, (n=6).

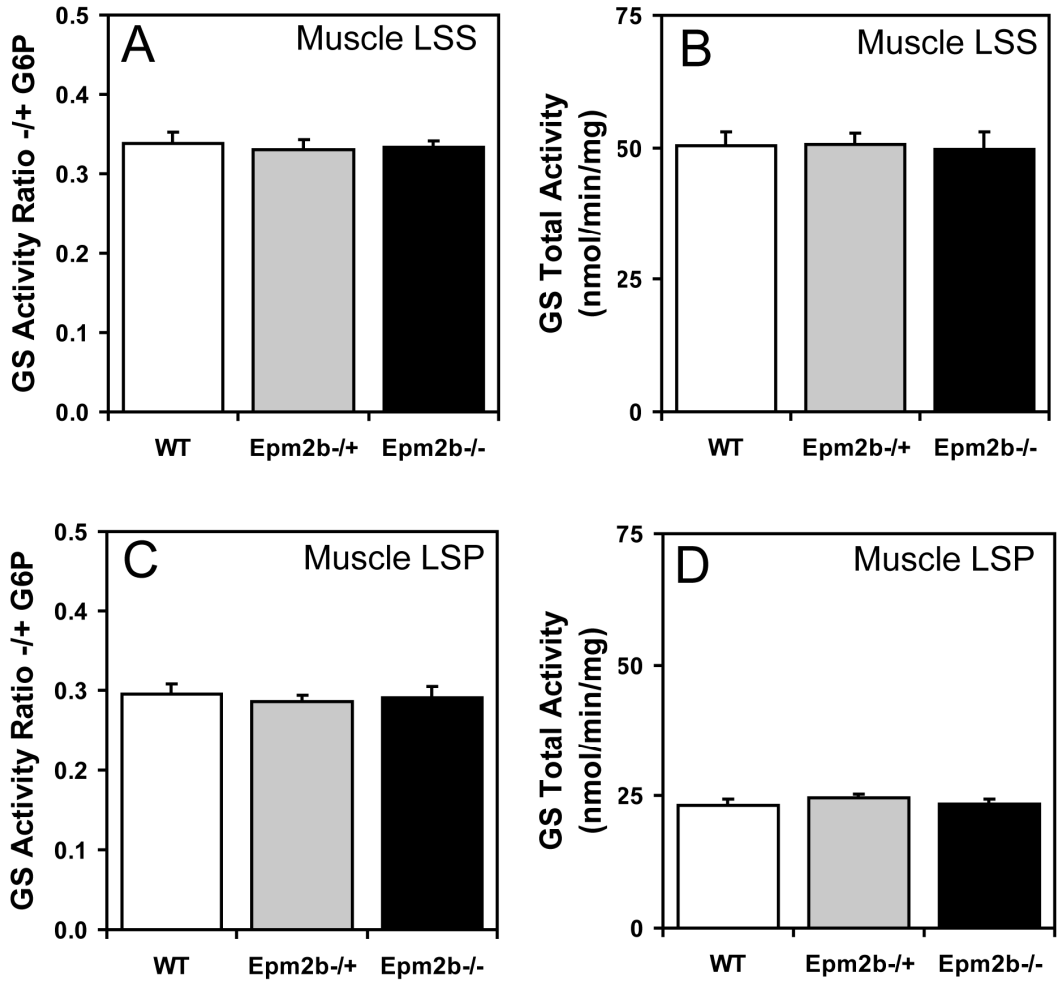

Figure 36. Glycogen synthase activity in skeletal muscle of *Epm2b-/-* mice. Skeletal muscle from 3 month old male WT, *Epm2b-/+* and *Epm2b-/-* mice was analyzed. **A.** Skeletal muscle glycogen synthase (GS) -/+ glucose-6P (G6P) activity ratio in the LSS, (n=8). **B.** Total skeletal muscle GS activity measured in the presence of G6P in the LSS, (n=8). **C.** Skeletal muscle GS -/+ G6P activity ratio in the LSP, (n=8). **D.** Total skeletal muscle GS activity in the LSP measured in the presence of G6P, (n=8).

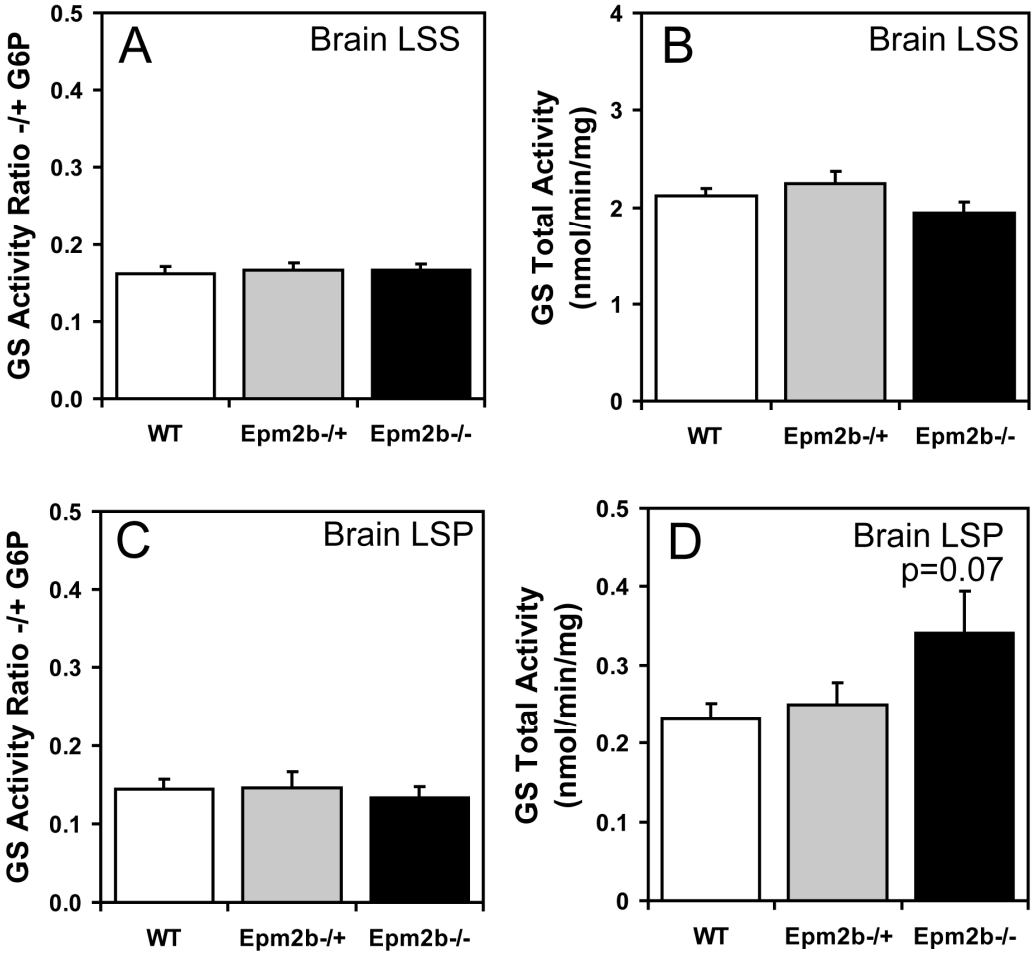

Figure 37. Glycogen synthase activity in brain of *Epm2b-/-* mice. Brain from 3 month old male WT, *Epm2b-/+* and *Epm2b-/-* mice was analyzed. **A.** Brain GS -/+ G6P activity ratio in the LSS, (n=8). **B.** Total brain GS activity in the LSS measured in the presence of G6P, (n=8). **C.** Brain GS activity ratio in the LSP -/+ G6P, (n=8). **D.** Total brain GS activity in the LSP measured in the presence of G6P, (n=8).

knockout animals (Figure 40A & 41A). In brain extracts, the signal by Western blotting was weak, and so the enzyme was enriched by high speed centrifugation of the LSS to produce a glycogen pellet. AGL levels in this pellet were the same in wild type and knockout mice (Figure 41B). Therefore, the only potentially significant changes associated with *Epm2b* disruption in these analyses was a slight increase in total glycogen and an enrichment of glycogen and glycogen synthase in the insoluble fraction in brain.

The type 1 protein phosphatase glycogen-binding subunit, PTG, has been proposed to be a target for malin-mediated ubiquitylation and degradation (117, 118). In order to detect PTG, it was necessary to prepare a high speed glycogen pellet. From analysis of this fraction, there was no change in PTG level in the *Epm2b-/-* mice (Figure 40C). We also analyzed the level of another glycogen-associated PP1 targeting subunit, R_{GL}/G_M (53) that is found in striated muscle, and observed no alteration in the *Epm2b-/-* mice (Figure 40B). As noted in the Introduction, GSK-3 was also considered a candidate to be a laforin substrate (104). We therefore analyzed GSK-3 total protein and phosphorylation of the inhibitory N terminal site. Neither parameter was affected by loss of the *Epm2b* gene, in either muscle or brain extracts (Figure 40B & 41C). We also analyzed the phosphorylation state of the eukaryotic initiation factor alpha (eIF2α), a marker for endoplasmic reticulum (ER) stress. No detectable changes were observed in the *Epm2b-/-* animals (Figure 40C).

Previous work has implicated laforin as a malin target (105) and has also suggested that malin and laforin function as a complex (122). Analysis of muscle extracts indicated a trend towards an increased distribution of laforin to the insoluble LSP (Figure 40A). However, from analysis of brain, there was a large increase in total laforin protein and a major, statistically significant redistribution of laforin to the LSP accompanied by clear depletion of the soluble LSS fraction in the *Epm2b-/-* mice (Figure 41A). In wild type animals, more than 90% of the laforin was in the soluble LSS fraction (Figure 41A & F) but in the knockout animals ~90% of the laforin was present in the insoluble LSP fraction (Figure 41A

& G). This result is the most striking biochemical difference that we have observed so far from study of the *Epm2b* knockout mice.

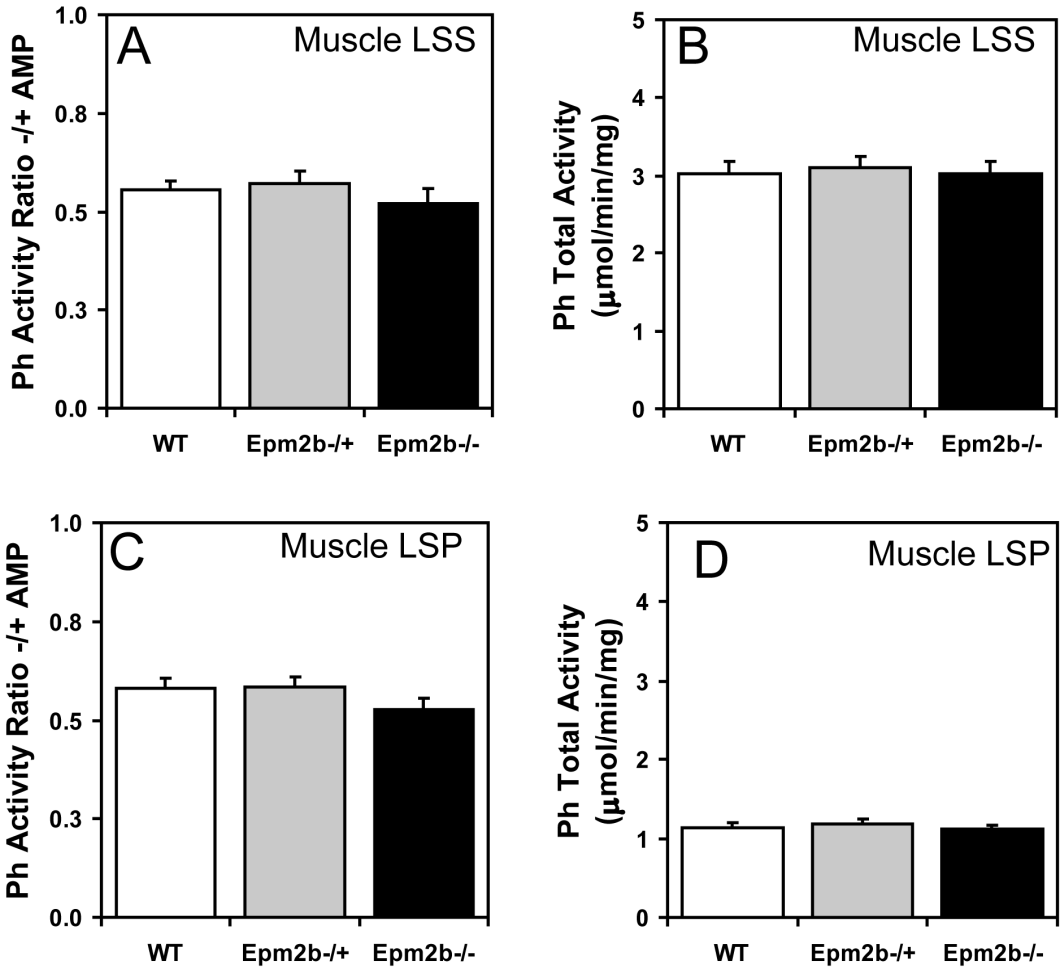

Figure 38. Glycogen phosphorylase activity in skeletal muscle of *Epm2b-/-* mice. Skeletal muscle from 3 month old male WT, *Epm2b-/+* and *Epm2b-/-* mice was analyzed. **A.** Skeletal muscle phosphorylase (Ph) -/+ AMP activity ratio in the LSS, (n=8). **B.** Total skeletal muscle Ph activity in the LSS, measured in the presence of AMP, (n=8). **C.** Skeletal muscle Ph -/+AMP activity ratio in the LSP, (n=8). **D.** Total skeletal muscle Ph activity in the LSP, measured in the presence of AMP, (n=8).

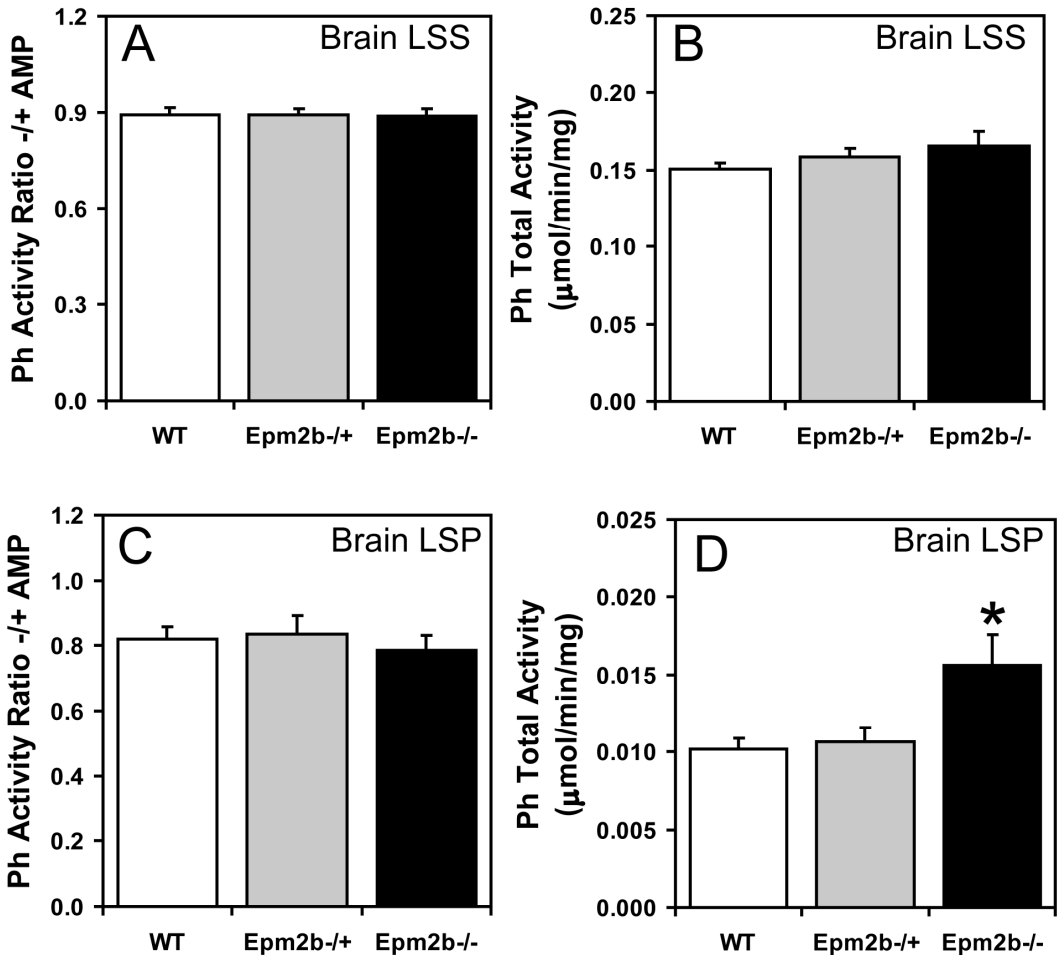

Figure 39. Glycogen phosphorylase activity in brain of *Epm2b-/-* mice. Brain from 3 month old male WT, *Epm2b-/+* and *Epm2b-/-* mice was analyzed. **A.** Brain phosphorylase (Ph) -/+ activity ratio in the LSP, (n=8). **B.** Total brain Ph activity in the LSS, measured in the presence of AMP, (n=8). **C.** Brain Ph -/+ AMP activity ratio in the LSP, (n=8). **D.** Total brain Ph activity in the LSP, measured in the presence of AMP. *p< 0.05 vs WT, (n=8).

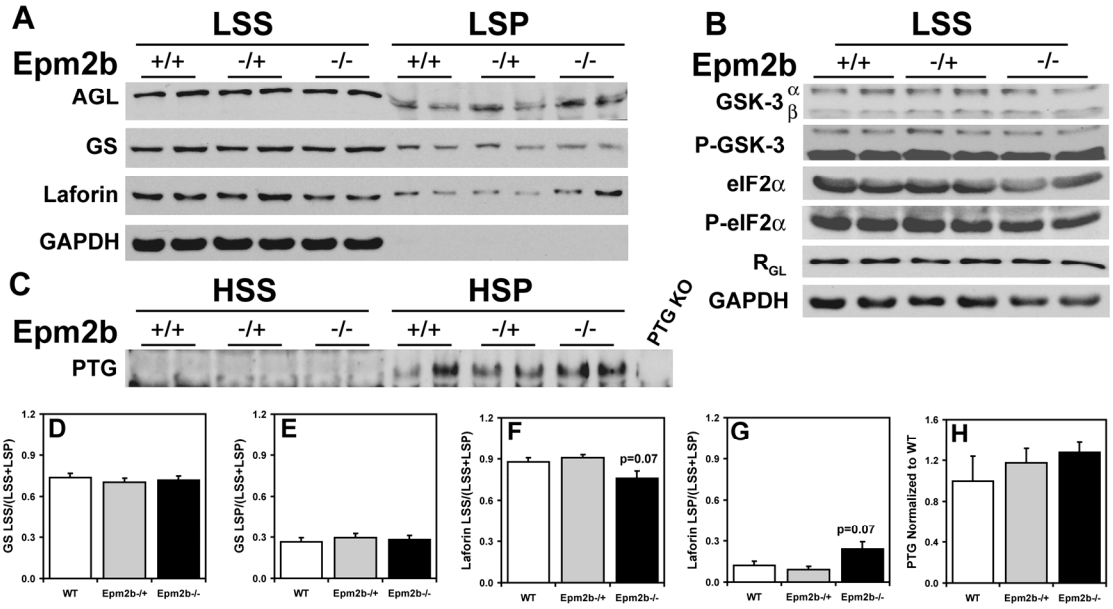

Figure 40. Glycogen metabolizing enzymes and related proteins in skeletal muscle of *Epm2b-/-* mice. Skeletal muscle from 3 month old male WT, *Epm2b-/+* and *Epm2b-/-* mice were analyzed**. A.** Distribution of AGL, GS and laforin protein levels in skeletal muscle LSS and LSP. Representative Western blots are shown from n=8. Comparable amounts of samples of the LSS and LSP were loaded. **B.** GSK-3, phospho-GSK-3, eIF2α, phospho-eIF2α and R_{GL} protein levels in the LSS. Representative Western blots are shown from (n=4). Same amounts of samples were loaded. GAPDH is used as loading control. **C.** PTG protein levels in the HSS and the HSP. Samples in the HSP pellet were enriched 5-times with respect to the HSS in order to allow detection. **D.** Quantitation of GS protein levels in the LSS, expressed as the ratio of protein in the LSS to the total protein (LSS + LSP), (n=8). **E.** Quantitation of GS protein levels in the LSP, expressed as the ratio of protein in the LSS to the total protein (LSS + LSP), (n=8). **F.** Quantitation of laforin protein levels in the LSS, expressed as the ratio of protein in the LSS to the total protein (LSS + LSP), (n=8). **G.** Quantitation of laforin protein levels in the LSP, expressed as the ratio of protein in the LSS to the total protein (LSS + LSP), (n=8). **H.** Quantitation of PTG protein levels in the HSP normalized to WT protein levels, (n=4).

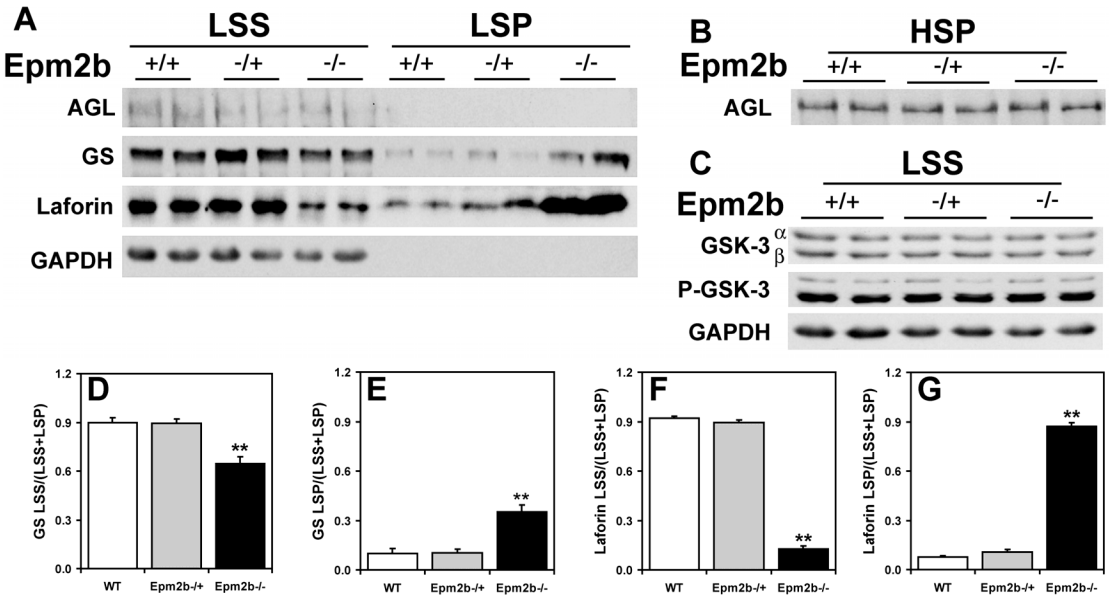

Figure 41. Glycogen metabolizing enzymes and related proteins in brain of *Epm2b-/-* mice. Skeletal muscle from 3 month old male WT, *Epm2b+/-* and *Epm2b-/-* mice were analyzed. **A.** Distribution of AGL, GS and laforin protein levels in brain LSS and LSP. Representative Western blots are shown from (n=5-8). LSP of AGL and GS are enriched ~2.5-fold as compared to LSS because of the low protein concentration in the pellet fraction whereas LSP of laforin are enriched only by 50%. **B.** AGL protein levels in the HSP enriched 2.5-fold with respect to the LSS, (n=4). **C.** GSK-3 and phospho-GSK-3 protein levels in the LSS, (n=4). **D.** Quantitation of GS protein levels in the LSS, expressed as the ratio of protein in the LSS to the total protein (LSS + LSP), normalized for equal sample loading. **p= 0.0002, (n=8). **E.** Quantitation of GS protein levels in the LSP, expressed as the ratio of protein in the LSS to the total protein (LSS + LSP), normalized for equal sample loading. **p= 0.0002, (n=8). **F.** Quantitation of laforin protein levels in the LSS, expressed as the ratio of protein in the LSS to the total protein (LSS + LSP), normalized for equal sample loading. **p< 0.0001, (n=5). **G.** Quantitation of laforin protein levels in the LSP, expressed as the ratio of protein in the LSS to the total protein (LSS + LSP), normalized for equal sample loading. **p< 0.0001, (n=5).

3.5 Effect of AMPK activation on glycogen metabolizing enzymes

Solaz-Fuster et al. (116) have proposed that AMPK phosphorylates laforin, controls its association with malin and thereby regulates laforin and malin targets. AMPK was also reported to phosphorylate the PTG protein phosphatase subunit and target it for degradation by the malin-laforin complex (120). Muscle AMPK was therefore activated *in vivo* by exercising wild type mice to exhaustion on a treadmill. Glycogen was significantly depleted by this exercise regimen (Figure 42C) with concomitant activation of glycogen synthase, as judged by the -/+ glucose-6P activity ratio (Figure 42A) and Western analysis of the phosphorylation of site 3a (Figure 42D). A six-fold increase in the activation state of AMPK was observed as judged by the ratio of phospho-AMPK to total AMPK (Figure 42E). Under these conditions, no changes were observed in the protein levels of glycogen synthase, debranching enzyme, laforin and R_{GL} (Figure 42D & E). Interestingly PTG protein levels were increased in response to exercise, opposite to what would be expected if AMPK phosphorylation targeted it for degradation (Figure 42F). This result is also consistent with activation of glycogen synthase (Figure 42A). We therefore find no evidence to support a role for AMPK in degradation of these proteins via malin or any other mechanism.

3.6 Glycogen phosphate levels are unchanged in skeletal muscle and liver of the *Epm2b-/-* mice

Our hypothesis is that Lafora bodies are formed by excessive glycogen phosphorylation that eventually alters the physico-chemical properties of the polysaccharide resulting in a loss of solubility. This hypothesis is supported by our analysis of the *Epm2a-/-* mice and the observation that glycogen phosphate levels are elevated. Analysis of muscle glycogen phosphate levels in the *Epm2b-/-* mice revealed no differences between genotypes (Figure 43A), consistent with the fact that Lafora bodies have not been observed in the majority of skeletal muscle sections analyzed by PASD staining. Lafora bodies were only detected in the soleus muscle of the *Epm2b-/-* mice, which represents a small fraction of the total skeletal muscle. Furthermore, Lafora bodies were detected in

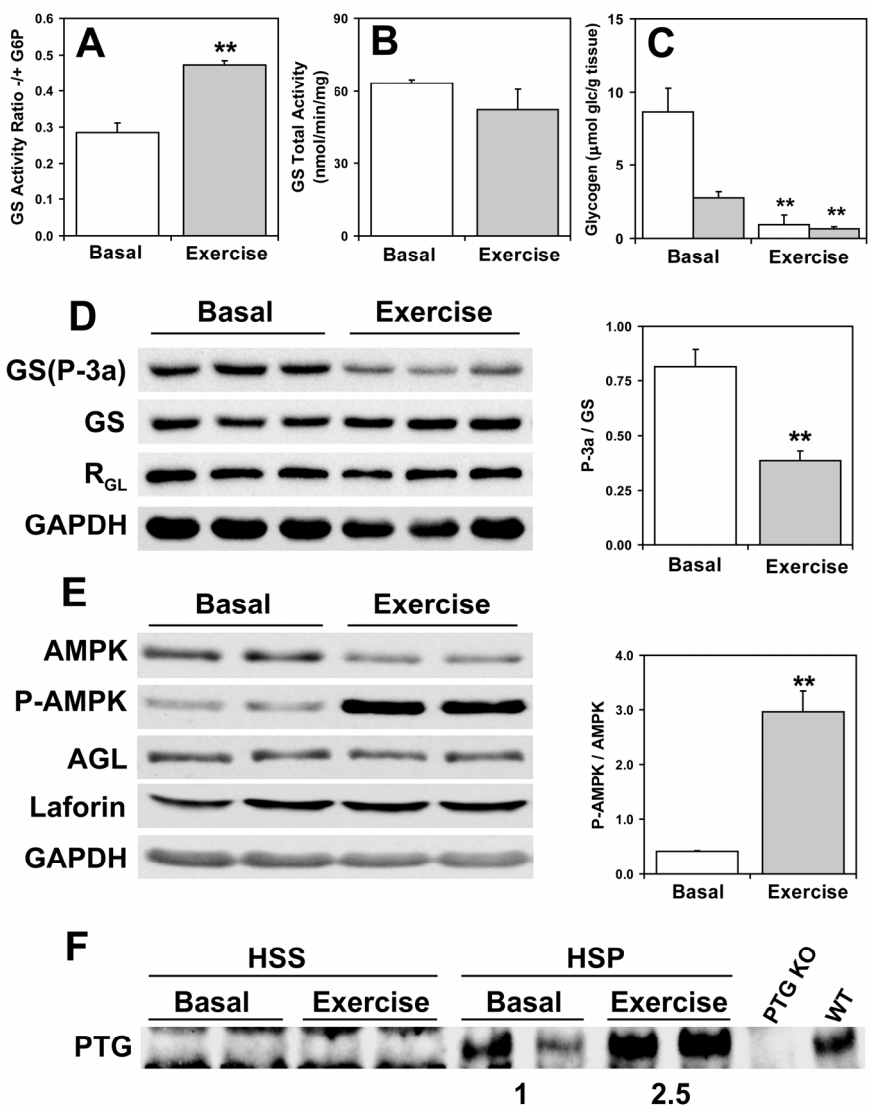

Figure. 42. Effect of AMPK activation on glycogen metabolizing enzymes and related proteins in skeletal muscle of exercised mice. Skeletal muscle of 3 month old WT male mice exercised to exhaustion were analyzed. **A.** GS -/+ G6P activity ratio in the LSS of basal and exercised mice. **p< 0.01, (n=3). **B.** Total GS activity in the LSS measured in the presence of G6P of basal and exercised mice, (n=3). **C.** Skeletal muscle glycogen levels in the LSS (open bars) and LSP (filled bars) of basal and exercised mice, (n=3). **D.** Western blots of phosphorylated GS (site 3a), total GS and R_{GL} in basal and exercised mice, and quantitation of GS site 3a phosphorylation. **p< 0.01, (n=3). **E.** Western blots of phosphorylated AMPK, total AMPK, AGL and laforin, and quantitation of AMPK phosphorylation in basal and exercised mice **p< 0.01, (n=3). **F.** PTG protein levels in the HSS and HSP of basal and exercised mice. HSP samples are enriched 4-fold with respect to the HSS.

a limited number of cells in soleus. Therefore it is unlikely that our measurements would be sensitive enough to detect alterations in glycogen phosphate levels associated with such a small fraction of the muscle positive for Lafora bodies. Consistent with the lack of Lafora bodies in liver sections, glycogen phosphate levels were normal in liver glycogen analyzed from the *Epm2b-/-* mice (Figure 43B). Due to the low quantity of brain glycogen, it was not feasible to measure covalent phosphate levels.

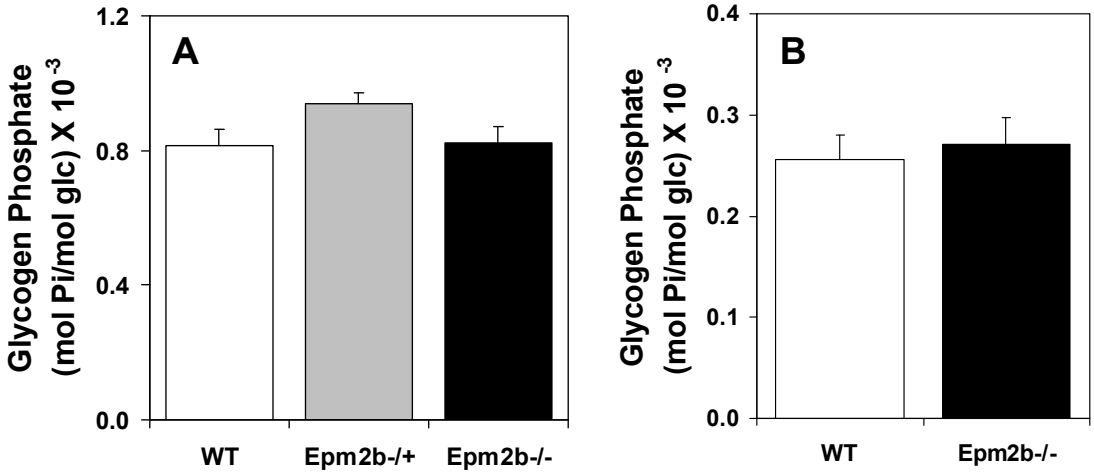

Figure 43. Glycogen phosphate levels in *Epm2b-/-* mice. Glycogen was purified from skeletal muscle and liver for analysis of covalent phosphate. **A.** Skeletal muscle glycogen phosphate levels of 3 month old WT (white bar), *Epm2b-/+* (grey bar) and *Epm2b-/-* (black bar) mice, (n=9-10). **B.** Liver glycogen phosphate levels of 3 month old WT (white bars) and *Epm2b-/-* (black bars) mice, (n=8).

4. The Incorporation of Phosphate into Glycogen

4.1 Synthesis of [β^{32}P]UDP-glucose, [β^{32}P]UDP-[2-deoxy]-glucose and [β^{32}P]UDP-[3-deoxy]-glucose

Lomako et al. (4) proposed that a UDP-glucose:glycogen:glucose-1-phosphotransferase transferred the β phosphate from UDP-glucose into glycogen when rabbit skeletal muscle extracts were incubated with [β-^{32}P]UDP-glucose and glycogen. However, the enzyme was never identified or characterized at the molecular level. In light of these results, we synthesized [β-^{32}P]UDP-glucose in an attempt to identify the enzyme responsible for phosphorylating glycogen. [β-^{32}P]UDP-glucose was synthesized enzymatically as described under Experimental Procedures (Figure 13) and purified using acid washed charcoal. Starting with [γ-^{32}P]ATP, UDP-glucose can be produced by the combined actions of hexokinase, phosphoglucomutase and UDP-glucose pyrophosphorylase. The purification is based on the fact that sugars do not bind activated charcoal, but nucleotides bind with high affinity. Given that UDP-glucose contains both a sugar and a nucleotide moiety, it can be purified from unreacted components of the reaction mixture by binding to charcoal and eluting under alkali conditions, sufficient to remove UDP-glucose from the charcoal without eluting non-sugar based nucleotides. HPTLC and autoradiography revealed the presence of one radiolabeled species that had an identical R_f value as UDP-[U-^{14}C]glucose (Figure 44A) and unlabelled UDP-glucose (data not shown). Treatment of [β-^{32}P]UDP-glucose with UDP-glucose pyrophosphatase, a NUDIX hydrolase that hydrolyses the pyrophosphate bond of UDP-glucose, generated glucose-1^{32}P (Figure 44A & B). The reaction is dependent on a divalent cation and was terminated with equimolar amounts of EDTA (see Results Section 7.1). Furthermore incubation of [β-^{32}P]UDP-glucose with glycogen synthase in the presence of rabbit liver glycogen resulted in the complete consumption of [β-^{32}P]UDP-glucose and a product that migrated with a similar R_f value as [β^{32}P]UDP (Figure 45). [β^{32}P]UDP-[2-deoxy]-glucose and

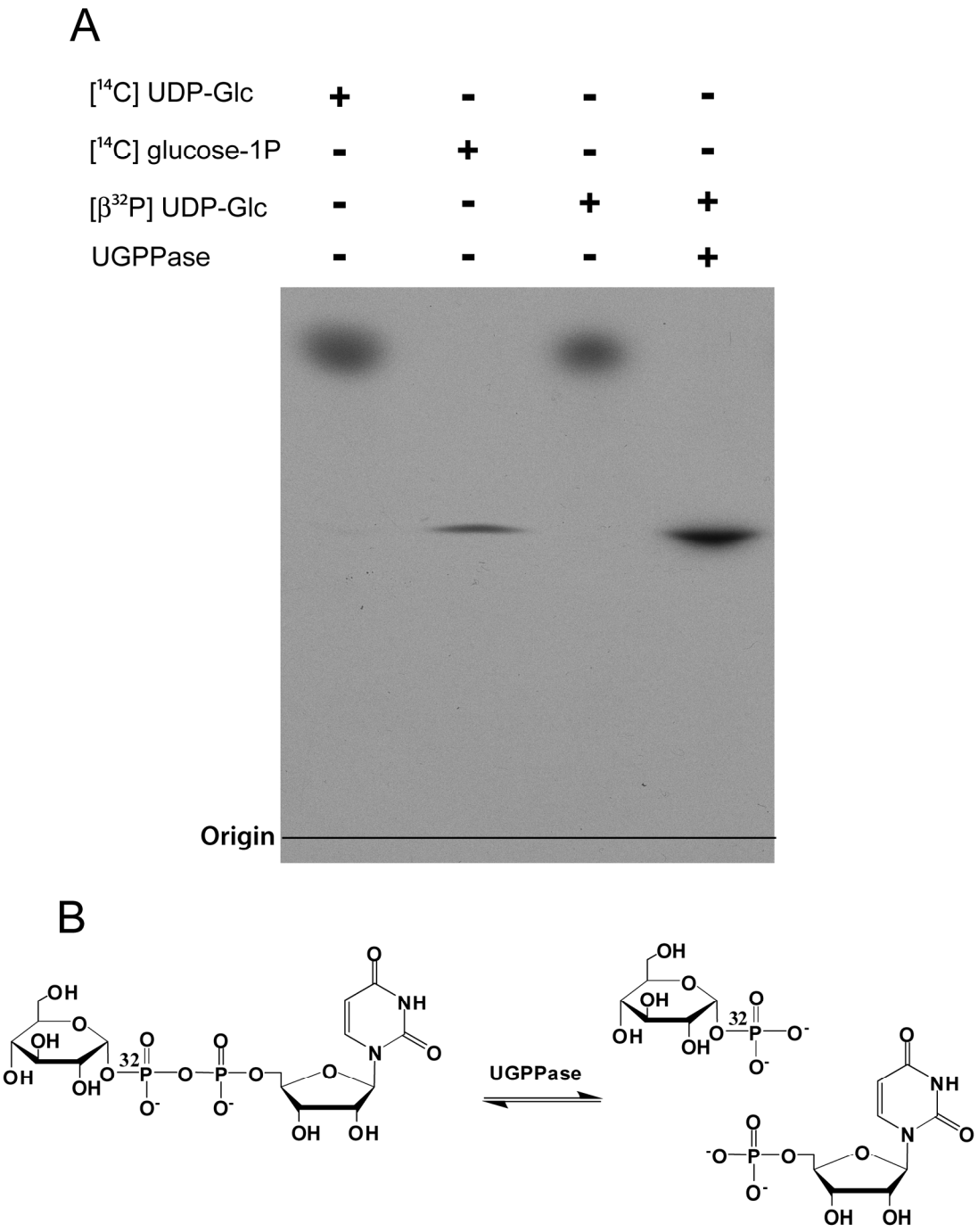

Figure 44. Synthesis of [β-^{32}P]UDP-glucose. [β-^{32}P]UDP-glucose was synthesized enzymatically and purified using acid washed charcoal. **A.** HPTLC and visualization by autoradiography of [β-^{32}P]UDP-glucose treated with and without UDP-glucose pyrophosphatase (UGPPase). Standard UDP-[U-^{14}C]glucose and [U-^{14}C]glucose-1P are shown. **B.** The reaction catalyzed by UGPPase.

[β^{32}P]UDP-[3-deoxy]-glucose were also synthesized as above with the exception that the starting product was 2-deoxy-glucose and 3-deoxyglucose instead of glucose, respectively. Both UDP-glucose derivatives migrated at the same R_f value as [β-^{32}P]UDP-glucose during HPTLC. Although less pure than [β-^{32}P]UDP-glucose, these derivatives were also consumed when incubated with glycogen synthase in the presence of glycogen (Figure 45).

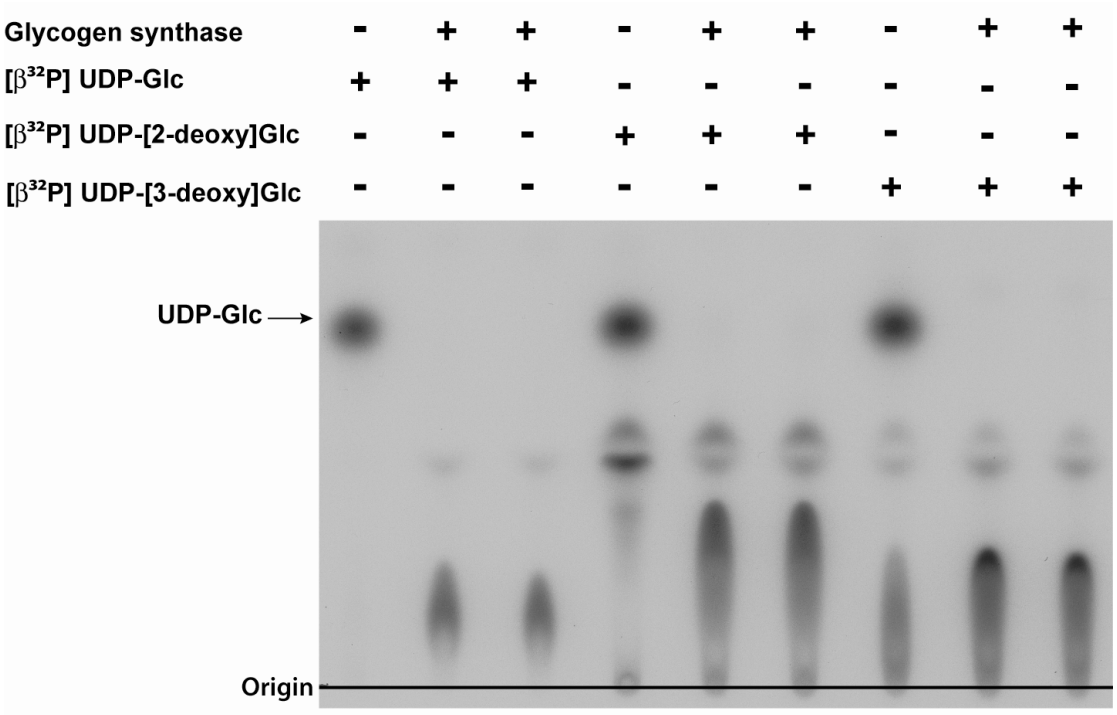

Figure 45 Reactivity of [β-^{32}P]UDP-glucose and derivatives towards glycogen synthase. HPTLC and visualization by autoradiography of [β-^{32}P]UDP-glucose, [β^{32}P]UDP-[2-deoxy]-glucose and [β^{32}P]UDP-[3-deoxy]-glucose treated with or without glycogen synthase. Radiolabeled UDP-glucose was consumed upon treatment with glycogen synthase

4.2 Glycogen synthase phosphorylates glycogen by transferring the β-phosphate from UDP-glucose into glycogen

In plant starch, C6 and C3 phosphomonoesters are formed by a unique set of dikinase enzymes, found only in plants, by transfer of the β-phosphate in ATP to C3 and C6 glucose hydroxyls in amylopectin (8). Extensive bioinformatic analysis of mammalian genomes has failed to reveal any analogous enzymes. However, we demonstrate that glycogen synthase transfers the β-phosphate from UDP-glucose into glycogen. Traditionally, glycogen synthase activity is measured by the incorporation of [U-^{14}C]glucose from UDP-[U-^{14}C]glucose using a filter paper assay (142). By this procedure, ^{14}C-labeled glycogen precipitates on filter papers when exposed to ethanol. The unreacted isotope is removed by extensive washing and the ^{14}C-labeled glycogen is quantified by scintillation counting. In our initial studies using purified rabbit skeletal muscle glycogen synthase to elongate exogenously added glycogen in the presence of [β^{32}P]UDP-glucose, using the filter paper assay, we noticed that the [β^{32}P]UDP formed bound to the filter papers (data not shown). Therefore we resorted to an additional purification step. The large molecular weight of glycogen does not allow it to enter polyacrylamide gels when subjected to SDS PAGE. The unreacted metabolites, such as UDP, will migrate through the gel leaving only the glycogen in the well. This method has been used successfully in the past to visualize ^{14}C-labeled glycogen (162). By this method we were able to demonstrate that the incorporation of phosphate into glycogen by glycogen synthase using [β^{32}P]UDP-glucose was time dependent (Figure 46B) and the rate of incorporation of phosphate, was in relative terms, equal to that of ^{14}C glucose incorporation using UDP-[U-^{14}C]glucose as the glucosyl donor (Figure 46 A-C). The absolute rate of phosphate incorporation was ~1 phosphate molecule introduced every 10,000 glucoses incorporated into glycogen. In an attempt to confirm that the radio-labeled spot on the gel was glycogen, and not an artifact of the reaction, the polysaccharide was digested with α-amylase and amyloglucosidase to hydrolyze the glycosidic linkages. Treatment with

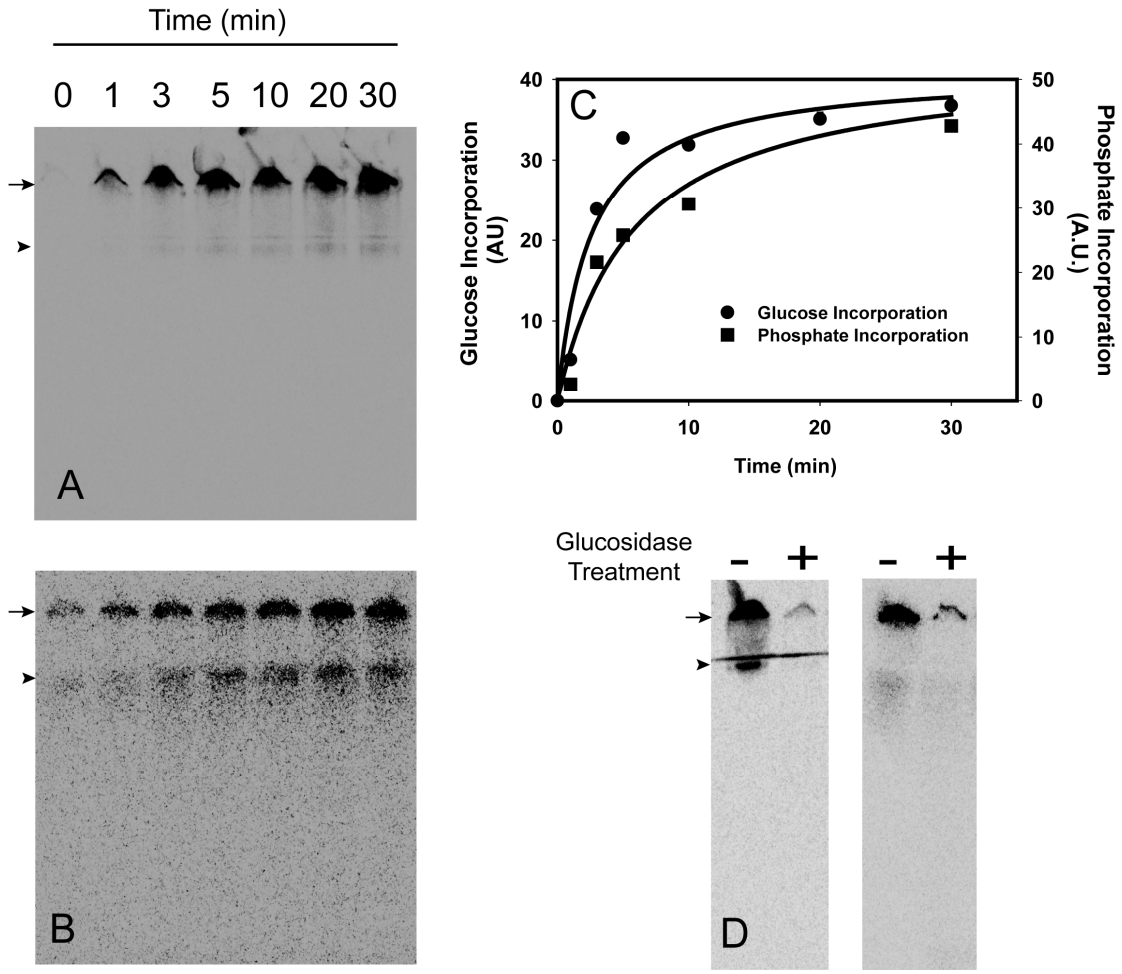

Figure 46. Glycogen synthase incorporates the β-phosphate of UDP-glucose into glycogen during synthesis. A 10% polyacrylamide gel was subjected to phosphorimaging to visualize radiolabeled glycogen**. A.** Phosphorimage depicting the time dependent incorporation of ^{14}C glucose into glycogen using UDP-[U-^{14}C]glucose as the glucosyl donor. **B.** Time dependent incorporation of ^{32}P into glycogen using [β-^{32}P]UDP-glucose as the phosphoryl donor. **C.** Relative quantitation of A. and B. **D.** Digestion of radiolabeled glycogen with the glycogen hydrolyzing enzymes α-amylase and amyloglucosidase. Arrows indicate the bottom of the well, and arrow heads the bottom of the stacking gel.

glucosidases eliminated all the radiolabel from both the ^{14}C and ^{32}P labeled glycogen.

Muscle glycogen synthase knockout mice, MGSKO, which lack the *Gys1* gene, do not accumulate glycogen in skeletal muscle and have no detectable glycogen synthase protein as judged by Western blotting (163). Extracts from muscle of these mice catalyzed minimal formation of ^{14}C-labeled glycogen (Figure 47, left panel). When extracts of wild type mice were incubated with [β-^{32}P]UDP-glucose, we observed high molecular ^{32}P-labeled material of the same mobility as the ^{14}C-labeled glycogen and which was also substantially reduced by treatment with glucosidases (Figure 47). Interestingly, formation of high molecular weight material was not above background when the extract came from MGSKO mice (Figure 47, right panel). We conclude first that ^{32}P can be incorporated into glycogen from [β-^{32}P]UDP glucose by enzyme(s) present in mouse muscle and secondly that the primary enzyme responsible is glycogen synthase.

4.3 Laforin removes phosphate incorporated by glycogen synthase

The UDP-glucose: glycogen glucose-1-phosphotransferase described by Lomako et al. (5) was proposed to transfer the β-phosphate of UDP-glucose into glycogen with the formation a C1-O-P-O-C6 bridging phosphodiester. Perhaps the most obvious mechanism for the incorporation of phosphate into glycogen catalyzed by glycogen synthase would be through the formation of a C1-O-P-O-C4 phosphodiester. This is based on the notion that the non-reducing C4-OH in the acceptor glycogen particle is thought to act as a nucleophile, attacking the C1 carbon of glucose in UDP-glucose with the subsequent formation of an α-1,4-glycosidic linkage. We originally hypothesized that the 4-OH of glycogen would attack the electrophilic β-phosphate of UDP-glucose forming a C1-O-P-O-C4 phosphodiester linkage necessitating the action of a phosphodiesterase prior to laforin action to remove the phosphate. In our *in vitro* characterization of laforin action, we were unable to detect activity towards the commercially available *p*-nitrophenolphosphocholine or *p*-nitrophenyl phenylphosphonate, two commonly

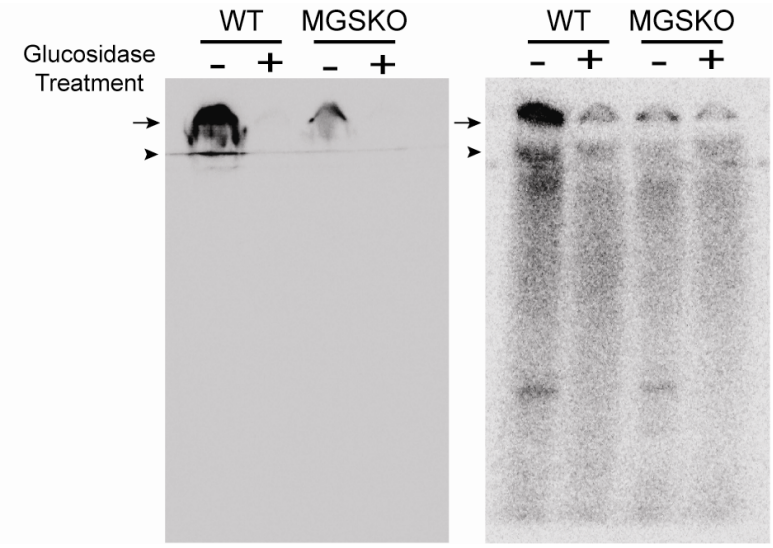

Figure 47. Phosphorylation of glycogen using mouse skeletal muscle extracts. Extracts from WT and MGSKO mice were used. Phosphorimage depicting the incorporation of [U-^{14}C]glucose (left) and ^{32}P (right) into glycogen from UDP-[U-^{14}C]glucose and [β-^{32}P]UDP-glucose respectively using mouse skeletal muscle extracts as the source of the enzyme. Treatment with α-amylase and amyloglucosidase is shown to confirm incorporation of radioactivity into glycogen. Arrows indicate the bottom of the well, and arrow heads the bottom of the stacking gel.

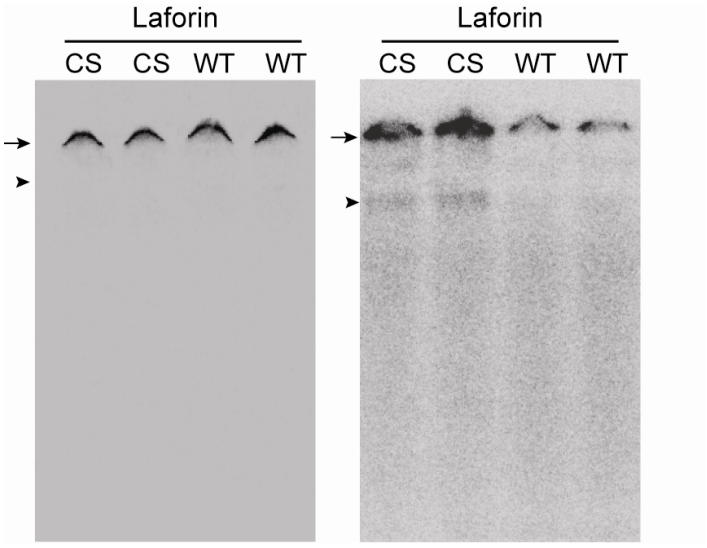

Figure 48. Laforin hydrolyzes phosphate introduced by glycogen synthase. ^{14}C labeled glycogen (left panel) and ^{32}P labeled glycogen (right panel was prepared, purified by ethanol precipitation and subjected to treatment with either catalytically inactive C266S, laforin (CS) or active (WT) laforin. Arrows indicate the bottom of the well, and arrow heads the bottom of the stacking gel.

used chromogenic phosphodiesterase substrates. An interesting phosphodiesterase candidate comes from examination of the human proteins containing carbohydrate binding domains. The CAZy database (www.cazy.org) lists a total of 37 human genes encoding proteins with predicted carbohydrate binding modules (CBM), grouped in four families (164). CBM20 has three entries, laforin, genethonin and an uncharacterized protein KIAA1434. KIAA1434 has a C terminal domain with similarity to glycerophosphoryl diester diesterases (GDPDs). We obtained the cDNA of this protein and subcloned it into pET28a and expressed the protein in bacteria followed by purification by affinity chromatography using Ni-NTA agarose. After incorporating ^{32}P into glycogen with glycogen synthase, we wondered whether the ^{32}P could be hydrolyzed by laforin in the presence of KIAA1434. Surprisingly laforin was able to hydrolyze the ^{32}P label whether KIAA1434 was included or not (data not shown). Incubation of ^{32}P labeled glycogen with either WT laforin or catalytically inactive C266S laforin clearly demonstrated that laforin was capable of removing the majority of the ^{32}P label incorporated by glycogen synthase (Figure 48, right panel), without affecting ^{14}C labeled glycogen that was prepared in a parallel experiment (Figure 48, left panel) and that the catalytic activity was required. Further evidence to support the notion of phosphomonoesters in glycogen comes from our *in vitro* observations that laforin can remove the majority of the phosphate in rabbit muscle glycogen in the presence of the glycogen degrading enzymes α-amylase and amyloglucosidase (Figure 16A). With this in mind we sought to determine the chemical nature of the phosphate linkage in glycogen using rabbit skeletal muscle glycogen as a convenient source.

5. Purification and Analysis of Phosphorylated Oligosaccharides from Rabbit Skeletal Muscle Glycogen

5.1 Purification of phosphorylated species from glycogen

Purified rabbit muscle glycogen contains 0.07% covalent phosphate by weight, which corresponds to approximately 1 phosphate every 650 glucose residues. Using this glycogen, we attempted to identify the chemical nature of the phosphate and more specifically the hydroxyl in glucose to which the phosphate is attached. Rabbit muscle glycogen was digested with α-amylase and amyloglucosidase and the anionic species were bound to DEAE sepharose resin. After extensive washing to remove glucose and neutral oligosaccharides, negatively charged species were eluted with ammonium bicarbonate and fractions analyzed for covalent phosphate by acid hydrolysis and detection of inorganic phosphate release by the Malachite Green method (140). Of the 20 fractions collected, seven contained a significant amount of covalent phosphate (labeled A-G, Figure 49).

5.2 Analysis of phosphorylated species by high performance thin layer chromatography (HPTLC)

The phosphorylated species collected by DEAE sepharose chromatography were subjected to high performance thin layer chromatography (HPTLC) analysis and were positive for carbohydrate as judged by reaction with N-(1-Naphthyl)ethylene-diamine dihydrochloride, a sensitive carbohydrate specific stain (Figure 50A). Each fraction analyzed by this method generated a single species that upon phosphate hydrolysis by laforin treatment caused a prominent change in the migration pattern of the oligosaccharides (Figure 50A). Removal of phosphate from the majority of the fractions resulted in a smear from the origin as well as three distinct species, that when developed with carbohydrate standards, migrated at similar R_f values as maltotriose, maltotetraose and maltopentaose (Figure 50B). This solvent system is unable to resolve monosaccharide phosphates from disaccharide phosphates, as glucose-

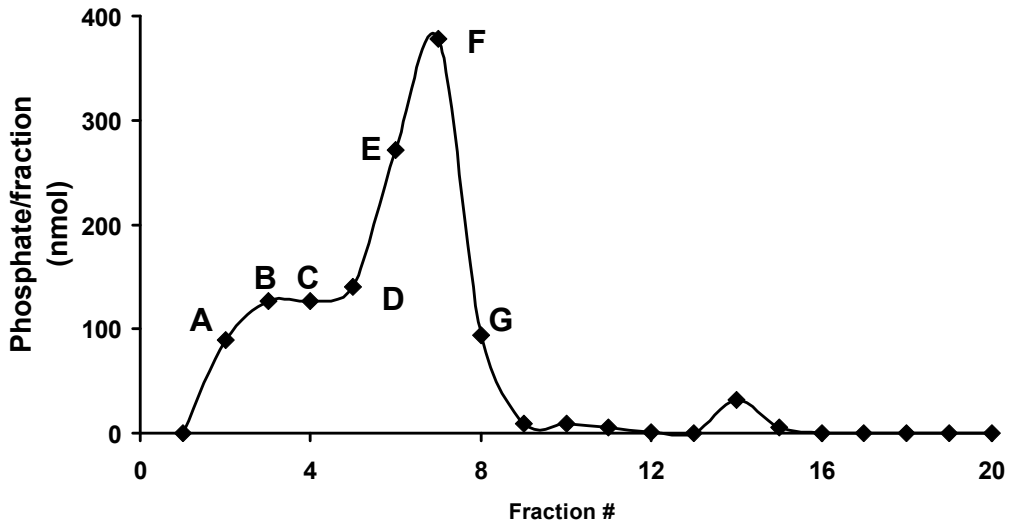

Figure 49. DEAE sepharose purification of phosphorylated species from glycogen. Anionic species from digested glycogen were bound to DEAE sepharose resin, eluted stepwise with increasing concentrations of NH_4HCO_3 .and analyzed for covalent phosphate. The chromatogram depicts the amount of phosphate in each fraction collected. Fractions 1-4, 10 mM NH_4HCO_3; Fractions 5-8, 50 mM NH_4HCO_3; Fractions 9-12, 100 mM NH_4HCO_3; Fractions 13-16, 500 mM NH_4HCO_3; Fractions 17-20, 1000 mM NH_4HCO_3.

6P and lactose-1P have similar R_f values (Figure 50B). Therefore it is not unreasonable to assume that the single species observed before dephosphorylation by laforin is a complex mixture of phosphorylated oligosaccharides that are not resolved by this method.

5.3 Analysis of phosphorylated oligosaccharides by high performance anion exchange chromatography (HPAEC)

Carbohydrates such as glucose have no charge at neutral pH but in alkali conditions, the sugar acquires a negative charge and can be separated by anion exchange chromatography. Therefore, we analyzed the phosphorylated oligosaccharides by high performance anion exchange chromatography (HPAEC). By this method the phosphorylated oligosaccharides eluted between 25-30 min (Figure 51B), retained by the column more than a series of

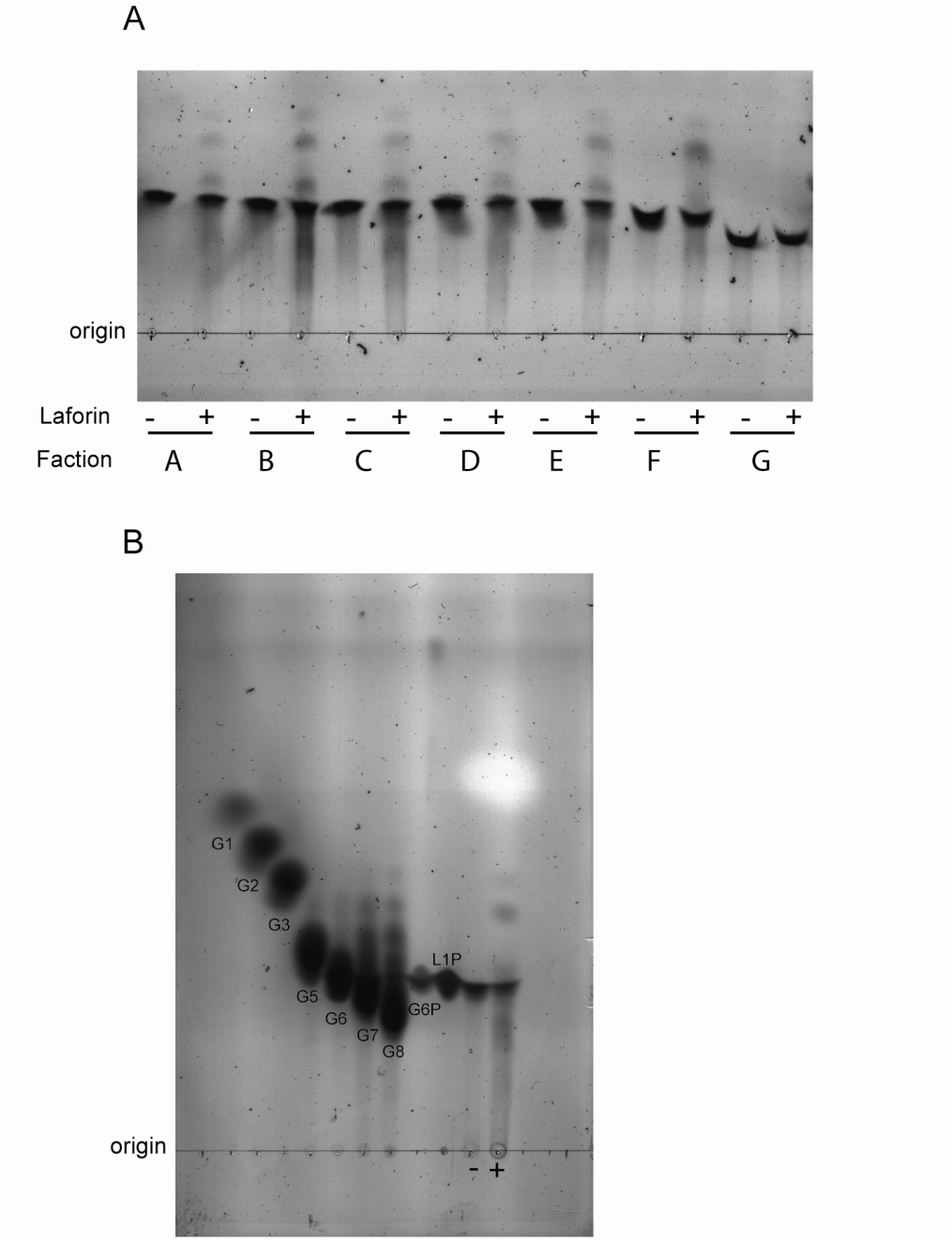

Figure 50. High performance thin layer chromatography analysis of phosphorylated oligosaccharides purified from glycogen. A. Analysis of DEAE sepharose fractions containing covalent phosphate. The fractions were either treated with catalytically inactive C266S laforin (-) or catalytically active WT laforin (+), developed by HPTLC and stained with N-(1-Naphthyl)ethylene-diamine dihydrochloride to visualize sugars. **B.** HPTLC analysis of Fraction E treated with inactive laforin (-) or active laforin (+). Malto-oligosaccharide and sugar phosphate standards are shown. G1, glucose; G2, maltose; G3, maltotriose; G5, maltopentaose; G6, maltohexaose; G7, maltoheptaose; G8, maltoocatose; G6P, glucose-6P; L1P, lactose-1P.

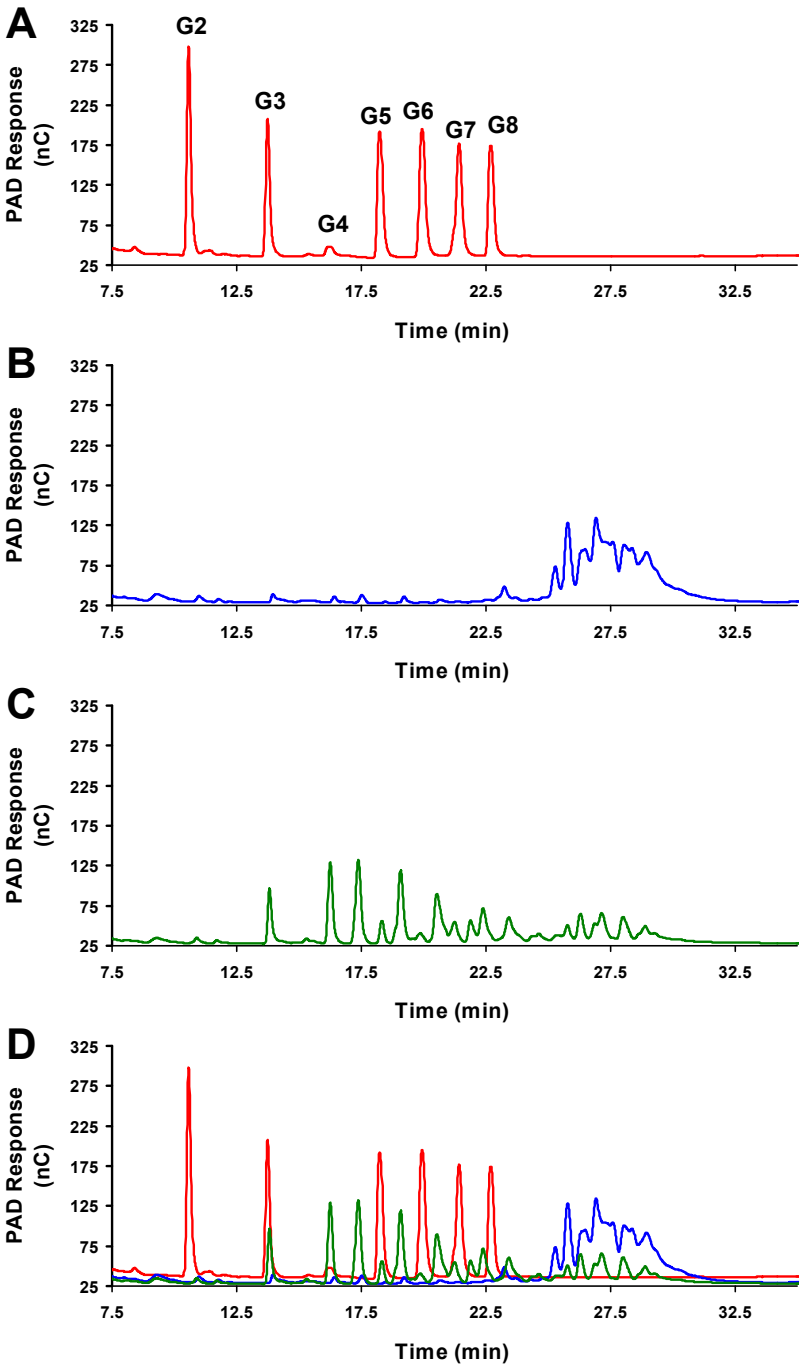

Figure 51. Analysis of purified phosphorylated oligosaccharides by high performance anion exchange chromatography (HPAEC). Approximately 5-10 nmoles (based on phosphate) of Fraction E from the DEAE sepharose column was analyzed after treatment with catalytically inactive C266S laforin or active WT laforin. **A.** HPAEC analysis of oligosaccharide standards. Abbreviations as in Figure 50. **B.** Phosphorylated oligosaccharides treated with catalytically inactive laforin. **C.** Phosphorylated oligosaccharides treated with active laforin. **D.** Overlay of A, B and C.

malto-oligosaccharide standards (Figure 51A), as would be expected for phosphorylated species. Treatment with laforin changed the elution profile producing a somewhat more complex mixture (Figure 51C). A series of peaks with retention times matching those of maltotriose, matotetraose, maltopentaose and maltohexaose were observed in the chromatogram (Figure 51D). This trend was observed in all fractions collected by DEAE sepharose chromatography (Figure 49) when treated with laforin and analyzed by HPAEC (data not shown). Given the highly branched nature of glycogen it is probable that the peaks produced after laforin treatment that do not correspond to the standard linear malto-oligosaccharides are branched oligosaccharides for which we do not have suitable standards.

Treatment of the phosphorylated oligosaccharides with alkaline phosphatase, a non specific phosphatase, produced many of the species produced by laforin treatment (Figure 52D & E). Alkaline phosphatase activity was not as efficient as laforin action as judged by the remaining area under the curve of the starting material after phosphate removal (Figure 52C & D). Interestingly, alkaline phosphatase treatment produced maltose, whereas the smallest oligosaccharide produced by laforin dephosphorylation was maltotriose, perhaps indicating specificity of laforin action based on chain length of the substrate. Incubation of the phosphorylated oligosaccharides with a non specific phosphodiesterase, snake venom phosphodiesterase, had no effect on the retention time on all fractions analyzed (data not shown).

5.4 Analysis of phosphorylated oligosaccharides by MALDI-TOF-MS

Further analysis of these fractions by matrix assisted laser desorption ionization time of flight mass spectrometry (MALDI-TOF-MS) confirmed a complex mixture of oligosaccharides, each containing a phosphate (Figure 53). Mass analysis indicated the presence of oligosaccharides varying in length from 3 glucoses plus a phosphate to 18 glucoses plus a phosphate in five of the fractions collected by anion exchange chromatography using DEAE sepharose. This methodology is only capable of identifying absolute mass quantities and the

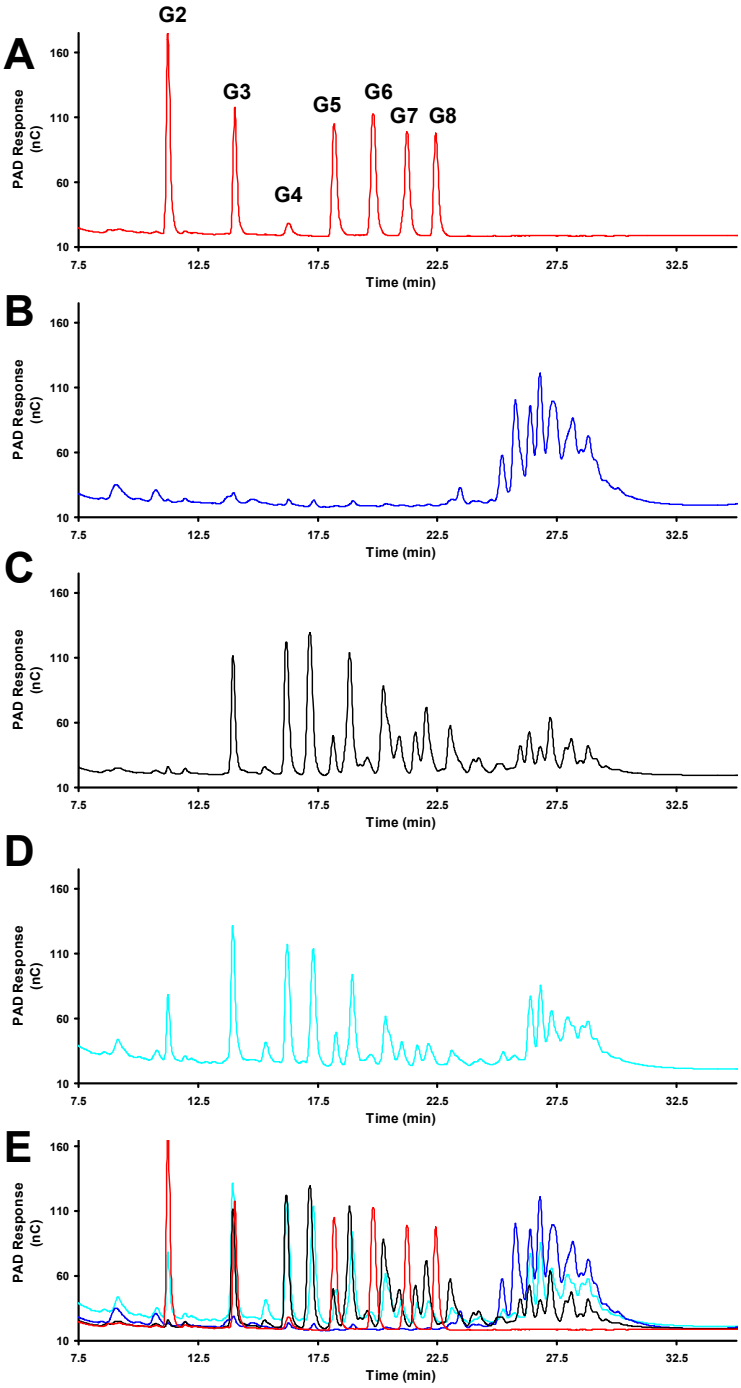

Figure 52. Alkaline phosphatase treatment of phosphorylated oligosaccharides. HPAEC analysis of phosphorylated oligosaccharides treated with laforin and alkaline phosphatase **A.** malto-oligosaccharide standards. Abbreviations as in Figure 50. **B.** Phosphorylated oligosaccharides from fraction E treated with catalytically inactive C266S laforin. **C.** Phosphorylated oligosaccharides from fraction E treated with C266S laforin. **D.** Phosphorylated oligosaccharides from fraction E treated with calf intestinal alkaline phosphatase. **E.** Overlay of A-D.

structure of these oligosaccharides cannot be determined from these analyses. However, our HPAEC analyses suggest that these oligosaccharide phosphates are not just linear, non-branched sugars, but a mixture of branched oligosaccharides which would not be resolved by mass analysis.

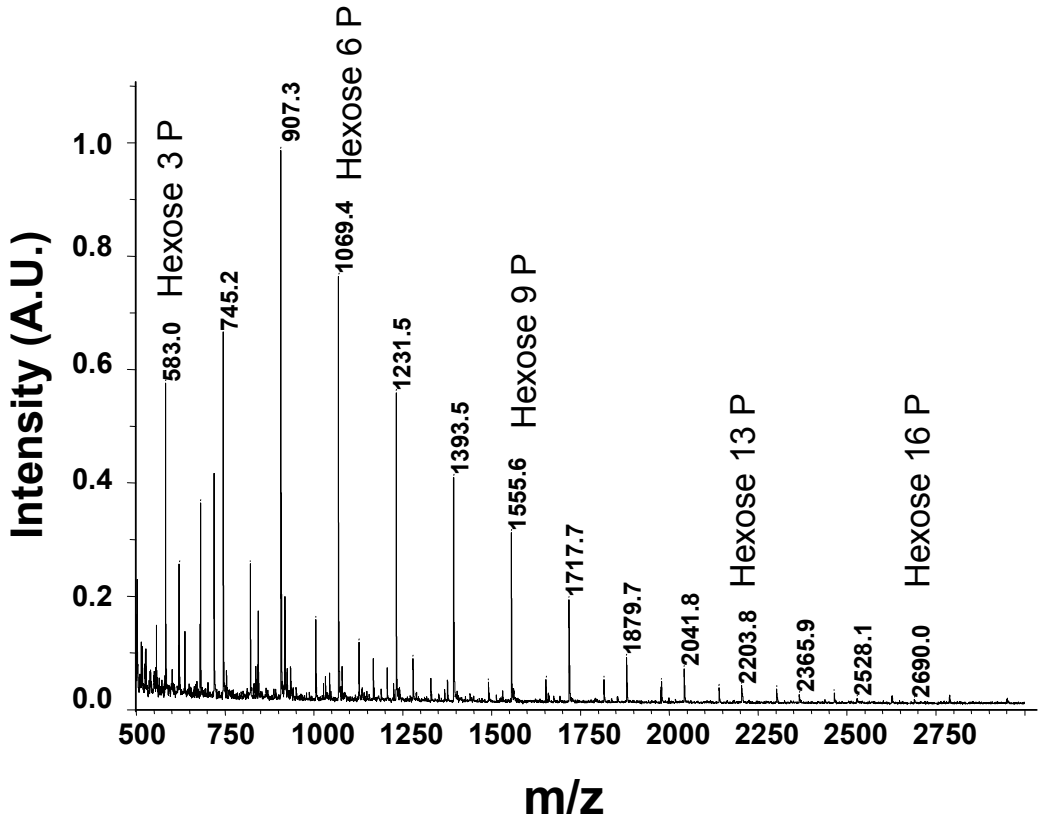

Figure 53. MALDI-TOF-MS analysis of phosphorylated oligosaccharides. MALDI/TOF-MS analysis was performed in the reflector negative ion mode using THAP as matrix. Two nmoles of sample E was analyzed.

6. Identification of the Phosphate Linkage in Glycogen

6.1 Acid hydrolysis of glycogen and phosphorylated oligosaccharides

Mild acid hydrolysis to cleave glycosidic bonds is used in carbohydrate chemistry to identify structural components of polysaccharides (165). Amylopectin, for example is hydrolyzed in 0.7M HCl for 3 hours at 100^{o}C to hydrolyze glycosidic linkages and the products can be analyzed enzymatically or chromatographically to determine the resulting monosaccharide phosphate structure. In an effort to detect glucose-6P in rabbit skeletal muscle glycogen, we hydrolyzed the polysaccharide under acidic conditions and attempted to measure glucose-6P levels enzymatically using glucose-6P dehydrogenase and spectrophotometrically determining the reduction of $NADP^+$ to NADPH. During these studies, we observed a rapid reduction in $NADP^+$ followed by a slow and steady increase in the rate of NADPH formation (Figure 54A). The amount of glucose-6P, taken as the theoretical saturation point of the initial burst in activity, accounted for about 25-30% of the total phosphate in glycogen. Since the reaction never went to completion at the time points analyzed, we wondered whether the high concentration of glucose present in the reaction mix after hydrolysis was being oxidized by glucose-6P dehydrogenase, albeit at a much slower rate. Using a reaction mixture consisting of glucose, initiated a reduction in $NADP^+$ catalyzed by glucose-6P dehydrogenase, suggesting that the enzyme has glucose dehydrogenase activity (Figure 54B). When a mixture of glucose and glucose-6P were incubated with glucose-6P dehydrogenase, there was a rapid reduction of $NADP^+$ followed by a slow and steady increase in the rate of NADPH formation (Figure 54B), reminiscent of the acid hydrolyzed glycogen sample (Figure 54A). Whether this activity is from glucose-6P dehydrogenase or from contaminating glucose dehydrogenase is not clear at the moment but this activity has been reported (166). In fact the authors warned about measuring glucose-6P levels in the presence of high concentrations of glucose.

In light of these results and the lack of specificity for substrates of glucose-6P dehydrogenase, we resorted to chromatographic analysis of acid hydrolyzed

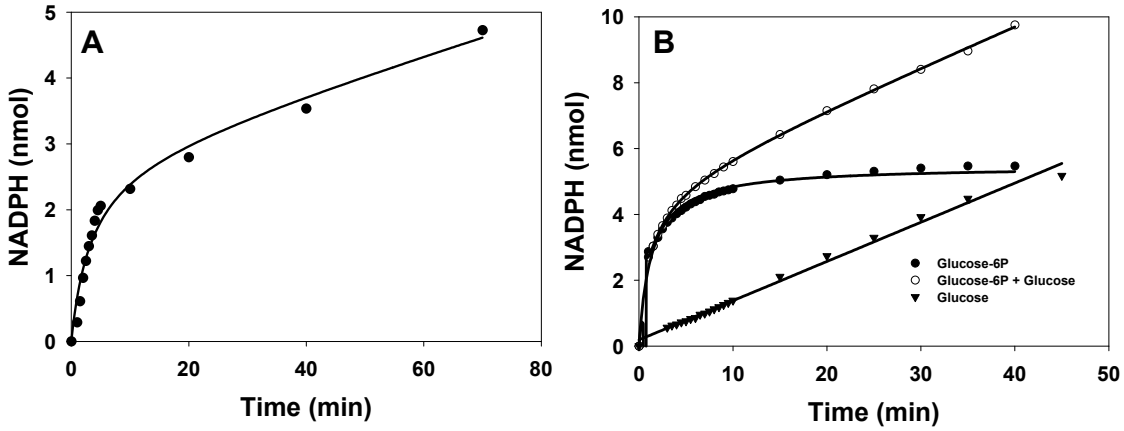

Figure 54. Glucose-6P dehydrogenase has glucose dehydrogenase activity. **A.** Time dependent reduction of $NADP^+$ by glucose-6P dehydrogenase in the presence of acid hydrolyzed rabbit muscle glycogen. **B.** Time dependent reduction of $NADP^+$ by glucose-6P dehydrogenase in the presence of glucose (▼), glucose-6P (●) and glucose + glucose-6P (○).

phosphorylated oligosaccharides. Our preliminary experiments involved hydrolysis in 2M trifluoroacetic acid (TFA) at 100^{o}C for 4 hours and resulted in complete hydrolysis of the glycosidic linkages and produced glucose-6P as judged by HPAEC (Figure 55A). Although we had evidence of glucose-6P production after acid hydrolysis of both glycogen and the phosphorylated oligosaccharides, glucose-6P is considerably more stable to acid treatment than glucose-1P (data not shown). We wondered whether our hydrolysis conditions were also hydrolyzing phosphate groups that may be attached at other positions of the glucose ring The only commercially available glucose phosphates are glucose-1P and glucose-6P, so we synthesized glucose-2P from glucose-1,2-cyclic phosphate with the rationale of determining whether glucose-2P is stable under the conditions used for acid hydrolysis of glycosidic linkages in the phosphorylated oligosaccharides. Glucose-1,2-cyclic phosphate was synthesized by the cyclization of glucose-1P with dicyclohexylcarbodiimide (DCC) in aqueous pyridine (147). It was originally discovered that the reaction of

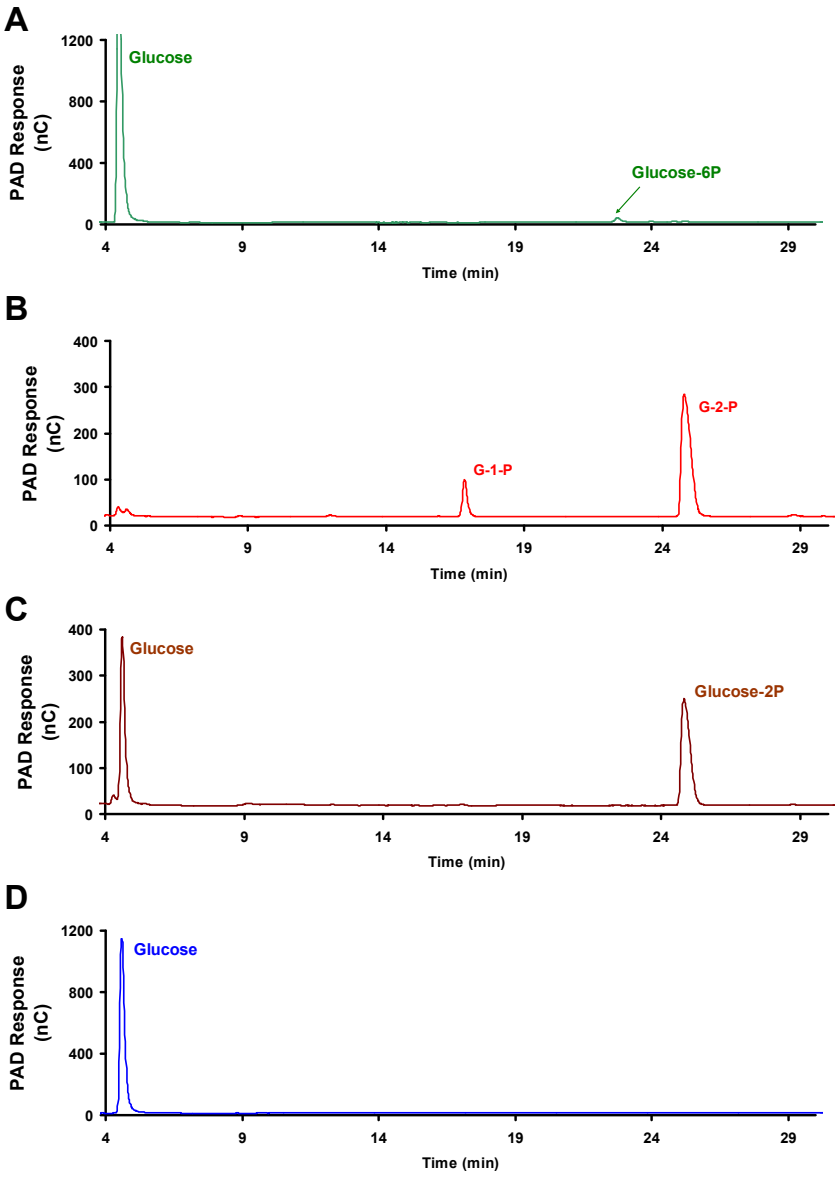

Figure 55. Acid hydrolysis of phosphorylated oligosaccharides. All samples were analyzed by HPAEC. **A.** Approximately 10 nmoles of phosphorylated oligosaccharides were subjected to acid hydrolysis in 2 M TFA at 100°C for 4 hours. Under these conditions, the phosphorylated oligosaccharides were hydrolyzed to glucose and glucose-6P. **B.** HPAEC analysis of glucose-2P detected contaminating glucose-1P. **C.** HPAEC analysis of mildly acid hydrolyzed glucose-2P (100 mM HCl, 5 minutes, 100°C). Under these conditions glucose-2P was stable and glucose-1P was hydrolyzed to glucose. **D.** Glucose-2P is hydrolyzed to glucose under conditions used to hydrolyze the phosphorylated oligosaccharides (2 M TFA at 100°C for 4 hours).

DCC with ribonucleoside '2',(3') phosphate esters which possessed adjacent *cis* hydroxyls formed five membered ribonucleoside 2',3' cyclic phosphates (167) The product of cyclization of glucose-1-phosphate with DCC depends entirely on the stereochemistry of the adjacent hydroxyl groups relative to the phosphate ester. Cyclization is possible when the relationship of a phosphate ester to the adjacent hydroxyl group is axial to equatorial or equatorial to equatorial (168). α-D-glucose-1P, for example contains a hydroxyl at the 2 position of the pyranose ring that lies equatorial (cis) to the phosphate ester, and therefore reaction with DCC will result in the formation of glucose-1,2-cyclic phosphate. In contrast, α-D-mannose-1-phosphate, in which the 2 hydroxyl and the phosphate ester lie axial (trans) does not undergo cyclization with DCC (168). Reaction of DCC with glucose-1P produced glucose-1-2-cyclic phosphate that was purified as the barium salt in about 60-70% yield. Hydrolysis of glucose-1-2-cyclic phosphate in 100 mM HBr for 5 min at 100^{o}C produced glucose-2P and glucose-1P; the latter is very labile under these conditions and was further hydrolyzed to glucose and inorganic phosphate. Glucose-2P was purified as the barium salt and analysis by HPAEC revealed the presence of 2 peaks, one minor peak of glucose-1P and a major peak corresponding to glucose-2P (Figure 55B), that was confirmed by NMR spectroscopy (data not shown). Acid hydrolysis, (5 min, 100^{o}C, 100mM HCl) converted the acid labile glucose-1P to glucose and inorganic phosphate, without affecting the glucose-2P (Figure 55C). However, subjecting glucose-2P to the acidic conditions required to hydrolyze glycosidic linkages in a parallel experiment to that of the phosphorylated oligosaccharides of Figure 55A, hydrolyzed the glucose-2P to glucose (Figure 55D). These results in addition to the observation that phosphoryl group migration can occur under acid conditions (169) prompted us to explore other methodologies to determine the position of the phosphate group in glycogen.

6.2 Determination of the phosphate position in glycogen by NMR spectroscopy

Although the phospho-oligosaccharide mixture is heterogeneous in terms of polymerization state, it is homogeneous in the sense that it consists primarily of glucose or glucose-phosphate residues. It was therefore amenable to analysis by NMR spectroscopy. Several spin systems were detected by ^{1}H-^{1}H COSY and TOCSY and ^{1}H-^{13}C HSQC. The spectra were dominated by a group of similar spin systems belonging to 4-α-Glc-(1$\rightarrow$4) residues. Other spin systems present included those of 4-α-Glc-(1$\rightarrow$6), terminal α-Glc-(1$\rightarrow$4), terminal α-Glc-(1$\rightarrow$6), and α and β reducing end residues that appeared to be mostly 4,6-linked (i. e. a branching residue glycosylated in both the 4 and the 6 positions), judging by their H-1 chemical shifts (170) (Table 2). In addition, two spin systems were identified, each with one proton resonance uncharacteristically far downfield for glucose, suggesting substitution by phosphate (Figure 56). On the basis of the connectivities established by the COSY, TOCSY, and ROESY experiments and the carbon chemical shifts determined by the HSQC experiment, one of these downfield signals appeared to be H-2 of a terminal glucose residue and the other H-3 of a 4-linked glucose. To confirm substitution by phosphate, we acquired a ^{1}H-^{31}P gHMQC spectrum, which showed two peaks, confirming substitution at the 2-OH and the 3-OH positions by phosphate (Figure 57). We also acquired a ^{1}H-^{31}P HMQC-TOCSY spectrum to ascertain that these two protons belong to the spin systems previously assigned. This spectrum showed the expected correlations of each of the peaks detected in gHMQC with their neighboring protons (Figure 58).

	Residue		1	2	3	4	5	6	NOE
I	t-α-Glc-2-P-(1→?)	^{1}H	5.69	4.00	3.76	3.50	3.69	3.83/3.77	
		^{13}C	100.0	77.3	74.8	72.0	75.0	63.3	
II	t-α-Glc-(1→4)	^{1}H	5.59	3.58	3.65	3.43	3.66	3.83/3.77	IV-4
		^{13}C	101.3	74.2	75.4	72.1	75.4	63.3	
III	4-α-Glc-(1→4)	^{1}H	5.40	3.60	3.97	3.64	3.84	3.83/3.77	III_{n-1}-4[a]
		^{13}C	102.2	74.1	76.0	79.7	73.8	63.3	
IV	4-α-Glc-3-P-(1→4)	^{1}H	5.35	3.75	4.46	3.81	3.87	n.d.[b]	III-4, VII-4, or VIII-4
		^{13}C	102.4	74.6	79.9	76.4	73.8	n.d.	
V	4,6-α-Glc_{red}	^{1}H	5.22	3.55	3.96	3.64	3.93	3.98/3.83	
		^{13}C	94.6	74.2	76.0	79.7	72.7	69.7	
VI	t-α-Glc-(1→6)	^{1}H	4.99	3.54	3.74	3.44	3.86	n.d.	
		^{13}C	101.5	74.7	74.2	72.1	73.8	n.d.	
VII	4-α-Glc-(1→6)	^{1}H	4.95	3.59	4.01	3.63	3.85	n.d.	
		^{13}C	100.7	74.1	73.0	80.6	74.0	n.d.	
VIII	4,6-β-Glc_{red}	^{1}H	4.65	3.25	3.77	3.62	3.60	3.97/3.73	
		^{13}C	98.5	76.7	78.9	80.6	77.3	68.8	

Table 2. Chemical shift assignments of phosphorylated oligosaccharides. [a]the next residue in the chain, [b]not determined.

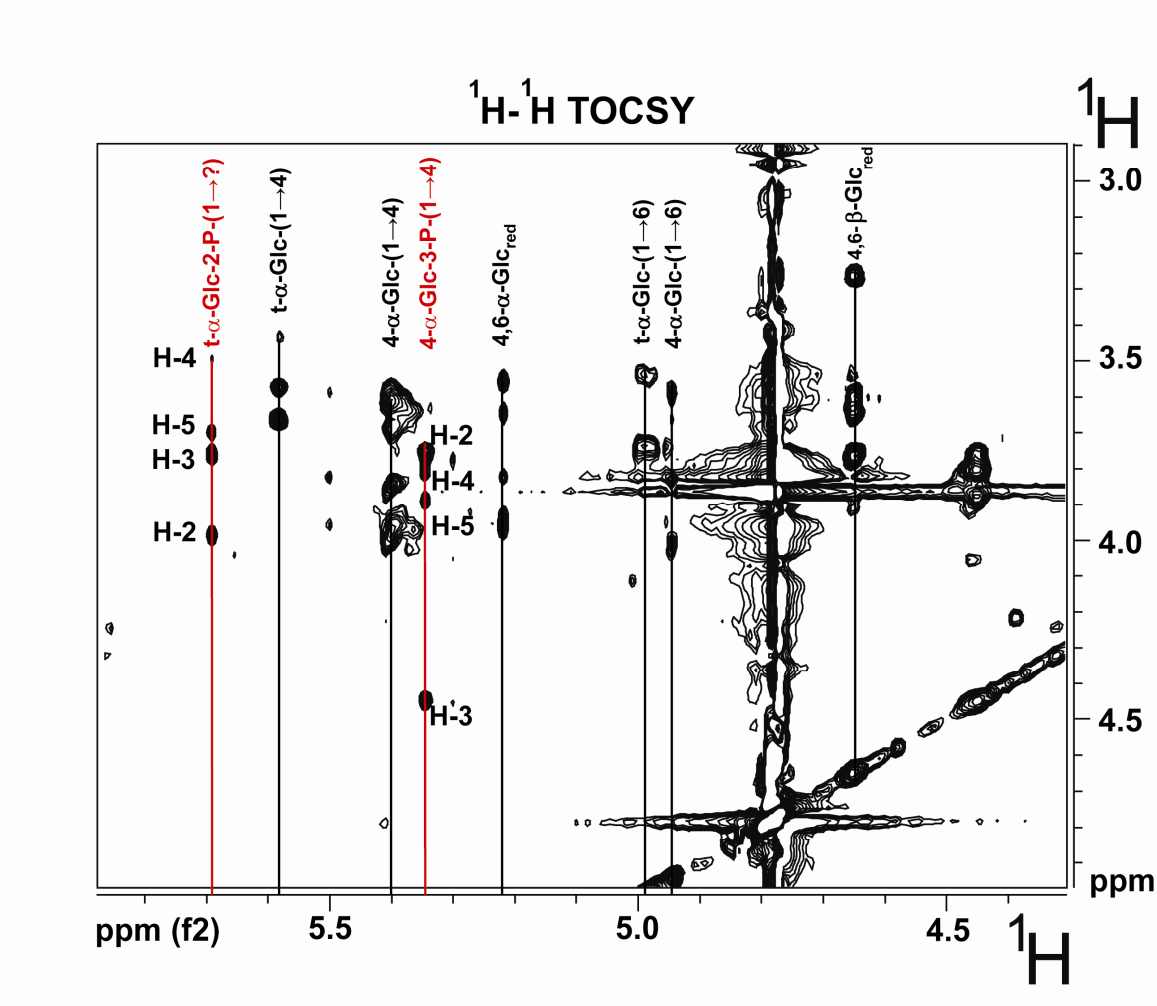

Figure 56. ^{1}H-^{1}H TOCSY NMR spectrum of phosphorylated oligosaccharides. A sample of phosphorylated oligosaccharides (Fraction C + D + E + F) was analyzed by ^{1}H-^{1}H TOCSY NMR. The spectrum was acquired at 25 ^{o}C and 18.7 T with a 1-s relaxation delay and 3.7 kHz spectral width, 100 ms spinlock time, 0.138 s acquisition time, 128 increments, and 32 transients per increment.

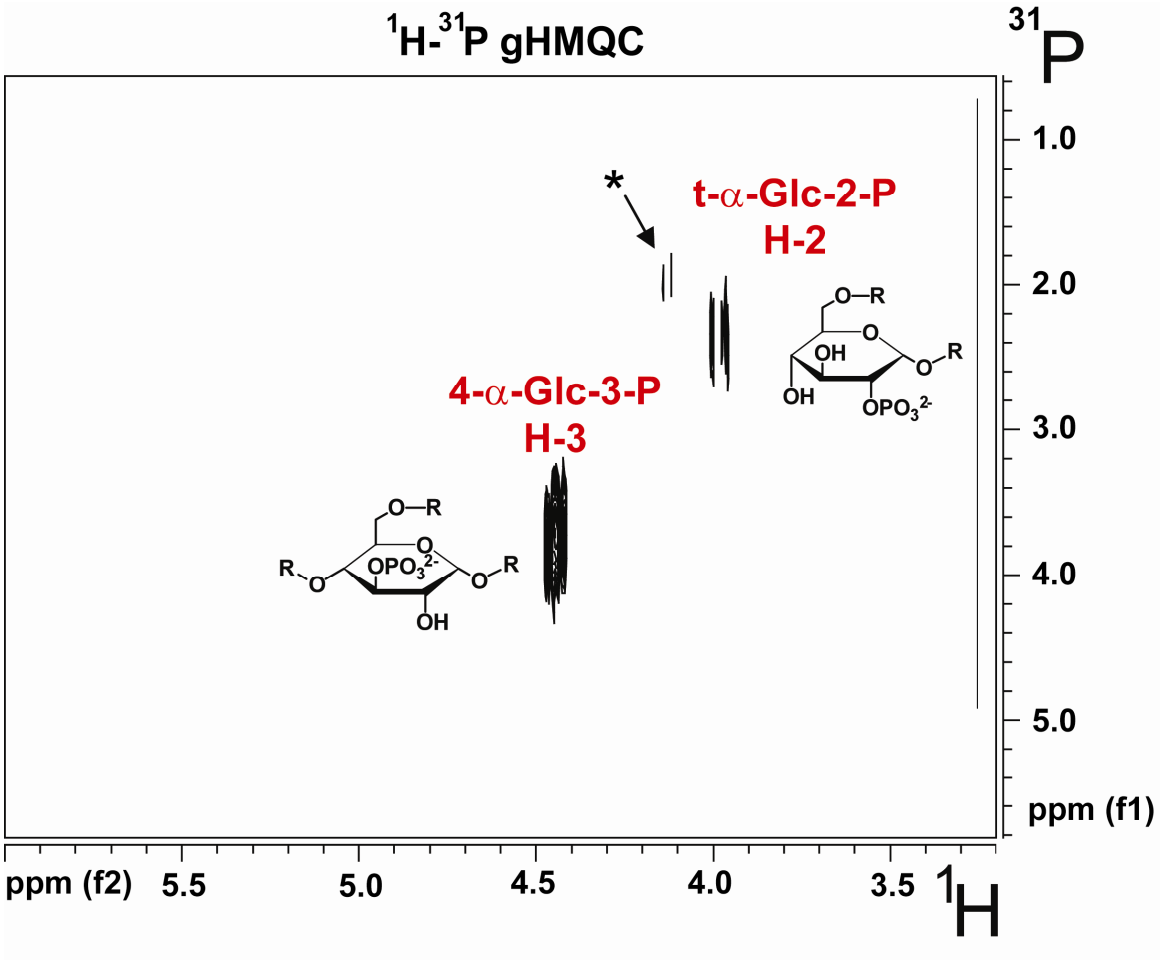

Figure 57. ^{1}H-^{31}P gHMQC NMR spectrum of phosphorylated oligosaccharides. A sample of phosphorylated oligosaccharides (Fraction C + D + E + F) was analyzed by gHMQC. The ^{1}H-^{31}P gHMQC spectrum was acquired with an 8.0 kHz spectral width in F_1, 0.4 s acquisition time, 32 increments, and 360 transients per increment. The signal marked with an asterisk is probably from a terminal glucose-2P residue linked in a different position but could not be clearly identified due to its low abundance.

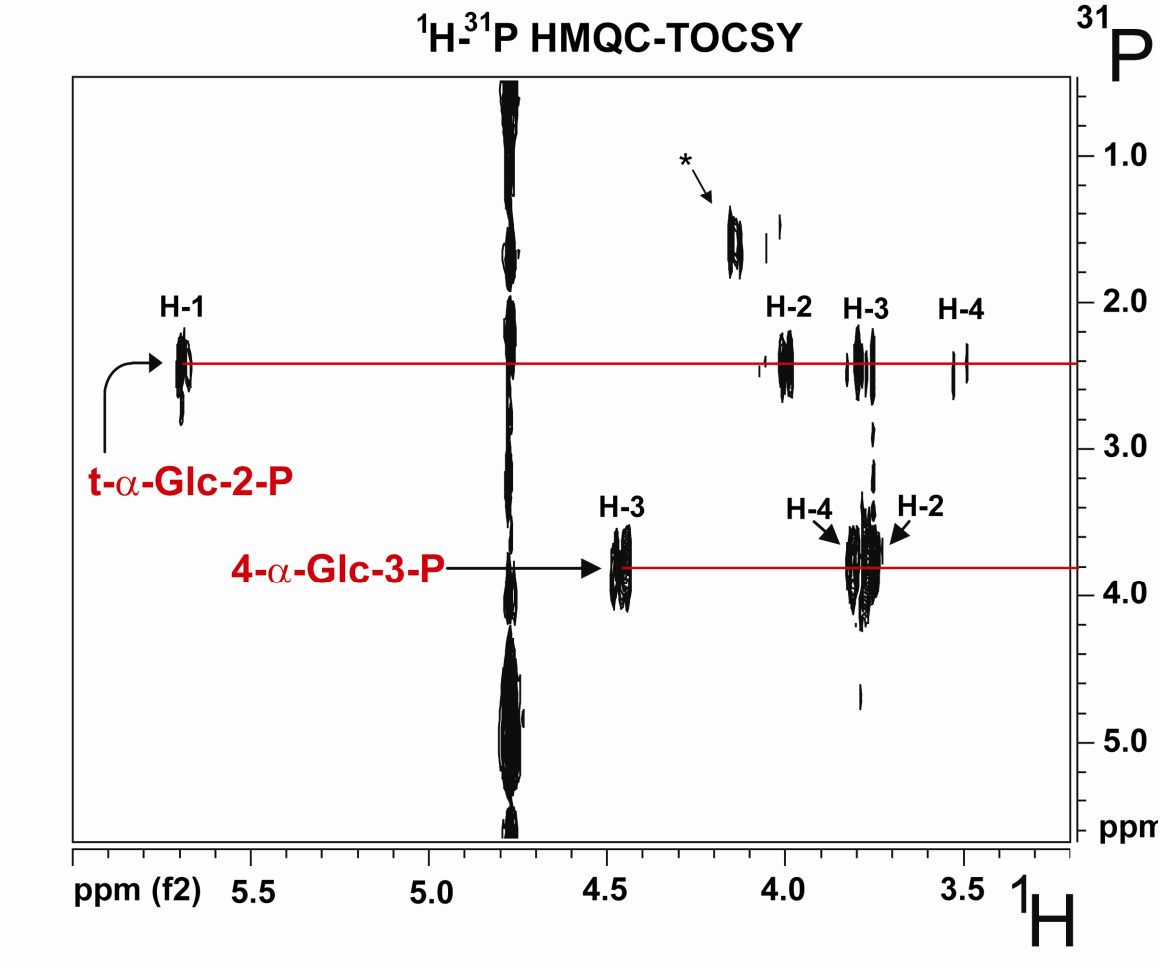

Figure 58. ^{1}H-^{31}P HMQC-TOCSY NMR spectrum of phosphorylated oligosaccharides. A sample of phosphorylated oligosaccharides (Fraction C + D + E + F) was analyzed by ^{1}H-^{31}P HMQC-TOCSY NMR. The ^{1}H-^{31}P HMQC-TOCSY spectrum was acquired with a 3.0 kHz spectral width in F_1, 0.3 s acquisition time, 40 ms spinlock time, 24 increments, and 400 transients per increment. Phosphorus decoupling was turned on during acquisition using the GARP-1 decoupling sequence. The signal marked with an asterisk is probably from a terminal glucose-2P residue linked in a different position but could not be clearly identified due to its low abundance.

7. Mechanism of Phosphate Incorporation by Glycogen Synthase

7.1 Cyclic phosphate formation

Perhaps the most obvious mechanism for the incorporation of phosphate into glycogen by glycogen synthase would be through the formation of a C1-O-P-O-C4 linkage. However, our data strongly suggest the occurrence of phosphomonoesters in glycogen. First of all, NMR analysis suggests the presence of phosphate at the C2 and C3 hydroxyls with no detectable C1, C4 or C6 phosphates. Furthermore, the NMR analysis suggests that these phosphates are monoesters. Secondly, our phosphorylated oligosaccharides are hydrolyzed by laforin, which in our hands has no phosphodiesterase activity, or alkaline phosphatase. Finally, laforin is capable of removing phosphate that has been incorporated by glycogen synthase. How is phosphate incorporated as a monoester by glycogen synthase during elongation of the polymer? Insight into the mechanism may come from an unexpected observation during our studies of UGPPase specificity for UDP-glucose. The reaction catalyzed by UGPPase (Figure 44B) is a metal dependent hydrolysis of the pyrophosphate bond in UDP-glucose. During the course of studying the enzyme's effects on [β-^{32}P]UDP-glucose, we noticed that in the presence of Mg^{2+} or Mn^{2+}, UDP-[U-^{14}C]glucose and [β-^{32}P]UDP-glucose would decompose to a species that, when analyzed by HPTLC, migrated slightly faster than UDP-glucose (Figure 59). This species was completely consumed by UGPPase treatment of the [β^{32}P]UDP-glucose but only partially in the reaction mix containing the UDP-[U-^{14}C]glucose (Figure 59). The latter is most likely due to the amount of substrate in the respective reactions, as the reaction containing UDP-[U-^{14}C]glucose had more substrate and was terminated prior to completion. Nevertheless, analysis of unlabelled UDP-glucose in the presence of Mg^{2+} revealed that the unknown species had no detectable UV absorption and contained carbohydrate, as judged by reactivity towards N-(1-Naphthyl)ethylene-diamine dihydrochloride (data not shown). Addition of equimolar amounts of EDTA or removing the divalent cation from the reaction mix prevented the formation of the species.

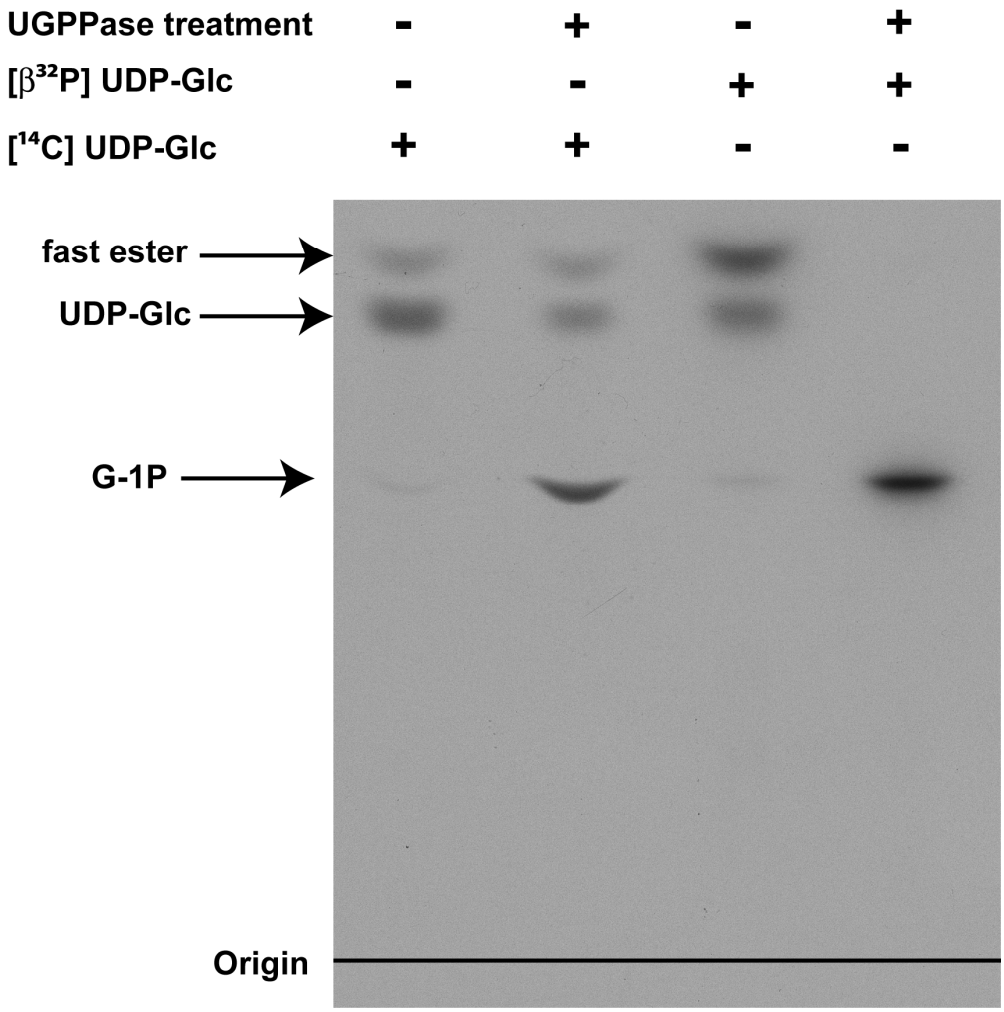

Figure 59. The formation of glucose-1,2-cyclic phosphate (fast ester) from UDP-glucose. UDP-[U-^{14}C]glucose and [β^{32}P]UDP-glucose were treated with or without 100 μg/mL UGPPase in 50 mM Tris-HCl, pH 8.8 containing 10 mM $MgCl_2$. The reaction was terminated by boiling in a water bath and the products analyzed by HPTLC. In contrast, the chromatogram of Figure 44 was terminated by the addition of equimolar amounts of EDTA, essentially eliminating the presence of fast ester.

Glucose,-1,2-cyclic phosphate (Figure 60A) was first described by Leloir, in the early 1950's as a contaminant in the enzymatic synthesis of UDP-glucose, that he termed "fast ester" (171). In addition to being prepared by reaction of glucose-1P with DCC (see Results Section 6.1), glucose-1,2-cyclic phosphate can be prepared by the metal ion or base catalyzed decomposition of UDP-glucose (172). We wondered whether cyclic phosphodiester formation during elongation of glycogen by glycogen synthase might be the phosphoryl donor responsible for phosphorylating glycogen. Our initial attempts to introduce phosphate into glycogen with glycogen synthase from [β-^{32}P]UDP-glucose in the presence of Mg^{2+} resulted in high background ^{32}P on the gel, most prominently in the well where glycogen resides. However the ^{32}P in the well was not glycogen as it was insensitive to glucosidase treatment. (data not shown). Furthermore,

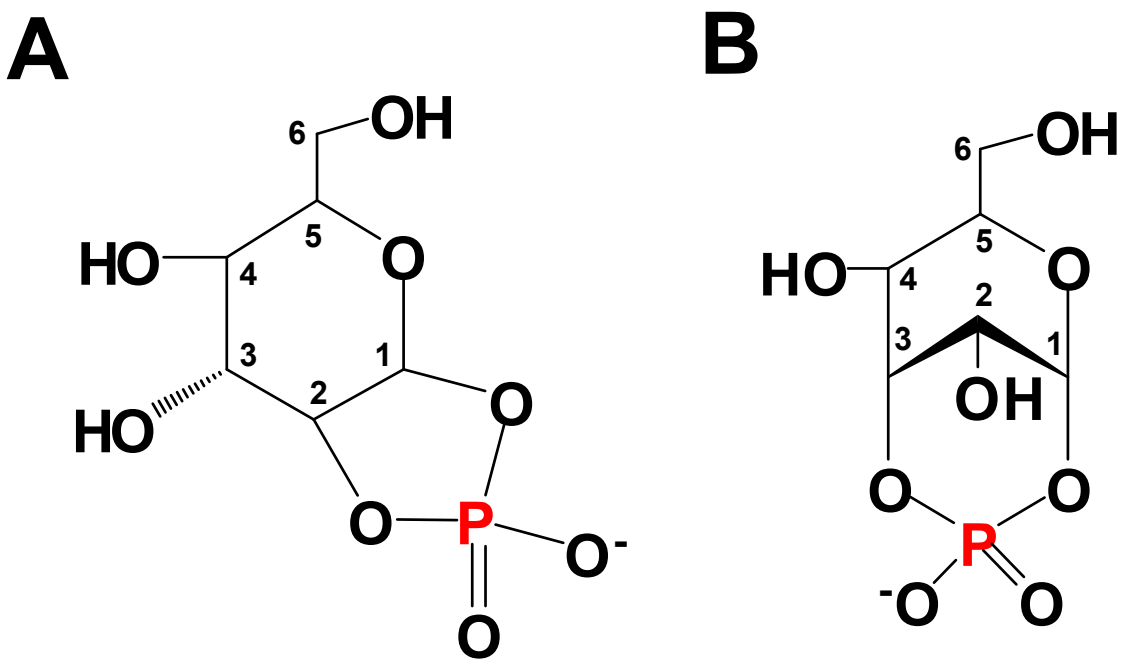

Figure 60. The structure of glucose-1,2-cyclic phosphate and glucose 1,3-cyclic phosphate. A. Glucose-1,2-cyclic phosphate is a five membered cyclic phosphate thought to form by the alkali and/or metal dependent decomposition of UDP-glucose. **B.** Glucose-1,3-cyclic phosphate is a seven membered cyclic phosphate.

we wondered whether the formation of glucose-1,2-cyclic phosphate or glucose-1,3-cyclic phosphate (Figure 59B) in the active site of glycogen synthase, independent of divalent cations, would allow for phosphate to be incorporated at the C2 or the C3 hydroxyls (Figure 66, see Discussion). In the event of the possible formation of a five membered cyclic phosphate ring or a six membered cyclic phosphate ring, the formation of the five membered ring would be favored (168). This is consistent with the preferential degradation of UDP-glucose to glucose-1,2-cyclic phosphate rather than glucose-1,3-cyclic phosphate, 5 and 6 membered cyclic phosphates respectively. However, [β^{32}P]UDP-[2-deoxy]-glucose undergoes cyclization in the presence of Mn^{2+} at alkaline pH as judged by HPTLC (Figure 61). Loss of the C2-OH would most likely cause cyclization to

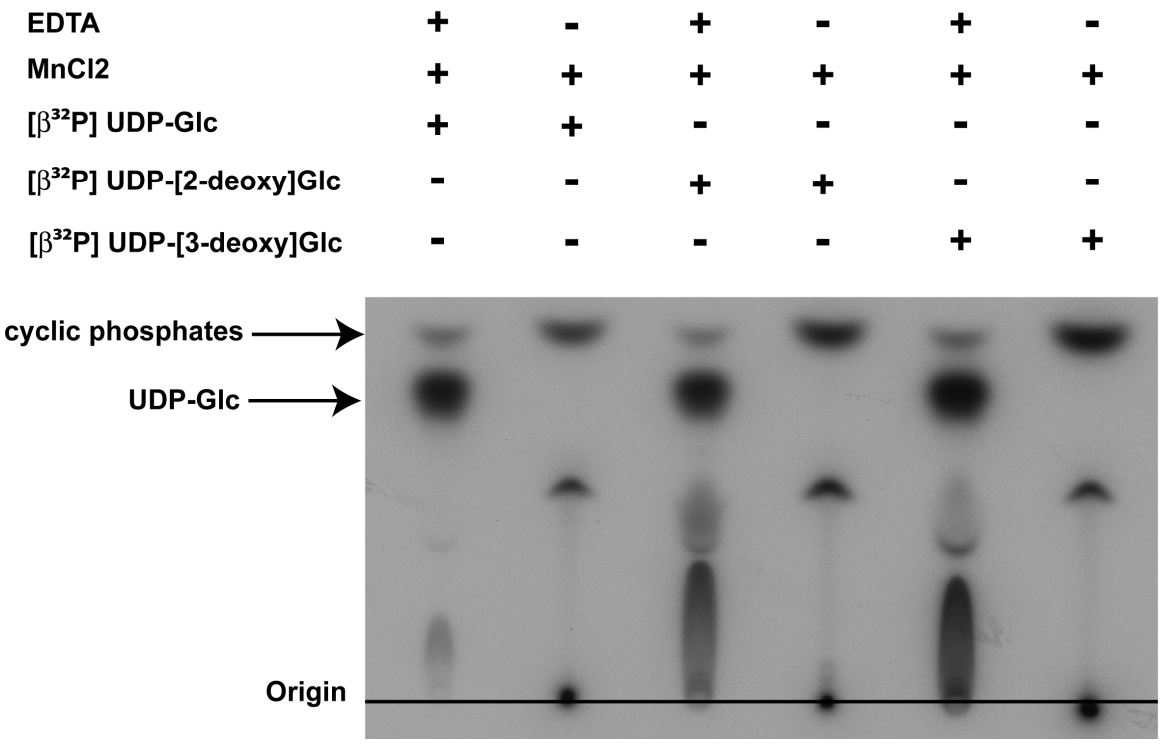

Figure 61. Cyclic phosphate formation from UDP-glucose derivatives. Incubation of [β^{32}P]UDP-glucose, [β^{32}P]UDP-[2-deoxy]-glucose and [β^{32}P]UDP-[3-deoxy]-glucose with Mn^{2+} results in the formation of cyclic phosphates as monitored by HPTLC. The addition of EDTA strongly inhibits cyclic phosphate formation by chelating the Mn^{2+}.

occur between the anomeric carbon and C3, forming a stable six membered cyclic phosphate. This is inferred because six-membered cyclic phosphates are more stable than seven membered cyclic phosphates (173), which would form between the C1 and C4/C6 hydroxyls. Likewise, cyclization of [β^{32}P]UDP-[3-deoxy]-glucose produced [^{32}P]glucose-1,2-cyclic phosphate (Figure 61). In addition to the formation of cyclic phosphates, the presence of Mn^{2+} also caused a notable change in the migration pattern of other ^{32}P labeled species. However, this may be an artifact since a precipitate of $Mn(OH)_2$ formed during the reaction in the samples without EDTA (Figure 61). Nevertheless, both UDP-glucose derivatives are capable of undergoing cyclization under these conditions. Interestingly, when these radioactive isotopes are incubated with glycogen synthase using glycogen as the acceptor, [β^{32}P]UDP-[3-deoxy]-glucose incorporates significantly more ^{32}P than [β^{32}P]UDP-[2-deoxy]-glucose and even more than [β^{32}P]UDP-glucose (Figure 62). The product of all three reactions was degraded by glucosidase treatment indicating that it was polysaccharide and that both UDP-glucose analogs could act as phosphate donors during glycogen synthesis. Why the three nucleotide sugars led to different phosphate incorporation is not immediately obvious. It is possible that loss of the hydroxyl at C2 forces cyclization at C3 while loss of the C3 hydroxyl forces the formation of a cyclic phosphate between C1 and C2 resulting in different kinetics of incorporation, also with respect to the normal UDP-glucose substrate.

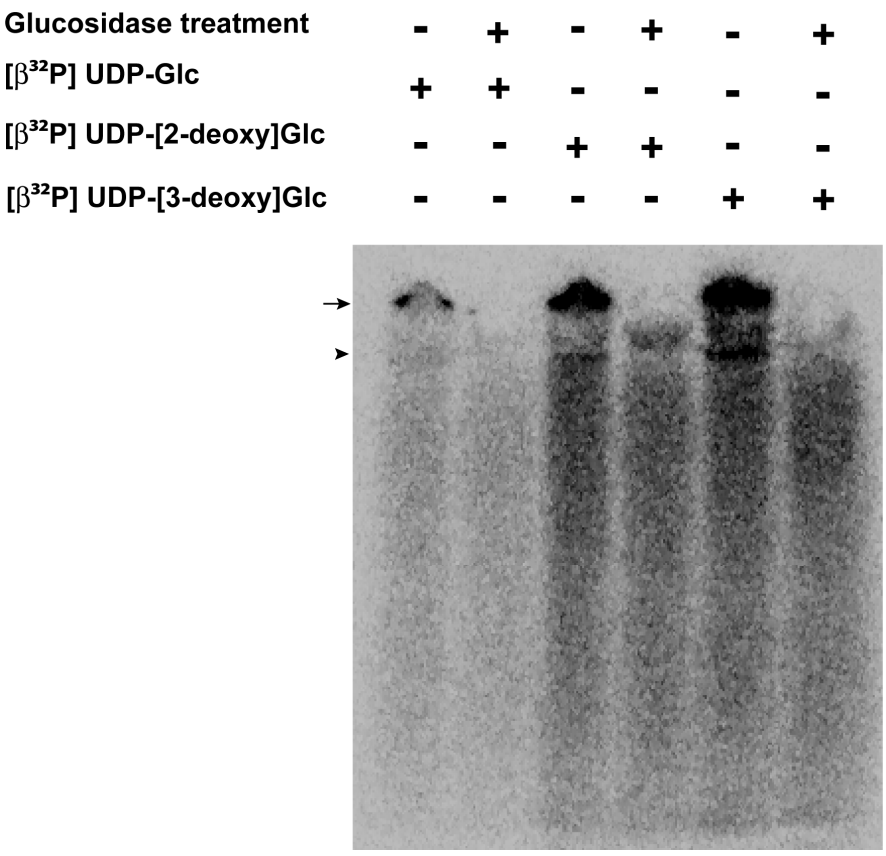

Figure 62. Glycogen synthase incorporates phosphate into glycogen using [β^{32}P]UDP-[2-deoxy]-glucose and [β^{32}P]UDP-[3-deoxy]-glucose. Glycogen synthase incorporates ^{32}P into glycogen using [β^{32}P]UDP-glucose, [β^{32}P]UDP-[2-deoxy]-glucose and [β^{32}P]UDP-[3-deoxy]-glucose as the phosphate donors. The arrow indicates the bottom of the well and the arrow head indicates the bottom of the stacking gel.

DISCUSSION

1. Laforin as a Glycogen Phosphatase

The first report of the presence of covalent phosphate in glycogen was in the early 1980's, (6) almost 125 years after the original discovery of the polysaccharide. The fact that covalent phosphate has been overlooked for all these years is a testimony to the low levels present in the glycogen molecule. The frequency of phosphorylation in rabbit muscle glycogen is around 1 phosphate every 650 glucoses residues. The average number of phosphates per glycogen molecule would of course depend on size. For example, a normal glycogen molecule of 9 tiers would have a diameter of ~31 nm and ~15,000 glucose residues (174). Such a particle would contain on average ~25 phosphate groups. Covalent phosphate in plant starch has been well studied, and starch metabolism is influenced by genetic depletion of the enzymes involved in starch phosphate metabolism. Although glycogen and amylopectin share the chemistry of their polymerization and branching linkages, their structures are quite different (175). Amylopectin has a generally higher molecular weight and is significantly less branched (1 in ~30 residues) than glycogen (1 in ~12 residues). Whereas glycogen is believed to be formed of concentric tiers of glucose residues (Figure 2), amylopectin has a more extended conformation that includes semi-crystalline regions of unbranched glucose chains lined up in parallel (176). This difference likely accounts for the fact that most of the phosphate in amylopectin is readily released by laforin, and is presumably superficial and available, while only a fraction of the phosphate is accessible on the surface of the glycogen molecule and phosphate from the inner tiers cannot be accessed until the structure is disrupted by hydrolyzing enzymes.

On the model of Gunja-Smith et al. (2) there are approximately equal numbers of A chains (unbranched) and B chains (branched), and there is a uniform distribution of chain lengths. Furthermore, each B chain has two chains attached to it, and all the unbranched chains are on the outermost tier. Assuming random distribution of phosphate, a full size glycogen molecule of 12

tiers, containing 55,000 glucose residues, with a frequency of phosphorylation of 1/650 would have about 85 phosphates, of which half would be located on the unbranched A chains of the outer most tier. In this hypothetical particle, laforin would release 25% of the total phosphate or ~21 phosphates. Only when the structure is disrupted by hydrolyzing enzymes would the remaining phosphate be removed. Perhaps this result suggests that phosphate is not equally distributed throughout the particle. If we assume that all phosphates on the A chains are sterically accessible to laforin, and the amount hydrolyzed is an absolute measure of the phosphate on the A chains, then the inner 11 tiers would contain 75% of the phosphate, far from equally distributed considering the inner 11 tiers would contain 50% of the glucose. It is interesting that the rate of phosphate release from both amylopectin and glycogen is saturable by substrate and follows approximately hyperbolic kinetics. The apparent K_m's for amylopectin and glycogen were 1.5 mg/ml and 4.5 mg/ml respectively. For glycogen with Mr 10^7, the K_m would be 0.45 μM. Expressed in terms of covalent phosphate concentrations, the values would be 47.3 μM and 42.5 μM for amylopectin and glycogen, respectively. However, if only 25% of the glycogen phosphate is assumed to be accessible, the K_m would be reduced to ~10 μM. Nonetheless, these K_m values are quite close to each other and would be consistent with some commonality in the reaction mechanism for phosphate removal from both polysaccharides. However, interpreting the kinetics of polysaccharide dephosphorylation by laforin is complex. First, both glycogen and amylopectin are polydisperse. Secondly, the analysis is complicated by the fact that laforin contains a carbohydrate binding domain separate from the catalytic site and that laforin activity requires a functional carbohydrate binding domain. In fact, if the inhibition of laforin *p*NPPase activity by polysaccharide (107) reflects binding, then even at the lowest substrate concentrations of Figures 14B and D, virtually all of the laforin would be bound. Thus, simple enzyme kinetic formulations may not be applicable.

2. Lafora Disease Mouse Models

Lafora disease is a progressive disorder and patients are relatively normal until they develop neurological symptoms starting in their teenage years with rapid progression and subsequent death within about 10 years (89-91). Therefore a molecular explanation for LD must account for the gradual nature of its onset and subsequent course, despite the fact that any genetically determined defects in proteins will be present from birth. Currently, a prevailing hypothesis is that the symptoms of the disease accompany the accumulation of the Lafora bodies which, in neurons, leads to cell death and the associated epilepsy, myoclonus, ataxia and other symptoms. Lafora bodies contain abnormally branched deposits of the normal cellular storage compound, glycogen (177, 178). In our studies of *Epm2a-/-*, mice we have observed age-dependent changes in the properties of glycogen that parallel the course of the disease and can explain its progressive nature. Based on these data, we believe that the initial hyperphosphorylation of glycogen in *Epm2a*-/- animals leads to altered physico-chemical properties that do not grossly affect the normal synthesis and degradation cycle of the polysaccharide. With time, the glycogen develops into a polysaccharide whose branching structure is substantially altered to form an insoluble polymer, with the characteristics of polyglucosan. We envisage a threshold in glycogen phosphorylation beyond which the glycogen is destined to become the insoluble polyglucosan that results in the pathology of the disease.

The frequency of phosphorylation measured for muscle glycogen from wild type mice, regardless of age, was around 1 per 1500 glucose residues. The value we reported for rabbit muscle glycogen was 1 per 650, which is similar to previous values cited in the literature (4, 5). This difference could be species related or could result from differences in the isolation protocols. In any case, phosphorylation is relatively rare and, in the 3 month old *Epm2a*-/- mice, is only increased to 1 in ~375 glucose residues. The average number of phosphates per glycogen molecule in mice, assuming 9 tiers (diameter of 30.6 nm and 15,386 glucose residues) would be ~10 which would increase to ~40 in young *Epm2a*-/- mice. It is difficult to conceive how addition of such a relatively small

number of charged groups could alone cause a dramatic change in ethanol solubility, especially as the phosphates are probably not all located on the outermost tiers of the molecule. More importantly, one might postulate that increased phosphorylation would actually make the polymer less soluble in a less polar solvent like ethanol. Phosphorylation is clearly responsible for the increased ethanol solubility since its removal with laforin reverts the solubility properties to that of wild type glycogen (Figure 21). We propose that the phosphates elicit a global change in glycogen structure. Experimental determination of glycogen structure is hampered by the fact that the polymer is polydisperse with respect both to size and to exact branching structure. However, there is a strong expectation that glycogen, like amylopectin, will contain polyglucose helices. A crystal structure of a cycloamylose has been determined (179). This molecule is a 26 residue cyclic polymer of glucose in α-1, 4- linkages (cyclomaltohexicosaose) that adopts a structure with two antiparallel polyglucose helices in which the glucose oxygen atoms are oriented towards the exterior surface and the carbon skeletons of the glucoses line the interior of the helix (Figure 63). While this molecule maintains the helical structures by constraints not present in native glycogen or amylopectin, it is not unreasonable to propose that some of the structural features occur in the native polysaccharides. It is notable in the cycloamylose structure that the helices are stabilized by intra-helical hydrogen bonding mediated by the physically adjacent 6', 2' and 3' hydroxyls (Figure 63). From inspection of the structure, it is apparent that the introduction of phosphate groups to virtually any glucose hydroxyl group would disrupt the local hydrogen bonding, destabilize the secondary structure, and potentially expose the more hydrophobic faces of the glucose residues to solvent. We propose that the glycogen molecule can maintain its compact structure with a low number of phosphorylations but that, past some threshold, too many helices lose their regular structure, resulting in altered packing of the polyglucose chains and global disruption of the structure of the molecule. In this situation, the ethanol solubility is actually enhanced by the disruption of the secondary structure caused by phosphorylation.

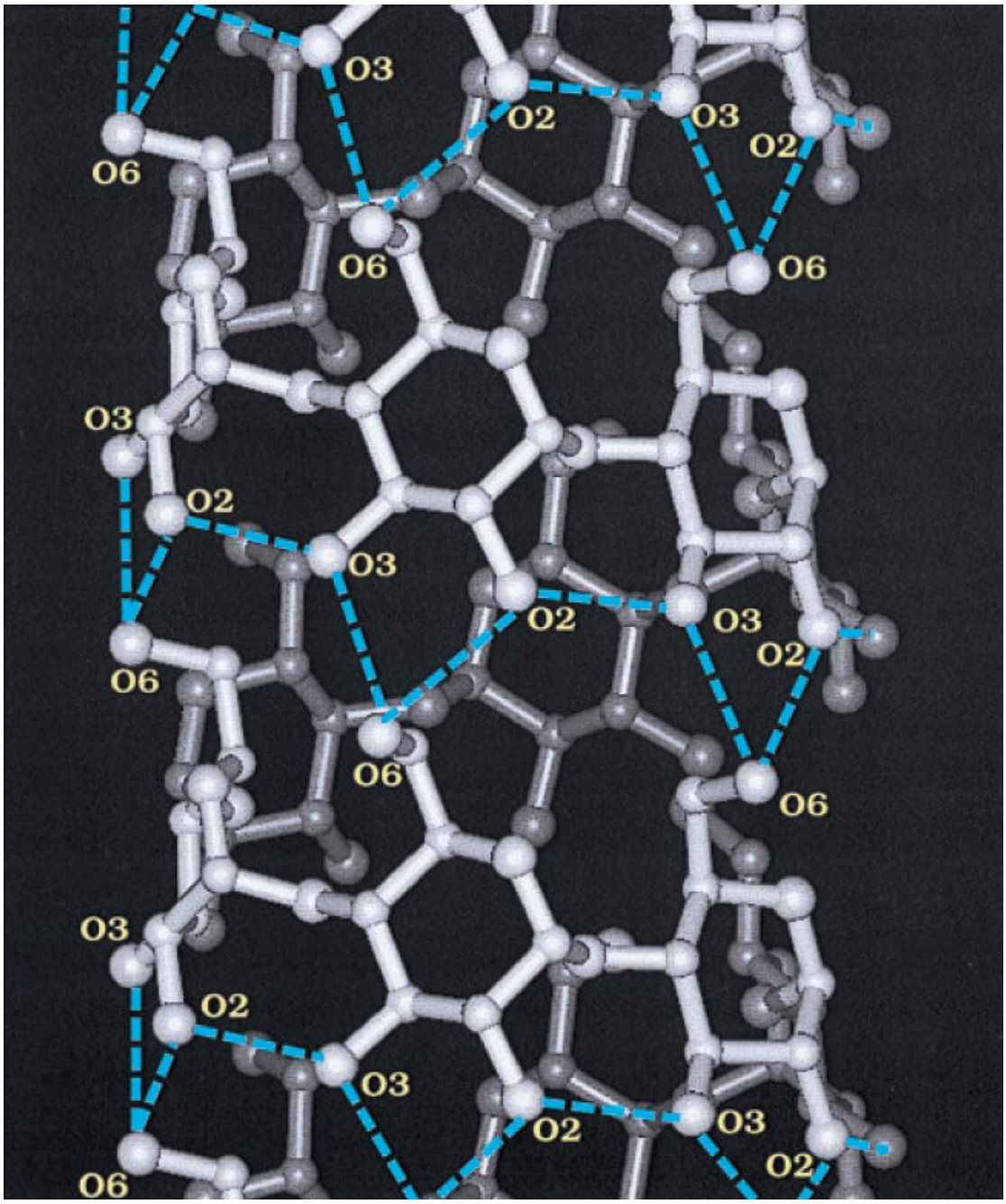

Figure 63. Crystal structure of v-amylose. View of the ideal left-handed, single-stranded v-amylose helix constructed on the basis of the central 6 glucoses in the four helical parts of the two symmetry-independent CA26 molecules in the triclinic unit cell. All C(6)–O(6) groups are oriented (2) *gauche*, hydrogen bonds $O(3)_n \cdots O(2)_{n+1}$ and $O(6)_n \cdots O(2)_{n+6}$; $O(6)_n \cdots O(3)_{n+6}$; drawn in blue. Adapted from Gessler et al. 96, 4246-4251. (1999) PNAS.

The glycogen purified from 9-12 month old *Epm2a*-/- mice has properties consistent with the formation of Lafora bodies. As the knockout mice age from 3 to 9-12 months, the increase in glycogen phosphorylation is relatively small but is accompanied by a major decrease in branching, acquisition of water insolubility, development of gross morphological abnormalities as observed by electron microscopy, and a tendency to aggregate. Aggregation is inferred from the appearance of large conglomerated structures by electron microscopy and also the fact that low speed centrifugation of tissue extracts recovers the majority of the glycogen in the pellet fraction. Normal glycogen particles in tissue extracts require high speed centrifugation (for example, 100,000 x g for 2 hours) to be removed from aqueous solution. Thus, the low speed centrifugation operationally defines two populations of glycogen particles. The glycogen particles present in the LSP are larger, have an altered iodine spectrum, are water insoluble and have an abnormal appearance by electron microscopy, as compared with the polysaccharide that remains in the supernatant which behaves more like normal glycogen. Based on the amount of covalently attached glycogenin, which essentially provides a count of the number of glycogen molecules present, the actual sizes of the glycogen molecules in the two fractions are not greatly different, only some 60% larger in the LSP fraction. This relatively small increase cannot explain the large change in hydrodynamic properties allowing sedimentation by low speed centrifugation and argues for the presence of aggregates in the LSP. In other words, the glycogen particles in the LSP must be formed of multiple, individual glycogen molecules. Both aggregation and water insolubility likely contribute to the formation of Lafora bodies. The insolubility can be attributed primarily to the reduced branching of the polysaccharide and is unaffected by dephosphorylation *in vitro* with laforin (data not shown). Aggregation requires the presence of the phosphate since its removal reverses much of the abnormal morphology seen by electron microscopy (Figure 23A & B). However, aggregation must also depend on the poorly branched structure since it is not observed with glycogen from the young *Epm2a*-/- animals, even though significant hyperphosphorylation has already

occurred. Thus, aberrant glycogen phosphorylation may be viewed as necessary but not sufficient for Lafora body formation in this model. How phosphorylation and reduced branching combine to favor aggregation of glycogen molecules in tissues is not clear at this time.

A major question in Lafora research is how loss of function of laforin or malin contributes to the generation of Lafora bodies. The first reported laforin substrate was the protein kinase GSK-3 (104, 180) that regulates glycogen synthase activity. However, not all reports support this hypothesis (3, 113, 138) which is also inconsistent with the observation that glycogen synthase -/+ glucose-6P activity ratio is not increased in *Epm2a*-/- or the *Epm2b-/-* animals and perhaps more importantly, the phosphorylation state of GSK3 is unchanged in both animal models. We favor the hypothesis that a primary function of laforin *in vivo* is as a glycogen phosphatase. It focuses on the idea that LD is essentially a metabolic disorder and that laforin is a glycogen metabolic enzyme. It could in fact be viewed as part of a repair or corrective mechanism, such as exists for the synthesis of other biopolymers, like DNA. Normal glycogen contains low levels of covalent phosphate and laforin will limit phosphorylation to what has evolved to be a structurally tolerated level. In the absence of functional laforin, as in the *Epm2a*-/- mice or LD patients, the usual cycles of glycogen synthesis and degradation in the various tissues initially proceed relatively normally but with time the glycogen gradually accumulates structural defects that set it on the course to develop into polyglucosan.

Defects in malin must also result in accumulation of polyglucosan. Malin could function in concert or upstream of laforin in the control of glycogen phosphorylation, resulting in an essentially identical mechanism to that proposed for laforin. Alternatively, it could regulate glycogen phosphorylation independently of laforin, for example down-regulating enzyme(s) responsible for introducing phosphate into glycogen. Finally, it could function to limit the transition from normally branched glycogen to polyglucosan. From our initial analyses of the *Epm2b-/-* mice, we favor the idea that malin prevents laforin sequestration in an insoluble fraction. Simple binding of malin and laforin could

be sufficient to maintain laforin in the soluble compartment to remove excessive phosphate from glycogen. Malin could actively oppose the formation of abnormally structured glycogen, as a positive regulator of laforin activity or by an unknown laforin-independent mechanism. Alternatively, rather than affecting the formation of abnormal glycogen, malin could prevent accumulation by promoting its disposal to lysosomes. In any event, the accumulation of structurally aberrant glycogen would disproportionately bind laforin which is known to interact preferentially with poorly branched polysaccharides like amylopectin (107) and polyglucosan (95).

Most Lafora research has focused on ways in which malin and laforin function to limit the transition from normally branched glycogen to polyglucosan and several potential malin targets have been proposed. Biochemically, malin has been shown to act as an E3 ubiquitin ligase (105) and studies with cultured cells have implicated multiple proteins as targets for malin action, including glycogen synthase, debranching enzyme, PTG and laforin (105, 117-119). In studies of hepatocytes (116) and neurons (117), the groups of Guinovart and de Cordoba proposed that a malin-laforin complex ubiquitylated the type 1 phosphatase regulatory subunit PTG and, in neurons, also glycogen synthase, leading to their degradation. Worby et al. (118) also reported that malin targets PTG for degradation in a laforin-dependent manner. Impaired degradation of either glycogen synthase or PTG should result in increased glycogen elongating activity, either by directly increasing glycogen synthase levels or, in the case of PTG, by increased targeting of PP1 to glycogen causing dephosphorylation and activation of glycogen synthase. An imbalance between elongating and branching activity has long been proposed as a potential mechanism for polyglucosan formation (181). If a functional laforin-malin complex targets these proteins for degradation by ubiquitylation, as proposed, one would expect their levels to be elevated when laforin or malin activity is defective, as in Lafora patients with *EPM2A* and *EPM2B* mutations or in mice with the *Epm2a* or the *Epm2b* gene disrupted. From our analysis of the *Epm2a-/-* and *Epm2b-/-* mice

we find no evidence for changes in the levels of debranching enzyme or PTG, arguing against laforin-malin dependent degradation in normal animals.

The results with glycogen synthase in the *Epm2a-/-* mice were more complex. At 3 months of age the *Epm2a*-/- mice have normal glycogen levels and a slight redistribution of glycogen synthase to the insoluble LSP. In the older animals total glycogen levels were significantly elevated in muscle and brain, and the majority of this glycogen was recoverable in the LSP/polyglucosan fraction as abnormally structured polysaccharide. Glycogen synthase protein, judged by Western blot, was significantly elevated in this fraction as compared with wild type samples. This result is also consistent with the *in vitro* observation that purified glycogen synthase binds more effectively to the abnormal glycogen isolated from old *Epm2a*-/- muscle. This increase in glycogen synthase could be consistent with laforin-dependent breakdown of glycogen synthase by malin. However, it is not a unique explanation since our experience with several genetically modified mouse models indicates that glycogen content correlates with glycogen synthase protein level. Binding to glycogen itself appears to stabilize glycogen synthase. For example, overexpression of another PP1 regulatory subunit, R_{GL}/G_M, leads to increased glycogen in muscle and elevated glycogen synthase protein (52). Decreased glycogen levels, as observed in R_{GL} knockout (53) or PTG knockout (DePaoli-Roach, unpublished data) animals, were associated with decreased glycogen synthase. The question then is whether the elevated glycogen synthase in the *Epm2a*-/- mice is secondary to the increased glycogen levels or the cause of the glycogen over-accumulation? In any event, the results from the old *Epm2a-/-* mice are confounding with respect to the enzymatic imbalance theory of polyglucosan formation in LD because the glycogen synthase recovered in the LSP has low activity. Normalizing activity in the presence of glucose-6P to the protein detected by Western blot, indicates a 2-3 fold decrease in specific activity in the LSP of *Epm2a*-/- mice compared to the LSS. Simplistically, these activity measurements do not indicate an enzymatic imbalance towards elongating activity in the knockout animals. The assessment is unchanged if activities determined in the

absence of glucose-6P are considered. The caveat would be if the enzyme assays, for some reason, do not reflect the true activity of the glycogen synthase in the LSP of the *Epm2a*-/- animals. One idea would be that association of glycogen synthase with the insoluble polyglucosan aggregates effectively removes the enzyme from the soluble phase, limiting our ability to measure activity by traditional assays, but *in vivo* allowing for effective elongation and synthesis of the glycogen. A different possibility would be that some unrecognized, stable modification of the enzyme is able to reduce activity, even in the presence of glucose-6P, an eventuality that would argue against the imbalance hypothesis. In the 3 month old *Epm2b-/-* mice, glycogen synthase total activity and -/+ glucose-6P activity ratios were unchanged, although in brain there was a trend to increased total activity in the LSP, consistent with our observations of the 3 month old *Epm2a-/-* mice. These results were confirmed by Western blotting with anti-glycogen synthase antibodies, and in the case of brain the increased proportion of glycogen synthase protein in the LSP was statistically significant.

An alternative mechanism for polyglucosan formation in *Epm2a*-/- mice would be loss of control of the branching/debranching system. The debranching enzyme, AGL, was proposed to be a malin target by Cheng et al. (119). Defects in malin function, then, should correlate with elevated AGL protein which the authors proposed would lead to less branched glycogen. The AGL protein level was unchanged in muscle or brain of *Epm2a*-/- and the *Epm2b-/-* mice arguing against increased debranching activity accounting for polyglucosan formation in this model. In any event, based on the two stage degradation of glycogen by phosphorylase and debranching enzyme, excessive AGL activity should only reduce branching frequency if phosphorylase, an abundant enzyme, becomes limiting. During synthesis, reduced branching enzyme activity could also potentially lead to impaired glycogen branching but in previous analyses of young *Epm2a*-/- (3) and C266S over-expressing mice (138), there was no evidence for a major decrease in branching enzyme activity in knockout animals. Our systematic analysis of glycogen metabolism in the *Epm2a-/-* and the *Epm2b-/-*

mice do not support the enzymatic imbalance hypothesis as being the predominant initial defect in the formation of Lafora bodies. Our model for Lafora body formation envisions a transition from relatively normal glycogen metabolism to a state in which incremental damage to glycogen molecules, triggered by hyperphosphorylation, leads to abnormal glycogen structure that in the long term becomes insoluble, poorly branched, aggregates of polyglucosan that can explain the formation of Lafora disease.

3. The Incorporation of Phosphate into Glycogen and the Chemistry of the Phosphorylation

The synthesis of biological polymers in nature, in many instances, is prone to errors by the polymerizing enzyme. The cell exhausts a great deal of energy in order to repair these mistakes, usually by recruiting "repair" proteins. The classic example is that of errors that occur during DNA replication, although errors in protein synthesis and the transcription of DNA to mRNA are also common (182-185). Incorporation of an incorrect nucleotide by DNA polymerase is rare, with a frequency of about 1 error every 100,000 nucleotides (186). At first glance, this rate seems almost negligible but in the case of humans with 6 billion base pairs in each diploid cell, this would account for ~120,000 errors every time the cell divides. Obviously, this is not the case due to the various DNA repair proteins which monitor the DNA for mistakes and repair them. Here we add another biopolymer, glycogen, to the list of those polymers prone to errors by their respective polymerizing enzymes.

Our *in vitro* and *in vivo* data support the notion that glycogen phosphorylation drives the formation of Lafora bodies and the subsequent neurological phenotype in Lafora patients. Therefore, understanding how the phosphate is incorporated and where the phosphate resides in the polymer is of fundamental importance not only for Lafora disease, but also for glycogen metabolism in general. We propose that phosphate incorporation into glycogen by glycogen synthase represents an enzymatic error not unlike mistakes in DNA

synthesis. As with DNA, we suggest that there is an evolved repair mechanism, in this case based on the action of the laforin phosphatase.

In vivo evidence for the incorporation of phosphate into glycogen by glycogen synthase comes from studies of mice exercised to exhaustion on a treadmill (J.M. Irimia unpublished observations). Exhaustive exercise in mice decreases muscle glycogen to about 20% of the normal value with a concomitant decrease in the total phosphate content of the glycogen. During recovery and subsequent glycogen synthesis, the total glycogen phosphate levels increase at a rate of about 1 phosphate every 6,500 glucoses, similar to our *in vitro* rate of phosphate incorporation by glycogen synthase. It is important to distinguish between the *rate* of phosphate incorporation and the *density* of basal phosphorylation or the frequency of phosphorylation. Glycogen synthase incorporates phosphate at a *rate* of 1 Pi every 5,000-10,000 glucose residues. However, the glycogen molecule has a *density* of basal phosphorylation of 1 phosphate every 1,500 glucose residues in mouse skeletal muscle for example. Although total phosphate levels increase during glycogen synthesis in the exercised mice, the density of phosphate (molPi / mol glc) decreases. This would be expected if only 1 phosphate is being incorporated approximately every 6,500 glucoses (Figure 64) and the basal density of phosphorylation in WT mice is about 1 phosphate every 1,500 glucoses. These data are consistent with phosphate being introduced *in vivo* during glycogen synthesis. Interestingly, the phosphate density never reaches the levels present in the basal, non exercised mice, even after a week of rest. We believe that this is due to the fact that glycogen synthase has not been through enough rounds of synthesis required to introduce phosphate back to basal levels. Perhaps an alternative explanation would be that during basal glycogen metabolism, only the outer tiers of the glycogen molecule are being turned over and the phosphate incorporated on the outer tier is rapidly hydrolyzed by laforin. Only after substantial depletion of glycogen such as after a bout of exercise, would the particle be degraded to an extent that the phosphate introduced during the subsequent re-synthesis by glycogen synthase would reside in the inner tiers of the molecule, shielded from

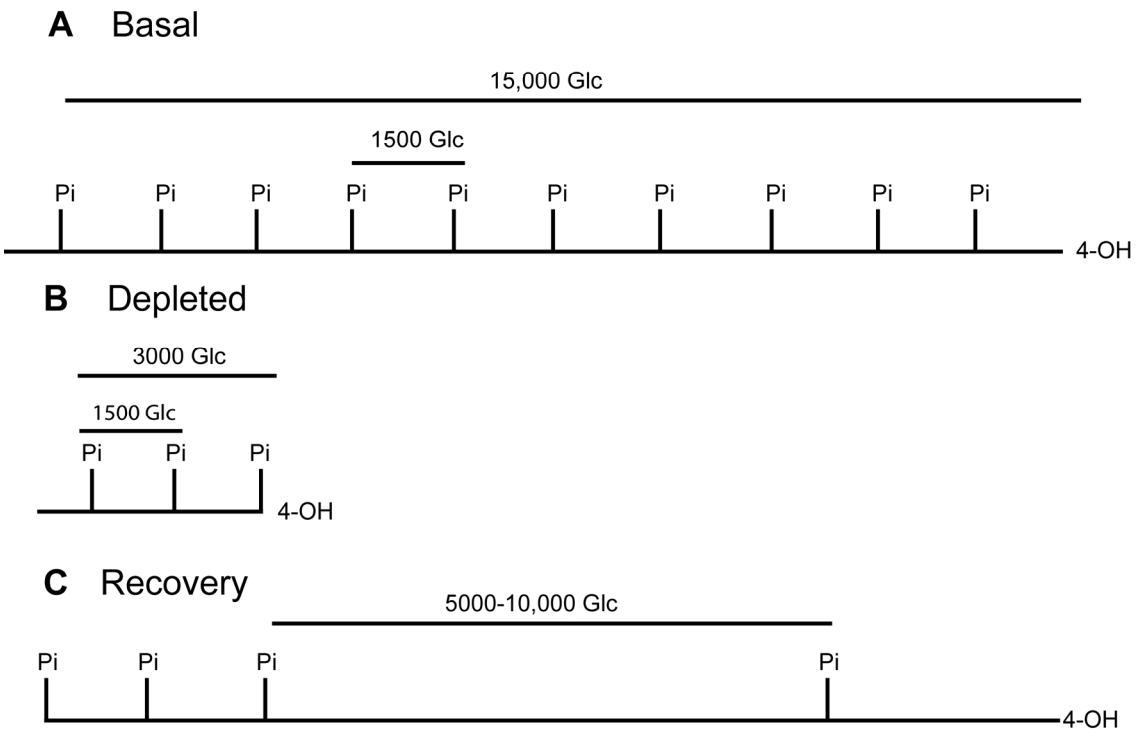

Figure 64. Linear model for phosphate metabolism in glycogen. A. Normal glycogen contains a basal level of phosphorylation. In mice, the frequency is about 1 Pi every 1500 glucose residues. **B.** After exhaustive exercise, mouse glycogen is depleted to about 20% the basal levels, total phosphate levels decrease due to laforin action but the density of phosphate increases slightly as the number of glucoses removed by phosphorylase must exceed the number of phosphates removed by laforin. **C.** In the recovery period, glycogen is synthesized and glycogen synthase incorporates phosphate at a rate of 1 Pi every 5000-10000 glucose residues. Although the total amount of phosphate increases, the density of phosphate decreases as the incorporation of glucose is far greater than that of phosphate. Only when glycogen synthase has gone through multiple rounds of synthesis will phosphate levels reach basal levels.

laforin action. In other words, the basal level of phosphorylation is restricted to the inner tiers of the particle or the B chains, consistent with laforin only being able to remove 25% of the phosphate from the intact glycogen molecule. Nevertheless, depletion of 80% of the glycogen in mouse muscle after exercise, assuming all glycogen molecules are degraded equally, would remove the two outer tiers plus about 50% of the third outermost tier of the molecule. However, Shearer and Graham (153) have suggested that different pools of glycogen granules appear to be degraded preferentially depending on exercise conditions, and whether or not this is dependent on the degree of phosphorylation of different pools of glycogen is unknown.

It is also of interest to note that liver glycogen phosphate levels decrease as mice age. Liver glycogen is turned over much more frequently than muscle glycogen, as the glucose stored as glycogen in the liver is mobilized to the bloodstream in the fasted state. The decrease in the frequency of phosphorylation as mice age may be explained by the same reasoning described for muscle glycogen after depletion by exercise.

The UDP-glucose: glycogen glucose-1-phosphotransferase described by Lomako et al. (5) was proposed to transfer the β-phosphate of UDP-glucose into glycogen with the formation a C1-O-P-O-C6 bridging phosphodiester. Perhaps the most obvious mechanism for the incorporation of phosphate into glycogen catalyzed by glycogen synthase would be through the formation of a C1-O-P-O-C4 phosphodiester. This is based on the idea that the non-reducing C4-OH in the acceptor glycogen molecule is thought to act as a nucleophile, attacking the C1 carbon of UDP-glucose with the subsequent formation of an α-1,4-glycosidic linkage. Our original hypothesis was that the C4-OH of glycogen would attack the electrophilic β-phosphate of UDP-glucose forming a C1-O-P-O-C4 phosphodiester linkage. However, there is no evidence that laforin has phosphodiesterase activity. In our *in vitro* characterization of laforin action, we were unable to detect activity towards the commercially available *p*-nitrophenolphosphocholine or *p*-nitrophenyl phenylphosphonate, two commonly used chromogenic phosphodiesterase substrates. Therefore, we originally

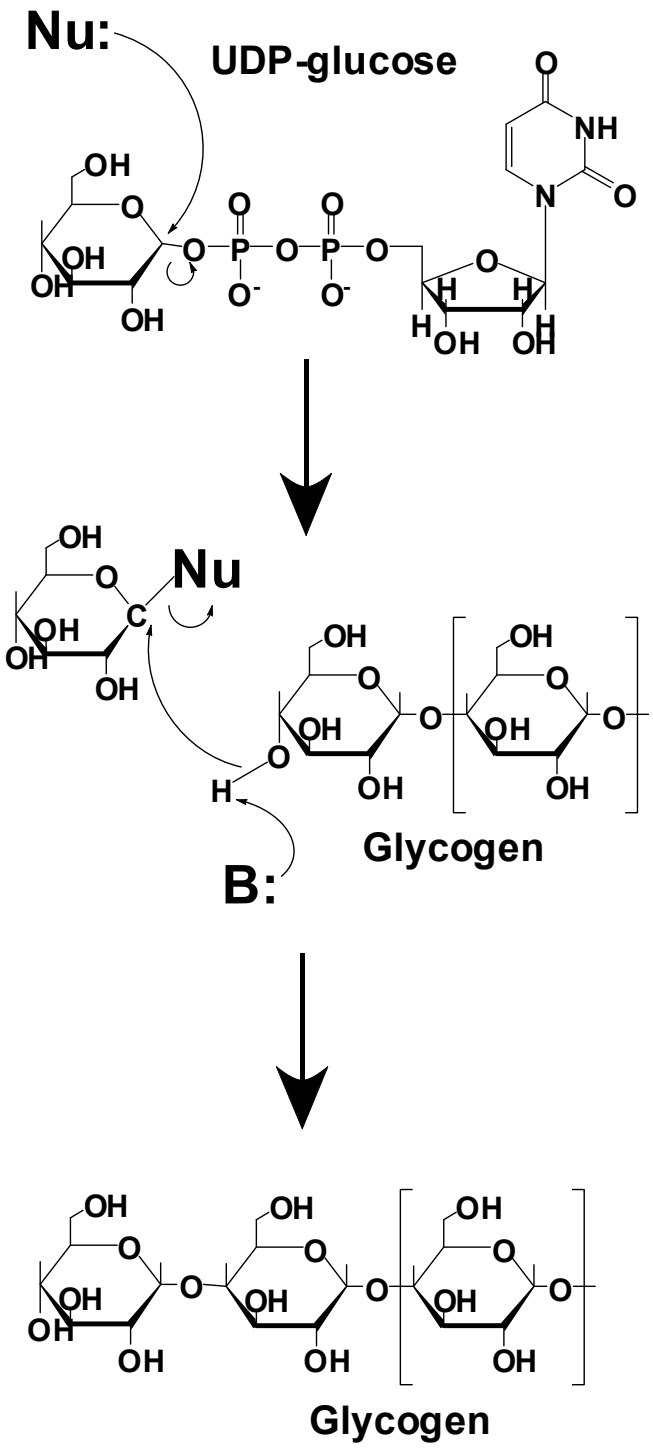

Figure 65. Proposed mechanism of glycogen polymerization catalyzed by glycogen synthase. An unknown amino acid in the active site of glycogen synthase acts as a nucleophile (Nu:) and attacks the anomeric carbon of UDP-glucose with the release of UDP. A basic residue (B:) deprotonates and activates the C4-OH making the oxygen a good nucleophile. Attack at C1 displaces the enzyme and forms an α-1,4-glycosidic linkage.

hypothesized that there must be a phosphodiesterase that would hydrolyze the phosphodiester bond and that laforin would then remove the phosphomonester. An interesting phosphodiesterase candidate was the putative glycerophosphoryl diester diesterases, KIA1434, that additionally contained a CBM20, but our unexpected observation that laforin could hydrolyze phosphate incorporated by glycogen synthase, avoids the necessity for a phosphodiesterase such as KIAA1434 to remove glycogen synthase incorporated phosphate.

Our initial attempts at determining the phosphate position of glycogen using acid hydrolysis were somewhat misleading since glucose-6P was detected in two separate experiments. The phenomenon of phosphoryl migration under acidic conditions has been observed in xylose phosphates (169) and our results suggest that this migration phenomenon also occurs in glucose. Acid hydrolysis of glycogen and subsequent determination of glucose-6P enzymatically via glucose-6P dehydrogenase revealed the presence of glucose-6P in the polysaccharide. Similarly, acid hydrolysis of the phosphorylated oligosaccharides prepared by the enzymatic hydrolysis of glycogen produced glucose-6P as judged by HPAEC. Nonetheless, glucose-6P was not detected by NMR spectroscopy analysis of the phosphorylated oligosaccharides, supporting the idea of phosphoryl group migration in glucose phosphates during acid hydrolysis.

Glycogen synthase normally transfers the glucosyl moiety of UDP-glucose to the non-reducing end of the glycogen particle. Mechanistically, an active site amino acid is thought to act as a nucleophile attacking the anomeric carbon, displacing UDP. A basic amino acid deprotonates the C4-OH of the acceptor glycogen molecule, thus making the non-reducing end of glycogen a nucleophile. Attack at the anomeric carbon recovers the stereochemistry with the formation of an α-1,4-glycosidic linkage (Figure 65). How the β-phosphate is incorporated at the 2-OH and the 3-OH is speculative at this time but we propose that a similar mechanism exists involving the spontaneous formation of glucose-1,2-cyclic phosphate and/or glucose-1,3-cyclic phosphate in the active site (Figure 66). Nucleophiilic attack at C1 of the cyclic phosphate would open the ring and the

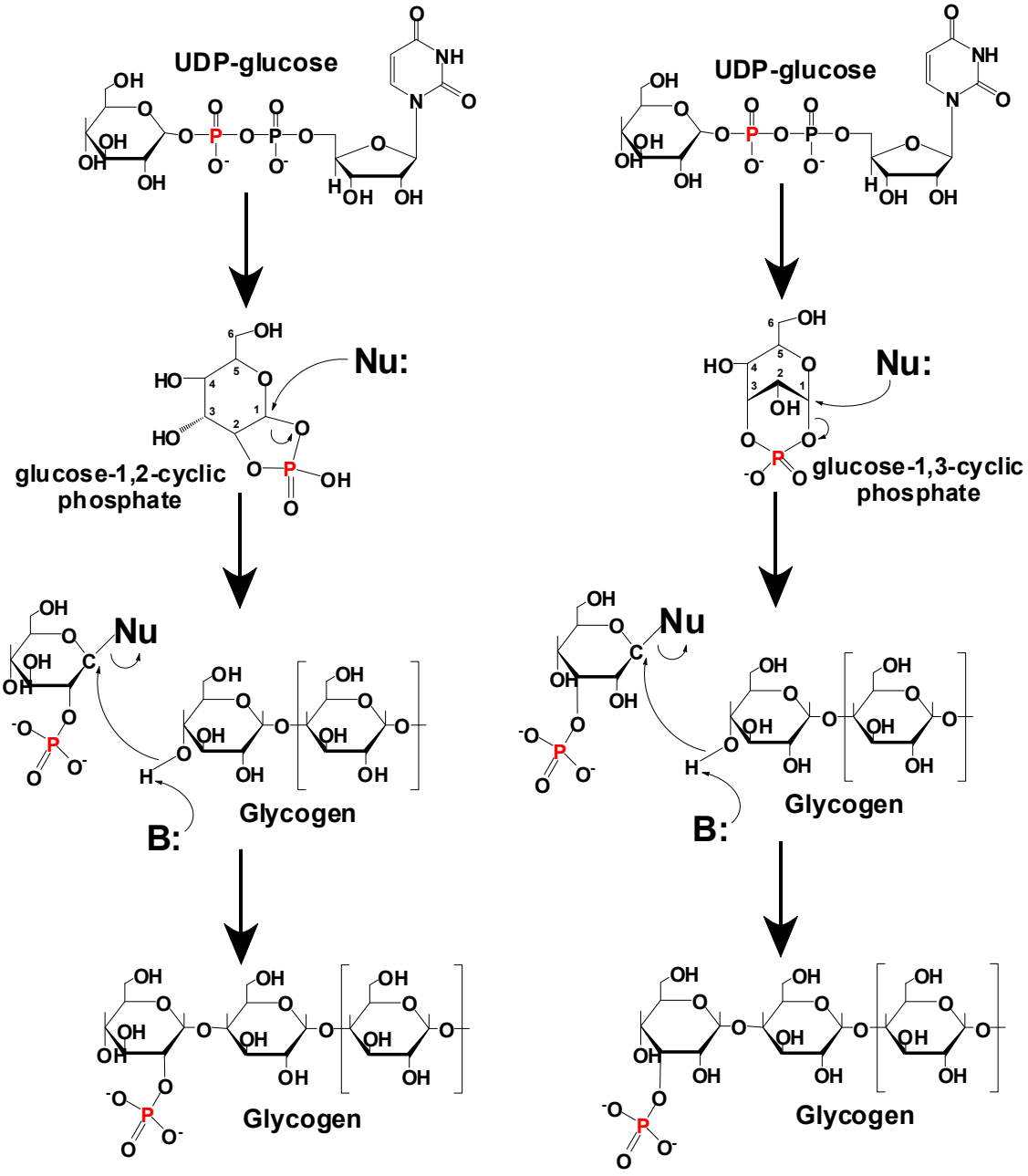

Figure 66. Proposed mechanism for the incorporation of phosphate at the C2-OH and the C3-OH in glycogen. We propose that during catalysis, one UDP-glucose molecule for every 5000-10000 that enters the active site of glycogen synthase breaks down to form glucose-1,2-cyclic phosphate (left) or glucose-1,3-cyclic phosphate (right). The active site nucleophile breaks the unstable cyclic phosphate by attack on C1. The activated 4-OH attacks the anomeric carbon forming an α-1,4-glycosidic linkage. By this mechanism, phosphate would be introduced at the C2 and C3 hydroxyls in glycogen by glycogen synthase.

activated C4-OH at the non-reducing end of glycogen would form an α-1-4-linkage (Figure 66). We propose that a small fraction of UDP-glucose will form a mixture of glucose-1,2-cyclic phosphate and glucose-1,3-cyclic phosphate, the former possibly being more prone to attack by a nucleophile at C1 due to the fact the five membered cyclic phosphates are less stable than six membered cyclic phosphates (168, 173).

It is perhaps not uncommon for enzymes to make mistakes. Most errors would go unnoticed, not affecting the cell's chance of survival in any way. If hexokinase, for example "accidently" phosphorylates one glucose-1P molecule for every 10,000 rounds of catalysis with glucose, the mistake would have virtually no impact on the survival of the cell. In the case of DNA synthesis, however, these mistakes could have profound impact on the survival of not only the cell but the organism. Therefore, evolution has found ways to correct these mistakes through repair proteins. Our data suggest that this is true for glycogen as well. The inadvertent incorporation of phosphate into glycogen during glycogen synthesis, over time, has profound implications for glycogen structure and metabolism, as highlighted in patients with Lafora disease. It is interesting, and perhaps very informative, that through evolution laforin is found for the most part, only in vertebrates. Do errors in glycogen synthesis only affect species that live long enough? Our attempts to measure total phosphate in the budding yeast, *S. cerevesiae* were unsuccessful, as we could never purify the glycogen sufficiently to remove contaminating material. Nonetheless, treatment with laforin was unable to release any detectable inorganic phosphate (data not shown), quite possibly because yeast glycogen does not contain significant levels of phosphate. One possibility could be that yeast do not live long enough for glycogen synthase to catalyze enough rounds of synthesis to incorporate detectable levels of phosphate. However, throughout evolution, multicellular eukaryotes such as vertebrates lived long enough for phosphate to accumulate in the glycogen molecule and subsequently become toxic to the cell. Natural selection would favor those species that were able to "repair" their glycogen by removing the phosphate via laforin.

A characteristic feature of Lafora bodies is that the frequency of α-1,6-glycosidic linkages is reduced. The mechanism by which phosphate affects branching of glycogen is speculative at this time. It remains to be seen if substrate specificity of the branching enzyme may be hindered by the presence of phosphate in a polysaccharide helix. There is precedent for this idea, as the glycogen hydrolyzing enzymes α-amylase and amyloglucosidase are not capable of quantitatively degrading glycogen to glucose. Perhaps this is due to the phosphate disrupting the secondary structure of a chain making phosphorylated regions of the polysaccharide resistant to enzymatic hydrolysis. In the cell, phosphorylated glycogen may prevent the branching enzyme from binding and forming an α-1,6-glycosidic linkage. Furthermore, it seems likely that glycogen phosphorylase will not be able to degrade past a phosphate during glycogenolysis. Phosphorylase is thought to degrade glycogen through transfer of a molecule of inorganic phosphate to the anomeric carbon at the non-reducing end, making glucose-1P a good leaving group with subsequent phosphorolysis. Incorporation of phosphate at the 2 or 3 hydroxyls would likely, for steric reasons, prevent the transfer of inorganic phosphate to C1, thus preventing glycogen degradation. Furthermore, phosphorylase may not be active towards a phosphorylated chain, as the secondary structure would be altered and binding may not be feasible. The end result would be an increase in total glycogen in the absence of laforin.

In summary, we envision a glycogen damage/repair process (Figure 67) that involves the transfer of the β-phosphate of UDP-glucose to the 2-OH and the 3-OH of a glycogen molecule during polymerization by glycogen synthase. Excessive phosphorylation “damages” the glycogen molecule by altering the physico-chemical properties of the polysaccharide that, if not “repaired” by laforin action, results in the formation of Lafora bodies in patients with Lafora disease.

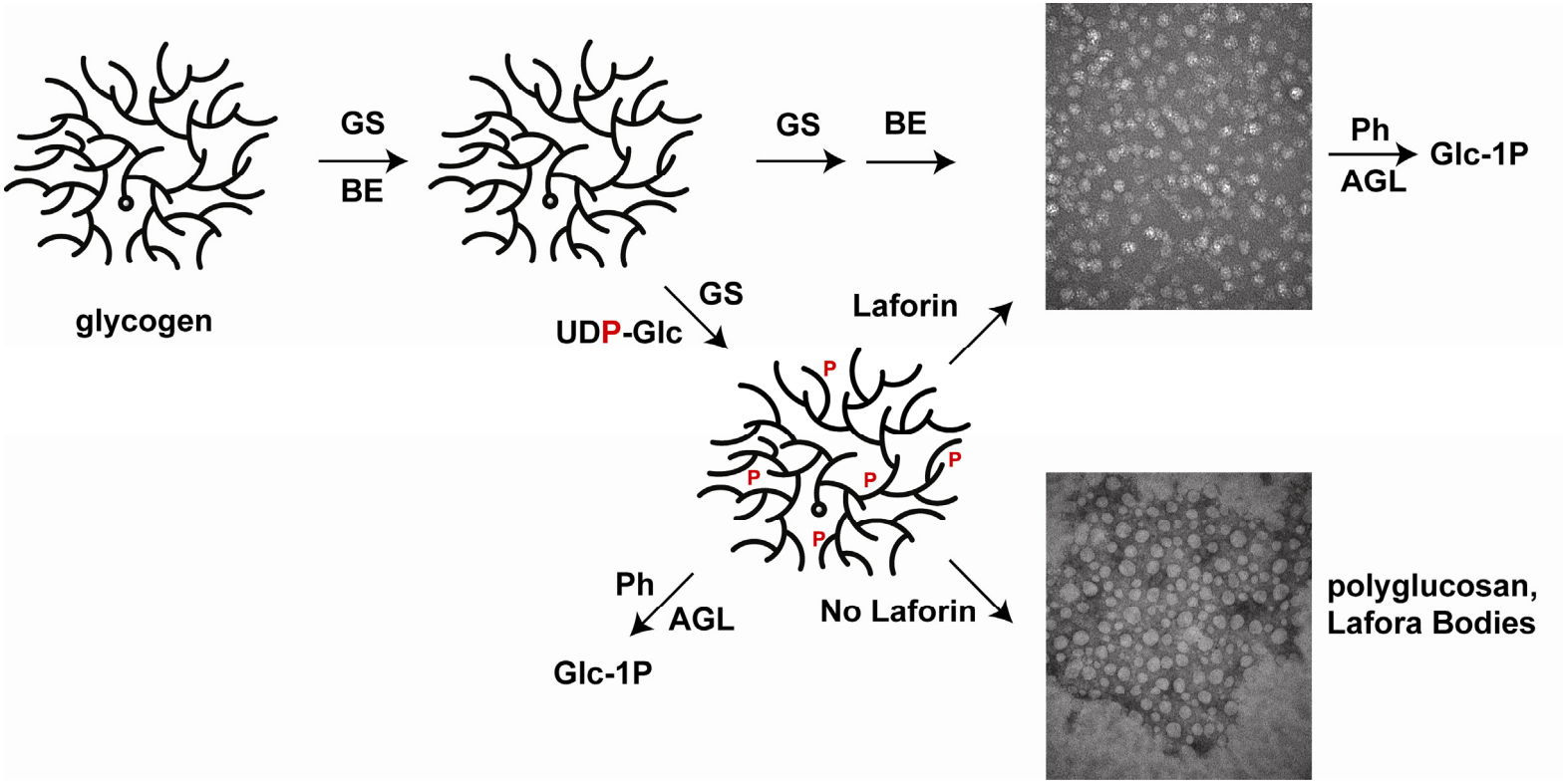

Figure 67. The metabolism of the covalent phosphate in glycogen. We envision a glycogen damage/repair process. During glycogen synthesis, glycogen synthase transfers the β-phosphate of UDP-glucose to glycogen with the formation of C2 and C3 phosphomonoesters. In the absence of the glycogen phosphatase laforin, such as in patients with Lafora disease, glycogen becomes excessively phosphorylated. The increase in phosphate disrupts the physico-chemical properties of the polysaccharide and with time, leads to the formation of Lafora bodies. We propose that laforin is a glycogen repair protein that repairs the damage incurred by glycogen synthase.

REFERENCES

1. Roach, P.J. 2002. Glycogen and its metabolism. *Curr Mol Med* 2:101-120.
2. Gunja-Smith, Z., Marshall, J.J., Mercier, C., Smith, E.E., and Whelan, W.J. 1970. A revision of the Meyer-Bernfeld model of glycogen and amylopectin. *FEBS Lett* 12:101-104.
3. Tagliabracci, V.S., Turnbull, J., Wang, W., Girard, J.M., Zhao, X., Skurat, A.V., Delgado-Escueta, A.V., Minassian, B.A., Depaoli-Roach, A.A., and Roach, P.J. 2007. Laforin is a glycogen phosphatase, deficiency of which leads to elevated phosphorylation of glycogen in vivo. *Proc Natl Acad Sci U S A* 104:19262-19266.
4. Lomako, J., Lomako, W.M., Whelan, W.J., and Marchase, R.B. 1993. Glycogen contains phosphodiester groups that can be introduced by UDPglucose: glycogen glucose 1-phosphotransferase. *FEBS Lett* 329:263-267.
5. Lomako, J., Lomako, W.M., Kirkman, B.R., and Whelan, W.J. 1994. The role of phosphate in muscle glycogen. *Biofactors* 4:167-171.
6. Fontana, J.D. 1980. The presence of phosphate in glycogen. *FEBS Lett* 109:85-92.
7. Tagliabracci, V.S., Girard, J.M., Segvich, D., Meyer, C., Turnbull, J., Zhao, X., Minassian, B.A., Depaoli-Roach, A.A., and Roach, P.J. 2008. Abnormal metabolism of glycogen phosphate as a cause for Lafora disease. *J Biol Chem* 283:33816-33825.
8. Blennow, A., Nielsen, T.H., Baunsgaard, L., Mikkelsen, R., and Engelsen, S.B. 2002. Starch phosphorylation: a new front line in starch research. *Trends Plant Sci* 7:445-450.
9. Ritte, G., Heydenreich, M., Mahlow, S., Haebel, S., Kotting, O., and Steup, M. 2006. Phosphorylation of C6- and C3-positions of glucosyl residues in starch is catalysed by distinct dikinases. *FEBS Lett* 580:4872-4876.
10. Niittyla, T., Comparot-Moss, S., Lue, W.L., Messerli, G., Trevisan, M., Seymour, M.D., Gatehouse, J.A., Villadsen, D., Smith, S.M., Chen, J., et al. 2006. Similar protein phosphatases control starch metabolism in plants and glycogen metabolism in mammals. *J Biol Chem* 281:11815-11818.
11. Kotting, O., Santelia, D., Edner, C., Eicke, S., Marthaler, T., Gentry, M.S., Comparot-Moss, S., Chen, J., Smith, A.M., Steup, M., et al. 2009. STARCH-EXCESS4 is a laforin-like Phosphoglucan phosphatase required for starch degradation in Arabidopsis thaliana. *Plant Cell* 21:334-346.
12. Kirkman, B.R., and Whelan, W.J. 1986. Glucosamine is a normal component of liver glycogen. *FEBS Lett* 194:6-11.
13. Cori, C.F.C.G.T. 1939. The activating effect of glycogen on the enzymatic synthesis of glycogen from glucose-1-phosphate. *JBC* 131:397-398.
14. Krisman, C.R., and Barengo, R. 1975. A precursor of glycogen biosynthesis: alpha-1,4-glucan-protein. *Eur J Biochem* 52:117-123.
15. Butler, N.A., Lee, E.Y., and Whelan, W.J. 1977. A protein-bound glycogen component of rat liver. *Carbohydr Res* 55:73-82.

16. Mu, J., Skurat, A.V., and Roach, P.J. 1997. Glycogenin-2, a novel self-glucosylating protein involved in liver glycogen biosynthesis. *J Biol Chem* 272:27589-27597.
17. Moslemi, A.R., Lindberg, C., Nilsson, J., Tajsharghi, H., Andersson, B., and Oldfors, A. Glycogenin-1 deficiency and inactivated priming of glycogen synthesis. *N Engl J Med* 362:1203-1210.
18. Lomako, J., Lomako, W.M., and Whelan, W.J. 1988. A self-glucosylating protein is the primer for rabbit muscle glycogen biosynthesis. *FASEB J* 2:3097-3103.
19. Hurley, T.D., Walls, C., Bennett, J.R., Roach, P.J., and Wang, M. 2006. Direct detection of glycogenin reaction products during glycogen initiation. *Biochem Biophys Res Commun* 348:374-378.
20. Rodriguez, I.R., and Whelan, W.J. 1985. A novel glycosyl-amino acid linkage: rabbit-muscle glycogen is covalently linked to a protein via tyrosine. *Biochem Biophys Res Commun* 132:829-836.
21. Smythe, C., Caudwell, F.B., Ferguson, M., and Cohen, P. 1988. Isolation and structural analysis of a peptide containing the novel tyrosyl-glucose linkage in glycogenin. *EMBO J* 7:2681-2686.
22. Gibbons, B.J., Roach, P.J., and Hurley, T.D. 2002. Crystal structure of the autocatalytic initiator of glycogen biosynthesis, glycogenin. *J Mol Biol* 319:463-477.
23. McVerry, P.H., and Kim, K.H. 1974. Purification and kinetic mechanism of rat liver glycogen synthase. *Biochemistry* 13:3505-3511.
24. Friedman, D.L., and Larner, J. 1963. Studies on Udpg-Alpha-Glucan Transglucosylase. Iii. Interconversion of Two Forms of Muscle Udpg-Alpha-Glucan Transglucosylase by a Phosphorylation-Dephosphorylation Reaction Sequence. *Biochemistry* 2:669-675.
25. Roach, R.J., and Larner, J. 1977. Covalent phosphorylation in the regulation glycogen synthase activity. *Mol Cell Biochem* 15:179-200.
26. Picton, C., Woodgett, J., Hemmings, B., and Cohen, P. 1982. Multisite phosphorylation of glycogen synthase from rabbit skeletal muscle. Phosphorylation of site 5 by glycogen synthase kinase-5 (casein kinase-II) is a prerequisite for phosphorylation of sites 3 by glycogen synthase kinase-3. *FEBS Lett* 150:191-196.
27. DePaoli-Roach, A.A., Ahmad, Z., Camici, M., Lawrence, J.C., Jr., and Roach, P.J. 1983. Multiple phosphorylation of rabbit skeletal muscle glycogen synthase. Evidence for interactions among phosphorylation sites and the resolution of electrophoretically distinct forms of the subunit. *J Biol Chem* 258:10702-10709.
28. Roach, P.J., DePaoli-Roach, A.A., and Larner, J. 1978. Ca2+-stimulated phosphorylation of muscle glycogen synthase by phosphorylase b kinase. *J Cyclic Nucleotide Res* 4:245-257.
29. Huang, T.S., and Krebs, E.G. 1977. Amino acid sequence of a phosphorylation site in skeletal muscle glycogen synthetase. *Biochem Biophys Res Commun* 75:643-650.

30. Flotow, H., and Roach, P.J. 1989. Synergistic phosphorylation of rabbit muscle glycogen synthase by cyclic AMP-dependent protein kinase and casein kinase I. Implications for hormonal regulation of glycogen synthase. *J Biol Chem* 264:9126-9128.
31. Flotow, H., Graves, P.R., Wang, A.Q., Fiol, C.J., Roeske, R.W., and Roach, P.J. 1990. Phosphate groups as substrate determinants for casein kinase I action. *J Biol Chem* 265:14264-14269.
32. Fiol, C.J., Mahrenholz, A.M., Wang, Y., Roeske, R.W., and Roach, P.J. 1987. Formation of protein kinase recognition sites by covalent modification of the substrate. Molecular mechanism for the synergistic action of casein kinase II and glycogen synthase kinase 3. *J Biol Chem* 262:14042-14048.
33. Carling, D., and Hardie, D.G. 1989. The substrate and sequence specificity of the AMP-activated protein kinase. Phosphorylation of glycogen synthase and phosphorylase kinase. *Biochim Biophys Acta* 1012:81-86.
34. Wilson, W.A., Skurat, A.V., Probst, B., de Paoli-Roach, A., Roach, P.J., and Rutter, J. 2005. Control of mammalian glycogen synthase by PAS kinase. *Proc Natl Acad Sci U S A* 102:16596-16601.
35. Skurat, A.V., and Dietrich, A.D. 2004. Phosphorylation of Ser640 in muscle glycogen synthase by DYRK family protein kinases. *J Biol Chem* 279:2490-2498.
36. Kuma, Y., Campbell, D.G., and Cuenda, A. 2004. Identification of glycogen synthase as a new substrate for stress-activated protein kinase 2b/p38beta. *Biochem J* 379:133-139.
37. Skurat, A.V., Wang, Y., and Roach, P.J. 1994. Rabbit skeletal muscle glycogen synthase expressed in COS cells. Identification of regulatory phosphorylation sites. *J Biol Chem* 269:25534-25542.
38. Roach, P.J. 1991. Multisite and hierarchal protein phosphorylation. *J Biol Chem* 266:14139-14142.
39. Zhang, W., DePaoli-Roach, A.A., and Roach, P.J. 1993. Mechanisms of multisite phosphorylation and inactivation of rabbit muscle glycogen synthase. *Arch Biochem Biophys* 304:219-225.
40. Skurat, A.V., and Roach, P.J. 1995. Phosphorylation of sites 3a and 3b (Ser640 and Ser644) in the control of rabbit muscle glycogen synthase. *J Biol Chem* 270:12491-12497.
41. Rutter, J., Probst, B.L., and McKnight, S.L. 2002. Coordinate regulation of sugar flux and translation by PAS kinase. *Cell* 111:17-28.
42. Bollen, M., Peti, W., Ragusa, M.J., and Beullens, M. The extended PP1 toolkit: designed to create specificity. *Trends Biochem Sci*.
43. Gibson, W.B., Illingsworth, B., and Brown, D.H. 1971. Studies of glycogen branching enzyme. Preparation and properties of -1,4-glucan- -1,4-glucan 6-glycosyltransferase and its action on the characteristic polysaccharide of the liver of children with Type IV glycogen storage disease. *Biochemistry* 10:4253-4262.

44. Caudwell, F.B., and Cohen, P. 1980. Purification and subunit structure of glycogen-branching enzyme from rabbit skeletal muscle. *Eur J Biochem* 109:391-394.
45. Titani, K., Koide, A., Ericsson, L.H., Kumar, S., Hermann, J., Wade, R.D., Walsh, K.A., Neurath, H., and Fischer, E.H. 1978. Sequence of the carboxyl-terminal 492 residues of rabbit muscle glycogen phosphorylase including the pyridoxal 5'-phosphate binding site. *Biochemistry* 17:5680-5693.
46. Gilboe, D.P., Larson, K.L., and Nuttall, F.Q. 1972. Radioactive method for the assay of glycogen phosphorylases. *Anal Biochem* 47:20-27.
47. Cohen, P.T. 2002. Protein phosphatase 1--targeted in many directions. *J Cell Sci* 115:241-256.
48. Yan, B., Heus, J., Lu, N., Nichols, R.C., Raben, N., and Plotz, P.H. 2001. Transcriptional regulation of the human acid alpha-glucosidase gene. Identification of a repressor element and its transcription factors Hes-1 and YY1. *J Biol Chem* 276:1789-1793.
49. Ceulemans, H., and Bollen, M. 2004. Functional diversity of protein phosphatase-1, a cellular economizer and reset button. *Physiol Rev* 84:1-39.
50. Ceulemans, H., Stalmans, W., and Bollen, M. 2002. Regulator-driven functional diversification of protein phosphatase-1 in eukaryotic evolution. *Bioessays* 24:371-381.
51. Stralfors, P., Hiraga, A., and Cohen, P. 1985. The protein phosphatases involved in cellular regulation. Purification and characterisation of the glycogen-bound form of protein phosphatase-1 from rabbit skeletal muscle. *Eur J Biochem* 149:295-303.
52. Aschenbach, W.G., Suzuki, Y., Breeden, K., Prats, C., Hirshman, M.F., Dufresne, S.D., Sakamoto, K., Vilardo, P.G., Steele, M., Kim, J.H., et al. 2001. The muscle-specific protein phosphatase PP1G/R(GL)(G(M))is essential for activation of glycogen synthase by exercise. *J Biol Chem* 276:39959-39967.
53. Suzuki, Y., Lanner, C., Kim, J.H., Vilardo, P.G., Zhang, H., Yang, J., Cooper, L.D., Steele, M., Kennedy, A., Bock, C.B., et al. 2001. Insulin control of glycogen metabolism in knockout mice lacking the muscle-specific protein phosphatase PP1G/RGL. *Mol Cell Biol* 21:2683-2694.
54. Munro, S., Cuthbertson, D.J., Cunningham, J., Sales, M., and Cohen, P.T. 2002. Human skeletal muscle expresses a glycogen-targeting subunit of PP1 that is identical to the insulin-sensitive glycogen-targeting subunit G(L) of liver. *Diabetes* 51:591-598.
55. Stalmans, W., Cadefau, J., Wera, S., and Bollen, M. 1997. New insight into the regulation of liver glycogen metabolism by glucose. *Biochem Soc Trans* 25:19-25.
56. Alemany, S., and Cohen, P. 1986. Phosphorylase a is an allosteric inhibitor of the glycogen and microsomal forms of rat hepatic protein phosphatase-1. *FEBS Lett* 198:194-202.

57. Printen, J.A., Brady, M.J., and Saltiel, A.R. 1997. PTG, a protein phosphatase 1-binding protein with a role in glycogen metabolism. *Science* 275:1475-1478.
58. Crosson, S.M., Khan, A., Printen, J., Pessin, J.E., and Saltiel, A.R. 2003. PTG gene deletion causes impaired glycogen synthesis and developmental insulin resistance. *J Clin Invest* 111:1423-1432.
59. Armstrong, C.G., Browne, G.J., Cohen, P., and Cohen, P.T. 1997. PPP1R6, a novel member of the family of glycogen-targetting subunits of protein phosphatase 1. *FEBS Lett* 418:210-214.
60. Munro, S., Ceulemans, H., Bollen, M., Diplexcito, J., and Cohen, P.T. 2005. A novel glycogen-targeting subunit of protein phosphatase 1 that is regulated by insulin and shows differential tissue distribution in humans and rodents. *FEBS J* 272:1478-1489.
61. Savage, D.B., Zhai, L., Ravikumar, B., Choi, C.S., Snaar, J.E., McGuire, A.C., Wou, S.E., Medina-Gomez, G., Kim, S., Bock, C.B., et al. 2008. A prevalent variant in PPP1R3A impairs glycogen synthesis and reduces muscle glycogen content in humans and mice. *PLoS Med* 5:e27.
62. Frame, S., Cohen, P., and Biondi, R.M. 2001. A common phosphate binding site explains the unique substrate specificity of GSK3 and its inactivation by phosphorylation. *Mol Cell* 7:1321-1327.
63. Dent, P., Lavoinne, A., Nakielny, S., Caudwell, F.B., Watt, P., and Cohen, P. 1990. The molecular mechanism by which insulin stimulates glycogen synthesis in mammalian skeletal muscle. *Nature* 348:302-308.
64. Brady, M.J., and Saltiel, A.R. 2001. The role of protein phosphatase-1 in insulin action. *Recent Prog Horm Res* 56:157-173.
65. Saltiel, A.R., and Steigerwalt, R.W. 1986. Purification of putative insulin-sensitive cAMP phosphodiesterase or its catalytic domain from rat adipocytes. *Diabetes* 35:698-704.
66. Cohen, P. 1989. The structure and regulation of protein phosphatases. *Annu Rev Biochem* 58:453-508.
67. MacKintosh, C., Campbell, D.G., Hiraga, A., and Cohen, P. 1988. Phosphorylation of the glycogen-binding subunit of protein phosphatase-1G in response to adrenalin. *FEBS Lett* 234:189-194.
68. Foulkes, J.G., and Cohen, P. 1979. The hormonal control of glycogen metabolism. Phosphorylation of protein phosphatase inhibitor-1 in vivo in response to adrenaline. *Eur J Biochem* 97:251-256.
69. Moorhead, G., MacKintosh, C., Morrice, N., and Cohen, P. 1995. Purification of the hepatic glycogen-associated form of protein phosphatase-1 by microcystin-Sepharose affinity chromatography. *FEBS Lett* 362:101-105.
70. Orho, M., Bosshard, N.U., Buist, N.R., Gitzelmann, R., Aynsley-Green, A., Blumel, P., Gannon, M.C., Nuttall, F.Q., and Groop, L.C. 1998. Mutations in the liver glycogen synthase gene in children with hypoglycemia due to glycogen storage disease type 0. *J Clin Invest* 102:507-515.

71. Irimia, J.M., Meyer, C.M., Peper, C.L., Zhai, L., Bock, C.B., Previs, S.F., McGuinness, O.P., DePaoli-Roach, A., and Roach, P.J. Impaired glucose tolerance and predisposition to the fasted state in liver glycogen synthase knock-out mice. *J Biol Chem* 285:12851-12861.
72. Cameron, J.M., Levandovskiy, V., MacKay, N., Utgikar, R., Ackerley, C., Chiasson, D., Halliday, W., Raiman, J., and Robinson, B.H. 2009. Identification of a novel mutation in GYS1 (muscle-specific glycogen synthase) resulting in sudden cardiac death, that is diagnosable from skin fibroblasts. *Mol Genet Metab* 98:378-382.
73. Pederson, B.A., Chen, H., Schroeder, J.M., Shou, W., DePaoli-Roach, A.A., and Roach, P.J. 2004. Abnormal cardiac development in the absence of heart glycogen. *Mol Cell Biol* 24:7179-7187.
74. Koeberl, D.D., Kishnani, P.S., Bali, D., and Chen, Y.T. 2009. Emerging therapies for glycogen storage disease type I. *Trends Endocrinol Metab* 20:252-258.
75. Chou, J.Y., Matern, D., Mansfield, B.C., and Chen, Y.T. 2002. Type I glycogen storage diseases: disorders of the glucose-6-phosphatase complex. *Curr Mol Med* 2:121-143.
76. Huijing, F. 1975. Glycogen metabolism and glycogen-storage diseases. *Physiol Rev* 55:609-658.
77. Koster, J.F., Busch, H.F., Slee, R.G., and Van Weerden, T.W. 1978. Glycogenosis type II: the infantile- and late-onset acid maltase deficiency observed in one family. *Clin Chim Acta* 87:451-453.
78. Raben, N., Plotz, P., and Byrne, B.J. 2002. Acid alpha-glucosidase deficiency (glycogenosis type II, Pompe disease). *Curr Mol Med* 2:145-166.
79. Raben, N., Nagaraju, K., Lee, E., Kessler, P., Byrne, B., Lee, L., LaMarca, M., King, C., Ward, J., Sauer, B., et al. 1998. Targeted disruption of the acid alpha-glucosidase gene in mice causes an illness with critical features of both infantile and adult human glycogen storage disease type II. *J Biol Chem* 273:19086-19092.
80. Raben, N., Danon, M., Lu, N., Lee, E., Shliselfeld, L., Skurat, A.V., Roach, P.J., Lawrence, J.C., Jr., Musumeci, O., Shanske, S., et al. 2001. Surprises of genetic engineering: a possible model of polyglucosan body disease. *Neurology* 56:1739-1745.
81. Douillard-Guilloux, G., Raben, N., Takikita, S., Ferry, A., Vignaud, A., Guillet-Deniau, I., Favier, M., Thurberg, B.L., Roach, P.J., Caillaud, C., et al. Restoration of muscle functionality by genetic suppression of glycogen synthesis in a murine model of Pompe disease. *Hum Mol Genet* 19:684-696.
82. Shen, J.J., and Chen, Y.T. 2002. Molecular characterization of glycogen storage disease type III. *Curr Mol Med* 2:167-175.
83. Wolfsdorf, J.I., and Weinstein, D.A. 2003. Glycogen storage diseases. *Rev Endocr Metab Disord* 4:95-102.

84. Raju, G.P., Li, H.C., Bali, D.S., Chen, Y.T., Urion, D.K., Lidov, H.G., and Kang, P.B. 2008. A case of congenital glycogen storage disease type IV with a novel GBE1 mutation. *J Child Neurol* 23:349-352.
85. Dimaur, S., Andreu, A.L., Bruno, C., and Hadjigeorgiou, G.M. 2002. Myophosphorylase deficiency (glycogenosis type V; McArdle disease). *Curr Mol Med* 2:189-196.
86. Ozen, H. 2007. Glycogen storage diseases: new perspectives. *World J Gastroenterol* 13:2541-2553.
87. Nakajima, H., Raben, N., Hamaguchi, T., and Yamasaki, T. 2002. Phosphofructokinase deficiency; past, present and future. *Curr Mol Med* 2:197-212.
88. Delgado-Escueta, A.V., Ganesh, S., and Yamakawa, K. 2001. Advances in the genetics of progressive myoclonus epilepsy. *Am J Med Genet* 106:129-138.
89. Chan, E.M., Andrade, D.M., Franceschetti, S., and Minassian, B. 2005. Progressive myoclonus epilepsies: EPM1, EPM2A, EPM2B. *Adv Neurol* 95:47-57.
90. Delgado-Escueta, A.V. 2007. Advances in lafora progressive myoclonus epilepsy. *Curr Neurol Neurosci Rep* 7:428-433.
91. Ganesh, S., Puri, R., Singh, S., Mittal, S., and Dubey, D. 2006. Recent advances in the molecular basis of Lafora's progressive myoclonus epilepsy. *J Hum Genet* 51:1-8.
92. Chan, E.M., Omer, S., Ahmed, M., Bridges, L.R., Bennett, C., Scherer, S.W., and Minassian, B.A. 2004. Progressive myoclonus epilepsy with polyglucosans (Lafora disease): evidence for a third locus. *Neurology* 63:565-567.
93. Edwards, T.A., Wilkinson, B.D., Wharton, R.P., and Aggarwal, A.K. 2003. Model of the brain tumor-Pumilio translation repressor complex. *Genes Dev* 17:2508-2513.
94. Ganesh, S., Delgado-Escueta, A.V., Sakamoto, T., Avila, M.R., Machado-Salas, J., Hoshii, Y., Akagi, T., Gomi, H., Suzuki, T., Amano, K., et al. 2002. Targeted disruption of the Epm2a gene causes formation of Lafora inclusion bodies, neurodegeneration, ataxia, myoclonus epilepsy and impaired behavioral response in mice. *Human Molecular Genetics.* 11:1251-1262.
95. Chan, E.M., Ackerley, C.A., Lohi, H., Ianzano, L., Cortez, M.A., Shannon, P., Scherer, S.W., and Minassian, B.A. 2004. Laforin preferentially binds the neurotoxic starch-like polyglucosans, which form in its absence in progressive myoclonus epilepsy. *Hum Mol Genet* 13:1117-1129.
96. Depaoli-Roach, A.A., Tagliabracci, V.S., Segvich, D.M., Meyer, C.M., Irimia, J.M., and Roach, P.J. Genetic depletion of the malin E3 ubiquitin ligase in mice leads to Lafora bodies and the accumulation of insoluble laforin. *J Biol Chem*.
97. Wang, W., Lohi, H., Skurat, A.V., DePaoli-Roach, A.A., Minassian, B.A., and Roach, P.J. 2007. Glycogen metabolism in tissues from a mouse model of Lafora disease. *Arch Biochem Biophys* 457:264-269.

98. Minassian, B.A., Lee, J.R., Herbrick, J.A., Huizenga, J., Soder, S., Mungall, A.J., Dunham, I., Gardner, R., Fong, C.Y., Carpenter, S., et al. 1998. Mutations in a gene encoding a novel protein tyrosine phosphatase cause progressive myoclonus epilepsy. *Nat Genet* 20:171-174.
99. Ganesh, S., Tsurutani, N., Amano, K., Mittal, S., Uchikawa, C., Delgado-Escueta, A.V., and Yamakawa, K. 2005. Transcriptional profiling of a mouse model for Lafora disease reveals dysregulation of genes involved in the expression and modification of proteins. *Neurosci Lett* 387:62-67.
100. Ganesh, S., Agarwala, K.L., Ueda, K., Akagi, T., Shoda, K., Usui, T., Hashikawa, T., Osada, H., Delgado-Escueta, A.V., and Yamakawa, K. 2000. Laforin, defective in the progressive myoclonus epilepsy of Lafora type, is a dual-specificity phosphatase associated with polyribosomes. *Hum Mol Genet* 9:2251-2261.
101. Wang, J., Stuckey, J.A., Wishart, M.J., and Dixon, J.E. 2002. A unique carbohydrate binding domain targets the lafora disease phosphatase to glycogen. *J Biol Chem* 277:2377-2380.
102. Gentry, M.S., Dowen, R.H., 3rd, Worby, C.A., Mattoo, S., Ecker, J.R., and Dixon, J.E. 2007. The phosphatase laforin crosses evolutionary boundaries and links carbohydrate metabolism to neuronal disease. *J Cell Biol* 178:477-488.
103. Fernandez-Sanchez, M.E., Criado-Garcia, O., Heath, K.E., Garcia-Fojeda, B., Medrano-Fernandez, I., Gomez-Garre, P., Sanz, P., Serratosa, J.M., and Rodriguez de Cordoba, S. 2003. Laforin, the dual-phosphatase responsible for Lafora disease, interacts with R5 (PTG), a regulatory subunit of protein phosphatase-1 that enhances glycogen accumulation. *Hum Mol Genet* 12:3161-3171.
104. Lohi, H., Ianzano, L., Zhao, X.C., Chan, E.M., Turnbull, J., Scherer, S.W., Ackerley, C.A., and Minassian, B.A. 2005. Novel glycogen synthase kinase 3 and ubiquitination pathways in progressive myoclonus epilepsy. *Hum Mol Genet* 14:2727-2736.
105. Gentry, M.S., Worby, C.A., and Dixon, J.E. 2005. Insights into Lafora disease: malin is an E3 ubiquitin ligase that ubiquitinates and promotes the degradation of laforin. *Proc Natl Acad Sci U S A* 102:8501-8506.
106. Ianzano, L., Zhao, X.C., Minassian, B.A., and Scherer, S.W. 2003. Identification of a novel protein interacting with laforin, the EPM2a progressive myoclonus epilepsy gene product. *Genomics* 81:579-587.
107. Wang, W., and Roach, P.J. 2004. Glycogen and related polysaccharides inhibit the laforin dual-specificity protein phosphatase. *Biochem Biophys Res Commun* 325:726-730.
108. Wang, W., Parker, G.E., Skurat, A.V., Raben, N., DePaoli-Roach, A.A., and Roach, P.J. 2006. Relationship between glycogen accumulation and the laforin dual specificity phosphatase. *Biochem Biophys Res Commun* 350:588-592.
109. Moses, S.W., and Parvari, R. 2002. The variable presentations of glycogen storage disease type IV: a review of clinical, enzymatic and molecular studies. *Curr Mol Med* 2:177-188.

110. Pederson, B.A., Csitkovits, A.G., Simon, R., Schroeder, J.M., Wang, W., Skurat, A.V., and Roach, P.J. 2003. Overexpression of glycogen synthase in mouse muscle results in less branched glycogen. *Biochem Biophys Res Commun* 305:826-830.
111. Cross, D.A., Alessi, D.R., Cohen, P., Andjelkovich, M., and Hemmings, B.A. 1995. Inhibition of glycogen synthase kinase-3 by insulin mediated by protein kinase B. *Nature* 378:785-789.
112. Wang, Y., Liu, Y., Wu, C., Zhang, H., Zheng, X., Zheng, Z., Geiger, T.L., Nuovo, G.J., Liu, Y., and Zheng, P. 2006. Epm2a suppresses tumor growth in an immunocompromised host by inhibiting Wnt signaling. *Cancer Cell* 10:179-190.
113. Worby, C.A., Gentry, M.S., and Dixon, J.E. 2006. Laforin, a dual specificity phosphatase that dephosphorylates complex carbohydrates. *J Biol Chem* 281:30412-30418.
114. Chan, E.M., Young, E.J., Ianzano, L., Munteanu, I., Zhao, X., Christopoulos, C.C., Avanzini, G., Elia, M., Ackerley, C.A., Jovic, N.J., et al. 2003. Mutations in NHLRC1 cause progressive myoclonus epilepsy. *Nat Genet* 35:125-127.
115. Pickart, C.M. 2001. Mechanisms underlying ubiquitination. *Annu Rev Biochem* 70:503-533.
116. Solaz-Fuster, M.C., Gimeno-Alcaniz, J.V., Ros, S., Fernandez-Sanchez, M.E., Garcia-Fojeda, B., Criado Garcia, O., Vilchez, D., Dominguez, J., Garcia-Rocha, M., Sanchez-Piris, M., et al. 2008. Regulation of glycogen synthesis by the laforin-malin complex is modulated by the AMP-activated protein kinase pathway. *Hum Mol Genet* 17:667-678.
117. Vilchez, D., Ros, S., Cifuentes, D., Pujadas, L., Valles, J., Garcia-Fojeda, B., Criado-Garcia, O., Fernandez-Sanchez, E., Medrano-Fernandez, I., Dominguez, J., et al. 2007. Mechanism suppressing glycogen synthesis in neurons and its demise in progressive myoclonus epilepsy. *Nat Neurosci* 10:1407-1413.
118. Worby, C.A., Gentry, M.S., and Dixon, J.E. 2008. Malin decreases glycogen accumulation by promoting the degradation of protein targeting to glycogen (PTG). *J Biol Chem* 283:4069-4076.
119. Cheng, A., Zhang, M., Gentry, M.S., Worby, C.A., Dixon, J.E., and Saltiel, A.R. 2007. A role for AGL ubiquitination in the glycogen storage disorders of Lafora and Cori's disease. *Genes Dev* 21:2399-2409.
120. Vernia, S., Solaz-Fuster, M.C., Gimeno-Alcaniz, J.V., Rubio, T., Garcia-Haro, L., Foretz, M., de Cordoba, S.R., and Sanz, P. 2009. AMP-activated protein kinase phosphorylates R5/PTG, the glycogen targeting subunit of the R5/PTG-protein phosphatase 1 holoenzyme, and accelerates its down-regulation by the laforin-malin complex. *J Biol Chem* 284:8247-8255.
121. Mittal, S., Dubey, D., Yamakawa, K., and Ganesh, S. 2007. Lafora disease proteins malin and laforin are recruited to aggresomes in response to proteasomal impairment. *Hum Mol Genet* 16:753-762.

122. Garyali, P., Siwach, P., Singh, P.K., Puri, R., Mittal, S., Sengupta, S., Parihar, R., and Ganesh, S. 2009. The malin-laforin complex suppresses the cellular toxicity of misfolded proteins by promoting their degradation through the ubiquitin-proteasome system. *Hum Mol Genet* 18:688-700.
123. Ramachandran, N., Girard, J.M., Turnbull, J., and Minassian, B.A. 2009. The autosomal recessively inherited progressive myoclonus epilepsies and their genes. *Epilepsia* 50 Suppl 5:29-36.
124. Gentry, M.S., Dixon, J.E., and Worby, C.A. 2009. Lafora disease: insights into neurodegeneration from plant metabolism. *Trends Biochem Sci* 34:628-639.
125. Cataldo, A.M., and Broadwell, R.D. 1986. Cytochemical identification of cerebral glycogen and glucose-6-phosphatase activity under normal and experimental conditions. II. Choroid plexus and ependymal epithelia, endothelia and pericytes. *J Neurocytol* 15:511-524.
126. Brown, A.M., and Ransom, B.R. 2007. Astrocyte glycogen and brain energy metabolism. *Glia* 55:1263-1271.
127. Phelps, C.H. 1972. Barbiturate-induced glycogen accumulation in brain. An electron microscopic study. *Brain Res* 39:225-234.
128. Cruz, N.F., and Dienel, G.A. 2002. High glycogen levels in brains of rats with minimal environmental stimuli: implications for metabolic contributions of working astrocytes. *J Cereb Blood Flow Metab* 22:1476-1489.
129. Hutchins, D.A., and Rogers, K.J. 1970. Physiological and drug-induced changes in the glycogen content of mouse brain. *Br J Pharmacol* 39:9-25.
130. Schurr, A., West, C.A., and Rigor, B.M. 1988. Lactate-supported synaptic function in the rat hippocampal slice preparation. *Science* 240:1326-1328.
131. Wender, R., Brown, A.M., Fern, R., Swanson, R.A., Farrell, K., and Ransom, B.R. 2000. Astrocytic glycogen influences axon function and survival during glucose deprivation in central white matter. *J Neurosci* 20:6804-6810.
132. Dringen, R., Gebhardt, R., and Hamprecht, B. 1993. Glycogen in astrocytes: possible function as lactate supply for neighboring cells. *Brain Res* 623:208-214.
133. Koehler-Stec, E.M., Simpson, I.A., Vannucci, S.J., Landschulz, K.T., and Landschulz, W.H. 1998. Monocarboxylate transporter expression in mouse brain. *Am J Physiol* 275:E516-524.
134. Pierre, K., Pellerin, L., Debernardi, R., Riederer, B.M., and Magistretti, P.J. 2000. Cell-specific localization of monocarboxylate transporters, MCT1 and MCT2, in the adult mouse brain revealed by double immunohistochemical labeling and confocal microscopy. *Neuroscience* 100:617-627.
135. Choi, I.Y., Seaquist, E.R., and Gruetter, R. 2003. Effect of hypoglycemia on brain glycogen metabolism in vivo. *J Neurosci Res* 72:25-32.
136. Criego, A.B., Tkac, I., Kumar, A., Thomas, W., Gruetter, R., and Seaquist, E.R. 2005. Brain glucose concentrations in patients with type 1 diabetes and hypoglycemia unawareness. *J Neurosci Res* 79:42-47.

137. Suh, S.W., Bergher, J.P., Anderson, C.M., Treadway, J.L., Fosgerau, K., and Swanson, R.A. 2007. Astrocyte glycogen sustains neuronal activity during hypoglycemia: studies with the glycogen phosphorylase inhibitor CP-316,819 ([R-R*,S*]-5-chloro-N-[2-hydroxy-3-(methoxymethylamino)-3-oxo-1-(phenylmet hyl)propyl]-1H-indole-2-carboxamide). *J Pharmacol Exp Ther* 321:45-50.
138. Wang, W., Lohi, H., Skurat, A.V., Depaoli-Roach, A.A., Minassian, B.A., and Roach, P.J. 2006. Glycogen metabolism in tissues from a mouse model of Lafora disease. *Arch Biochem Biophys*.
139. Maehama, T., Taylor, G.S., Slama, J.T., and Dixon, J.E. 2000. A sensitive assay for phosphoinositide phosphatases. *Anal Biochem* 279:248-250.
140. Hess, H.H., and Derr, J.E. 1975. Assay of inorganic and organic phosphorus in the 0.1-5 nanomole range. *Anal Biochem* 63:607-613.
141. Bradford, M.M. 1976. A rapid and sensitive method for the quantitation of microgram quantities of protein utilizing the principle of protein-dye binding. *Anal Biochem* 72:248-254.
142. Thomas, J.A., Schlender, K.K., and Larner, J. 1968. A rapid filter paper assay for UDPglucose-glycogen glucosyltransferase, including an improved biosynthesis of UDP-14C-glucose. *Anal Biochem* 25:486-499.
143. Skurat, A.V., Cao, Y., and Roach, P.J. 1993. Glucose control of rabbit skeletal muscle glycogenin expressed in COS cells. *J Biol Chem* 268:14701-14707.
144. Orellana, A., Neckelmann, G., and Norambuena, L. 1997. Topography and Function of Golgi Uridine-5[prime]-Diphosphatase from Pea Stems. *Plant Physiol* 114:99-107.
145. Dhugga, K.S., and Ray, P.M. 1994. Purification of 1,3-beta-D-glucan synthase activity from pea tissue. Two polypeptides of 55 kDa and 70 kDa copurify with enzyme activity. *Eur J Biochem* 220:943-953.
146. Kennedy, L.D., Kirkman, B.R., Lomako, J., Rodriguez, I.R., and Whelan, W.J. 1985. The biogenesis of rabbit-muscle glycogen. *Membranes and Muscle.* IRL Press, Oxford:65-84.
147. Zmudzka, B.S., D. 1964. Preparation and chemical and enzymic properties of cyclic phosphates of D-glucopyranose and synthesis of derivatives of N-(D-glucopyranosyl) pyridine. *Acta Biochimica Polonica* 11:509-525.
148. De Clercq, E., Zmudzka, B., and Shugar, D. 1972. Antiviral activity of polynucleotides: role of the 2'-hydroxyl and a pyrimidine 5-methyl. *FEBS Lett* 24:137-140.
149. Piras, R. 1963. Synthesis of Some Aldose 2-Phosphates. *Arch Biochem Biophys* 103:291-292.
150. Wishart, D.S., Bigam, C.G., Yao, J., Abildgaard, F., Dyson, H.J., Oldfield, E., Markley, J.L., and Sykes, B.D. 1995. 1H, 13C and 15N chemical shift referencing in biomolecular NMR. *J Biomol NMR* 6:135-140.

151. Ganesh, S., Delgado-Escueta, A.V., Sakamoto, T., Avila, M.R., Machado-Salas, J., Hoshii, Y., Akagi, T., Gomi, H., Suzuki, T., Amano, K., et al. 2002. Targeted disruption of the Epm2a gene causes formation of Lafora inclusion bodies, neurodegeneration, ataxia, myoclonus epilepsy and impaired behavioral response in mice. *Hum Mol Genet* 11:1251-1262.
152. Krisman, C.R. 1962. A method for the colorimetric estimation of glycogen with iodine. *Anal Biochem* 4:17-23.
153. Shearer, J., and Graham, T.E. 2004. Novel aspects of skeletal muscle glycogen and its regulation during rest and exercise. *Exerc Sport Sci Rev* 32:120-126.
154. Smythe, C., and Cohen, P. 1991. The discovery of glycogenin and the priming mechanism for glycogen biogenesis. *Eur J Biochem* 200:625-631.
155. Lomako, J., Lomako, W.M., and Whelan, W.J. 2004. Glycogenin: the primer for mammalian and yeast glycogen synthesis. *Biochim Biophys Acta* 1673:45-55.
156. Roach, P.J., and Skurat, A.V. 1997. Self-glucosylating initiator proteins and their role in glycogen biosynthesis. *Prog Nucleic Acid Res Mol Biol* 57:289-316.
157. Rubinsztein, D.C. 2006. The roles of intracellular protein-degradation pathways in neurodegeneration. *Nature* 443:780-786.
158. Moreno, D., Towler, M.C., Hardie, D.G., Knecht, E., and Sanz, P. The Laforin-Malin Complex, Involved in Lafora Disease, Promotes the Incorporation of K63-linked Ubiquitin Chains into AMP-activated Protein Kinase Beta Subunits. *Mol Biol Cell*.
159. McBride, A., and Hardie, D.G. 2009. AMP-activated protein kinase--a sensor of glycogen as well as AMP and ATP? *Acta Physiol (Oxf)* 196:99-113.
160. McBride, A., Ghilagaber, S., Nikolaev, A., and Hardie, D.G. 2009. The glycogen-binding domain on the AMPK beta subunit allows the kinase to act as a glycogen sensor. *Cell Metab* 9:23-34.
161. Kahn, B.B., Alquier, T., Carling, D., and Hardie, D.G. 2005. AMP-activated protein kinase: ancient energy gauge provides clues to modern understanding of metabolism. *Cell Metab* 1:15-25.
162. Skurat, A.V., Lim, S.S., and Roach, P.J. 1997. Glycogen biogenesis in rat 1 fibroblasts expressing rabbit muscle glycogenin. *Eur J Biochem* 245:147-155.
163. Pederson, B.A., Schroeder, J.M., Parker, G.E., Smith, M.W., DePaoli-Roach, A.A., and Roach, P.J. 2005. Glucose metabolism in mice lacking muscle glycogen synthase. *Diabetes* 54:3466-3473.
164. Boraston, A.B., Bolam, D.N., Gilbert, H.J., and Davies, G.J. 2004. Carbohydrate-binding modules: fine-tuning polysaccharide recognition. *Biochem J* 382:769-781.
165. Haebel, S., Hejazi, M., Frohberg, C., Heydenreich, M., and Ritte, G. 2008. Mass spectrometric quantification of the relative amounts of C6 and C3 position phosphorylated glucosyl residues in starch. *Anal Biochem* 379:73-79.

166. Anderson, W.B., and Nordlie, R.C. 1968. Glucose dehydrogenase activity of yeast glucose 6-phosphate dehydrogenase. I. Selective stimulation by bicarbonate, phosphate, and sulfate. *Biochemistry* 7:1479-1485.
167. Dekker, C.A., and Khorana, H.G. 1954. Carbodiimides. VI. The reaction of dicyclohexylcarbodiimide with yeast adenylic acid. A new method for the preparation of monoesters of ribonucleoside 2'- and 3'-phosphates *JACS* 76:3522–3527
168. Khorana, H.G., Tener, R.S., Wright, R.S., and Moffatt, J.G. 1957. Cyclic phosphates. III. Some general observations on the formation and properties of five-, six- and seven-membered cyclic phosphate esters *JACS* 79:430–436
169. Levene, P.A., and Raymond, A.L. 1934. Xylosephosphoric Acids II *J Biol Chem* 107:75-83.
170. van Leeuwen, S.S., Kralj, S., van Geel-Schutten, I.H., Gerwig, G.J., Dijkhuizen, L., and Kamerling, J.P. 2008. Structural analysis of the alpha-D-glucan (EPS35-5) produced by the Lactobacillus reuteri strain 35-5 glucansucrase GTFA enzyme. *Carbohydr Res* 343:1251-1265.
171. Paladini, A.C., and Leloir, L.F. 1952. Studies on uridine-diphosphate-glucose. *Biochem J* 51:426-430.
172. Nunez, H.A., and Barker, R. 1976. The metal ion catalyzed decomposition of nucleoside diphosphate sugars. *Biochemistry* 15:3843-3847.
173. Szabo, P., and Szabo, L. 1961. Phosphorylated sugars. Part III. The formation of five-, six-, and seven-membered cyclic phosphates of 1,2-*O*-isopropylidene-D-glucofuranose, and the synthesis of two new cyclic phosphates of D-glucose. *J Chem Soc*:448-457.
174. Graham, T.E. 2009. Glycogen: an overview of possible regulatory roles of the proteins associated with the granule. *Appl Physiol Nutr Metab* 34:488-492.
175. Ball, S., Guan, H.P., James, M., Myers, A., Keeling, P., Mouille, G., Buleon, A., Colonna, P., and Preiss, J. 1996. From glycogen to amylopectin: a model for the biogenesis of the plant starch granule. *Cell* 86:349-352.
176. Zeeman, S.C., Smith, S.M., and Smith, A.M. 2007. The diurnal metabolism of leaf starch. *Biochem J* 401:13-28.
177. Sakai, M., Austin, J., Witmer, F., and Trueb, L. 1970. Studies in myoclonus epilepsy (Lafora body form). II. Polyglucosans in the systemic deposits of myoclonus epilepsy and in corpora amylacea. *Neurology* 20:160-176.
178. Yokoi, S., Austin, J., Witmer, F., and Sakai, M. 1968. Studies in myoclonus epilepsy (Lafora body form). I. Isolation and preliminary characterization of Lafora bodies in two cases. *Arch Neurol* 19:15-33.
179. Gessler, K., Uson, I., Takaha, T., Krauss, N., Smith, S.M., Okada, S., Sheldrick, G.M., and Saenger, W. 1999. V-Amylose at atomic resolution: X-ray structure of a cycloamylose with 26 glucose residues (cyclomaltohexaicosaose). *Proc Natl Acad Sci U S A* 96:4246-4251.

180. Liu, Y., Wang, Y., Wu, C., Liu, Y., and Zheng, P. 2006. Dimerization of Laforin Is Required for Its Optimal Phosphatase Activity, Regulation of GSK3beta Phosphorylation, and Wnt Signaling. *J Biol Chem* 281:34768-34774.
181. Minassian, B.A. 2001. Lafora's disease: towards a clinical, pathologic, and molecular synthesis. *Pediatr Neurol* 25:21-29.
182. Fredrick, K., and Ibba, M. 2009. Protein synthesis: Errors rectified in retrospect. *Nature* 457:157-158.
183. Zaher, H.S., and Green, R. 2009. Quality control by the ribosome following peptide bond formation. *Nature* 457:161-166.
184. Thomas, M.J., Platas, A.A., and Hawley, D.K. 1998. Transcriptional fidelity and proofreading by RNA polymerase II. *Cell* 93:627-637.
185. Erie, D.A., Hajiseyedjavadi, O., Young, M.C., and von Hippel, P.H. 1993. Multiple RNA polymerase conformations and GreA: control of the fidelity of transcription. *Science* 262:867-873.
186. Kunkel, T.A., and Bebenek, K. 2000. DNA replication fidelity. *Annu Rev Biochem* 69:497-529.

CURRICULUM VITAE

Vincent S. Tagliabracci

EDUCATION

2000-05 BS Chemistry and Biology. University of Indianapolis, Indianapolis IN.

2005-10 Ph.D. Biochemistry and Molecular Biology, Indiana University, Indianapolis IN

APPOINTMENTS

2004-05 Intern: Eli Lilly and Company, Laboratory of Ann Dantzig

2005 Technician: Indiana University School of Medicine Department of Neurology, Laboratory of Yansheng Du.

HONORS AND AWARDS

2001 The National Deans List of America

2000-04 Academic All Conference Team in Men's Golf at the University of Indianapolis

2002 Rho Chapter of Sigma Zeta Honorary Society

2003 Outstanding student in chemistry award, University of Indianapolis

2003 Alpha Chi Honor Society of America

2004 Phi Alpha Epsilon Honor Society of America

2004 Collegiate All American Scholar Award

2008 Sigma Xi, Graduate Student Research Competition. 2nd Place

2008 Biochemistry Retreat Poster Award

2009 IUSM/CTSI Poster Session, 1st Place Student Category

2010 Peggy Gibson Award for Best Paper by a Graduate Student

2010 Jack Davis Award for Best Seminar by a Graduate Student

2010 Sigma Xi. Graduate Student Research Competition. Raymond Paradise Award for 1st Place

2010 Nominated for the Esther L. Kinsley Dissertation Award

GRANT SUPPORT

2006 Devault Diabetes Fellowship

2007-09 American Heart Association Pre-Doctoral Fellowship

SERVICES

2008-09 Department of Biochemistry and Molecular Biology Student Representative

ORAL PRESENTATIONS

1. Deficiency of laforin, a glycogen phosphatase, leads to age dependent aberrations of glycogen structure *in vivo*. FASEB Conference on Protein Phosphatases Snowmass, CO. 2008.
2. Glycogen Phosphorylation and Lafora Disease. Europhosphatases: Protein Phosphatases in Development and Disease, Egmund Ann Zee, the Netherlands. 2009.
3. Glycogen Phosphorylation and Lafora Disease: University of Pisa, Pisa Italy. 2009.
4. Glycogen Phosphorylation and Lafora Disease. Progressive Myoclonus Epilepsies in the New Millenium. Venice, Italy. 2010. Invited Speaker

POSTER PRESENTATIONS

1. Novel Insight into the Role of Covalent Phosphate of Glycogen in its Metabolism and Structure. **Tagliabracci VS**, Girard JM, Turnbull J, Zhao X, Skurat AV, Ackerley C, Minassian BA, DePaoli-Roach AA, and. Roach PJ. American Diabetes Association, 68th Annual Scientific Sessions, San Francisco, CA. 2008.
2. Deficiency of laforin, a glycogen phosphatase, leads to age dependent aberrations of glycogen structure *in vivo*. **Tagliabracci VS**, Girard JM, Turnbull J, Zhao X, Skurat AV, Ackerley C, Minassian BA, DePaoli-Roach AA, and. Roach PJ. FASEB Conference on Protein Phosphatases Snowmass, CO. 2008.

3. Silencing SREBP1 in Liver of db/db Mice Uncovers a Role in Glucose Metabolism. Ruiz R, **Tagliabracci VS**, Irimia-Dominguez J., Roach PJ, Morral N. American Diabetes Association, 69th Annual Scientific Sessions, New Orleans, LA. 2009.
4. Role of p38MAPK in Epinephrine Control of Glycogen Metabolism. DePaoli-Roach AA, Segvich D, **Tagliabracci VS**, Nakai C, Wojtaszewski and Roach PJ. American Diabetes Association, 69th Annual Scientific Sessions, New Orleans, LA. 2009.

PUBLICATIONS

1. Lin, S., **Tagliabracci, V.S**., Chen, X., and Du, Y. 2005. Albumin protects cultured cerebellar granule neurons against zinc neurotoxicity. *Neuroreport* 16:1461-1465.
2. **Tagliabracci, V.S**., Turnbull, J., Wang, W., Girard, J.M., Zhao, X., Skurat, A.V., Delgado-Escueta, A.V., Minassian, B.A., Depaoli-Roach, A.A., and Roach, P.J. 2007. Laforin is a glycogen phosphatase, deficiency of which leads to elevated phosphorylation of glycogen in vivo. *Proc Natl Acad Sci U S A* 104:19262-19266.
3. Wei, X., Ma, Z., Fontanilla, C.V., Zhao, L., Xu, Z.C., **Tagliabracci, VS**., Johnstone, B.H., Dodel, R.C., Farlow, M.R., and Du, Y. 2008. Caffeic acid phenethyl ester prevents cerebellar granule neurons (CGNs) against glutamate-induced neurotoxicity. *Neuroscience* 155:1098-1105.
4. **Tagliabracci, V.S**., Girard, J.M., Segvich, D., Meyer, C., Turnbull, J., Zhao, X., Minassian, B.A., Depaoli-Roach, A.A., and Roach, P.J. 2008. Abnormal metabolism of glycogen phosphate as a cause for Lafora disease. *J Biol Chem* 283:33816-33825.
5. Heyen, C.A., **Tagliabracci, V.S**., Zhai, L., and Roach, P.J. 2009. Characterization of mouse UDP-glucose pyrophosphatase, a Nudix hydrolase encoded by the Nudt14 gene. *Biochem Biophys Res Commun* 390:1414-1418.

6. Depaoli-Roach, A.A.*, **Tagliabracci, V.S**.*, Segvich, D.M., Meyer, C.M., Irimia, J.M., and Roach, P.J. Genetic depletion of the malin E3 ubiquitin ligase in mice leads to Lafora bodies and the accumulation of insoluble laforin. Epub ahead of print *J Biol Chem*.
***** denotes co-first authors